Non-locality and Back-reaction in Acoustic Black Holes and Non-linearity in Quantum Fluid Dynamics

Giorgio Ciliberto

THESE DE DOCTORAT

NNT : 2024UPASP174

Non-locality and Back-reaction in Acoustic Black Holes and Non-linearity in Quantum Fluid Dynamics

Non-localité et rétro-action dans les trous noirs acoustiques et non-linéarité dans les fluides quantiques

Thèse de doctorat de l'université Paris-Saclay et de l'université de Freiburg

École doctorale n°564, Physique en Île-de-France
Spécialité de doctorat : Physique
Graduate School : Physique. Référent : Faculté des sciences d'Orsay

Thèse préparée dans les unités de recherche **LPTMS (Université Paris-Saclay, CNRS)** et **QOS (Universität Freiburg)** , sous la direction de **Nicolas PAVLOFF**, Professeur, et la co-direction de **Andreas BUCHLEITNER**, Professeur

Thèse soutenue à Paris-Saclay, le 19 décembre 2024, par

Giorgio CILIBERTO

Composition du jury

Membres du jury avec voix délibérative

Jacqueline BLOCH Directrice de recherche, CNRS C2N Académie des Sciences	Présidente
Augusto SMERZI Directeur de recherche, CNR-INO LENS	Rapporteur & Examinateur
Marek KUŚ Professeur, Warsaw University of Technology QuantMath research group	Rapporteur & Examinateur
Heidi RZEHAK Professeure, Universität Freiburg Physikalisches Institut	Examinatrice

université PARIS-SACLAY | ÉCOLE DOCTORALE Physique en Île-de-France (PIF)

Titre: Non-localité et rétro-action dans les trous noirs acoustiques et non-linéarité dans les fluides quantiques

Mots clés: condensat de Bose-Einstein, radiation de Hawking acoustique, intrication, non-localité, rétro-action, turbulence quantique

Résumé: Cette thèse porte essentiellement sur les corrélations quantiques et les fluctuations non-lineaires dans les fluides quantiques. Elle se concentre spéficiquement sur les fluctuations quantiques collectives, à savoir les ondes sonores, dans le flux stationnaire d'un quasi-condensat 1D de Bose-Einstein qui présente un horizon acoustique, c'est-à-dire une transition du flux d'un régime subsonique à un régime supersonique. Les phénomènes quantiques générés par la présence de l'horizon sont étudiés. La thèse présente également un bref excursus sur les turbulences dans un fluide quantique bidimensionnel.

Nous étudions la non-séparabilité quantique, la non-localité et la rétro-action du rayonnement acoustique de Hawking émis par un trou noir analogue. L'intrication et les corrélations non locales au sein du système tripartite de quasi-particules émises par l'horizon acoustique sont d'abord étudiées. Les équations de rétro-action qui régissent l'effet de ce rayonnement acoustique sur le fond inhomogène sont dérivées et des solutions stationnaires sont considérées. Enfin, une théorie phénoménologique basée sur des contraintes topologiques pour la création et l'annihilation de vortex est appliquée efficacement aux données expérimentales, permettant ainsi de rendre compte des phases de croissance et de décroissance des turbulences.

Title: Non-locality and Back-reaction in Acoustic Black Holes and Non-linearity in Quantum Fluid Dynamics

Keywords: : Bose-Einstein condensate, acoustic Hawking radiation, entanglement, nonlocality, back- reaction, quantum turbulence

Abstract: This thesis is mainly about quantum correlations and non-linear fluctuations in quantum fluids. It focuses especially on collective quantum fluctuations, i.e. sound waves, in the stationary flow of a 1D Bose-Einstein quasi-condensate which exhibits an acoustic horizon, i.e. a transition from subsonic to supersonic flow. Quantum phenomena generated by the presence of the horizon are investigated. The thesis also presents a brief excursus on two-dimensional turbulence in a quantum fluid.

We study quantum non-separability, non-locality and back-reaction of the acoustic Hawking radiation emitted by an analog black hole. The entanglement and non-local correlations within the tripartite system of quasi-particles emitted from the acoustic horizon are first investigated. Back-reaction equations governing the effect of such acoustic radiation on the inhomogeneous background are derived and stationary solutions are considered. Finally, a phenomenological theory based on topological constraints for vortex creation and annihilation is effectively applied to experimental data, thus accounting for the growth and decay of turbulence.

Résumé en français

Cette thèse porte principalement sur la théorie des fluides quantiques et les phénomènes non linéaires dans les systèmes quantiques. Elle se concentre en particulier sur les fluctuations quantiques collectives, c'est-à-dire les ondes sonores, dans les condensats de Bose-Einstein (BEC) en écoulement stationnaire présentant des horizons acoustiques, c'est-à-dire des transitions d'écoulements subsoniques à supersoniques. Les phénomènes quantiques générés par la présence de l'horizon sont étudiés. La thèse présente également un bref excursus sur la turbulence quantique dans les fluides quantiques d'excitons-polaritons.

Un premier chapitre introductif présente brièvement la gravité analogue, les condensats de Bose-Einstein et les contraintes topologiques à la turbulence quantique. Un deuxième chapitre 2 présente la modélisation des trous noirs avec des systèmes analogues et un troisième chapitre 3 les trous noirs analogues, réalisés dans des BECs, que nous considérons spécifiquement dans ce travail. Un quatrième chapitre 4 fournit les résultats de notre étude de la violation des inégalités de Bell dans notre système analogue. Un cinquième chapitre 5 étudie la dérivation des équations de rétro-action dans des condensats analogue et quelques résultats préliminaires sur les solutions stationnaires. Enfin, un dernier chapitre 6, sans rapport avec la gravité analogue, présente l'ajustement numérique des données expérimentales obtenues à partir d'une théorie phénoménologique pour la croissance et la décroissance du nombre de tourbillons dans un fluide bidimensionnel quantique.

Plus précisément, le deuxième chapitre 2 et le troisième chapitre 3 sont des chapitres d'introduction à la modélisation des trous noirs avec des systèmes analogues 2 et plus spécifiquement dans des quasi-condensats 1D 3. Le troisième chapitre présente les trous noirs de Schwarzschild et la modélisation de la dynamique des champs scalaires dans l'espace-temps courbe par la propagation d'ondes sonores dans une métrique courbe effective donnée par le champ moyen d'un écoulement non homogène. Il présente également la dérivation du rayonnement de Hawking et de son analogue hydronymique. Le quatrième chapitre présente les différentes configurations analogues de trous noirs dans un quasi-condensat 1D utilisées dans cette étude, ainsi que les transformations de Bololiubov définissant les modes entrants et sortants comme des fluctuations quantiques émergeant de la linéarisation de Bogoliubov de l'équation de Gross-Pitaevskii.

Le quatrième chapitre 4 ainsi que le cinquième chapitre 5 présentent les recherches spécifiques que nous avons menées sur les corrélations quantiques 4 et la rétro-action dans des trous noirs analogues 1D réalisés dans des

BECs 5. Le quatrième chapitre 4, après une introduction aux inégalités de Bell et au formalisme de la fonction de Wigner, se concentre sur l'étude des corrélations quantiques entre les trois modes sortants de notre système et caractérise les conditions de non-localité pour les mesures de pseudospin GKMR dans nos configurations analogues de trous noirs. Le cinquième chapitre 5 dérive les équations de rétro-réaction décrivant l'effet du rayonnement de Hawking sur la métrique du trou noir analogue qui le génère : quelques résultats asymptotiques préliminaires sont fournis.

Le dernier chapitre 6 considère les contraintes topologiques sur la turbulence quantique d'un fluide 2D d'excitons-polaritons. Un tel fluide est décrit par une équation de Schrödinger non linéaire qui est analogue à l'équation de Gross-Pitaevskii d'un BEC de vapeur atomique. L'étude montre que la croissance et la décroissance du nombre de tourbillons sont régies par des contraintes topologiques dictées par les lois de conservation des nombres quantiques.

***

Il apparaît donc que le domaine de la gravité analogue vise à pallier le manque de théorie et d'expérience dans le domaine de la gravité quantique en transposant certaines de ses principales questions et préoccupations à des systèmes de matière condensée. En suivant cette stratégie, nous avons étudié la non-séparabilité quantique, la non-localité et la rétro-réaction du rayonnement acoustique de Hawking émis par un trou noir analogue réalisé dans l'écoulement d'un quasi-condensat 1D.

Dans le chapitre 4, notre travail théorique prépare le terrain pour de futures études expérimentales en fournissant des prédictions quantitatives du degré d'intrication et de violation des inégalités de Bell dans une configuration analogue réaliste, à la fois pour les systèmes bi- et tri-partites. En effet, alors que le processus de Hawking relativiste n'implique, dans le cas stationnaire, que deux modes, un troisième mode est présent dans le système étudié : tout en n'affectant pas l'analogie avec le rayonnement de Hawking, le troisième mode conduit à une phénoménologie plus riche. Nous avons donc mené une étude systématique du système, confirmant le caractère non classique, c'est-à-dire non séparable et non local, du rayonnement de Hawking analogue grâce à des critères expérimentaux pertinents. En outre, notre étude des différents critères de non-localité démontre que les modes quantiques de grande longueur d'onde du système consistent en une superposition de versions dégénérées d'états GHZ à variables continues. Il est intéressant de noter que la nature continue des degrés de liberté, à la différence des états GHZ construits sur des qbits, permet à ces modes de rester intriqués

après un traçage partiel. Cela confirme que l'information quantique à variables continues avec des modèles analogues de trous noirs ouvre de nouvelles perspectives de traitement robuste de l'information dans une variété de protocoles, tels que le partage de secrets ou le brouillage d'informations.

Dans le chapitre 5, nous avons dérivé des équations de rétro-action qui sont génériquement valables pour l'écoulement d'un condensat inhomogène dans n'importe quelle dimension. Nous les avons spécifiquement appliquées à une configuration analogue de trou noir dans un quasi-condensat 1D. Nous avons trouvé des solutions asymptotiques et fourni quelques résultats préliminaires pour des choix cohérents de paramètres. Les travaux futurs seront consacrés à l'étude de la dynamique exacte de l'horizon sous l'effet de la rétro-action et à la détermination de la correction de la température de Hawking du système qui en découle. Étant donné que dans le cadre gravitationnel, la source quantique de la rétro-action s'est avérée difficile à évaluer, les configurations hydrodynamiques analogues semblent être des systèmes précieux pour tester des modèles au-delà de la gravité (semi-)classique. Dans cette perspective, puisque la dérivation de l'effet Hawking ne prend pas en compte la rétro-action, un prolongement naturel de notre étude sera d'écrire les équations de Bogoliubov modifiées avec un champ moyen intégrant la rétro-action. L'effet de la rétro-réaction sur le rayonnement de Hawking, la « rétro-rétro-réaction » pour ainsi dire, pourrait alors être étudié et la thermalité du rayonnement reconsidérée dans cette nouvelle perspective. Cela ouvrirait de nouvelles perspectives sur la nature de l'information transportée par le rayonnement de Hawking.

Enfin, dans le chapitre 6, nous avons mené une étude expérimentale et théorique combinée de la cinétique des tourbillons dans un fluide quantique compressible 2D composé d'excitons-polaritons. Ainsi, en considérant un modèle phénoménologique minimal basé sur des contraintes topologiques, nous avons dérivé des équations cinétiques de formation et d'annihilation de points critiques du champ de vitesse. Ces équations sont capables de reproduire le taux de création et d'annihilation de tourbillons quantifiés observé expérimentalement dans les phases de croissance et de décroissance de la turbulence quantique. Ces résultats devront être approfondis par des simulations numériques plus poussées. De plus, même si ce dernier chapitre n'est pas lié à la gravité analogue, on peut penser à de futurs modèles 2D, impliquant la vorticité, qui exploiteraient les contraintes décrites ici : dans cette perspective, les charges topologiques considérées dans notre modèle phénoménologique effectif de turbulence quantique, pourraient également s'avérer utiles pour étudier la physique des trous noirs rotatifs analogues et de phénomènes tels que la superradiance.

ACKNOWLEDGEMENTS

This PhD was conducted under the co-supervision of Prof. Nicolas PAVLOFF at the *Laboratoire de Physique Théorique et Modèles Statistiques* (LPTMS, Paris-Saclay) in Orsay and Prof. Andreas BUCHLEITNER at the *Quantum Optics and Statistics* group (QOS, Freiburg University) in Freiburg. It was financed by Paris-Saclay and Freiburg Universities (RTG-DynCAM) as well as by the CNRS and I am grateful to these institutions for this opportunity.

Of course, I first would like to thank my two supervisors, Nicolas and Andreas. Working with them was both an enlightening scientific undertaking and a sincere human experience. It all started with my Master internships with Nicolas and I really thank him for trusting me and for the really great pleasure it was to work with him on a daily basis. I also thank Andreas for all the great discussions we had. I learned a lot from both of them and it will be my pleasure to work with them again in the future.

The study of Bell's inequalities would not be what it is without Mathieu Isoard : I really thank him for his time. Over the months, working with him became more as talking with a friend than exchanging with a colleague. And I am grateful to him for that. I would also like to thank Alessandro Fabbri and Roberto Balbinot for the long discussions we had on the back-reaction phenomenon as well as all the people involved in the topological constraints project.

I would like to thank the referees for accepting to review my work and all the jury members for agreeing to take part to the PhD defense.

I would like to thank all the PhD students and the Post-docs both in Paris and in Freiburg, for sharing their time and experience and office with me, Lucas, Li, Jules, Romain and all the others.

I would like to thank the former director of the LPTMS, Emmanuel TRIZAC, and the present director, Alberto ROSSO, for making the LPTMS in Orsay such an inspiring and dynamic working place. The same holds true for the QOS led by Andreas BUCHLEITNER in Freiburg.

In the administration of the two research groups, I would like to thank Claudine LE VAOU and Delphine HANNOY at the LPTMS and Gislinde BÜHLER and Elena WIGGERT at the QOS. The co-supervision agreement was established thanks to the daily efforts of Claudine, Gislinde and Elena : I am grateful to them for their time. A huge special thank goes to Claudine for taking care of my numerous travels back-and-forth Paris-Freiburg and to Gislinde who helped me so much on my arrival in Freiburg. I also thank Zhiqiang QIN for the IT assistance at the LPTMS.

I also would like to thank the housekeepers and maintenance team without whom the buildings would not be so comfortable places to work in.

Finally, I would like to thank all the people who helped me succeed in my Bachelor and Master Degrees and without whom I would not be writing these lines for my PhD thesis : I am indebted to them all. Among them, a special thank goes to my father, for his time and for the pleasure of discussing physics with him.

Last but not least, I would like to thank all my closest family, my father Sergio again, my mother Margherita and my two sisters Elena and Silvia, as well as my oldest and best friends, Jean-Sébastien, Emanuele, Benjamin and Andrea, my cousin Alessandro : I just thank all of them for Beurizot and for all what we did and will do together, for the infinite discussions we had and will have, for what we were and will be.

Contents

1 - INTRODUCTION

1.1 . Outline of the thesis

This thesis is mainly about quantum fluid theory and non-linear phenomena in quantum systems. It focuses especially on collective quantum fluctuations, i.e. sound waves, in stationary flowing Bose-Einstein condensates (BECs) which exhibit acoustic horizons, i.e. transitions from subsonic to supersonic flows. Quantum phenomena generated by the presence of the horizon are investigated. The thesis also presents a brief excursus on quantum turbulence in quantum fluids of exciton-polaritons.

This chapter introduces Analog Gravity, Bose-Einstein condensates and quantum turbulence constraints. A second chapter 2 presents the modeling of black holes with analog systems and a third chapter 3 the BEC analog black hole we specifically consider in this work. A fourth chapter 4 provides the results of our inquiry of Bell's inequalities violation in our BEC analog. A fifth chapter 5 investigates the derivation of the back-reaction equations in our BEC analog and some preliminary results on stationary solutions. Finally, a last chapter 6, unrelated to analog gravity, presents the numerical fitting of experimental data obtained from a phenomenological theory for the growth and decay of the number of vortices in a quantum two-dimensional fluid.

More specifically, the second chapter 2 and third chapter 3 are introductory chapters to the modeling of black holes with analog systems 2 and more specifically in 1D quasi-condensates 3. The third chapter presents Schwarzschild black holes and the modeling of scalar field dynamics in curved-space time by sonic waves propagation in an effective curved metric given by a non-homogenously flowing background. It also presents the derivation of Hawking radiation and of its hydronymical analog. The fourth chapter presents the different analog black hole configurations in a 1D quasi-condensate used in the current study, as well as the Bololiubov transformations defining the ingoing and outgoing modes emerging as quantum fluctuations from the Bogoliubov linearization of the Gross-Pitaevskii equation.

The fourth chapter 4 and fifth chapter 5 presents the the specific research we conducted on quantum correlations 4 and back-reaction in an analog 1D BEC black hole 5. The fourth chapter 4, after providing an introduction to Bell's inequalities and Wigner function formalism, focuses on the study of the quantum correlations between the three outgoing modes of our system and characterizes the non-locality conditions for GKMR pseudospin measurements in our analog black hole configurations. The fifth chapter 5 derives the back-reaction equations describing the effect of Hawking radiation on the analog black hole metrics which generates it : some preliminary asymptotic results are provided.

The final chapter 6 considers the topological constraints on the quantum turbulence of a 2D fluid of exciton-polaritons. Such a fluid is described by a non-linear Schrödinger equation which is analog to the Gross-Pitaevskii equation of an atomic vapour BEC. The growth and decay of the number of vortices are found to be driven by topological constraints dictated by quantum number conservation laws.

1.2 . Introduction to Analog Gravity

From black holes to non-locality

The Lorentzian invariance of the speed of light in vacuum asserted by Einstein's Special Relativity (1905) constrained *causality* in the past and future light cones of an event. Einstein's theory of General Relativity (1915), reformulating Newtonian gravity as a geometric theory of gravitation, generalized the causal constraint to the Riemannian geometry of curved space-time [1, 2]. In 1916, Schwarzschild [3] found a solution to the non-linear field equations of Einstein's theory, defining the metric of a gravitational field generated on its outside by a a non-charged spherical mass distribution with null angular momentum : the *Schwarzschild metric*. If this mass distribution were to collapse to a radius r_m smaller than a critical

radius, the *Schwarzschield radius*, all the mass would end up in a finite time into the singularity $r = 0$ of the metric. As soon as $r_m < r_s$, the interior of the the sphere of radius r_s would become a *causally disconnected region* with respect to the exterior, no signal emitted in the interior being able to propagate outwards because of the gravity enforced tilting of the light cones [1]. The interior region is then called a *black hole*[2].

In 1935 Einstein, Podolsky and Rosen [4] published a paper questioning the definition of reality implied by quantum mechanics. In this paper, the existence of states appearing to give an inconsistent definition of reality was seen as a proof of the incompleteness of quantum mechanics. Soon after, Schrödinger [5] named such states *verschränkt* states, i.e. *entangled* states, while Bohr [6] argued quantum mechanics to be perfectly complete and consistent in its contextual definition of reality, the very existence of complementary (or conjugate) observables, that could not be both simultaneously measured with arbitrary precision, implying to define as *real* only what was actually measured. The *non-locality* of such entangled states, i.e. their exhibiting correlations that appeared to contradict the light-cone causality constraints of special relativity, was also seen by Bohr as consistent with a wave function formalism describing a composite system as an irreducible whole.

According to Einstein-Podolski and Rosen, in order for such correlations to be *local* and therefore congruent with special relativity, one should think at them as being in some way predetermined : but this is impossible when one does not know in advance which one of two non-commuting measurements, e.g. momentum and position, would be performed since these two measurements cannot have *simultaneous* reality and cannot therefore both be predetermined in advance. Then, appearing to violate *realism* and *locality*, quantum mechanics should be considered as incomplete[3]. In 1964 Bell [7] defined a mathematical constraint, known as *Bell's inequality*, through the violation of which non-locality and/or non-realism can be revealed [8]. Throughout the 70s and 80s, quantum mechanics was experimentally found to violate Bell-type inequalities for some entangled states and non-commuting measurements[4]. Thus, such and similar violations are signatures of fully quantum, i.e. highly non-classical, regimes. In the framework of the hydrodynamic analogs of black holes, where the full system can be measured, the non-locality of bipartite and tripartite correlations in the radiated waves can be investigated.

1970s : Quantum Field Theory in Curved Space-Time

At the end of the 60s, Parker showed how, through the Bogoliubov transformation formalism, the time-dependence of the metric in an expanding universe would yield particle creation out of the vacuum. In the first 70s Pennrose and Floyd predicted that energy could be extracted from a rotating black hole and Misner prooved that a rotating black hole could amplify incident waves, a phenomenon known as *superradiance* [9]. Also relying on Quantum Field Theory (QFT) in curved-space-time (CSP), Hawking demonstrated in 1974-75 the existence of a thermal radiation from the event horizon of a non-rotating black hole , the emission of such a radiation leading eventually to the total evaporation of the black-hole [10, 11]. This thermal radiation, generated by the time-dependence of the metric during the gravitation collapse forming the black hole, is predicted tohave a Planck spectrum emitted at a temperature T_H known as Hawking temperature and only determined by the mass, the angular momentum and the electric charge of the black hole.

These radiation phenomena such as superradiance and Hawking radiation all rely on stimulated or spontaneous particle emission processes through the existence of negative energy particles absorbed by the black-hole. In the Hawking process, each particle of the thermal emission is entangled with a negative energy particle falling in the black-hole. Similar to the Hawking effect is the Unruh effect (1976), according to which an accelerating observer sees a thermal radiation proportional to its acceleration [12].

[1] The reverse is not true : the causal disconnection between the two regions is asymmetric.

[2] The possibility of the existence of black holes, as massive objects generating gravitational fields with escape velocity higher than the speed of light, had already been considered in the 18th century by Laplace and Michell. The physics of black holes can nevertheless only be apprehended by the geodesic modeling of light ray trajectories as theorized by Einstein's General relativity.

[3] By *realism* we loosely refer to any theory that postulates the outcome of a measurement to be predetermined.

[4] See section 4.1 for a more detailed treatment of Bell's inequalities.

The temperature T_H of the Hawking thermal radiation should be for a black hole of solar mass, of order 10^{-8} K, which makes it imperceptible within a Cosmic Microwave Background (CMB) of order 3 K. Thus, since astrophysical observation is not nowdays within reach, other ways of testing such predictions had to be devised. It is in this perspective that one can resort to hydrodynamic experiments simulating these gravitational predictions.

1980s-2020s : Hydrodynamical models

Indeed, the domain of analog gravity aims at providing laboratory models for gaining insight on general relativity phenomena that cannot be directly observed in the usual gravitational context or for which there exists no complete theoretical framework. Two such phenomena are black hole superradiance [13, 14, 15] and Hawking radiation [10, 16]. In 1981, Unruh noticed that sound waves in a fluid behave like a massless scalar field propagating in a curved Lorentzian geometry [16]. His article gave birth to Analog Gravity. Indeed, noticing that the mathematical formalism for describing the propagation of a perturbation in a fluid can be presented in terms of a an effective curved space-time metric [17], transsonic flows can be thought of and implemented experimentally both for classical and quantum systems. Such inhomogeneous systems, where in a supersonic (subsonic) region the fluid flows at a speed higher (lower) than the speed of a sonic wave in the fluid at rest, can then mimic the Schwarzschild metric with light cones and light horizons becoming sound cones and sonic horizons respectively. We will then be facing an acoustic analog of a gravitational black hole.

Let us consider a fluid with a (in)homogeneous flow of speed $\mathbf{v}$ in the laboratory frame. In the reference frame where the fluid is locally at rest, the space-time interval is locally defined as

$$ds^2_{\text{resting}} = c_s^2 dt^2 - d\mathbf{x}^2 \tag{1.1}$$

whereas in the laboratory frame, i.e. in the reference frame where the fluid is flowing, the same interval is given

$$ds^2_{\text{flowing}} = c_s^2 dt^2 - (d\mathbf{x} - \mathbf{v}dt)^2 \tag{1.2}$$

for a Galilean transformation[5] [9], with therefore an effective metric

$$g_{\mu\nu} = \begin{pmatrix} \mathbf{c}^2 - \mathbf{v}^2 & \mathbf{v}^T \\ \mathbf{v} & \mathbb{1} \end{pmatrix} \tag{1.3}$$

with $\mathbf{v}^T$ the transposed of the column vector $\mathbf{v}$ and $\mathbb{1}$ a 3×3 identity matrix. Where the flow is locally supersonic, i.e. where $\mathbf{c}^2 - \mathbf{v}^2 < 0$, sound waves can no longer propagate against the local flow. It is then possible to induce flowing configurations with acoustic horizons that sound waves can only cross in one direction : one side of the horizon is then *causally disconnected* from the other with respect to sound cones, in the sense that no event of the supersonic side can influence the subsonic side.

The fluid must be considered at large length scales, where the system can be described in the hydrodynamic limit, i.e. by macroscopic hydrodynamical variables. In this limit, only low energy excitations, i.e. with large wave length, can be appropriately described. The simplest models that can be experimentally realized are one-dimensional flows of classical or quantum fluids[6]. As an example[7], event horizons have been implemented with surface waves [18, 19, 20, 21, 22, 23] and acoustic waves [24], nonlinear optical systems [25, 26, 27, 28], cavity polaritons [29, 30, 31] and Bose-Einstein condendates (BECs) of atomic vapors [32, 33, 34, 35]. Because of their low temperature and coherence properties BECs appear particularly well suited for demonstrating quantum features.

Furthermore, Unruh [16] noticed that the existence of an acoustic (optical) horizon implied the existence of an acoustic (optical) radiation analogous to Hawking radiation. However, even experimentally,

[5] We consider $v << c$ with c the speed of light. $x \to x - vt$.

[6] Quantum fluids are systems that show macroscopic quantum effects such as superfluidity. In such systems the de Broglie wave length must be greater than the averaged distance between particles. When this is so, the wave-like behavior of the particle can indeed no longer be ignored.

[7] See Ref. [9] for a brief review of other hydrodynamical models, such as the ones for particle creation in an expanding universe.

this radiation is extremely hard to be detected since it is "hidden" in the thermal noise of the system. For this reason, non-local methods of two-point density-correlation functions [36], robust with respect to the thermal noise of the fluid, have been considered to detect the correlation between the unique phonon propagating against the current (detected in the subsonic region) and the two phonons propagating with the current (detected in the supersonic region) [37] [38]. In Bose-Einstein condensates (BECs) a signal that could correspond to an analog Hawking radiation is claimed to have been detected in 2016, and more convincingly in 2019 (see Fig. 1.1), by Steinhauer in a fluid of ultra-cold rubidium atoms [33].

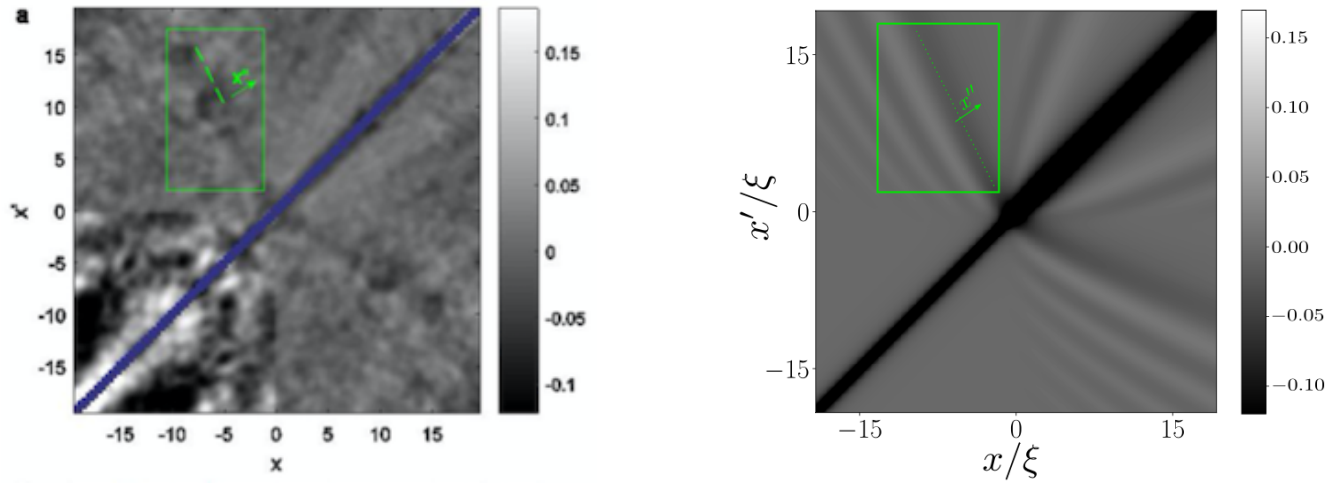

Figure 1.1: Two-point density-correlation function $G^{(2)}(x,x') = \langle : \hat{n}(x,t)\hat{n}(x',t) : \rangle - \langle \hat{n}(x,t) \rangle \langle \hat{n}(x',t) \rangle$. Left Plot : Experimental signature of Analog Hawking radiation (2019) [34]. Right Plot : Theoretical simulation of Analog Hawking radiation (2020) [39]. The condensate is flowing from the positive x or x' region to the negative x or x' region : the positive region is subsonic and the negative region is supersonic. The dotted lines in the two plots represent the line of correlation between an outgoing phonon in the exterior or subsonic region (positive x') and an outgoing phonon in the interior or supersonic region (negative x), with the acoustic horizon at $x, x' = 0$. The main diagonal $x = x'$ line just represents self-correlations induced by short-range two-body repulsion. The off-diagonal signal is not at 45 degrees since the two phonons propagate at two different effective speeds, approximately $V_u - c_u$ for the upstream phonon (Hawking phonon) and $V_d - c_d$ for downstream phonon (partner phonon) : the correlation in position is given by the ratio of these two effective speeds. A more detailed inspection of the figure reveals a third correlation line in the $x, x' > 0$ region, which relates to the existence of a third outgoing phonon in the interior or supersonic region propagates at approximately $V_d + c_d$. These speeds are computed taking the limit $\omega \to 0$ of the group velocity $d\omega/dQ$, with Q the wavevector, of the three branches of the dispersion relation that generate outgoing (with respect to the horizon) phonons. The ratios of thus computed speeds fit the experimental correlations lines since most of analog Hawking physics unfold in the long wavelength regime.

1.3 . Introduction to BECs

Theory and Experiments with BECs

Phase transitions to higher ordered states of matter are often symmetry-breaking processes. In the same manner as crystallisation breaks the translation symmetry of a homogeneous fluid, the Bose-Einstein condensate (BEC) phase transition is associated with the breaking of the U(1) symmetry of the global phase. In 3D the complex scalar order parameter describing the BEC can be identified to the macroscopic wavefunction of the condensate, associated to the off-diagonal long-range order in the one body-density matrix of the system [40].

The Bose-Einstein statistical distribution was defined in 1924 by Bose and Einstein as describing the mean number of non-interacting identical bosons occupying a same quantum state [41, 42]. At a sufficiently low temperature, a macroscopic fraction of bosons occupies the same quantum state of lower

energy, then generating a *macroscopic state of matter* called a *Bose-Einstein condensate*. The theory was later extended to systems of interacting bosons by Bogoliubov [43] and others.

The superfluidity of liquid helium was experimentally achieved in 1938 by Allen and Misener [44] and simultaneously by Kapitza [45]. Soon after, London established the connection between BECs and superfluidity [46]. In 1947, Bogoliubov modeled small excitations in a weakly interacting gas as phonons of the BEC and connected their dispersion relation to superfluidity [43]. Within the theoretical research on quantum vortices, superfluidity and liquid helium pioneered by Landau in 1941, Onsager in 1949 [47], Penrose in 1951 [48] and Feynman in 1955 [49], in 1961 the Gross-Pitaevskii equation was theorized by Gross and Pitaevskii [50, 51] for the description of weakly interacting systems [8].

It is nevertheless only in 1995 that the first BECs are experimentally realized in a gas of rubidium atoms by Cornell and Wieman [52][9], and in a gas of sodium atoms by Ketterle [53]. The BECs experiments in Analog Gravity [54, 33, 34] conducted in the last decade have to be framed in this tradition of theoretical and experimental knowledge [37].

2010s : Analog experiments in one-dimensional quasi-condensates

There is no true Bose-Einstein condensation at low dimension: thermal or quantum phase fluctuations prevent off-diagonal long range order in a 1D or 2D Bose system. At finite temperature this can be seen as resulting from Hohenberg-Mermin-Wagner theorem [55, 56], and at $T = 0$ from its generalization by Pitaevskii and Stringari [40]. Nevertheless, a 1D mean-field theory [57] can be applied as long as $d < \xi$, with d the average distance between particles and ξ the healing length of the system. In 1D, where the transverse motion is freezed, the zero temperature one-body density matrix behaves as

$$\langle \hat{\Psi}^\dagger(x)\hat{\Psi}(x')\rangle \propto \exp\left(-\frac{mc}{2\pi\hbar n_1}\ln\frac{r}{\xi}\right) \tag{1.4}$$

with $r = |x - x'|$, c the speed of sound and n_1 the linear density. In the above expression (1.4) a low energy approximation is made, relying on a hydrodynamic description valid only for distances r much greater than the healing length ξ and involving momenta up to $\hbar/\xi$. Expression (1.4) corresponds to a phase coherence length

$$\ell_\phi = \xi \exp\left[\pi\sqrt{n_1 a_\perp^2/2a}\right] \tag{1.5}$$

where a is the 3D s-wave scattering length and $a_\perp = \sqrt{\hbar/m\omega_\perp}$, $\omega_\perp$ being the angular frequency of the transverse trapping potential. It turns out that experimental conditions can be worked out such as to extend the long-range order to *macroscopic distances* [58]. Indeed, as long as quantum correlations are measured over distances which are smaller than the phase coherence length ℓ_ϕ one can still be, at zeroth order in the expansion of the field operator, in a *1D meanfield regime*[10]. Hence, for a quasi-1D guided BEC, the Bogoliubov approximation, i.e. the expansion of the field operator in a classical mean field term and a small quantum fluctuation term (see (3.3) in Chapter 3), is valid in the "1D mean field regime" [57] defined by

$$\left(\frac{a}{a_\perp}\right)^2 \ll n_{\rm typ}a \ll 1 \tag{1.6}$$

where $n_{\rm typ}$ is the typical linear density (number of atoms per unit length). The left inequality in (1.6) ensures that the phase coherence length ℓ_ϕ is exponentially large compared to the healing length, see. (1.5). The inequality at the right ensures that the transverse degrees of freedom are frozen [11]. For a

[8] In a weakly interacting system the scattering length characterizing the interactions is smaller than the average distance between particles.

[9] The signature of Bose-Einstein condensation was recognized in a narrow peak exhibiting "a nonthermal, anisotropic velocity distribution expected of the minimum-energy quantum state of the magnetic trap" over a broad isotropic thermal velocity distribution [52].

[10] Corrections to this leading order approximation will be considered in Chapter 5.

[11] Taking the kinetic energy per particle E_{kin} to be of the order of $\hbar^2 n_1^2/2m$ and the interaction energy per particle E_{int} to be of the order of $g_{1D}n_1 \sim 2a\hbar\omega_p erp$ and imposing and imposing $E_{int} \ll \hbar\omega_\perp$ and $E_{int} \ll E_{kin}$, one retrieves the relations given in (1.6).

transverse trap of frequency of 1 kHz, one gets $(a_\perp/a)^2 = 1.7 \times 10^{-5}$ and 2.6×10^{-4}, for ^{23}Na and ^{87}Rb, respectively. Hence the domain of validity of the 1D mean field approximation used in the present work typically ranges over four orders of magnitudes in density. In the regime where (1.6) holds, the background classical field Φ of expansion (3.3) is solution of a Gross-Pitaekskii equation which is the stationary and classical version of Eq. (3.2), where the non-linear interaction parameter g is defined as $g = 2\hbar\omega_\perp a$.

The experimental realization of an analog black hole by the Technion Group [34, 35] is close to what is here called the "waterfall" configuration (see Chapter 3). With this theoretical configuration, where the potential $U(x)$ is a step function and the upstream profile $\phi_u(x)$ is half that of a dark soliton, one can reproduce important aspects of the experimental density-correlation pattern reported in [34][12]. In the experiment, a trapped quasi 1D BEC[13] of 8000 ^{87}Rb atoms[14] is swept from right to left at constant velocity $0.18\,\mathrm{mm\,sec}^{-1}$ by a potential step created by a laser beam[15]. In the laser frame, the BEC is then flowing from right to left. The apparent velocity of the flow in the laser frame is, by current nv conservation, in the the upstream and downstream asymptotic regions $v_u \sim 0.2\,\mathrm{mm.s}^{-1}$ and $v_d \sim 0.9\,\mathrm{mm.s}^{-1}$ respectively. The upstream density and upstream speed of sound are of the order $n_u \sim 90\,\mu m^{-1}$ and $c_u \sim 0.5\mathrm{mm.s}^{-1}$ respectively, the downstream density and downstream speed of sound of $n_d \sim 20\,\mu m^{-1}$ and $c_d \sim 0.3\mathrm{mm.s}^{-1}$. The BEC is therefore subsonic upstream and supersonic downstream. Measurements are performed in a region of the order $100\mu\mathrm{m}$ and the measured analog Hawking temperature is of the order of $T_H \sim 0.35$ nK[16].

1.4 . Introduction to the topology of quantum vortices

In classical fluids the identification of topological critical points proves helpful for classifying flow patterns [59, 60] and studying two-dimensional spatio-temporal chaos and turbulence [61, 62, 63, 64, 65]. As they do in the classical context [66, 67, 68, 69, 70], vortices plays a major role in the route to two-dimensional quantum turbulence [71, 72, 73, 74, 75, 76, 77, 78, 79]. Indeed, in 2D quantum fluids, vortices are both topological singularities and the building blocks of turbulent scaling regimes. The quantization of vorticity was already understood in the 50's by Onsager, Feynman, Gross and Pitaevskii [47, 49, 50, 51] as part of a broader theoretical research on Bose-Einstein condensation, superfluidity and liquid helium. In the study presented in Chapter 6 we describe the onset and decay of 2D quantum turbulence through a temporal study of the number of critical points and show that a topologically constrained kinetic theory gives an excellent account of the experimental survey of the group of Dario Ballarini at Lecce Institute of Nanotechnology.

Indeed, we present here a new approach to two-dimensional quantum turbulence that incorporates key topological constraints previously overlooked in the field. While quantum turbulence is typically associated with the proliferation of quantum vortices, in two-dimensional systems, fundamental topological rules demand the involvement of additional critical points indentified by specific sets of *topological charges*, namely the vorticity index I_V and the Poincaré-Hopf index I_P. We enumerate these points in a compressible polariton superfluid and identify their elementary creation mechanisms. This allows us to develop a model that accurately captures the formation kinetics of vortices and of all the critical points. Our results highlight the crucial role of topological conservation laws in both the growth and decay of two-dimensional quantum turbulence.

[12] There are nonetheless some caveats, see [39] for a discussion.

[13] The condensate is trapped radialy by a laser beam of $3.6\mu m$ waist and 812 nm. "The radial trap frequency of 140 Hz is greater than the maximum interaction energy of 70 Hz, so the behavior is 1D" [33].

[14] In the state $F = 2$, $m_F = 2$.

[15] "The horizon is created by a very sharp potential step, achieved by short-wavelength laser light ($0.442\mu m$), and high resolution optics (NA 0.5)"[33]. In order to create the step potential the Gaussian beam is half blocked.

[16] The experimental temperature of the BEC is difficult to evaluate but the theoretical two-point density correlation function can fit the experimental data up to two times the Hawking temperature [39].

2 - MODELING BLACK HOLES WITH ANALOG SYSTEMS

In this section we will consider the mathematical formalism that justifies the analogy between gravitational systems and hydrodynamical flows. We intend to show how the evolution of a perturbation in a fluid can be modeled mathematically in terms of propagation in an effective curved space-time metric. To this end, we will start from Einstein equations and recall their expression in vacuum in order to define from them the Schwarzschild metric. The Klein-Gordon equation for a massless scalar field in a Schwarzschild curved space-time will then be mapped to the evolution of a sonic wave in a fluid in order to justify the hydrodynamical analogy in classical and quantum fluids. Then, Hawking radiation will be derived in the gravitational framework by considering the simplest case of a collapsing mass distribution, i.e. the Vaidya metric. Finally the expression of the the analog Hawking radiation in hydrodynamical systems will also be derived, thus completing the analogy.

2.1 . THE SCHWARZSCHILD BLACK HOLE

2.1.1 . From Einstein Equations to Schwarzschild Black Hole

Einstein equations [1, 2] are given by the tensorial equations[1]

$$R_{\mu\nu} - \frac{1}{2} R\, g_{\mu\nu} = \frac{8\pi G}{c^4} T_{\mu\nu} \tag{2.1}$$

where $R_{\mu\nu}$ is the Ricci tensor, $R = g^{\mu\nu} R_{\mu\nu}$ the scalar curvature, $g_{\mu\nu}$ the metric tensor, G Newton's gravitational constant, c the speed of light in vacuum and $T_{\mu\nu}$ the energy-momentum tensor[2]. Greek indices refer to the four components of the position four-vector. On the left hand side, the Ricci tensor is given by

$$R_{\mu\nu} = R^{\rho}{}_{\mu\rho\nu} = \partial_\rho \Gamma^{\rho}{}_{\mu\nu} - \partial_\mu \Gamma^{\rho}{}_{\mu\rho} + \Gamma^{\rho}{}_{\mu\nu} \Gamma^{\sigma}{}_{\rho\sigma} - \Gamma^{\rho}{}_{\mu\sigma} \Gamma^{\sigma}{}_{\nu\rho} \tag{2.2}$$

where $R^{\rho}{}_{\mu\rho\nu} = g^{\sigma\rho} R_{\sigma\mu\rho\nu}$ is the Riemann curvature tensor, with the Christoffel symbols given by

$$\Gamma^{\mu}{}_{\nu\rho} = \frac{1}{2} g^{\mu\sigma} (\partial_\nu g_{\sigma\rho} + \partial_\rho g_{\sigma\nu} - \partial_\sigma g_{\nu\rho}) \tag{2.3}$$

This means that the left hand side of (2.1) is only a function of the metric tensor $g^{\mu\nu}$ and of its first and second derivatives. Contracting (2.1) with $g^{\mu\nu}$ one gets

$$R = -\frac{8\pi G}{c^4} T$$

with $T = g^{\mu\nu} T_{\mu\nu}$. Replacing this expression of R in (2.1) one gets another covariant expression of the same Einstein equations (2.1), i.e.

$$R_{\mu\nu} = \frac{8\pi G}{c^4} \left(T_{\mu\nu} - \frac{1}{2} g_{\mu\nu} T \right) \tag{2.4}$$

For a non-rotating electrically-neutral macroscopic matter distribution of total mass M considered as punctual and fixed at the origin, all the components of the energy-momentum tensor are zero for any $\mathbf{x}(t) \neq \mathbf{0}$, which means that in vacuum Einstein equations reduce to

$$R_{\mu\nu} = 0 \tag{2.5}$$

Then, for our mass distribution, it can be shown after some algebra[3] that the most general spherically symmetric vacuum (i.e. outside the mass) solution of the Einstein field equations (2.5) is the metric tensor

[1] We neglect here the term $+\Lambda g_{\mu\nu}$, with Λ the cosmological constant, that should also appear on the left-hand-side of equation (2.1).

[2] In General Relativity the tensors $g_{\mu\nu}$, $R_{\mu\nu}$ and $T_{\mu\nu}$ are all symmetric, which means that for any tensor $X_{\mu\nu}$ of order 2 one has $X_{\mu\nu} = X_{\nu\mu}$.

[3] For example, see Refs. [[1], [2]]. The computation is performed knowing that :(1) in General Relativity, the choice of coordinates system is arbitrary ; (2) in the limit cases where there is no mass ($M \to 0$) or when we are far from it ($r \to \infty$) one must retrieve the Minkowski space-time with signature $(+ - - -)$; (3) the different components $g_{\mu\nu}$ of the metric tensor must of course verify Einstein equations in vacuum (2.5); (4) the limit of weak field must be compatible with Newton's potential $\phi = -MG/r$ with M the global mass of the punctual body.

$g_{\mu\nu}$ defining, in spherical coordinates, the interval $ds^2 = g_{\mu\nu}dx^\mu dx^\nu$ as

$$\begin{aligned} ds^2 &= \left(1 - \frac{r_s}{r}\right) c^2 dt^2 - \frac{1}{1 - \frac{r_s}{r}} dr^2 - r^2 d\Omega^2 \\ d\Omega^2 &= \sin^2(\theta) d\phi^2 + d\theta^2 \\ r_s &= \frac{2MG}{c^2} \end{aligned} \tag{2.6}$$

where r_s is the Schwarzschild radius or gravitational radius. This metric is called the *Schwarzschild metric*. It is immediately seen that for $r_s = 0$ this metric reduces to the pseudo-euclidian metric, i.e. to Minkowski space-time. On the contrary, when $r_s \neq 0$ this metric has two singularities : one in $r = 0$ and the other in $r = r_s$. Furthermore, if $r > r_s$ the signature (i.e. the sign of the $g_{\mu\mu}$) of the metric is $(+---)$ whereas if $r < r_s$ the signature is $(-+++)$. Therefore r_s constitutes an *horizon* that distinguishes two regions of space-time : in one ($r > r_s$) the variable t if of type *time* and the variable r of type *space* whereas in the other ($r < r_s$) it is the other way around with t of type *space* and r of type *time*.

Of the two singularities, the one at $r = r_s$ is unphysical, i.e. it is only related to the choice of the coordinate system. Defining

$$c d\bar{t} = c dt + \frac{\sqrt{r_s/r}}{1 - \frac{r_s}{r}} dr \tag{2.7}$$

the metric (2.6) can be expressed in the so-called *Painlevé-Gullstrand* coordinates

$$ds^2 = \left(1 - \frac{r_s}{r}\right) c^2 d\bar{t}^2 - 2\sqrt{\frac{r_s}{r}} c\, d\bar{t}\, dr - dr^2 - r^2 d\Omega^2 \tag{2.8}$$

where it can be seen that the singularity at $r = r_s$ has disappeared and the only singularity left is the one at the origin.

The Schwarzschild observer is a far observer. The Painlevé-Gullstrand observer is a free-falling observer. By definition for the propagation of a light beam one has $ds^2 = 0$, which implies that a radial null geodesic, i.e. $ds^2 = 0$ for $d\Omega = 0$ (purely radial trajectory), is described in our two reference frames as[4]

$$c\frac{dt}{dr} = \pm\frac{1}{1 - \frac{r_s}{r}} \qquad c\frac{d\bar{t}}{dr} = \frac{1}{\pm 1 - \sqrt{\frac{r_s}{r}}} \tag{2.9}$$

As expected when $r \to \infty$ the light-cones are just the 45 degrees slopes of the Minkowski space-time. But, according the Schwarzschild observer, as one comes closer to r_s then the slopes get steeper with the cone merging in a vertical line at r_s. This means that an observer located in the Minkowski-like region of the metric, i.e. at $R_{obs} \gg r_s$, will never see ingoing rays crossing r_s because of the *infinite gravitational red-shift* exhibited by any light ray leaving the Schwarzschild gravitational field. Indeed in this reference frame, one can define a local proper time at the r_i position as

$$d\tau_i = \sqrt{1 - \frac{r_s}{r_i}} dt \tag{2.10}$$

with t the proper time at infinity, and then the ratio of the frequencies ν_a and ν_b (measured in their respective proper times) of an outgoing light ray emitted at r_a and propagating to r_b, with $r_s < r_a < r_b$, will be given by

$$\frac{\nu_b}{\nu_a} = \frac{d\tau_a}{d\tau_b} = \frac{\sqrt{1 - \frac{r_s}{r_a}}}{\sqrt{1 - \frac{r_s}{r_b}}} < 1 \tag{2.11}$$

since $r_a < r_b$. For $r_a = r_s$, the ratio (2.11) goes to zero and the red-shift is infinite.

[4]The given expressions are obtained just by solving $ds^2 = 0$ as a second order equation for dt/dr and $d\bar{t}/dr$ respectively .

According to the Painlevé-Gullstrand observer, which can be taken, contrary to the Schwarzschild observer, as a local observer at r_s, we see from (2.9) that an ingoing light ray can freely pass (inwards) through r_s but no outgoing ray emitted at $r < r_s$ can pass (outwards) through r_s. We will therefore say that a neutral non-rotating spherical mass distribution whose total mass M concentrates in a sphere of radius lower than the Schwarzschild radius r_s generates a stationary black hole that is named a *Schwarzschild Black Hole*, with the Schwarzschild radius r_s being the *event horizon* of the Schwarzschild black-hole[5]. Then the mass of the body collapses to the origin in what is called a *gravitational singularity*. The name *black hole* refers to the fact that there is no way out once any massive or massless particle penetrates the region $r < r_s$. A non-rotating neutral black-hole is completely determined by its mass.

Finally, the surface gravity κ [80], which has the dimension of an acceleration, is computed by evaluating at r_s the variation of $dr/d\bar{t}$ with respect to r for a null radial geodesic

$$\kappa = \left(c \frac{d}{dr} \frac{dr}{d\bar{t}} \right)_{r=r_s} = \frac{c^2}{2\, r_s} \tag{2.12}$$

We will see that the Hawking temperature T_H of the Hawking radiation is proportional to the surface gravity κ of the black hole.

2.1.2 . Klein-Gordon equation in curved space-time

We are interested in the propagation of a massless scalar field in the Schwarzschild space-time. The dynamics of such a field is obtained through the Klein-Gordon equation. This equation is simply obtained by promoting to quantum operators the terms $E \to i\hbar\partial_t$ and $p \to -i\hbar\nabla$ in the Einstein's relation $E^2 = (mc^2)^2 + (pc)^2$. For a massless scalar field $\psi(t, \mathbf{r})$ one obtains

$$\left[\frac{1}{c^2} \partial_t^2 - \Delta \right] \psi = 0 \tag{2.13}$$

where $\frac{1}{c^2}\partial_t^2 - \Delta$ is the d'Alembert operator. Using $\eta^{\mu\nu} = \mathrm{diag}(+1, -1, -1, -1)$ and $x^\mu = (ct, \mathbf{x})$, this relation can be rewritten as

$$\eta^{\mu\nu} \partial_\mu \partial_\nu \psi = 0 \Rightarrow \partial_\mu \partial^\mu \psi = 0$$

which corresponds to a dynamics determined by a pseudo-euclidian metric. In curved space-time the partial derivatives ∂_μ have to be promoted to *covariant derivates* ∇_μ defined as

$$\nabla_\mu A^\nu = \partial_\mu A^\nu + \Gamma^\nu_{\rho\mu} A^\rho \tag{2.14}$$

with A^μ a contravariant four-vector. When $\nu = \mu$, one can show [1] that

$$\nabla_\mu A^\mu = \frac{1}{\sqrt{-g}} \partial_\mu \left(\sqrt{-g} A^\mu \right) \tag{2.15}$$

with g the (negative) determinant of the metric tensor $g_{\mu\nu}$. Knowing that $\nabla^\mu = g^{\mu\nu}\nabla_\nu$ and $\nabla_\nu \psi = \partial_\nu \psi$ for ψ a scalar, one gets $\nabla^\mu \psi = g^{\mu\nu}\nabla_\nu \psi = g^{\mu\nu}\partial_\nu \psi$. But $\nabla^\mu \psi$ is a contravariant four-vector just as A^μ. Hence, substituting A^μ in the last relation by our expression of $\nabla^\mu \psi$, one obtains eventually the d'Alembert operator in curved space-time

$$\nabla_\mu \nabla^\mu \psi = \frac{1}{\sqrt{-g}} \partial_\mu \left(\sqrt{-g} g^{\mu\nu} \partial_\nu \psi \right) \tag{2.16}$$

With the d'Alembert operator so defined, the Klein-Gordon equation for a massless scalar field in curved space-time reads

$$\nabla_\mu \nabla^\mu \psi = 0 \tag{2.17}$$

[5] Let us recall that the Schwarzschild metric is valid for describing the vacuum around any neutral non-rotating spherical mass distribution. The radius of this mass distribution does not have to be smaller than r_s. If it does, the mass distribution collapses to the $r = 0$ singularity of the metric, thus generating a black-hole.

2.2 . ACOUSTIC ANALOGS OF SCHWARZSCHILD METRIC

Now that we have our dynamic equation for a scalar field in curved space-time and that we can implement this equation with the Schwarzschild metric, we are going to see how a sonic perturbation in a fluid can indeed be modeled by such a formalism. We will then quickly see how BECs dynamics can fit in this hydrodynamical approach.

2.2.1 . Fluid equations and acoustic approximation

As already said, Unruh [16] noticed that a sonic wave in a fluid behaves as a massless scalar field in curved-space time. Therefore, taking $g_{\mu\nu}$ to be the Schwarzschild metric generating a curved space-time close to a black hole horizon, we can use (2.17) to study the behavior of a massless scalar field ψ near the horizon. Furthermore, if one considers a flow where there is a subsonic region and a supersonic region, the sonic waves will propagate in an *effective curved space-time* with the supersonic region being the acoustic analog (i.e. a dumb hole) of a gravitational black hole [37]. Likewise the immaterial frontier between subsonic and supersonic flow will be an acoustic analog of the *event horizon* of a gravitational black hole.

Knowing that a sonic wave is a massless scalar field, for a non-relativistic non-viscous barotropic[6] fluid, the dynamics is described by equations

$$\partial_t \rho + \nabla \cdot (\rho \mathbf{v}) = 0 \tag{2.18}$$

$$\partial_t \mathbf{v} + (\mathbf{v} \cdot \nabla)\mathbf{v} = -\frac{1}{\rho}\nabla p \tag{2.19}$$

$$p = p(\rho) \tag{2.20}$$

where $\rho(t, \mathbf{r})$ is the density of the fluid, $\mathbf{v}(t, \mathbf{r})$ its speed and $p(t, \mathbf{r})$ the pressure field. The first equation (2.18) is the equation for mass conservation, the second one (2.19) is the Euler equation whereas the third one (2.20) allows for closing the system by defining the pressure p as an increasing function of the density ρ. One wants also the fluid to have null vorticity, which means that for every t, one must have $\nabla \wedge \mathbf{v} = 0$. This last expression allows to set $\mathbf{v} = \nabla\psi$ with $\psi(t, \mathbf{r})$ a scalar field that can be identified with the velocity potential [37].

We can now resort to perturbation theory in order to model the propagation of small fluctuations in a fluid. For (ψ_0, ρ_0, p_0) an exact solution of previous equations (2.18), (2.19) and (2.20), we look for a general solution (ψ, ρ, p) at first order of the form

$$\begin{pmatrix} \psi(t,\mathbf{r}) \\ \rho(t,\mathbf{r}) \\ p(t,\mathbf{r}) \end{pmatrix} = \begin{pmatrix} \psi_0(t,\mathbf{r}) \\ \rho_0(t,\mathbf{r}) \\ p_0(t,\mathbf{r}) \end{pmatrix} + \varepsilon \begin{pmatrix} \psi_1(t,\mathbf{r}) \\ \rho_1(t,\mathbf{r}) \\ p_1(t,\mathbf{r}) \end{pmatrix} \tag{2.21}$$

with (ψ_1, ρ_1, p_1) the perturbation and ε a small dimensionless parameter. We then linearizes the fluid equations [37]. After some algebra, setting $dp(\rho_0)/d\rho = c^2(\rho_0) = c^2$ with c the sound speed in the moving fluid frame, one obtains, without loss of information, a unique partial differential equation of second order

$$\partial_t \left(\frac{\rho_0}{c^2}(\partial_t\psi_1 + \nabla\psi_0 \cdot \nabla\psi_1) \right) = \nabla \cdot \left(\rho_0 \nabla(\psi_1) - \frac{\rho_0}{c^2}(\partial_t\psi_1 + \nabla\psi_0 \cdot \nabla\psi_1)\nabla(\psi_0) \right) \tag{2.22}$$

The resolution of (2.22) for ψ_1 allows then to find ρ_1 and p_1. One can also notice that for a non flowing fluid, i.e. for $\nabla\psi_0 = 0$, the relation (2.22) reduces to

$$\left(\frac{1}{c^2}\partial_t^2 + \Delta \right) \psi_1 = 0$$

which is, as expected, the Klein-Gordon equation in flat space-time for a massless scalar field, i.e. here the d'Alembert equation for the velocity potential of an acoustic perturbation propagating at speed c in a static medium.

[6] In a barotropic fluid the lines of equal pressure (isobar) are parallel to the lines of equal density (isopycnal).

2.2.2 . Sonic wave in a fluid as a massless scalar field in curved space-time

In order to demonstrate (see Refs. [37] and [17]) that the propagation of sonic waves in a fluid is analogous to the dynamics of massless scalar fields in curved space-time, we will denote the temporal index t as 0 and the spatial indices as i or j and will use Einstein's convention for sommation over repeated indices. Relation (2.22) thus becomes

$$\partial_0\left(\frac{\rho_0}{c^2}\partial_0\psi_1\right)+\partial_0\left(\frac{\rho_0}{c^2}\partial^j(\psi_0)\partial_j(\psi_1)\right)+\partial_i\left(\frac{\rho_0}{c^2}\partial^i(\psi_0)\partial_0\psi_1\right)+\partial_i\left(\frac{\rho_0\partial^j(\psi_0)\partial^i(\psi_0)-\rho_0c^2\delta^{ji}}{c^2}\partial_j(\psi_1)\right)=0$$

We can then compare this last relation to

$$\partial_0\left(\sqrt{-g}g^{00}\partial_0\psi_1\right)+\partial_0\left(\sqrt{-g}g^{0j}\partial_j(\psi_1)\right)+\partial_i\left(\sqrt{-g}g^{i0}\partial_0\psi_1\right)+\partial_i\left(\sqrt{-g}g^{ij}\partial_j(\psi_1)\right)=0 \tag{2.23}$$

which is nothing else but $\nabla_\mu\nabla^\mu\psi_1=\frac{1}{\sqrt{-g}}\partial_\mu\left(\sqrt{-g}g^{\mu\nu}\partial_\nu\psi_1\right)=0$ with $\nabla_\mu\nabla^\mu$ the d'Alembert operator in curved space-time (2.16) and g the determinant of the matrix $g_{\mu\nu}$. Consequently, a term-to-term identification between our two relations allows for determining the 4×4 matrix $g_{\mu\nu}$ as

$$g_{\mu\nu}=\frac{\rho_0}{c}\begin{pmatrix}\left(c^2-\mathbf{V}^2\right) & V_j\\ V_i & -\delta_{ij}\end{pmatrix} \tag{2.24}$$

where $\mathbf{V}=\nabla\psi_0$ and $V^i=\partial^i\psi_0$. One immediately recognizes the metric of curved space-time with signature $(+---)$ expressed in cartesian coordinates. Then, for a speed $\mathbf{V}$ purely radial, i.e. for $V_\theta=0$ and $V_\phi=0$, one sees that the metric has same shape as the gravitational Painlevé-Gullstrand metric (2.8), since it generates an interval of the form

$$ds^2=\frac{\rho_0}{c}\left[\left(c^2-{V_r}^2\right)d\bar{t}^2-2V_rd\bar{t}dr-dr^2-r^2d\Omega^2\right] \tag{2.25}$$

The choice of coordinates being arbitrary, one can modify the time origin by setting

$$dt=d\bar{t}-\frac{V_r}{c^2-V_r^2}dr \tag{2.26}$$

One then recovers an interval analogous to the Schwarzschild interval (2.6)

$$ds^2=\frac{\rho_0}{c}\left[\left(1-\left(\frac{V_r}{c}\right)^2\right)c^2dt^2-\frac{1}{1-\left(\frac{V_r}{c}\right)^2}dr^2-r^2d\Omega^2\right] \tag{2.27}$$

Indeed, ρ_0/c being only a multiplying factor, one can see that here $1-\left(V_r/c\right)^2$ plays the role of $1-(r_s/r)$ in (2.6), with V_r the speed of a radial transsonic flow [16]. Close enough to the horizon, i.e. at zero order, $\rho_0(r)$ can be considered as a constant ϱ, and since c is a function of $\rho_0(r)$, it will be constant too. One could therefore manipulated the metric (2.27) without worrying about the constant multiplying factor. Finally, for a one-dimensional flow along the x axis and towards positive x, our analog Schwarzschild metric reduces to

$$g_{\mu\nu}=\frac{\varrho}{c}\begin{pmatrix}\left(c^2-V^2\right) & 0\\ 0 & -\frac{1}{1-\left(\frac{V}{c}\right)^2}\end{pmatrix} \tag{2.28}$$

which, in Painlevé-Gullstrand coordinates, corresponds to

$$g_{\mu\nu}=\frac{\varrho}{c}\begin{pmatrix}\left(c^2-V^2\right) & -V\\ -V & -1\end{pmatrix} \tag{2.29}$$

2.2.3 . Gross-Pitaevskii equation and curved space-time

In this work, we will be interested in a one-dimensional quasi-condensate, whose dynamics is described by the time-dependent Gross-Pitaevskii equation for the field operator $\hat{\Psi}(x,t)$ of an indistiguishable bosonic many-particle system :

$$i\hbar\partial_t\hat{\Psi}=-\frac{\hbar^2}{2m}\partial_x^2\hat{\Psi}+[U(x)+g_0\hat{n}]\hat{\Psi} \tag{2.30}$$

with $U(x)$ an external potential, g_0 a coupling constant[7] and $\hat{n} = \Psi^\dagger\Psi$. In the *classical mean-field approximation* of our field operator one can set

$$\hat{\Psi}(x,t) \to \psi_0(x,t) = \sqrt{\rho(x,t)}e^{i\theta(x,t)} \tag{2.31}$$

using the density-phase representation of the complex mean-field. It is then easily shown that this equation can be recast in such a way as to describe the propagation of a real massless scalar field in an curved effective metric modeling the curvature of a space-time gravitational metric [81]. Indeed, in the density-phase representation, the previous time-dependent Gross-Pitaevskii equation reduces to the continuity equation and Euler equation of hydrodynamics for an irrotational inviscid fluid

$$\begin{aligned} \partial_t\rho + \partial_x\rho v &= 0 \\ \hbar\partial_t\theta = -\tfrac{\hbar^2}{2m}(\partial_x\theta)^2 - \tfrac{\hbar^2}{2m}\tfrac{\partial_x^2\sqrt{\rho}}{\sqrt{\rho}} &- g\rho - U(x) \end{aligned} \tag{2.32}$$

where $v = \frac{\hbar}{m}\partial_x\theta$ and where the second term on the right hand side represents a "quantum pressure". Taking into account small first-order fluctuations ρ_1 and θ_1 around the mean-field defined by ρ_0 and θ_0, i.e.

$$\begin{aligned} \rho(x,t) &\to \rho_0(x,t) + \rho_1(x,t) \\ \theta(x,t) &\to \theta_0(x,t) + \theta_1(x,t) \end{aligned} \tag{2.33}$$

the density-phase Gross-Pitaevskii equations (2.32) can be expanded at first order. When the system is considered at scales much larger than the healing length ξ[8], i.e. in the hydrodynamic approximation, after some algebra (see [81]), an equation for the scalar field θ_1, representing the dynamics of the condensate phase fluctuations, is obtained. This dynamics is given by a curved space-time equation

$$\frac{1}{\sqrt{-g}}\partial_\mu\left(\sqrt{-g}g^{\mu\nu}\partial_\nu\theta_1\right) = 0 \tag{2.34}$$

with

$$g_{\mu\nu} = \frac{\rho_0}{mc_0}\begin{pmatrix} \left(c_0^2 - {v_0}^2\right) & -v_0 \\ -v_0 & -1 \end{pmatrix} \tag{2.35}$$

which is nothing else but our analog Schwarzschild metric in Painlevé-Gullstrand coordinates (2.29), parametrized by the zeroth-order mean-field density ρ_0 and velocity v_0 (given by $v_0 = (\hbar/m)\partial_x\theta_0$ where θ_0 is the velocity potential) of the condensate, with c_0 (given by $mc_0^2 = g_0\rho_0$) the speed of sound in the condensate. Hence, the Gross-Pitaevskii equation can be transposed in the curved space-time formalism in order to study the dynamics of a scalar field evolving in an effective metric. The sign of $c_0^2 - v_0^2$ changes from $+1$ to -1 when the system is brought from a subsonic regime to a supersonic regime respectively. One will have an acoustic horizon at $c_0 = v_0$ and the system will be referred to as an *acoustic black-hole*.

2.3 . HAWKING RADIATION

2.3.1 . Klein-Gordon inner product

The Klein-Gordon inner product in curved space-time is defined as :

$$(f_1, f_2) = -i\int_\Sigma d\Sigma^\mu(f_1\partial_\mu f_2^* - f_2^*\partial_\mu f_1) \tag{2.36}$$

[7] In the Gross-Pitaevskii equation the coupling constant is usually referred to simply as g. We named it here g_0 in order to avoid confusion with the determinant of the metric tensor that we already referred to as g.

[8] The healing length ξ of the system can be defined either as : (1) the typical length-scale over which, for a trapped condensate, the uniform density in the bulk of the system varies in order to vanish at the confining borders ; (2) the wavelength at which the dispersion relation of the excitations of the system goes from a linear regime (collective excitations) to a quadratic regime in the wavevector (quasi-particle regime) [58].

with Σ a Cauchy hyper-surface, i.e. a hyper-surface of constant time, and $d\Sigma^\mu = d\Sigma n^\mu$ the volume element where n^μ is a future directed unit normal vector to Σ. In Minkowski flat spacetime the Klein-Gordon inner product reduces to[9]

$$(f_1, f_2) = -i \int d^3x (f_1 \partial_t f_2^* - f_2^* \partial_t f_1) \tag{2.37}$$

It has been proven, using Gauss's theorem, that the Klein-Gordon inner product is independent of the chosen Cauchy hyper-surface [82]. Defining a positive energy function as

$$f_\omega = \frac{e^{-i\omega t}}{2\pi r\sqrt{2\omega c}} e^{\pm ikr} \tag{2.38}$$

with $\omega = ck$ and c the speed of light, one obtains straightforwardly in Minkowski spacetime

$$\begin{array}{rcl} (f_\omega, f_{\omega'}) & = & \delta(\omega - \omega') \\ (f_\omega, f^*_{\omega'}) & = & 0 \\ (f^*_\omega, f^*_{\omega'}) & = & -\delta(\omega - \omega') \end{array} \tag{2.39}$$

for ω and ω' two positive energies. Then $\{f_\omega, f^*_\omega\}$ constitutes (see section 2.3.5) a complete orthonormal basis for the space of positive/negative energy/norm solutions of the flat spacetime Klein-Gordon equation (2.17).

2.3.2 . Bogoliubov transformation and Hawking radiation

In a curved spacetime, contrary to the flat Minkowski spacetime, there is no natural splitting of modes between positive and negative frequency solutions : different choices may lead uppon quantization to different vacua [82]. Consequently, there is no clear way to formalise a definite particle state. However, when the spacetime is asymptotically stationary one can define a natural notion of positive frequency mode in the asymptotic regions. For ξ^μ a timelike vector field, a natural notion of **positive frequency modes** u_i is given by

$$\xi^\mu \nabla_\mu u_j = -i\omega_j u_j \tag{2.40}$$

with $w_j > 0$ [82]. In Minkowski spacetime the *Killing time* t obeys $\xi^\mu \nabla_\mu t = 1$ for $\xi^0 = \partial_t$. Then one can define a positive frequency mode $u_j \propto \exp -i\omega_j t$, with (2.40) reducing to

$$\frac{\partial}{\partial t} u_j = -i\omega_j u_j \tag{2.41}$$

Hence, in his 1974 paper *Black hole explosions ?* [10], Hawking considers, "in an asymptotically flat space time containing a star which collapses to produce a black hole", a massless Hermitian scalar field $\hat{\phi}$ obeying the Klein-Gordon equation in curved spacetime 2.17 and given by

$$\hat{\phi} = \sum_i [f_i \hat{a}_i + f_i^* \hat{a}_i^\dagger] \tag{2.42}$$

with $\hat{a}_i$ and $\hat{a}_i^\dagger$ being respectively the annihilation and creation operator for incoming scalar particles and f_i complex functions of space $\vec{x}$ and time t for a given positive energy ω_i[10], with f_i^* the complex conjugate of f_i. The *initial vacuum state* is defined as the state containing no incoming particles, that is to say, for all i,

$$\hat{a}_i \left|0_{in}\right\rangle = 0 \tag{2.43}$$

The f_i are a complete orthonormal family of complex valued solutions of the wave equation (2.17). On past null infinity $\mathcal{I}^-$, i.e. in $u = ct - r = -\infty$ for the black-hole singularity located in $r = 0$, $\mathcal{I}^-$ these f_i are asymptotically *in-going* and *positive* frequency, which means that at $\mathcal{I}^-$ they contain only positive frequencies.

[9] Just by taking $n^\mu = (1, 0, 0, 0)$, one is left with $d\Sigma^0 = dxdydz$.

[10] Here, as in Hawking's paper [10], the energy space is discretized but one can easily take $\sum_i \to \int d\omega$ without modifying the reasoning.

One can also express $\hat{\phi}$ in terms of outgoing waves p_i and waves q_i crossing the event horizon

$$\hat{\phi} = \sum_i [p_i \hat{b}_i + p_i^* \hat{b}_i^\dagger + q_i \hat{c}_i + q_i^* \hat{c}_i^\dagger] \tag{2.44}$$

The p_i are solutions of the wave equation (2.17) which are zero on the event horizon and are asymptotically outgoing, positive frequency waves, i.e. positive frequency on future null infinity $\mathcal{I}^+$, i.e. in $v = ct + r = +\infty$ The q_i are solutions of the same wave equation which contain no outgoing component, i.e. they are zero on future null infinity $\mathcal{I}^+$. It is of course possible to write the p_i and the q_i as linear combinations of the f_i and f_i^*, that is to say as

$$\begin{aligned} p_i &= \sum_j \alpha_{ij} f_j + \beta_{ij} f_j^* \\ q_i &= \sum_j \gamma_{ij} f_j + \eta_{ij} f_j^* \end{aligned} \tag{2.45}$$

Then, in the Hawking effect, the **time dependence of the metric during the collapse** will cause a certain amount of **mixing of positive and negative frequencies**, which means that the β_{ij} and η_{ij} will *not* be zero. Equating the *ingoing* and *outgoing* definitions of $\hat{\phi}$, i.e. writing

$$\hat{\phi} = \sum_i [f_i \hat{a}_i + f_i^* \hat{a}_i^\dagger] = \sum_i [p_i \hat{b}_i + p_i^* \hat{b}_i^\dagger + q_i \hat{c}_i + q_i^* \hat{c}_i^\dagger] \tag{2.46}$$

one finds, by simply rearranging the terms of this last relation, that

$$\begin{aligned} \hat{a}_j &= \sum_i \alpha_{ij} \hat{b}_i + \beta_{ij}^* \hat{b}_i^\dagger + \gamma_{ij} \hat{c}_i + \eta_{ij}^* \hat{c}_i^\dagger \\ \hat{a}_j^\dagger &= \sum_i \beta_{ij} \hat{b}_i + \alpha_{ij}^* \hat{b}_i^\dagger + \eta_{ij} \hat{c}_i + \gamma_{ij}^* \hat{c}_i^\dagger \end{aligned} \tag{2.47}$$

This last expression is a Bogoliubov transformation. Then one has

$$\sum_j [\alpha_{hj}^* \hat{a}_j - \beta_{hj}^* \hat{a}_j^\dagger] = \hat{b}_h \tag{2.48}$$

as long as

$$\begin{aligned} \textstyle\sum_j \alpha_{hj}^* \alpha_{ij} - \beta_{hj}^* \beta_{ij} = \delta_{ih} \qquad & \textstyle\sum_j \alpha_{hj}^* \beta_{ij}^* - \beta_{hj}^* \alpha_{ij}^* = 0 \\ \textstyle\sum_j \alpha_{hj}^* \gamma_{ij} - \beta_{hj}^* \eta_{ij} = 0 \qquad & \textstyle\sum_j \alpha_{hj}^* \eta_{ij}^* - \beta_{hj}^* \gamma_{ij}^* = 0 \end{aligned} \tag{2.49}$$

The definitions of $\hat{b}_h^\dagger$, $\hat{c}_h$ and $\hat{c}_h^\dagger$ are obtained in a similar way. Now, *if there are no incoming particles*, i.e. if the initial state is $|0_{in}\rangle$, one has by definition

$$\langle 0_{in}| \hat{a}_i^\dagger \hat{a}_i |0_{in}\rangle = 0 \tag{2.50}$$

But one can see that in $\hat{b}_i^\dagger \hat{b}_i$ a term (summed over h and j) in $\hat{a}_j \hat{a}_h^\dagger$ appears. Since this term is nothing but $\hat{a}_j^\dagger \hat{a}_h + \delta_{jh}$, taking the average of $\hat{b}_i^\dagger \hat{b}_i$ on the same initial state $|0_{in}\rangle$ one is left with

$$\langle 0_{in}| \hat{b}_i^\dagger \hat{b}_i |0_{in}\rangle = \sum_{jh} \delta_{hj} \beta_{ij} \beta_{ih}^* = \sum_j \beta_{ij} \beta_{ij}^* = \sum_j |\beta_{ij}|^2 \tag{2.51}$$

Therefore if $\beta_{ij} \neq 0$ the vacua of $\hat{a}_i$ and $\hat{b}_i$ are not the same : there is particle creation, i.e. presence of outgoing particles without ingoing particles. In order to compute the β_{ij}, one must consider the Klein-Gordon inner product (p_i, f_j^*). Indeed from relation (2.45), one obtains, with the Klein-Gordon inner product (2.36),

$$(p_i, f_j^*) = -\beta_{ij} \tag{2.52}$$

The previous Klein-Gordon inner product is defined on a given Cauchy surface of constant time. The difficulty of evaluating such an inner product relies in the fact that an asymptotic outgoing solution must

be traced back to the ingoing region (or vice versa) in order to evaluate its inner product with an ingoing mode defined in this region. In the case of a black-hole, $\mathcal{I}^+$ alone is not a Cauchy surface since the asymptotic future is given by $\mathcal{I}^+ \cup \mathcal{I}^H$, with $\mathcal{I}^H$ representing the future of the ingoing modes falling in the black hole and $\mathcal{I}^+$ the future of the ingoing modes escaping at $r = +\infty$ after crossing $r = 0$. Therefore, the best Cauchy hyper-surface over which to evaluate the inner product (2.52) is $\mathcal{I}^-$.

Ignoring the $\hat{c}_i$ and $\hat{c}_i^\dagger$ in Rel. (2.47), this last relation can be applied to the vacuum $|0_{in}\rangle$ of the $\hat{a}_i$, leading to

$$\hat{a}_j |0_{in}\rangle = 0 \quad \Rightarrow \quad \alpha_{ij} \hat{b}_i |0_{in}\rangle = -\beta^*_{ij} \hat{b}_i^\dagger |0_{in}\rangle \tag{2.53}$$

with implicit summation on index i. Writing

$$|0_{in}\rangle = \hat{S} |0_{out}\rangle \tag{2.54}$$

with $\hat{S}$ some generic invertible operator, one obtains

$$\hat{b}_k \hat{S} = -V_{ki} \hat{b}_i^\dagger \hat{S} \tag{2.55}$$

with implicit summation on index j and $V_{ki} = [(\alpha^T)^{-1}]_{kj} [\beta^\dagger]_{ji}$ a matrix where α^T and $\beta^\dagger$ are the transpose of α and the hermitian conjugate of β, respectively. Then, recalling that $[\hat{x}, \hat{p}] = i\hbar$ and that for bosons $[\hat{b}, \hat{b}^\dagger] = 1$ with $\hat{p} = -i\hbar\partial_{\hat{x}}$ in position representation, one can write $\hat{b}_k = \partial_{\hat{b}_k^\dagger}$, thus obtaining, for $\partial_{\hat{b}_k^\dagger} b_q^\dagger = \delta_{kq}$,

$$\partial_{\hat{b}_k^\dagger} \hat{S} = -V_{ki} \hat{b}_i^\dagger \hat{S} \quad \Rightarrow \hat{S} = \mathcal{N} \exp\left(-V_{qi} \hat{b}_i^\dagger b_q^\dagger\right) \tag{2.56}$$

with $\mathcal{N}$ a normalization constant. The in-vacuum $|0_{in}\rangle$ is therefore obtained by squeezing the out-vacuum $|0_{out}\rangle$, with $\hat{S}$ the squeezing operator, i.e.

$$|0_{in}\rangle = \mathcal{N} e^{\sum_{q,i} -V_{qi} \hat{b}_i^\dagger b_q^\dagger} |0_{out}\rangle \tag{2.57}$$

If $\beta = 0$ it can then be seen, according to the definition of the matrix V, that $|0_{in}\rangle = |0_{out}\rangle$.

2.3.3 . Eddington-Finkelstein coordinates

In order to derive Hawking radiation in the Swarzschild metric several coordinate changes are needed. As we have seen in (2.9), in Schwarzschild coordinates radial null geodesic are given by

$$c^2 \frac{dt^2}{dr^2} = \left(1 - \frac{r_s}{r}\right)^{-2} \tag{2.58}$$

Then, one can define for $r \neq r_s$

$$r^* = r + r_s \ln \frac{|r - r_s|}{r_s} \tag{2.59}$$

where r^* is called the *Regge-Wheeler* or *tortoise* coordinate. The absolute value $|r - r_s|$ implies that r^* is defined for any r greater or smaller than r_s and is such that

$$r^* \underset{r=0}{=} 0 \qquad \lim_{r \to r_s} r^* = -\infty \qquad \lim_{r \to +\infty} r^* = +\infty \tag{2.60}$$

One has therefore

$$\frac{dr^*}{dr} = 1 + \frac{r_s}{r - r_s} = \frac{r}{r - r_s} = \left(1 - \frac{r_s}{r}\right)^{-1} \tag{2.61}$$

both for $r > r_s$ and $r < r_s$, which leads to

$$\left(c \frac{dt}{dr^*}\right)^2 = 1 \qquad \Rightarrow \qquad cdt = \pm dr^* \tag{2.62}$$

This last relation implies

$$d(ct \mp r^*) = 0 \tag{2.63}$$

One then usually defines new coordinates v and u such that any fixed value of variables v and u given by

$$v = ct + r^* \qquad u = ct - r^* \tag{2.64}$$

will represent an *ingoing* radial null geodesic and an *outgoing* radial null geodesic respectively[11]. Taking the *ingoing* radial null geodesic[12], one can therefore parametrize the non-angular part of the Schwarzschild

[11] One has $cdt/dr^* = -1$ for v and $cdt/dr^* = +1$ for u : hence *ingoing* and *outgoing* respectively.
[12] One could take the *outgoing* radial null geodesic as well.

metric with (v, r) or (t, v) instead of (t, r), since from the definitions (2.64) and (2.59) one can take v and r as independent variables and consider t to be fixed as a function $t(v, r)$ or v and t as independent variables and considered r to be fixed as a function $r(t, v)$. Considering that one has by definition

$$dv = cdt + dr^* = cdt + \left(1 - \frac{r_s}{r}\right)^{-1} dr \tag{2.65}$$

one obtains[13] in the first case

$$ds^2(v, r, \theta, \phi) = \left(1 - \frac{r_s}{r}\right) dv^2 - 2drdv - r^2 d\Omega^2 \tag{2.66}$$

and in the second case

$$ds^2(t, v, \theta, \phi) = -\left(1 - \frac{r_s}{r}\right) \left(dv^2 - 2cdtdv\right) - r^2 d\Omega^2 \tag{2.67}$$

Dropping the angular part it can then be notice that

$$\det g_{\mu\nu}(v, r) = -1 \qquad \det g_{\mu\nu}(v, t) = -\left(1 - \frac{r_s}{r}\right)^2 \tag{2.68}$$

Hence, whereas the second metric $g_{\mu\nu}(v, t, \theta, \phi)$ is not invertible both in $r = 0$ and $r = r_s$ since there $\det g_{\mu\nu}(t, v, \theta, \phi) = 0$, the first metric, while still diverging in the g_{vv} component for $r = 0$, is now invertible in $r = r_s$ where the determinant is finite. Therefore the metric $g_{\mu\nu}(v, r)$ is now regular at r_s, with no divergence appearing when going from r_s^+ to r_s^-. Let us therefore take this metric where v/c is a time coordinate.

In this metric parametrized by coordinates (v, r, θ, ϕ), usually referred to as the *ingoing (or advanced) Eddington-Finkelstein* coordinates, with v the time coordinate, we are interested in time-like and null-like geodesics. We want therefore $ds^2 \geq 0$, that is to say for radial geodesics,

$$\left(1 - \frac{r_s}{r}\right) dv^2 - 2drdv \geq 0 \tag{2.69}$$

and therefore, after dividing by dv^2 which doesn't change the inequality sign,

$$\left(1 - \frac{r_s}{r}\right) \geq 2\frac{dr}{dv} \tag{2.70}$$

We are interested in *future* oriented geodesics, i.e. $dv > 0$. The left-hand-side of the inequality is strictly positive for $r > r_s$, which means that dr can have both positive and negative values. But for $r < r_s$ the left-hand-side of the inequality is strictly negative and this implies that the right-hand-side must be negative : in this case the propagation of any (be it massive or massless) particle can therefore only occur towards $r = 0$. Furthermore, since there is no more divergence in $r = r_s$, the propagation from the region $r > r_s$ to the region $r < r_s$ can occur and the surface $r = r_s$ can be crossed : since once this surface crossed for any particle there is no way back, the only possible direction of propagation being inwards, the region $r < r_s$ is called a *black-hole*. The surface of the sphere of radius $r = r_s$ is called the *future event horizon* of the black hole, the term *future* referring to the fact that this horizon is located at constant $u = +\infty$.

An analogous reasoning for the metric parametrized by coordinates (u, r, θ, ϕ), usually referred to as *outgoing (or retarded) Eddington-Finkelstein*, with u the time coordinate, leads to the interval

$$ds^2(u, r, \theta, \phi) = \left(1 - \frac{r_s}{r}\right) du^2 + 2drdu - r^2 d\Omega^2 \tag{2.71}$$

and to the radial geodesic relation

$$ds^2 \geq 0 \qquad \Rightarrow \qquad \left(1 - \frac{r_s}{r}\right) \geq -2\frac{dr}{du} \tag{2.72}$$

where the region $r < r_s$ allows only for outwards propagation. In this metric the region $r < r_s$ is therefore called a *white-hole* and the surface of the sphere of radius $r = r_s$ is referred as the *past event horizon* of the white hole, the term *past* referring to the fact that this horizon is located at constant $v = -\infty$. In both set of coordinates the horizon is therefore located at infinity with respect to the time coordinate (u or v) of the metric. The *Kruskal* coordinates can bring the horizons to a finite value (see [82]).

[13] The coordinate v represents time in one case and space in in the other.

2.3.4 . Collapse in Vaidya spacetime

Vaidya spacetime is the simplest exact solution to Einstein's equation that describes the formation of a black hole and hence the simplest *non-stationary* spacetime describing particle creation from a black hole [82]. In (v, r) coordinates, the mass M in (2.6) is taken to be v dependent, and the stress-energy tensor T_{vv} is considered to be proportional to $dM/dv = M\delta(v - v_0)$. Therefore, since[14]

$$M(v) = M\Theta(v - v_0) \tag{2.73}$$

the black hole is considered to be formed by a collapse of matter modeled by an ingoing null shock wave at time v_0. Before the formation of the black hole, i.e. for $v < v_0$, one has the usual Minkowski space-time. Since there is no black-hole this space-time is obtained from the Schwarzschild space-time (2.6) by setting $r_s = 0$ and therefore $r^* = r$ from Eq. (2.59). We will call this region "IN" and write it as

$$\begin{aligned} ds^2_{in} &= c^2 dt^2_{in} - dr^2_{in} - r^2_{in} d\Omega^2 \\ &= dv^2_{in} - 2dv_{in}dr_{in} - r^2_{in} d\Omega^2 \\ &= du^2_{in} + 2du_{in}dr_{in} - r^2_{in} d\Omega^2 \\ &= du_{in}dv_{in} - r^2_{in} d\Omega^2 \end{aligned} \tag{2.74}$$

Once the black-hole is formed, i.e. for $v > v_0$, we are in the stationary configuration of the Schwarzschild black-hole, i.e. $r_s \neq 0$ and $r^* \neq r$. This region, that we call "OUT", is most easily written, using (2.61), as

$$\begin{aligned} ds^2_{out} &= \left(1 - \frac{r_s}{r_{out}}\right)\left(c^2 dt^2_{out} - (dr^*_{out})^2\right) - r^2_{out} d\Omega^2 \\ &= \left(1 - \frac{r_s}{r_{out}}\right)\left(dv^2_{out} - 2dv_{out}dr^*_{out}\right) - r^2_{out} d\Omega^2 \\ &= \left(1 - \frac{r_s}{r_{out}}\right)\left(du^2_{out} + 2du_{out}dr^*_{out}\right) - r^2_{out} d\Omega^2 \\ &= \left(1 - \frac{r_s}{r_{out}}\right) du_{out}dv_{out} - r^2_{out} d\Omega^2 \end{aligned} \tag{2.75}$$

Since the Schwarzschild metric is parametrized by r, with $r(r^*, t)$, $r(v, t)$, $r(u, t)$ or $r(u, v)$[15], the continuity of the metric imposes a matching at $v = v_0$, i.e. at $v_{in} = v_{out} = v_0$. This matching condition is written

$$r_{in}(v_0, t_{in}) = r_{out}(v_0, t_{out}) \tag{2.76}$$

or

$$r_{in}(v_0, u_{in}) = r_{out}(v_0, u_{out}) \tag{2.77}$$

according to the chosen coordinate system. For the sake of clarity, let us rewrite relations (2.64) defining r^* in each region when working with the (u, v) coordinates. One has in the "IN" region

$$r_{in}(v_{in}, u_{in}) = \frac{v_{in} - u_{in}}{2} \tag{2.78}$$

since here $r^*_{in} = r_{in}$ because (2.59) is defined for $r_s = 0$ in region "IN". In the "OUT" regions one has instead

$$r^*_{out}(v_{out}, u_{out}) = \frac{v_{out} - u_{out}}{2} = r_{out}(v_{out}, u_{out}) + r_s \ln\left(\frac{|r_{out}(v_{out}, u_{out}) - r_s|}{r_s}\right) \tag{2.79}$$

Applying the matching condition (2.77) in the previous relation (2.79) evaluated at v_0, yields straightforwardly

$$\frac{v_0 - u_{out}}{2} = r_{in}(v_0, u_{in}) + r_s \ln\left(\frac{|r_{in}(v_0, u_{in}) - r_s|}{r_s}\right) \tag{2.80}$$

[14] Here Θ is the usual unit step function.
[15] Of course $r(r^*, t) = r(r^*)$ since the metric is stationary.

and eventually, applying (2.78),

$$u_{out} = u_{in} - 2\,r_s \ln\left(\frac{|v_0 - u_{in} - 2\,r_s|}{2\,r_s}\right) \tag{2.81}$$

Now u_{out} is a function of u_{in}. We have seen that the horizon is located at $u = +\infty$ (what we called the *future* horizon, i.e. the horizon of a black hole) in a Schwarzschild metric. Here our metric is such in the "OUT" region and therefore the horizon is located at $u_{out} = +\infty$. From expression (2.81) we can see that when $u_{in} = -\infty$ one has $u_{out} \approx u_{in}$ which means that at early times $u_{out} = -\infty$, i.e. long before the black hole was formed, a positive frequency mode of frequency $\omega/2\pi$ is not altered when going from the first region to the second : because the whole space is a Minkowski space when $u_{out} = -\infty$, there is no scattering and hence no mixing of frequencies. But the more u_{in} gets closer to $v_H = v_0 - 2r_s$ the more u_{out} differs from u_{in} since one has $u_{out} \to +\infty$ when $u_{in} \to v_H$.

2.3.5 . Real Massless Scalar Field in Vaidya space-time

This space-time we considered is the simplest space-time for the Hawking effect. The simplest field to quantize in such a space-time is a real massless scalar field. This field obeys the Klein-Gordon equation in curved space-time given in (2.17). Since the configuration is spherically symmetric one can write the massless scalar field ψ as

$$\psi(x^\mu) = \sum_{l,m} \frac{f_l(r,t)}{r} Y_l^m(\theta,\phi) \tag{2.82}$$

with Y_l^m the spherical harmonics. In the "OUT" region the equation (2.17) can easily be computed with the (r^*, t) coordinates and, after some algebra, it reads[16]

$$\left(\partial_t^2 - \partial_{r^*}^2 + V_l(r)\right) f_l(r,t) = 0 \qquad V_l(r) = \left(1 - \frac{r_s}{r}\right)\left(\frac{l(l+1)}{r^2} + \frac{r_s}{r^3}\right) \tag{2.83}$$

In the "IN" region, the equation is obtained from the previous (2.83) just by setting $r_s = 0$, i.e. $r^* = r$: in this region, the equation is simply the one of flat space. The heart of the Hawking process takes place at the horizon where the potential $V_l(r)$ vanishes in both regions for $l = 0$. We will therefore take here the potential $V_l(r)$ to be identically zero everywhere in both regions and rename f_l as f, with f solution of (2.83) with $V_l(r)$ identically zero everywhere in both regions. A positive frequency solution will be given by a harmonic time dependence in $f(r,t)$, i.e.

$$f(r,t) = e^{-i\omega t} f(r) \tag{2.84}$$

which leads straightforwardly to

$$\frac{d^2 f(r)}{dr^{*2}} + \omega^2 f(r) = 0 \tag{2.85}$$

with $r^* = r$ in the "IN" region. One can also solve (2.17) using (u, v) coordinates. Then the equation reads[17]

$$\left(4\partial_u\partial_v + V_l(r)\right) f_l(r,t) = 0 \tag{2.86}$$

with $V_l(r)$ as defined in Eq. (2.83). With the potential $V_l(r)$ taken to be identically zero everywhere in both regions, one can then define

$$f(r,t) = F(u) + G(v) \tag{2.87}$$

which is solution of equation

$$\partial_u\partial_v f(r,t) = 0 \tag{2.88}$$

[16] The relation $r^2\nabla^2 Y_l^m = -l(l+1)Y_l^m$ for spherical harmonics has been used, with ∇^2 the Laplacian in spherical coordinates. Relation (2.61) must also be used since $r^*(r)$.

[17] Equation(2.86) is obtained straightforwardly from (2.83) just by applying relations $\partial_{r^*} = \partial_u - \partial_v$ and $\partial_t = \partial_u + \partial_v$.

2.3.6 . Hawking radiation in Vaidya space-time

On past null infinity $\mathcal{I}^-$, the ingoing asymptotic solutions f_ω of (2.88) defined as

$$\psi^{in}_\omega = \frac{g_\omega}{r} = \frac{e^{-i\omega v_{in}/c}}{4\pi r\sqrt{\omega c}} \tag{2.89}$$

are such that[18]

$$(\psi^{in}_\omega, \psi^{in}_{\omega'}) = -4\pi\, i \int_{\mathcal{I}^-} dv_{in}\, r^2 (\psi^{in}_\omega \partial_{v_{in}} \psi^{in*}_{\omega'} - \psi^{in*}_{\omega'} \partial_{v_{in}} \psi^{in}_\omega) = \delta(\omega - \omega') \tag{2.90}$$

Similarly, we define on future null infinity $\mathcal{I}^+$, the outgoing asymptotic solutions f_ω of (2.88)

$$\psi^{out}_\omega = \frac{f_\omega}{r} = \frac{e^{-i\omega u_{out}/c}}{4\pi r\sqrt{\omega c}} \tag{2.91}$$

are such that[19]

$$(\psi^{out}_\omega, \psi^{out}_{\omega'}) = -4\pi\, i \int_{\mathcal{I}^+} du_{out}\, r^2 (\psi^{out}_\omega \partial_{u_{out}} \psi^{out*}_{\omega'} - \psi^{out*}_{\omega'} \partial_{u_{out}} \psi^{out}_\omega) = \delta(\omega - \omega') \tag{2.92}$$

In the Schwarzschild black hole metric the past null infinity $\mathcal{I}^-$ is a Cauchy surface where the $\beta_{\omega\omega'}$ coefficients can be determined from[20]

$$\beta_{\omega\omega'} = -(\psi^{in}_\omega, \psi^{out*}_{\omega'}) = 4\pi\, i \int_{\mathcal{I}^-} dv_{in}\, r^2 (\psi^{in}_\omega \partial_{v_{in}} \psi^{out*}_{\omega'} - \psi^{out*}_{\omega'} \partial_{v_{in}} \psi^{in}_\omega) \tag{2.93}$$

once the mode ψ^{out}_ω has been traced back to this region. To do so, we have to consider a last condition.

Because of the spherical symmetry of the problem, while working in the (r,t) space-time a light ray that is crossing $r = 0$ (before the black-hole is formed) "reflects" at 45° on the t-axis and one must therefore have in region "IN" the condition

$$f(r = 0, t) = 0 \tag{2.94}$$

The ingoing light ray v_0 represents the shock wave of the black hole formation and the ingoing light ray v_H, with $v_H < v_0$ the last ray to escape to infinity without falling in the black hole : it is the ray that generates the horizon along $u_{out} = +\infty$. These two rays reach $r = 0$ at ct_H and ct_0 respectively with $ct_0 - ct_H = 2r_s$ as can be seen from Fig. 2.1, hence, using (2.63), $v_0 - v_H = 2\,r_s$. Before v_H/c the scalar field is constituted by both ingoing modes (not yet "reflected" on $r = 0$) and outgoing modes (already "reflected" on $r = 0$). After v_H there are no more outgoing modes since all the ingoing modes fall in the black hole. Since nothing happens when crossing $r = 0$, the "reflected" outgoing mode $u_{out}(u_{in})$ is just $u_{out}(v_{in})$ with the function u_{out} defined in (2.81)[21]. Then, condition (2.94), implies

$$\psi^{out}_\omega = \frac{e^{-i\omega u_{out}(u_{in})/c}}{4\pi r\sqrt{\omega c}} - \frac{e^{-i\omega u_{out}(v_{in})/c}}{4\pi r\sqrt{\omega c}} \Theta(v_H - v_{in}) \tag{2.95}$$

At early times, i.e. when $v_{in} \to -\infty$, one has

$$u_{out}(v_{in}) \underset{v_{in}\to-\infty}{\approx} v_{in} \qquad u_{out}(u_{in}) \underset{v_{in}\to-\infty}{\approx} u_{in} \tag{2.96}$$

[18] Let us remark that v/c is a time coordinate whereas v is a space coordinate. On $\mathcal{I}^-$, the space coordinate varies from $-\infty$ to $+\infty$, with $u_{out} = -\infty$. The integration over $\sin\theta d\theta d\phi$ has already been performed, leading to the factor 4π.

[19] Rigorously, the following definition would only be true in a Minkowski spacetime where $\mathcal{I}^+$ is indeed a Cauchy surface at $v_{out} = +\infty$. In a black hole configuration the Cauchy surface is $\mathcal{I}^+ \cup \mathcal{I}^H$, with $\mathcal{I}^H$ the horizon drawn by the last outgoing light ray escaping to infinity before the creation of the black hole. This is the reason why we have to choose $\mathcal{I}^-$ as a Cauchy surface for evaluating the $\beta_{\omega\omega'}$ coefficients. Let us also remark that $r_{in} = r_{out} = r$.

[20] The Cauchy surface $\mathcal{I}^-$ is defined far all v_{in} and v_{out} when $u_{out} \to -\infty$. But for $v > v_H$, i.e. for v_{out}, all the ingoing null rays fall into the null horizon $u_{out} = +\infty$ and there are no "reflect" modes to $\mathcal{I}^+$, hence here ψ^{out}_ω. The integration over $\mathcal{I}^-$ can then be taken on the v_{in} at $u_{out} = -\infty$.

[21] The "reflection" at $r = 0$ happens only in the (r,t) coordinates : in an (x,t) coordinate the v_{in} light ray would just continue to go straight. This is why one has just to change $v_{in} \leftrightarrow u_{in}$ in the function u_{out} when crossing $r = 0$.

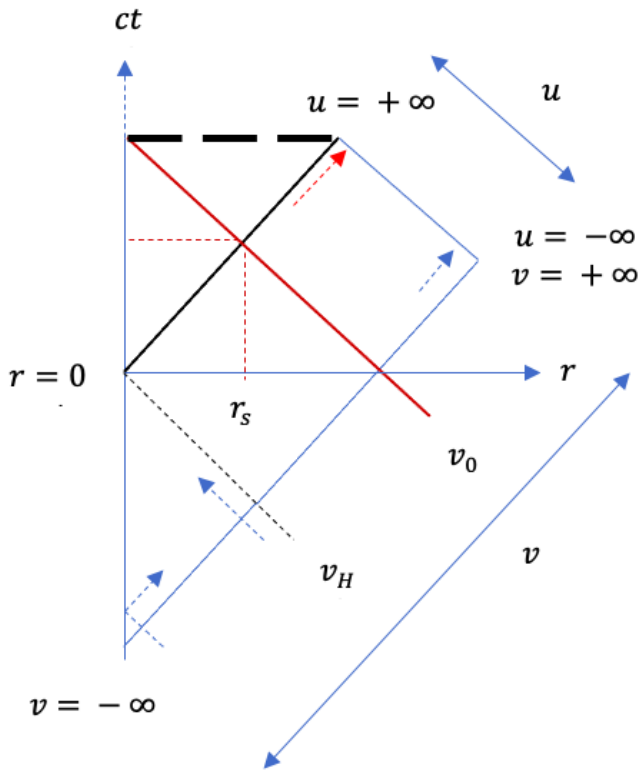

Figure 2.1: Penrose diagram of a Vaidya space-time. Due to spherical symmetry, the (ct, x) plane has been folded in the the (ct, r) plane, with r the radial coordinate centered at the black-hole singularity, with r_s the Schwarzschild event horizon. The lines of constant u and v define ingoing and outgoing null rays, respectively (see (2.64)). The ingoing light ray v_0 represents the shock wave of the black hole formation (it separates the "IN" region from the "OUT" region of spacetime) whereas v_H represents the last ingoing ray escaping $u = +\infty$: therefore the u constant black line is the null horizon of the black hole. The thick dashed dark line is the black hole singularity : every ingoing ray emitted after v_H falls into the singularity. At early times an ingoing positive frequency mode ω is mapped to an outgoing mode of identical frequency (blue dashed arrows). At late times, close to v_H, an outgoing positive energy mode gets infinitely blue shifted (see (2.98)) when traced back to an ingoing mode (red dashed arrow to blue dashed arrow).

and upon "reflection" at $r = 0$ an ingoing positive frequency ω is mapped to the same outgoing positive frequency ω. There is no particle creation and from (2.81) one has

$$\beta_{\omega\omega'} \underset{v_{in}\to-\infty}{\approx} 0 \tag{2.97}$$

At late times, i.e. when $u_{out} \to +\infty$ and $v_{in} \to v_H$, one must also have $u_{in} \to v_H$, i.e.[22]

$$\begin{aligned} u_{out}(u_{in}) &\underset{v_{in}\to v_H}{\approx} v_H - 2\,r_s \ln\left(\frac{|v_H - u_{in}|}{2\,r_s}\right) \\ u_{out}(v_{in}) &\underset{v_{in}\to v_H}{\approx} v_H - 2\,r_s \ln\left(\frac{|v_H - v_{in}|}{2\,r_s}\right) \end{aligned} \tag{2.98}$$

An outgoing positive frequency ω is no longer mapped, upon "reflection" at $r = 0$, to an ingoing positive frequency ω, since $u_{out}(v_{in}) \neq v_{in}$ and $u_{out}(u_{in}) \neq u_{in}$. Hence,

$$\beta_{\omega\omega'} \underset{v_{in}\to-v_H}{\neq} 0 \tag{2.99}$$

and one has particle creation. The explicit computation of the $\beta_{\omega\omega'}$ can be found in Ref. [82]. It leads to

$$|\alpha_{\omega\omega'}|^2 = e^{\hbar\omega/k_B T_H}|\beta_{\omega\omega'}|^2 \qquad \text{with} \qquad T_H = \frac{\hbar c}{4\pi k_B r_s} \tag{2.100}$$

[22] With $v_H = v_0 - 2\,r_s$ by definition.

Introducing a discretized ω_i [23] and taking into account[24]

$$\int_0^\infty d\omega' \left[|\alpha_{\omega_i\omega'}|^2 - |\beta_{\omega_i\omega'}|^2\right] = 1 \tag{2.101}$$

one obtains[25]

$$\langle \hat{b}_i^\dagger \hat{b}_i \rangle_{in} = \int_0^\infty d\omega' |\beta_{\omega_i\omega'}|^2 = \frac{1}{e^{\hbar\omega_i/k_B T_H} - 1} \tag{2.102}$$

which corresponds to a thermal spectrum of temperature T_H.

2.3.7 . Analog Hawking temperature

In order to conclude this section on the hydrodynamical analogy for Hawking radiation, we will show how an analogous Hawking temperature for the analogous thermal radiation can indeed be well defined in the hydrodynamical frame. In fact, considering quantum field theory in curved space-time, Hawking theorized the existence of a thermal black body radiation emitted from a gravitational black hole. By virtue of vacuum quantum fluctuations close to the event horizon, a black hole radiates at

$$T_H = \frac{\hbar c^3}{8\pi k_B G M} = \frac{\hbar}{2\pi k_B c}\kappa \tag{2.103}$$

where c is the speed of light in vacuum , $\hbar$ the reduced Planck constant , k_B Boltzmann's constant, G Newton's constant , M the mass of the black hole and κ the surface gravity of the black hole. The surface gravity is by definition the gravitational acceleration at the event horizon. For a Schwarzschild black hole, the surface gravity was given in (2.12) and one obtains eventually the Hawking temperature

$$T_H|_{\text{Schwarz.}} = \frac{\hbar c}{4\pi k_B r_s} \tag{2.104}$$

One clearly sees that the smaller the radius (or the mass) the higher the temperature of the black hole. Knowing that the thermal radiation of a solar mass black hole is of order 10^{-8} K whereas the Cosmic Microwave Background is of order 3 K, any astronomical observation of Hawking radiation is highly unlikely. On the contrary, experiments in Analog Gravity can allow an experimental verification of the analog radiation.

Indeed, comparing (2.27) and (2.6), one can define an analog Hawking temperature [83]. To this end, let us arbitrarily state that the flow becomes supersonic in R and let us, from (2.27), expand with respect to r to first order $f(r) = 1 - (V_r(r)/c(r))^2$ around R. Close to R one has $f(r) \approx f(R) + f'(R)(r-R) = f'(R)(r-R)$ since, by definition of the acoustic horizon, $V_r(R)/c(R) = 1$ and therefore $f(R) = 0$. Hence, having

$$f'(R) = -\frac{2V_r V_r' c^2 - 2{V_r}^2 c c'}{c^4} = 2\frac{c'(R) - V_r'(R)}{c}$$

and also, from (2.6), expanding with respect to r to first order $g(r) = 1 - r_s/r$ around r_s, i.e. $g(r) \approx g(r_s) + g'(r_s)(r-r_s) = g'(r_s)(r-r_s)$ since by definition $g(r_s) = 0$, with $g'(r_s) = 1/r_s$, one clearly sees that $2(c' - V_r')/c$ plays the same role in the acoustic frame as the one played by $1/r_s$ in the gravitational frame. Therefore, looking at (2.12), one can define an acoustic analog surface gravity term

$$\kappa_{\text{ac}} = c(R)\left|\frac{\partial\left(c - V_r\right)}{\partial_r}\right|_R \tag{2.105}$$

Eventually this analog surface gravity leads to a well defined acoustic analog Hawking temperature

$$T_H|_{\text{Acoustic}} = \frac{\hbar}{2\pi k_B c}\kappa_{\text{ac}} \tag{2.106}$$

[23] With a continuous normalization of the modes, the quantity $\langle \hat{b}_\omega^\dagger \hat{b}_\omega \rangle_{in}$ would represent the Hawking flux at frequency ω integrated for all times : it would then be infinite [82].
[24] See (2.49).
[25] See (2.51).

This completes our acoustic analogy and allows us to state, in Unruh's words, that indeed " [t]he model of behavior of quantum field in a classical gravitational field is the motion of sound waves in a convergent fluid flow " [16]. The radial dimension can then be modeled by a one dimensional flow along the x axis with an acoustic horizon in x_h defined by $c(x_h) = v(x_h)$[26] and with a one-to-one mapping of the relevant physical observables between the analog system and the gravitational one. This bijective mapping is summarized in Table 2.1.

Gravitational Black Hole	**Acoustic Black Hole**
light speed c	sound speed $c(x)$
radius $r_s = 2GM/c^2$	x_h such that $V(x_h) = c(x_h)$
surface gravity $\kappa = c^2/2r_s$	$\kappa_{\rm ac} = c(x_h)\lvert\partial(c-V)/\partial x\rvert_{x_h}$
temperature $T_H \propto \kappa$	$T_H\lvert_{\rm Acoustic} \propto \kappa_{\rm ac}$

Table 2.1: Analogy terms between a gravitational Schwarzschild black hole of mass M, with G the gravitational constant, and an acoustic black hole implemented in a fluid as a one-dimensional flow with an acoustic horizon located at x_h and $V(x)$ the velocity of the flow. Clearly, if the central symmetry of the gravitational configuration is lost in such an analog configuration, this acoustic model still captures the relevant radial dynamics of the gravitational black-hole.

2.3.8 . Limit of the Analogy

As a final remark, we will just signal the main limit of the analogy : the existence of supersonic modes due to the violation of Lorentz invariance. The Doppler shifted Bogoliubov dispersion relation (see Rel. (3.24) and Fig. 3.2 in Chapter 3) generates, due to dispersion effects, a zoology of modes that is richer than in the gravitational framework. The analog system is thus tripartite where the gravitational one is bipartite. This is a drawback of the analogy but, by considering the analog hydrodynamic system *per se*, it is a nice feature that allow to study tripartite entanglement and nonlocality.

Furthermore, the existence of these supersonic modes allows us to translate the emission process generated by the gravitational collapse into a stationary scattering process on the horizon. Due to the dispersion effects, the physics of the analog Hawking radiation is mainly driven by long wavelength phenomena. Then, the Hawking temperature that is given by the analog surface gravity (2.105) can also be obtained by considering the scattering coefficient S_{02} of the "in" partner mode (2) onto the "out" Hawking mode (0), as can be seen in Chapter 3. Indeed, the far exterior region of our one-dimensional black hole is given by the asymptotic region $x \to -\infty$, where the average energy current at zero temperature [38] reads

$$\Pi_0 = -\int_0^\Omega \frac{d\omega}{2\pi}\hbar\omega|S_{02}(\omega)|^2 \tag{2.107}$$

The transmission coefficient $|S_{02}(\omega)|^2$ is directly related to the presence of the acoustic horizon and exists only for $\omega < \Omega$. This coefficient is a signature of the analog Hawking radiation [38] and it can be fitted by a thermal spectrum $\Gamma \times n_{T_H}$ with Γ a constant[27] and $n_{T_H}(\omega)$ the thermal Bose occupation number

$$n_{T_H}(\omega) = \frac{1}{\exp\left(\frac{\hbar\omega}{k_B T_H}\right) - 1} \tag{2.108}$$

where T_H is the analog Hawking temperature. Because of the cut-off energy Ω the fitting to a thermal spectrum is only partial. Indeed, as can be seen from Fig. 2.2 the fitting at low energy is quite good and becomes less precise when $\omega \to \Omega$ because of the cut-off. The given estimations of the Hawking

[26] An infinte one-dimensional system will mimic the relevant physics generated by the presence of the event horizon but, contrary to the gravitational configuration, will have no singularity at $r = 0$.

[27] It is the "greybody factor". At $\Gamma = 1$ the radiation is the purely thermal radiation of a black body.

temperature T_H and greybody factor Γ can therefore be considerably improved by considering only a long wavelength expansion of $|S_{02}|^2$.

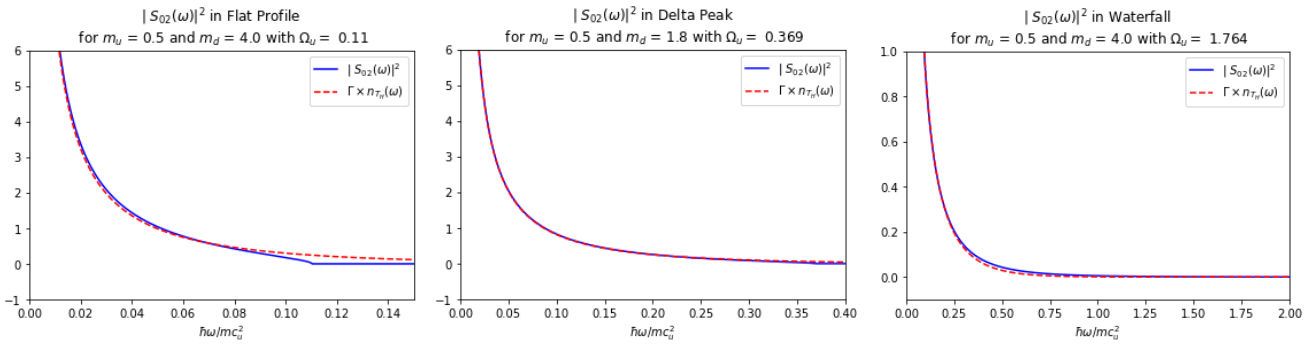

Figure 2.2: Fit of $|S_{02}(\omega)|^2$ by a Bose thermal spectrum $n_{T_H}(\omega)$ of temperature T_H for the Flat Profile, Delta Peak and Waterfall configurations (see Chapter 3. The values of the fitting parameters are : $\Gamma = 1.143$ and $k_B T_H/mc_u^2 = 0.067$ for Flat Profile, $\Gamma = 0.997$ and $k_B T_H/mc_u^2 = 0.125$ for Delta Peak, $\Gamma = 0.924$ and $k_B T_H/mc_u^2 = 0.142$ for Waterfall. For a description of the three analog black hole configurations see Chapter 3.

3 - BECs ANALOG BLACK HOLES

BECs are promising analog systems. One can enumerate at least four main reasons for this : (1) BECs are quantum systems and therefore exhibits quantum fluctuations, which are the core of Hawking radiation phenomenon ; (2) in such systems, the two-point density correlation function allows for a robust signature of the Hawking radiation [36][1] ; (3) 1D configurations can be theoretically devised, which make the phenomenon mathematically easier to study ; (4) some of such 1D configurations have been experimentally implemented [33, 34], thus allowing for comparison between theoretical predictions and experimental data. In this chapter we will review, within the Bogoliubov approximation, such zeroth order background configurations as well as the first order quantum excitations defining the ingoing and outgoing modes in the scattering process on the acoustic horizon.

3.1 . THE GROSS-PITAEVSKII EQUATION AND THE BOGOLIUBOV APPROXIMATION

3.1.1 . The 1D meanfield

The dynamics of BECs is well described by the Gross-Piatevskii equation [58]. This non-linear equation allows for a precise characterization of the zeroth order mean-field and first order quantum fluctuations. We consider here a stationary flow of a 1D Bose-Einstein-Condensate described by 1D Heisenberg field operator

$$\hat{\Psi}(x,t) = \hat{\Phi}(x,t)e^{-i\mu t/\hbar} \tag{3.1}$$

where μ is the chemical potential fixed by boundary conditions at infinity. This field operator is solution of the Gross-Piatevskii field equation :

$$i\hbar\partial_t\hat{\Phi} = -\frac{\hbar^2}{2m}\partial_x^2\hat{\Phi} + [U(x) + g(x)\hat{n} - \mu]\hat{\Phi} \tag{3.2}$$

where $U(x)$ is an external potential, $\hat{n} = \hat{\Phi}^\dagger\hat{\Phi}$ the density operator and $g > 0$ a nonlinear parameter which accounts for a repulsive effective two body-interaction and for a transverse harmonic trapping. In the quasicondensate regime, i.e. in the so-called 1D mean-field regime [57], the Bogoliubov approximation for stationary flows consists in writing the quantum field as

$$\hat{\Phi}(x,t) = \Phi(x) + \delta\hat{\Psi}(x,t) \tag{3.3}$$

where the quantum field operator $\hat{\Phi}$ has been split in a stationary classical contribution Φ describing the background flow pattern and a small quantum fluctuation $\hat{\Psi}$. Whereas the decomposition (3.3) is legitimate in 3D, it has a finite range of validity in the 1D configurations we consider; however, its conditions of applicability are commonly met in standard experimental situations [84].

The classical contribution $\Phi(x)$ is solution of the classical stationary Gross-Pitaevskii equation

$$\mu\Phi = -\frac{\hbar^2}{2m}\partial_x^2\Phi + [U(x) + g(x)|\Phi|^2]\Phi \tag{3.4}$$

An acoustic analog black hole configuration is defined as an inhomogeneous stationary flow exhibiting an asymptotic subsonic upstream flow in the $x < 0$ region, an asymptotic supersonic downstream flow in the region $x > 0$ and, close to $x = 0$, the acoustic horizon where the local velocity of the flow V equals the local speed of sound c. The chosen potential $U(x)$ and parameter interaction g in (3.4) will shape different configurations. Several such flows have been considered in the past. The so-called "waterfall configuration" is close to the experimental realization of Refs. [33, 34].

[1] In the gravitational case Hawking radiation is completly lost in the Cosmic Microwave Background (CMB). In the BEC even if the temperature is very low, the analog Hawking radiation has a temperature very low compared to the one of the BEC. But in an analog black hole the interior (supersonic) region is not precluded to measurements : the two-point densisty correlation function provides a robust measure of the signal.

Using the subscript *u* for upstream (subsonic) and *d* for downstream (supersonic) we can write

$$\Phi(x) = \begin{cases} \sqrt{n_u}\exp(ik_u x)\phi_u(x) & \text{for } x < 0 \\ \sqrt{n_d}\exp(ik_d x)\phi_d(x) & \text{for } x > 0 \end{cases} \tag{3.5}$$

In order for n_u and n_d to be respectively the upstream and downstream asymptotic densities, we define $\lim_{x\to-\infty}|\Phi_u| = 1$ and $\lim_{x\to+\infty}|\Phi_d| = 1$, i.e. $\lim_{x\to-\infty}\Phi_u = \exp(i\beta_u)$ and $\lim_{x\to-\infty}\Phi_d = \exp(i\beta_d)$ with $\beta_{u,d}$ a constant. Hence, an analog black hole horizon is realized if the flow takes asymptotically the form an upstream subsonic and downstream supersonic plane wave. The functions $\phi_u(x)$ and $\phi_d(x)$ specify the precise form of the flow pattern. In all our three configurations treated below we have

$$\phi_d(x) = \exp(i\beta_d) \tag{3.6}$$

meaning that $\phi_d(x)$ is a constant and that the downstream flow pattern is flat with constant density and velocity. Finally, we define, for $\alpha = u$ or d, the upstream and downstream asymptotic flow velocities V_α, asymptotic speed of sound c_α, healing lengths ξ_α, and Mach numbers m_α as

$$\hbar k_\alpha = mV_\alpha \qquad mc_\alpha^2 = g_\alpha n_\alpha \qquad mc_\alpha = \hbar/\xi_\alpha \qquad m_\alpha = V_\alpha/c_\alpha \tag{3.7}$$

For a black hole configuration, one has, by definition, $m_u < 1$ and $m_d > 1$. Since a stationary flow requires equality of asymptotic chemical potentials one can plug (3.5) in (3.4) and get a first asymptotic relation. Knowing that a stationary flow also requires current conservation, we get a second asymptotic relation[2]. One finally gets respectively

$$\frac{\hbar^2 k_\alpha^2}{2m} + U_\alpha + g_\alpha n_\alpha = \mu \qquad n_u V_u = n_d V_d \tag{3.11}$$

3.1.2 . Flat Profile configuration

In the Flat Profile configuration [85, 38] the flow pattern is flat with constant density and velocity, i. e. $V_u = V_d = V_0$ and $n_u = n_d = n_0$. Therefore, in order for this configuration to be an acoustic black hole, one must have $c_d < V_d = V_u < c_u$. Since the density is flat everywhere one can also take $\phi_u(x) = \phi_d(x) = 1$, i.e. $\beta_u = \beta_d = 0$. This means that (3.5) reduces for all x to $\phi(x) = \sqrt{n_0}\exp(ik_0 x)$ with $k_0 = mV_0/\hbar$. By virtue of (3.7) one has immediately :

$$\frac{c_d}{c_u} = \frac{m_u}{m_d} = \frac{\xi_u}{\xi_d} \tag{3.12}$$

Taking a steplike configuration for $U(x)$ and $g(x)$, that is

$$U(x) = \begin{cases} U_u & \text{for } x < 0 \\ U_d & \text{for } x > 0 \end{cases} \text{ and } g(x) = \begin{cases} g_u & \text{for } x < 0 \\ g_d & \text{for } x > 0 \end{cases} \tag{3.13}$$

with $g_u > g_d$ in order to fulfill the second relation in (3.7) for $c_u > c_d$, one finally gets, by virtue of the first relation of (3.11),

$$U_u + g_u n_0 = U_d + g_d n_0 \tag{3.14}$$

and thefore $U_u = n_0(g_d - g_u) + U_d < U_d$ since $g_u > g_d$[3]. High sensitivity to total atom number [38] and complexity of local monitoring of g(x) make this configuration experimentally unrealistic.

[2] In the mean-field approximation, the current is both upstream and downstream given by

$$j_\alpha(x,t) = \frac{\hbar}{m} Im(\Psi^* \partial_x \Psi) = V_\alpha n_\alpha - \frac{t}{m} n_\alpha |\phi_\alpha(x)|^2 \partial_x \mu \tag{3.8}$$

Then taking

$$\partial_x \mu = 0 \tag{3.9}$$

one has a stationary flow with $j_\alpha(x,t) = j_\alpha(x)$ since V_α and n_α are asymptotic constants. Then current conservation implies

$$j_u(x) = j_d(x) \tag{3.10}$$

[3] Note that if one takes smooth profiles for $U(x)$ and $g(x)$ imposing to $U(x)+g(x)n_0$ to be a constant as required by the first relation in (3.11) then $\hat{\Psi}(x,t)$ can only be determined numerically whereas it can be determined analytically for the steplike configuration of $U(x)$ and $g(x)$

3.1.3 . Delta Peak configuration

If one imposes $g(x) = g$ to be a constant and $U(x) = \Lambda\delta(x)$ to be a repulsive δ peak with $\Lambda > 0$, a transonic stationary profile, i.e. an acoustic black hole configuration, can also be obtained. In this case, one gets [38] for $x < 0$ a portion of a dark soliton profile

$$\phi_u(x) = \cos\theta \tanh\left(\frac{x - x_0}{\xi_u}\cos\theta\right) - i\sin\theta \tag{3.15}$$

with $0 < \sin\theta = m_u < 1$, which implies that one can take $\theta \in]0, \pi/2[$, and therefore $\lim_{x\to-\infty}\phi_u(x) = -\exp(i\theta)$, that is to say $\beta_u = \pi + \theta$. Furthermore, with g a constant and $U_{u,d} = 0$, one gets from (3.11) and (3.7) that

$$\frac{mV_\alpha^2}{2} + gn_\alpha = \mathrm{C}^{\mathrm{st}}$$

and then, setting

$$\frac{n_u}{n_d} = \frac{V_d}{V_u} = y$$

from the second relation of (3.11) and factorizing out gn_u in the first relation of (3.11), that

$$1 + \frac{m_u^2}{2} = \frac{m_u^2}{2}y^2 + \frac{1}{y}$$

This last relation can be rewritten as

$$(1 - y)\left(\frac{m_u^2}{2}y^2 + \frac{m_u^2}{2}y - 1\right) = 0$$

whose positive solution, ignoring the solution $y = 1$ that is not compatible with a black hole configuration, is

$$y = \frac{1}{2}\left(-1 + \sqrt{1 + \frac{8}{m_u^2}}\right)$$

This being set, from (3.7), one obtains immediately

$$\frac{n_u}{n_d} = \frac{V_d}{V_u} = y \qquad \frac{m_d}{m_u} = y^{\frac{3}{2}} \qquad \frac{c_d}{c_u} = \frac{1}{\sqrt{y}} = \frac{\xi_u}{\xi_d} \tag{3.16}$$

Since $\phi_d(x) = \exp(i\beta_d)$ is constant, by continuity of the wave function in $x = 0$ one has $\phi(0) = \sqrt{n_u}\phi_u(0) = \sqrt{n_d}\phi_d(0)$, i.e. $\sqrt{y}\phi_u(0) = \cos\beta_d + i\sin\beta_d$, and therefore, by identification of the imaginary part on each side, $-\sqrt{y}\sin\theta = \sin\beta_d$, and by identification of the real part on each side,

$$-\sqrt{y}\cos\theta\tanh\left(\frac{x_0}{\xi_0}\cos\theta\right) = \cos\beta_d$$

Hence $\cos\beta_d < 0$. Knowing that

$$\cos\beta_d = -\sqrt{1 - \sin^2\beta_d} = \sqrt{1 - y\sin^2\theta} = \sqrt{1 - ym_u^2}$$

we obtain

$$\cos\theta\tanh\left(\frac{x_0}{\xi_0}\cos\theta\right) = \sqrt{\frac{1}{y} - m_u^2} = m_u\sqrt{\frac{y-1}{2}}$$

Therefore one has finally

$$\begin{aligned} \beta_d &= \pi - \arcsin(-m_u\sqrt{y}) \\ \frac{x_0}{\xi_u} &= \frac{1}{\cos\theta}\tanh^{-1}\left(\sqrt{\frac{y-1}{2}}\tan\theta\right) \end{aligned} \tag{3.17}$$

From the appropriate matching of its derivative

$$\partial_x\phi(0^+) - \partial_x\phi(0^-) = 2m\hbar^{-2}\phi(0)$$

and from the relations (3.17) one finally gets

$$\Lambda = \frac{\hbar^2\lambda}{m\xi_u} \quad \text{with } \lambda = m_u\sqrt{\frac{y-1}{2}} \tag{3.18}$$

In this configuration one has $V_u < c_d < c_u < V_d$.

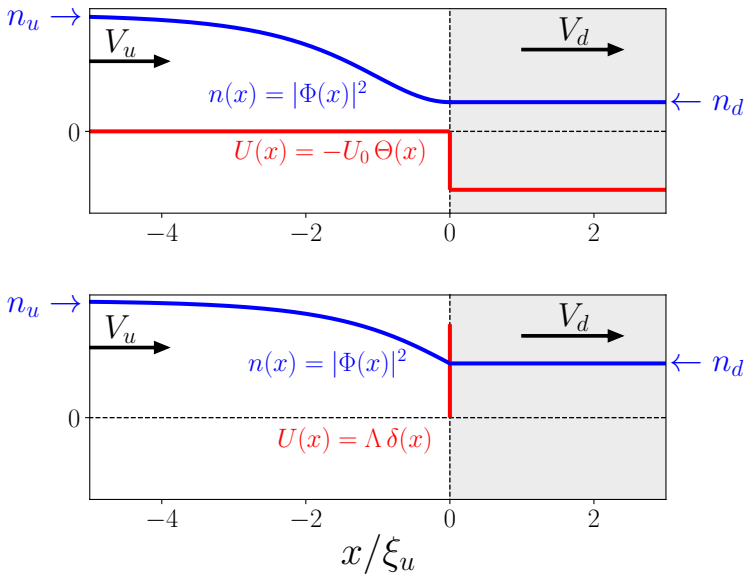

Figure 3.1: Schematic representation of the background density profile of the waterfall configuration (upper plot) and of the delta peak configuration (lower plot). The shaded region corresponds to the interior of the analog black hole (see the main text). The whole $x > 0$ region is supersonic, while the upstream region is asymptotically subsonic (i.e., in the limit $x \to -\infty$).

3.1.4 . Waterfall configuration

Here one imposes $g(x) = g$ to be a constant and $U(x) = -U_0\Theta(x)$ with $U_0 > 0$ and Θ the Heaviside function. The $\phi_u(x)$ profile is as defined in (3.15) for the δ peak configuration but with $x_0 = 0$ which means that here $\phi_u(x)$ is exactly one half of a dark soliton. One still has $\sin\theta = m_u$ and therefore, from the continuity of the order parameter ϕ in $x = 0$, one gets $n_u m_u^2 = n_d$, from which one can obtain $\exp i\beta_d = -i$ knowing that $\phi_d(x) = \sqrt{n_d}\exp i\beta_d$. Using first current conservation and then first relation in (3.11) one finally comes to

$$\frac{V_d}{V_u} = \frac{n_u}{n_d} = \frac{1}{m_u^2} = m_d = \left(\frac{\xi_d}{\xi_u}\right)^2 = \left(\frac{c_u}{c_d}\right)^2 \qquad \frac{U_0}{g n_u} = \frac{m_u^2}{2} + \frac{1}{2m_u} - 1 \tag{3.19}$$

In this configuration one has $V_u = c_d < c_u < V_d$.

The delta peak and waterfall configurations are depicted in Fig. 3.1. In this figure the region $x > 0$ is shaded in order to remind that it corresponds to the interior of the analog black hole. It is however important to recall that the precise location of the horizon separating the interior and the exterior of an analog black hole is ill-defined, see, e.g., the discussion in Sec. II.A of Ref. [86].

3.1.5 . First order fluctuations around the stationary condensate

In order to study spontaneous quantum effects let us first consider $\delta\hat{\Psi}$ in (3.2) as a small time-dependent classical field composed of normal modes of the form

$$\delta\Psi(x,t) = e^{ik_\alpha x}\left[\bar{u}_\alpha(x,\omega)e^{-i\omega t} + \bar{v}^*_\alpha(x,\omega)e^{i\omega t}\right] \tag{3.20}$$

with $\alpha = u$ for $x < 0$ and $\alpha = d$ for $x > 0$. Linearizing the classical Gross-Pitaevskii field equation (3.2) to first order in $\delta\Psi(x,t)$ and setting $X_\alpha = x/\xi_\alpha$ (which implies $k_\alpha x = m_\alpha X_\alpha$) and $\varepsilon_\alpha = \hbar\omega/g_\alpha n_\alpha$, one obtains

$$L_\alpha \begin{pmatrix} \bar{u}_\alpha \\ \bar{v}_\alpha \end{pmatrix} = \varepsilon_\alpha \begin{pmatrix} \bar{u}_\alpha \\ \bar{v}_\alpha \end{pmatrix} \tag{3.21}$$

where L_α is the Bogoliubov-de Gennes Hamiltonian defined as

$$L_\alpha = \begin{pmatrix} H_\alpha - im_\alpha\partial_{X_\alpha} & \phi_\alpha^2 \\ -(\phi_\alpha^*)^2 & -H_\alpha - im_\alpha\partial_{X_\alpha} \end{pmatrix} \tag{3.22}$$

with

$$H_\alpha = -\frac{1}{2}\partial^2_{X_\alpha} + 2|\phi_\alpha|^2 - 1$$

Taking the eigenvectors of Bogoliubov-de Gennes equation (3.21) for $X_\alpha \in \mathbb{R}$ to be of the form

$$\begin{pmatrix} \bar{u}_\alpha(x,\omega) \\ \bar{v}_\alpha(x,\omega) \end{pmatrix} = e^{iQ_l X_\alpha} \begin{pmatrix} U_l(x) \\ V_l(x) \end{pmatrix} \tag{3.23}$$

with $U_l(x)$ and $W_l(x)$ constant when $\phi_\alpha(x)$ is constant, i.e. when $|x| \to \infty$, the dimensionless wave vectors Q_l must be solutions of

$$(\varepsilon_\alpha - m_\alpha Q_l)^2 = \omega_B^2(Q_l) \tag{3.24}$$

where

$$\omega_B(Q_l) = Q_l\sqrt{1 + \frac{Q_l^2}{4}} \tag{3.25}$$

is the dimensionless Bogoliubov dispersion relation in a condensate at rest. The different branches of this dispersion relation are represented in Fig. 3.2.

The wavevectors Q_l are dimensionless and defined as $Q_l = q_l\xi_\alpha$. When the solutions Q_l are complex, one should discard the wave vectors with $\mathrm{Im}(Q_l) > 0$ for $\alpha = u$ and $\mathrm{Im}(Q_l) < 0$ for $\alpha = d$ in order to avoid divergence and keep only the evanescent solutions. The index l identifies the branch of the dispersion relation to which the excitation pertains and is actually a double index. Indeed, calling $in\,(out)$ a branch whose group velocity points towards (outwards) the horizon and eva an evanescent mode, for $\alpha = u$ one has $l \in \{0|in, 0|out, 0|eva\}$ whereas for $\alpha = d$ one has $l \in \{1|in, 1|out, 2|in, 2|out\}$ if $\omega < \Omega$ and $l \in \{1|in, 1|out, 2|eva\}$ if $\omega > \Omega$, with Ω a threshold that exists only for a supersonic flow and is defined by the positive energy $\varepsilon_d(Q_d^*) = \Omega_d$ for $\Omega_d = m_d Q_d^* - \omega_B(Q_d^*)$ being a maximum (FIG. 3.2), with $\Omega_d = \Omega/g_d n_d$.Thus Ω corresponds to the value of Q_l defined as

$$q^*\xi_d = Q_d^* = \left(-2 + m_d^2 + \frac{m_d}{2}\sqrt{8 + m_d^2}\right)^{\frac{1}{2}} \tag{3.26}$$

The 0 and 1 in/out modes are positive norm eigenvectors whereas the 2 in/out modes are negative norm eigenvectors. The group velocity of each mode is given by $\partial\omega/\partial q < 0$. A mode is therefore "in"-going when propagating towards $x = 0$ and "out"-going when propagating away from $x = 0$ [38]. Hence at $Q_l = Q_d^*$ one has exactly $\partial\omega_B/\partial Q_l = m_d$. But for $Q_l > Q^*$ one has $\partial\omega_B/\partial Q_l > m_d$, which means that the excitations have here a dimensionless group velocity larger than the dimensionless flow velocity $m_d > 1$: these are supersonic modes.

One can check that if $(\bar{u}_\alpha, \bar{v}_\alpha)^T$ is a solution of (3.21) for the eigenvalue ε_α so is $(\bar{v}_\alpha^*, \bar{u}_\alpha^*)^T$ for $-\varepsilon_\alpha$. And since both solutions describe the same excitation (3.20), we can take $\omega \in \mathbb{R}^+$ without loss of generality. This is related [87] to the fact that $|U_l|^2 - |V_l|^2$ can be positive, negative or null, this sign being the same as the one of $E_l = \varepsilon_\alpha - m_\alpha Q_l$. Finally, it has been shown [88] that the current J_l associated to the eigenvector $(\bar{u}_\alpha, \bar{w}_\alpha)^T$ is a conserved quantity defined by

$$J_l = \frac{i}{2}c\left[f\partial_{X_\alpha}f^* - f^*\partial_{X_\alpha}f + g\,\partial_{X_\alpha}g^* - g^*\partial_{X_\alpha}g\right] \tag{3.27}$$

with $f = e^{im_\alpha X_\alpha}\bar{u}_\alpha$ and $g = e^{-im_\alpha X_\alpha}\bar{v}_\alpha$.

3.1.6 . Downstream and Upstream Eigenvectors

Downstream, where the flow is supersonic, the $U_l(x)$ and $W_l(x)$ of the eigenvectors (3.23) of the linearized Gross-Pitaevskii field equation (3.21) are, for all configurations (flat profile, delta peak, waterfall), given by [38]

$$\begin{pmatrix} U_l(x) \\ V_l(x) \end{pmatrix} = \frac{1}{C_l}\begin{pmatrix} \left(\frac{Q_l^2}{2} + E_l\right)e^{i\beta_d} \\ \left(\frac{Q_l^2}{2} - E_l\right)e^{-i\beta_d} \end{pmatrix} \tag{3.28}$$

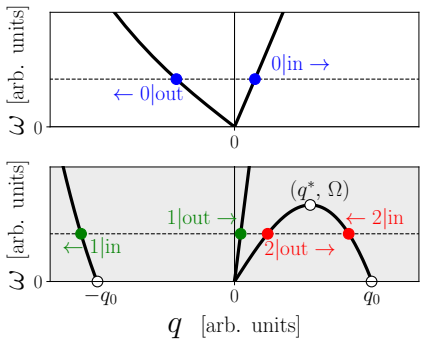

Figure 3.2: Graphical representation of the positive frequency part of the dispersion relation (3.24) in the far upstream subsonic (upper plot) and downstream supersonic (lower plot) regions. The background color of the lower plot is greyed for recalling that it concerns the interior of the analog black hole. In both plots the horizontal dashed line represents the angular frequency ω of a given excitation. In the upstream region there are two channels of propagation associated to each value of ω. In the downstream region there are four (two) propagation channels when ω is smaller (larger) than the threshold Ω defined in Eq. (3.26). The channels are denoted as 0, 1 or 2, with an additional "in" ("out") label indicating if the wave propagates towards (away from) the horizon. The direction of propagation of each channel is marked with an arrow.

with $E_l = \varepsilon_d - m_d Q_l$ and C_l a normalization constant. Defining the group velocity [38] as

$$V_g(Q_l) = \frac{\partial \omega}{\partial q_l} = c_\alpha \frac{\partial \varepsilon_\alpha}{\partial Q_l} = V_\alpha + c_\alpha \frac{Q_l \left(Q_l^2/2 + 1\right)}{E_l} \tag{3.29}$$

one can set the normalization constant to

$$C_l = |2\mathrm{Re}(E_l^* Q_l^2) V_g(Q_l)|^{\frac{1}{2}}$$

in order to have the normalization

$$|U_l|^2 - |W_l|^2 = \frac{\pm 1}{|V_g(Q_l)|^2} \tag{3.30}$$

This normalization allows $J_l = \pm 1$ in (3.27) for all non-evanescent modes.

Upstream, where the flow is subsonic, the $U_l(x)$ and $W_l(x)$ are not the same for all configurations. For the flat profile, the two components are the same as in the downstream region, with index d replaced by index u. On the contrary, for the other two configurations (delta peak and waterfall), one has [38]

$$\begin{pmatrix} U_l(x) \\ W_l(x) \end{pmatrix} = \frac{1}{D_l} \begin{pmatrix} \left[\frac{Q_l}{2} + \varepsilon_u/Q_l + i\chi(X_u)\right]^2 \\ \left[\frac{Q_l}{2} - \varepsilon_u/Q_l + i\chi(X_u)\right]^2 \end{pmatrix} \tag{3.31}$$

with D_l a normalization constant and $\chi(X_u) = \cos\theta \tanh\left[(X_u - X_0)\cos\theta\right]$ for $X_0 = x_0/\xi_u$. We choose to evaluate D_l at $X_u \to -\infty$. In order to obtain again $J_l = \pm 1$, the normalization constant is found to be, for real Q_l,

$$D_l = \sqrt{8} i \frac{Q_l}{|Q_l|} |E_l V_g(Q_l)|^{\frac{1}{2}} \left|\frac{\varepsilon_u}{Q_l}\right| \tag{3.32}$$

The choice of the phase of D_l allows the eigenvectors in (3.31) to have the same shape as the upstream eigenvectors of the flat profile configuration in the limit $\omega \to 0$ and is therefore motivated by practical and aesthetic reasons[4].

[4]For completeness, the normalization for Q_l complex, is given by

$$D_l = |V_g(Q_l)|^{\frac{1}{2}} \left| 8\mathrm{Re}[E_l(\varepsilon_u/Q_l)^2] + 4\varepsilon_u(\cos^2\theta)\frac{(Q_l - Q_l^*)^2}{|Q_l|^2} + 2i\varepsilon_u(\cos\theta)\frac{Q_l - Q_l^*}{|Q_l|^2}[Q_l^2 + (Q_l^*)^2] \right|^{\frac{1}{2}}$$

3.2 . THE "IN" AND "OUT" BASES FOR QUANTUM FLUCTUATIONS

3.2.1 . The quantum fluctuation operator $\delta\hat{\Psi}$

Considering the previous section 3.1, the normal modes defined in (3.20), can be written in the form

$$\left(\bar{u}_{j|in}e^{im_\alpha X_\alpha}\right)e^{-i\omega t}b_j+\left(\bar{v}_{j|in}e^{-im_\alpha X_\alpha}\right)^* e^{i\omega t}b_j^* \tag{3.33}$$

for the ingoing modes and in the form

$$\left(\bar{u}_{j|out}e^{im_\alpha X_\alpha}\right)e^{-i\omega t}c_j+\left(\bar{v}_{j|out}e^{-im_\alpha X_\alpha}\right)^* e^{i\omega t}c_j^* \tag{3.34}$$

for the outgoing modes for modes $j=0,1$. Because of the negative norm $|U_l|^2-|V_l|^2$ the mode 2 must be written

$$\left(\bar{u}_{2|in}e^{im_\alpha X_\alpha}\right)e^{-i\omega t}b_2^*+\left(\bar{v}_{2|in}e^{-im_\alpha X_\alpha}\right)^* e^{i\omega t}b_2 \tag{3.35}$$

for the ingoing mode and

$$\left(\bar{u}_{2|out}e^{im_\alpha X_\alpha}\right)e^{-i\omega t}c_2^*+\left(\bar{v}_{2|out}e^{-im_\alpha X_\alpha}\right)^* e^{i\omega t}c_2 \tag{3.36}$$

for the outgoing mode. This specific treatment of mode 2 will be required upon quantization by the fluctuation field $\delta\hat{\Psi}$ fulfilling the bosonic commutation relation

$$[\delta\hat{\Psi}(x,t),\delta\hat{\Psi}^\dagger(x',t)]=\delta(x-x') \tag{3.37}$$

The outgoing coefficients can then be expanded in the ingoing basis according to

$$\begin{aligned} c_j &\underset{j=0,1}{=} S_{j0}\,b_0+S_{j1}\,b_1+S_{j2}\,b_2^* \\ c_2^* &= S_{20}\,b_0+S_{21}\,b_1+S_{22}\,b_2^* \end{aligned} \tag{3.38}$$

The evanescent modes must be considered as outgoing modes, i.e.

$$\left(\bar{u}_{j|eva}e^{im_\alpha X_\alpha}\right)e^{-i\omega t}c_j^{eva}+\left(\bar{v}_{j|eva}e^{-im_\alpha X_\alpha}\right)^* e^{i\omega t}[c_j^{eva}]^* \tag{3.39}$$

for $j=0,2$. Then one obtains

$$c_j^{eva}\underset{j=0,2}{=}S_{j0}^{eva}\,b_0+S_{j1}^{eva}\,b_1+S_{j2}^{eva}\,b_2^* \tag{3.40}$$

Upon the quantization procedure $b_j\to\hat{b}_j$ and $b_j^*\to\hat{b}_j^\dagger$ with $\hat{b}_j$ and $\hat{b}_j^\dagger$ the annihilation and creation operators respectively of the ingoing scattering modes $j=0,1,2$, the quantum fluctuation operator $\delta\hat{\Psi}$ given in (3.3) can now be expanded as

$$\begin{aligned} \delta\hat{\Psi}(x,t) &= e^{ik_\alpha x}\int_0^\infty\frac{d\omega}{\sqrt{2\pi}}\sum_{L=0,1}\left[\bar{u}_L(x,\omega)e^{-i\omega t}\hat{b}_L(\omega)+\bar{v}_L^*(x,\omega)e^{i\omega t}\hat{b}_L^\dagger(\omega)\right] \\ &\quad+e^{ik_\alpha x}\int_0^\Omega\frac{d\omega}{\sqrt{2\pi}}\left[\bar{u}_2(x,\omega)e^{-i\omega t}\hat{b}_2^\dagger(\omega)+\bar{v}_2^*(x,\omega)e^{i\omega t}\hat{b}_2(\omega)\right] \end{aligned} \tag{3.41}$$

with $\bar{u}_L$ and $\bar{v}_L$ for $L=0,1,2$ being linear combinations of $\bar{u}_l$ and $\bar{v}_l$ given by the coefficients S_{ij} and S_{ij}^{eva}, as can be explicitly seen from relation (3.46)[5]. One has the usual bosonic commutation relations

$$[\hat{b}_L(\omega),\hat{b}_{L'}^\dagger(\omega)]=\delta_{L,L'}\delta(\omega-\omega') \tag{3.42}$$

The expression of the scattering coefficients S_{ij} and S_{ij}^{eva} is determined by the matching conditions.

[5]This expansion does not take into account the zero energy modes that are necessary to obtain the right bosonic commutation relation (3.37) for the field operator $\delta\hat{\Psi}$ (see Refs. [87, 89, 90]).

3.2.2 . Matching conditions and scattering modes

From the normal mode (3.20) and the eigenvectors (3.23) definitions, one can define

$$\Xi_l(x,\omega) = \begin{pmatrix} u_l(x,\omega) \\ v_l(x,\omega) \end{pmatrix} = \begin{pmatrix} \exp\left((iQ_l + m_\alpha)\right) U_l(x) \\ \exp\left((iQ_l - m_\alpha)\right) V_l(x) \end{pmatrix} \tag{3.43}$$

Calling Ξ_u^L a linear combination of the Ξ_l in the upstream region, i.e. with $l \in \{0|in, 0|out, 0|eva\}$, and Ξ_d a linear combination of the Ξ_l in the downstream region, i.e. with $l \in \{1|in, 1|out, 2|in, 2|out\}$ if $\omega < \Omega$ and $l \in \{1|in, 1|out, 2|eva\}$ if $\omega > \Omega$, one can define the two matching conditions as

$$\begin{aligned} \Xi_u^L(x=0,\omega) &= \Xi_d^L(x=0,\omega) \\ \frac{\hbar}{2m}\left[\frac{d\Xi_d^L}{dx}(x=0,\omega) - \frac{d\Xi_u^L}{dx}(x=0,\omega)\right] &= \Lambda\, \Xi_u^L(x=0,\omega) \end{aligned} \tag{3.44}$$

with $\Lambda = 0$ for the flat profile and waterfall configurations. These two conditions correspond to the (dis)continuity of the wavefunction and its first derivative implied by the Gross-Pitaevskii field equation (3.2). Then, the **scattering modes** $\Xi^L(x,\omega)$ are defined to be the three modes $L = 0, 1, 2$ generated by the scattering of the three ingoing modes $l = 0, 1, 2$ on the potential $U(x)$. They read

$$\Xi^L(x,\omega) = \begin{pmatrix} \bar{u}_L(x,\omega) e^{im_\alpha X_\alpha} \\ \bar{v}_L(x,\omega) e^{-im_\alpha X_\alpha} \end{pmatrix} \tag{3.45}$$

with $\bar{u}_L(x,\omega)$ and $\bar{v}_L(x,\omega)$ appearing in (3.41). In the upstream and downstream region, the three linear combination Ξ^0, Ξ^1 and Ξ^2 are given by[6]

$$\begin{aligned} \Xi_u^0 &= \Xi_{0|in} + S_{00}\, \Xi_{0|out} + S_{00}^{eva}\, \Xi_{0|eva} \\ \Xi_d^0 &= S_{10}\, \Xi_{1|out} + \Theta(\Omega-\omega)\, S_{20}\, \Xi_{2|out} + \Theta(\omega-\Omega)\, S_{20}^{eva}\, \Xi_{2|eva} \\ \Xi_u^1 &= S_{01}\, \Xi_{0|out} + S_{01}^{eva}\, \Xi_{0|eva} \\ \Xi_d^1 &= \Xi_{1|in} + S_{11}\, \Xi_{1|out} + \Theta(\Omega-\omega)\, S_{21}\, \Xi_{2|out} + \Theta(\omega-\Omega)\, S_{21}^{eva}\, \Xi_{2|eva} \\ \Xi_u^2 &= \Theta(\Omega-\omega)\, \left(S_{02}\, \Xi_{0|out} + S_{02}^{eva}\, \Xi_{0|eva}\right) \\ \Xi_d^2 &= \Theta(\Omega-\omega)\, \left(\Xi_{2|in} + S_{12}\, \Xi_{1|out} + S_{22}\, \Xi_{2|out}\right) \end{aligned} \tag{3.46}$$

where Θ is the Heaviside function and the $|S_{ll'}(\omega)|^2$ are the scattering coefficients of transmission or reflexion from l'-ingoing mode at energy $\hbar\omega$ to l-outgoing mode at same energy $\hbar\omega$. Defining the scattering matrix

$$S_{\omega<\Omega} = \begin{pmatrix} S_{00} & S_{01} & S_{02} \\ S_{10} & S_{11} & S_{12} \\ S_{20} & S_{21} & S_{22} \end{pmatrix} \tag{3.47}$$

the current conservation can be written as

$$S^\dagger \eta S = \eta = S \eta S^\dagger \qquad \eta = \mathrm{diag}(1,1,-1) \tag{3.48}$$

which is implied by the bosonic canonical commutation relations that the creation and annihilation operators must fulfill. Note that the S_{ij}^{eva} coefficients do not appear in the S matrix since, being related to evanescent modes, they are not involved in current conservation. Note also that for $\omega > \Omega$ the mode 2 becomes evanescent and therefore the matrix S becomes the 2×2 matrix

$$S_{\omega>\Omega} = \begin{pmatrix} S_{00} & S_{01} \\ S_{10} & S_{11} \end{pmatrix} \tag{3.49}$$

with current conservation $S^\dagger S = S S^\dagger = \mathrm{diag}(1,1)$.

[6] The x and ω dependence has been dropped for legibility.

3.2.3 . Propagation channels and quantum modes

In order to summarize the main points of our approach, it must recall that the decomposition (3.3) is meaningful in a regime of small quantum fluctuations where the operator $\hat{\Psi}$ can be treated within a Bogoliubov approach. In this case $\hat{\Psi}$ is naturally expanded along the asymptotic ingoing and outgoing channels of the flow. The dispersion relation of elementary excitations (3.24) in the asymptotic upstream subsonic and downstream supersonic regions ($x \to -\infty$ and $+\infty$, respectively) is of Bogoliubov type, with a Doppler shift accounting for the finite velocity of the background.

From the identification of the relevant channels and of their direction of propagation it is possible to define quantum modes forming a basis enabling to describe all the elementary excitations of the background flow. To each such mode is associated a quantum operator: $\hat{b}_i^\dagger(\omega)$ and $\hat{b}_i(\omega)$ ($i = 0$, 1 or 2) are the creation and annihilation operators of an excitation of energy $\hbar\omega$ which is ingoing in channel $i|\mathrm{in}$ and scattered by the horizon onto the three outgoing channels $0|\mathrm{out}$, $1|\mathrm{out}$ and $2|\mathrm{out}$. Since each $\hat{b}$ mode is associated with a single ingoing channel, it is denoted as an "ingoing mode". It is also relevant to define "outgoing modes" associated with a single outgoing channel. The corresponding operators are denoted as $\hat{c}_i(\omega)$ and $\hat{c}_i^\dagger(\omega)$. For instance $\hat{c}_0^\dagger$ is the creation operator of an excitation where the three ingoing channels are implied and form an outgoing excitation in channel $0|\mathrm{out}$. The corresponding quantum mode is the analogous Hawking mode. As can be seen from the quantization of the coefficients in (3.38), the outgoing modes are related to the incoming ones via the scattering matrix $S(\omega)$:

$$\begin{pmatrix} \hat{c}_0 \\ \hat{c}_1 \\ \hat{c}_2^\dagger \end{pmatrix} = \begin{pmatrix} S_{00} & S_{01} & S_{02} \\ S_{10} & S_{11} & S_{12} \\ S_{20} & S_{21} & S_{22} \end{pmatrix} \begin{pmatrix} \hat{b}_0 \\ \hat{b}_1 \\ \hat{b}_2^\dagger \end{pmatrix}, \tag{3.50}$$

where all the ω dependencies have been omitted for legibility. The modes $\hat{b}_2$ and $\hat{c}_2$ are particular in the sense that they have a negative norm and should be quantized inverting the usual role of the creation and annihilation operators [87] in order to satisfy the standard Bose commutation relations. The mode $\hat{c}_2$ is analogous to what is called the partner is the context of Hawking radiation. We denote the mode associated with $\hat{c}_1$ the companion; Lorentz invariance prevents such a mode to exist in a gravitational black hole, but it is unavoidable in an analog system.

The fact that the outgoing operators fulfil the canonical commutation relations implies that the scattering matrix $S(\omega)$ obeys the skew-unitarity condition (3.48).For $\omega > \Omega$ the mode with subscript 2 (the partner) disappears because the corresponding ingoing and outgoing channels do (cf. Fig. 3.2) and the S-matrix becomes 2×2 and unitary. In this case the vacuum of the outgoing modes (the $\hat{c}$'s) is identical to the vacuum of the incoming ones (the $\hat{b}$'s) and the analogous Hawking effect disappears. The value of the corresponding threshold energy is given in (3.26). It has been shown in Ref. [86] that the three-mode system describing the analogous black hole horizon can be modeled by an optical setup simply composed of a parametric amplifier and a beam splitter, as depicted in Fig. 4.1.

4 - VIOLATION OF BELL INEQUALITIES IN AN ANALOG BLACK HOLE

In this chapter we conduct a theoretical study of violation of bipartite and tripartite Bell inequalities in an analog black hole implemented in the flow of a quasi-one dimensional Bose-Einstein condensate[1]. In the BEC system we consider, the asymptotic upstream region is subsonic while the asymptotic downstream region is supersonic. Such a flow induces the mismatch of the asymptotic dispersion relations illustrated in Fig. 3.2. In the downstream region, the appearance of additional (negative norm) channels gives rise to the Bogoliubov transformation (3.50) which enforces the mismatch (4.82) between the ingoing and outgoing vacua. Therefore, in an analog system, the Hawking radiation appears to be driven by the very same mechanism as the one suggested by Hawking for the radiation of a gravitational black hole [11] : the vacuum of the outgoing modes is not the same as the vacuum of the ingoing modes.

The Bogoliubov transform we consider is attached to a standard quadratic Bose Hamiltonian [87] and to the production of correlated and entangled pairs of quasi-particles. In this perspective, the sonic character of the Doppler-shifted dispersion relation in the long wavelength limit not only results in the low energy divergence of the coefficients of the S matrix involving the incoming negative norm mode, i.e. the $S_{j,2}$ coefficients, [92] and in a finite analog Hawking temperature [93, 94], but also in the existence of three and not simply two quasi-particle modes. It will be shown that such a three-quasi-particle system can then be mimicked by a simple optical setting involving a standard parametric downconversion process and the presence of a beam-splitter as illustrated in Fig. 4.1. In this setup, the presence of the beam-splitter incorporates the greybody factor which - from a gravitational perspective - accounts for the back-scattering of Hawking radiation by the curved geometry surrounding the black hole [86].

We will not address here the question of the actual experimental demonstration of quantum entanglement in a BEC analog black hole (see, e.g., Ref. [86] for a recent discussion) but rather take the theoretical analysis a little further by asking: which general insight can we reach by studying quantum correlations of the Hawking signal emitted by an analog black hole? A natural approach for such an investigation is a test of nonlocality via violation of Bell inequality. The epistemological query of refutation of local hidden variable theories has already received an unambiguous answer in many contexts (see, e.g., Ref. [95] and references therein) and important progresses have also been achieved in the field of BEC matter waves [96, 97, 98, 99] we consider here. Such a test is nonetheless a nontrivial extension of the scope of analog gravity and would constitute a primer for continuous variables entanglement in a matter wave environment (see also Refs. [100, 101, 102] for related proposals). In view of future experimental studies it is relevant to quantitatively evaluate in realistic configurations to what extent Bell inequalities can be violated in BEC analogs. This is a natural question to ask, all the more so as we argue in the following that in some (exotic) limits the analog black hole we consider exactly realizes a Einstein-Podolsky-Rosen (EPR) pair. Furthermore, as will be shown, the specifics of the system provide a natural testing ground for genuine *tripartite* nonlocality. Our theoretical investigation of the matter reveals an unexpected generic feature of black hole analogs: in the long wave-length limit, the state of the system realizes an infinite sum of degenerate Greenberger-Horne-Zeilinger (GHZ) states. Interestingly, thanks to the continuous nature of its degrees of freedom, and despite the clear GHZ nature of its long wavelength modes, the analog system remains entangled after partial tracing.

4.1 . BELL INEQUALITIES : A SHORT HISTORY

4.1.1 . Premisses

In quantum mechanics two canonically conjugate variables cannot be determined simultaneously with arbitrary precision, i.e. for "two physical quantities described by non-commuting operators, the

[1]Regarding the entanglement properties of our system, a primary reference for this chapter is Ref. [86]. Furthermore, a preliminary work on bipartite violation of Bell inequalities is to be found in the unpublished Ref. [91].

knowledge of one precludes the knowledge of the other" and either "these two quantities cannot have simultaneous reality" or the quantum wave function encoding our knowledge of the system provides an incomplete description of reality [4]. It is then not possible to construct a state in which they are both perfectly known, viz. well-defined simultaneously. With two non-commuting observables, such as position and momentum, the measurement (i.e. the experimental setting) decides which one is real or definite and which one is not, since reducing the uncertainty (i.e. the variance) of one increases the uncertainty of the other. According to Einstein, Podolsky and Rosen this is on its own a puzzling outcome and their famous 1935 paper [4] is mainly about the inconsistent definition of reality implied by the existence of non-commuting observables. The *Gedankenexperiment* of the non-factorizable two-particle state that is presented there, is brought into as a proof of the inconsistency of quantum mechanics formalism.

To this end, Einstein, Podolsky and Rosen (EPR) define a criterion taken "not as a necessary, but merely a sufficient, condition of reality", which reads : "[a] **sufficient condition for the reality of a physical quantity is the possibility of predicting it with certainty, without disturbing the system**" [4]. In quantum mechanics this is possible : (1) when the measurement is performed on an eigenstate of the measured quantity ; (2) when after the measurement of one subsystem the state of the other subsystem is known with certainty from the outcome of the first measurement. When dealing only with one-particle system, the commutation relation, for example, between the position $\hat{x}$ and the momentum $\hat{p}_x$ is given by

$$[\hat{x}, \hat{p}_x] = i\hbar \tag{4.1}$$

In the $\{|x\rangle\}$ basis, on can define the one-particle wave-function ψ_0 as

$$\begin{aligned} \psi_{p_0}(x) = e^{ip_0 x/\hbar} \qquad \hat{p}_x = -i\hbar\partial_x \\ \hat{p}_x \psi_{p_0}(x) = p_0\, \psi_{p_0}(x) \end{aligned} \tag{4.2}$$

and consider the EPR criterion to be fulfilled since ψ_{p_0} is here an eigenfunction of the momentum operator $\hat{p}_x$. Then one can say that, when the system is in state $|\psi_{p_0}\rangle$, the physical quantity p_0 is "an element of physical reality" since $\hat{p}_x$ can take a "particular value" : one says that the particle associated to the wave function ψ_{p_0} has a *definite* momentum p_0. But taking the position operator $\hat{x}$ for the particle in state $|\psi_{p_0}\rangle$ one obtains by definition

$$\hat{x}\, \psi_{p_0}(x) = x\, \psi_{p_0}(x) \tag{4.3}$$

with x being *indefinite* since corresponding to any real value. Therefore $\psi_{p_0}(x)$ is not an eigenfunction of operator $\hat{x}$ and hence position is not in this case "an element of physical reality" since its measurement "disturbs the particle and thus alters its state" yielding a random (i.e. impredictable) outcome [4]. For non-commuting observables, measuring one observable in the eigenstate of the other alters the system state, which implies that "*when the operators corresponding to two physical quantities do not commute the two quantities cannot have simultaneous reality*" [4] or that the quantum wave function formalism is incomplete.

And here comes the *Gedankenexperiment* of the two-particle non-factorizable state to make things worse. Indeed, for a two-particle system described by the wave function $\Psi(x_1, x_2)$ one can define the observables

$$\hat{X}_\pm = \hat{x}_1 \pm \hat{x}_2 \qquad \hat{P}_\pm = \hat{p}_1 \pm \hat{p}_2 \tag{4.4}$$

It can be easily checked that $\hat{X}_-$ and $\hat{P}_+$ commute thus making it possible for state $|\Psi\rangle$ to be simultaneously eigenvector of both $\hat{X}_-$ and $\hat{P}_+$, let us say for eigenvalues u and 0 respectively, i.e.

$$\hat{X}_- |\Psi\rangle = u\, |\Psi\rangle \qquad \hat{P}_+ |\Psi\rangle = 0 \tag{4.5}$$

Thus, knowing that the initial state $\langle x_1, x_2|\Psi\rangle = \Psi(x_1, x_2)$ is characterized by definite relative position u and definite total momentum 0, it can be inferred from (4.4) that measuring $\hat{x}_1$ or $\hat{p}_1$ on system 1 (one particle) will *immediately* constrain system 2 (the other particle) to be either in $x_2 = x_1 - u$ or in $p_2 = -p_1$ respectively. Let us say that the measurement on subsystem 1 (either $\hat{x}_1$ or $\hat{p}_1$) and the measurement on subsystem 2 (either $\hat{x}_2$ or $\hat{p}_2$ respectively) are space-like events, i.e. that they are causally disconnected.

Then **one faces a contradiction unless quantum mechanics is incomplete**. Indeed : (1) both x_1 and p_1 are *random* outcomes ; (2) based on the *random* outcome of its own measurement of position or momentum, observer 1 now knows "with certainty" and "without disturbing the system" what will be the outcome of the measurement of position or momentum (respectively) by observer 2, i.e. observe 1 knows that if x_1 is measured then $x_2 = x_1 - u$ and if p_1 is measured then $p_2 = -p_1$; (3) since, due to the measurement on the first subsystem, the second subsystem ends up either in a state of definite position or definite momentum while not knowing which measurement has been performed on subsystem 1, its definite values must have been settled from the start, thus making the subsystem 2 in a state of definite position x_2 **and** definite momentum p_2 ; (4) but this is forbidden by non-commutativity and is therefore contradictory unless the x_i and p_i (with $i = 1, 2$) are some functions $x_i(\lambda)$ and $p_i(\lambda)$ of some unknown or hidden possibly random[2] variable λ that would justify the correlations by making at the same time quantum formalism incomplete.

The contradiction arises from the fact that the two measurements are causally disconnected and that the collapse of the wave function after measurement 1 appears to be as a **non-local** phenomenon. We will therefore consider a process to be non-local if not governed by relativistic causality. This does not mean that it violates relativistic causality (indeed, **it does not**) but that the correlations exhibited by the system cannot be explained by any (classical) relativistic propagation of information and must therefore be of quantum nature. This being said, it appears clearly that what really bothers Einstein, Podolski and Rosen, is not *non-locality* per se but rather quantum *contextuality*[3], the phenomenon of non-locality being for them just (so to say) a proof of inconsistency of quantum mechanics. Indeed, what seems to be really inconceivable for Einstein, Podolski and Rosen is that the "same reality", i.e. the state of system 2 and therefore the "reality" of its momentum or position, "depend upon the process of measurement carried out on the first system" which should "not disturb the second system in any way" : in other words, they simply deny, by their reasoning, that "two or more physical quantities can be regarded as simultaneous elements of reality *only when they can be simultaneous measured or predicted* " [4]. From there, they conclude that the very existence of non-commuting observables in the formalism of quantum mechanics implies that "the quantum mechanical description of reality given by the wave function is not complete" [4]. It is therefore worth stressing that the question of non-locality of quantum mechanics is not addressed per se in the EPR paper but is rather considered as a decisive inconsistency in a more general inspection about the notion of "reality" implied by the existence of non-commuting observables in quantum mechanics formalism.

As it is well known Bohr (1935) disagreed with the previous argumentation by Einstein, Podolsky and Rosen [6]. Understanding that the real physical question asked by the EPR paper [4] was the one of the "criterion of reality" defining "physical reality", he argued that quantum mechanics provides a "completely rational description of physical phenomena" [6]. This is why, according to Bohr, the fact that one can never "attach definite values to both of two canonically conjugate variables" is not an argument for incompleteness of quantum mechanics but rather implies "a final renunciation of the classical ideal of causality" and a "radical revision" of what is "physical reality", hence a notion of "*individuality* completely foreign to classical physics" [6]. Considering position and momentum, he claims that quantum mechanics is nothing else than "a rational discrimination between essentially different experimental arrangements and procedures which are suited either for an unambiguous use of the idea of space location, or for a legitimate application of the conservation theorem of momentum" : this characteristics he calls "***complementarity***", specifying that it has to do with a "*free choice* on what we want to measure" and not "with an ignorance of the value of certain physical quantities, but with the impossibility of defining these quantities in an unambiguous way" [6][4].

[2] It has to be not random if one wants to restore determinism.

[3] We will refer by "quantum *contextuality*" to the fact that it is the chosen quantum measurement that selects what has to be taken as real. According to quantum contextuality, the definition of reality is then contextual to the undertaken experiment. This is related mathematically to the *non-commutativity* of canonically conjugated observables.

[4] "The last remarks apply equally well to the special problem treated by Einstein, Podolsky and Rosen, which has been referred to above, and which does not actually involve any greater intricacies than the simple examples discussed above. The particular quantum-mechanical state of two free particles, for which they give an explicit

If the answer by Bohr is generically about the completeness of quantum mechanics, the one by Schrödinger (1935) is specifically about the entangledness of the EPR state [5][5]. The fact that two systems that have interacted cannot be described by two independent wave functions but must be apprehended as a unique (entangled) state, is considered by Schrödinger as being not "*one* but rather *the* characteristic trait of quantum mechanics, the one that enforces its entire departure from classical lines of thought" : only a measure on one subsystem (after which the state of the other subsystem can be "inferred simultaneously") can disentangle them since a new measurement of the first subsystem will no longer simultaneously affect the second one [5][6]. As can be seen **entanglement** is defined by Schrödinger as characterizing the state of a system where a measurement of a subsystem can instantly modify the state of the other subsystem no matter how remote the two subsystems are. Interestingly, after a first measurement on one subsystem, the two subsystems are disentangled since a second measurement on one of the two subsystems would not modify the state of the other.

The question of non-locality raised by the EPR paper is explicitly addressed by Bell in his 1964 paper [7] in which he gave a mathematical formulation of the locality constraints of the phenomenon, thus making it possible to test local-hidden-variable theories experimentally (see 4.1.3). Indeed, in 1957, Bohm and Aharonov [103] had already suggested to test in a realistic discrete setting the EPR paradox through the "polarization properties of pairs of photons". Instead of spin singlet state (at first considered), discrete-variable two-photon states were implemented in experiments relying on photon counting [8, 104]. Then, the 1964 argument by Bell [7] to rule out hidden-variable theories was generalized in 1969 by Clauser et. al. [105] in the (here adopted) CHSH inequality for the study of "the polarization correlation of a pair of optical photons". Therefore, whereas the EPR paradox was first thought in a continuous variable setting, Bell inequalities were first derived in a discrete variable setting[7]. Thus, experiments confirming the completeness of quantum mechanics were performed [107], among others, by Freedman and Clauser in 1972 [108], with time-varying analyzers by Aspect, Dalibard and Roger in 1982 [109] for two-particle systems and in 2000 by Zeilinger et al. [110] with an entangled three-photon GHZ state and an experimental setting relying, in this last case, on a Mermin-type argument [111, 112] for the refutation of the EPR incompleteness assumption rather than on a Bell-type inequality. If, in the wake of these experiments, the EPR paradox and Bell inequalities were understood to be an invaluable resource for quantum technologies [107], nowadays the question is not only investigated with small systems of a few particles but also in "massive many-particle systems", among which atomic Bose-Einstein condensates (BECs) appear to be "particularly well suited to investigate nonclassical phenomena at the quantum-to-classical boundary" through measurement of collective spin correlations [99][8], therefore similarly to what was first suggested

mathematical expression, may be reproduced, at least in principle, by a simple experimental arrangement, comprising a rigid diaphragm with two parallel slits, which are very narrow compared with their separation, and through each of which one particle with given initial momentum passes independently of the other. If the momentum of this diaphragm is measured accurately before as well as after the passing of the particles, we shall in fact know the sum of the components perpendicular to the slits of the momenta of the two escaping particles, as well as the difference of their initial positional coordinates in the same direction; while of course the conjugate quantities, i.e., the difference of the components of their momenta, and the sum of their positional coordinates, are entirely unknown. In this arrangement, it is therefore clear that a subsequent single measurement either of the position or of the momentum of one of the particles will automatically determine the position or momentum, respectively, of the other particle with any desired accuracy; at least if the wave-length corresponding to the free motion of each particle is sufficiently short compared with the width of the slits. As pointed out by the named authors, we are therefore faced at this stage with a completely free choice whether we want to determine the one or the other of the latter quantities by a process which does not directly interfere with the particle concerned" [6].

[5] It is indeed (see [8]) Schrödinger himself that introduced the notion of entanglement in his answer [5] to the EPR paper [4].

[6] "Another way of expressing the peculiar situation is : the best possible knowledge of a *whole* does not necessarily include the best possible knowledge of all its *parts*, even though they may be entirely separated and therefore virtually capable of being "best possibly known", i.e. of possessing, each of them, a representative of its own" [5].

[7] The question of translating Bell inequalities in terms of continuous unbounded variables is still an open one [8]. Most of the works testing Bell inequalities with continuous variables rely on some discretization procedure of the possible outcomes. This is for example the case with the GKMR pseudospins used in this work [106].

[8] More specifically, what is considered is the splitting of one BEC in two BECs that exhibit bipartite entanglement between the collective spins of each BEC [99].

by Bohm for spin correlations [103]. We will not dive further in the history of Bell inequalities and just stress that experiments such as Colciaghi's [99] suggest that the pseudospin approach of our work can eventually be translated to a realistic experimental setting[9].

Before considering the violation of Bell inequalities in our analog black-hole (from 4.2 on), we will present in the following : the notions of entanglement and non-locality with continuous variables as stated by the EPR paper (see 4.1.2) ; the mathematical constraints on local realism implied by Bell inequalities (see 4.1.3) ; the measures of genuine bipartite and tripartite entanglement and nonlocality (see 4.1.4).

4.1.2 . The 1935 EPR : Entanglement and Non-locality with Continuous Variables

In EPR the notion of entanglement appears without any reference to a discrete variable setting. The thought experiment is indeed conducted within a fully continuous variable approach, with the position $\hat{x}$ and momentum $\hat{p}$ non-commuting operators involved. As a matter of fact, in the two-particle state invoked in the paper, the two particles are correlated in position and momentum. Thus, despite later insightful research based on discrete variable systems, the notion itself of entanglement came out from a continuous variable setting after being more explicitly introduced by Schrödinger in his reply to the EPR paper [8]. Indeed, as stated in 4.1.1, the two particles sharing the entangled state (4.11) are perfectly correlated in their positions and momenta, thus making it possible to infer (with absolute certainty) the outcome of a position (momentum) measurement on particle 2 from a position (momentum) measurement on particle 1 and without disturbing the state of the second particle since the first measure has indeed disentangled the state of the full system. Then, because EPR's realism postulates an *objective reality* and refuses the idea of an *action at a distance*, it is inferred that both position and momentum of the second particle must be *predetermined*. But such states of both definite position and momentum are forbidden by quantum mechanics and consequently, according to the EPR reasoning, quantum mechanics formalism must be incomplete.

In order to understand the quantum structure of such a state, let us define, as usual, the single-particle position $\{|x\rangle\}$ and momentum $\{|p\rangle\}$ representations

$$|x\rangle = \frac{1}{\sqrt{2\pi}} \int_{-\infty}^{+\infty} dp\, e^{-ipx}\, |p\rangle \qquad |p\rangle = \frac{1}{\sqrt{2\pi}} \int_{-\infty}^{+\infty} dx\, e^{ipx}\, |x\rangle \tag{4.6}$$

and

$$\langle x|p\rangle = \frac{1}{\sqrt{2\pi}} e^{ipx} \qquad \langle x'|x\rangle = \delta(x-x') \qquad \langle p'|p\rangle = \delta(p-p') \qquad \int_{-\infty}^{+\infty} dp\, e^{ipx} = 2\pi\, \delta(x) \tag{4.7}$$

with x and p dimensionless and δ the Dirac-function. The two-particle state vector is then written

$$|\psi\rangle = \int_{-\infty}^{+\infty} dx_1 dx_2\, \psi(x_1,x_2)\, |x_1,x_2\rangle = \int_{-\infty}^{+\infty} dp_1 dp_2\, \bar{\psi}(p_1,p_2)\, |p_1,p_2\rangle \tag{4.8}$$

Considering [5] the state (4.8) as being the eigenstate of operators $\hat{X}_- = \hat{x}_1 - \hat{x}_2$ (relative position) and $\hat{P}_+ = \hat{p}_1 + \hat{p}_2$ (total momentum) for real eigenvalues u and 0 respectively (see (4.4)), i.e.

$$\hat{X}_-\, |\psi\rangle = u\, |\psi\rangle \qquad \hat{P}_+\, |\psi\rangle = 0 \qquad [\hat{X}_-, \hat{P}_+] = 0 \tag{4.9}$$

one can define, for u some real constant and C some *vanishing* normalization constant, the unphysical and unnormalizable state

$$\langle x_1,x_2|\psi\rangle = \psi(x_1,x_2) = C\, \delta(x_1 - x_2 - u) \quad \Leftrightarrow \quad \langle p_1,p_2|\psi\rangle = \bar{\psi}(p_1,p_2) = C\, \delta(p_1+p_2)\, e^{ip_2 u} \tag{4.10}$$

i.e.

$$|\psi\rangle = C \int_{-\infty}^{+\infty} dx\ |x, x-u\rangle = C \int_{-\infty}^{+\infty} dp\, e^{-ipu}\, |p,-p\rangle \tag{4.11}$$

[9] It must be noted that the collective pseudospins used in [99] are not the the GKMR pseudo-spins introduced in Ref. [106] and here adopted in our work (see 4.4).

as being the limiting case of a physical and normalizable two-mode squeezed state with squeezing parameter r, which in the position basis $\{|x\rangle\}$ representation reads[10]

$$\begin{aligned}
\psi(x_1,x_2) &= \frac{1}{\sqrt{\pi}}\exp\left\{-\frac{(x_1+x_2+v)^2}{4}e^{-2r}-\frac{(x_1-x_2-u)^2}{4}e^{2r}\right\}\\
\psi(x_1+x_2,x_1-x_2) &= \left[\frac{1}{(2\pi e^{2r})^{1/4}}\exp\left\{-\frac{(x_1+x_2+v)^2}{4}e^{-2r}\right\}\right]\left[\frac{1}{(2\pi e^{-2r})^{1/4}}\exp\left\{-\frac{(x_1-x_2-u)^2}{4}e^{2r}\right\}\right]\\
&= C\left[\frac{1}{(2\pi e^{-2r})^{1/4}}\exp\left\{-\frac{(x_1-x_2-u)^2}{4}e^{2r}\right\}\right]\\
&\underset{r\to+\infty}{\longrightarrow} C\,\delta(x_1-x_2-u)
\end{aligned} \tag{4.12}$$

with v also real and C a vanishing constant. In the momentum basis $\{|p\rangle\}$ representation, one would have

$$\bar{\psi}(p_1,p_2)\frac{1}{\sqrt{\pi}}\exp\left\{-\frac{(p_1-p_2)^2}{4}e^{-2r}-\frac{(p_1+p_2)^2}{4}e^{2r}+\frac{i}{2}\left[v(p_1+p_2)+u(p_2-p_1)\right]\right\}\underset{r\to+\infty}{\longrightarrow} C\,\delta(p_1+p_2)\,e^{ip_2u} \tag{4.13}$$

Let us indeed consider the unitary two-mode displacing and squeezing operator $\hat{D}_1(\alpha_1)\hat{D}_2(\alpha_2)\hat{S}(\zeta)$ with, for $(j=1,2)$,

$$\hat{D}_j(\alpha_j)=\exp\left\{\alpha_j a_j^\dagger-\alpha_j^*\hat{a}_j\right\}\qquad\Rightarrow\qquad \hat{D}_j^\dagger(\alpha_j)a_j\hat{D}_j(\alpha_j)=\hat{a}_j+\alpha_j \tag{4.14}$$

and[11]

$$\begin{aligned}
&\hat{S}(\zeta)=\exp\left\{\zeta^* a_1a_2\ -\zeta\hat{a}_1^\dagger a_2^\dagger\right\}\\
&\hat{A}_j=\hat{S}^\dagger(\zeta)\hat{a}_j\hat{S}(\zeta)\\
&\hat{S}^\dagger(\zeta)\hat{a}_1\hat{S}(\zeta)=\hat{a}_1\cosh r-\hat{a}_2^\dagger\,e^{i\theta}\sinh r\\
&\hat{S}^\dagger(\zeta)\hat{a}_2\hat{S}(\zeta)=\hat{a}_2\cosh r-\hat{a}_1^\dagger\,e^{i\theta}\sinh r
\end{aligned} \tag{4.15}$$

for $\zeta=re^{i\theta}$. In the position representation, the two-mode displaced squeezed vacuum is then given[12] by

$$\langle X_1,X_2|\,\hat{S}^\dagger(\zeta)\hat{D}_2^\dagger(\alpha_2)\hat{D}_1^\dagger(\alpha_1)\hat{a}_1\hat{a}_2\hat{D}_1(\alpha_1)\hat{D}_2(\alpha_2)\hat{S}(\zeta)\,|0_1,0_2\rangle_A=\langle X_1|\,(\hat{A}_1+\alpha_1)\,|0_1\rangle_A\,\langle X_2|\,(\hat{A}_2+\alpha_2)\,|0_2\rangle_A=0 \tag{4.16}$$

with $|0_1,0_2\rangle_A$ the vacuum of A_j. Using the dimensionless definitions

$$\hat{X}_j=\frac{1}{\sqrt{2}}\left(\hat{A}_j+\hat{A}_j^\dagger\right)\qquad \hat{P}_j=\frac{1}{i\sqrt{2}}\left(\hat{A}_j-\hat{A}_j^\dagger\right) \tag{4.17}$$

and

$$\langle X_j|\,A_j=\frac{1}{\sqrt{2}}\left(X_j+\frac{d}{dX_j}\right)\qquad \langle P_j|\,A_j=\frac{1}{\sqrt{2}}\left(i\frac{d}{dX_j}+iP_j\right) \tag{4.18}$$

this two-mode displaced squeezed vacuum is straightforwardly proven to be associated to the Gaussian wave function

$$\varphi_0(X_1,X_2)\propto\exp\left\{-\frac{(X_1+\sqrt{2}\alpha_1)^2}{2}\right\}\exp\left\{-\frac{(X_2+\sqrt{2}\alpha_2)^2}{2}\right\} \tag{4.19}$$

or, in the momentum representation,

$$\bar{\varphi}_0(P_1,P_2)\propto\exp\left\{-\frac{(P_1-i\sqrt{2}\alpha_1)^2}{2}\right\}\exp\left\{-\frac{(P_2-i\sqrt{2}\alpha_2)^2}{2}\right\} \tag{4.20}$$

[10] To be consistent with the definitions (4.17) of our $\hat{x}$ and $\hat{p}$ operators, the factor $1/4$ in the exponential is taken in order to have $\langle X_i^2\rangle=\int_{-\infty}^{+\infty}dx_idx_j\,x_i^2|\psi(x_i,x_j)|^2=1/2$ when $r=0$ and the two particles are uncorrelated.

[11] See Appendix A.1 for the squeezing operator $\hat{S}(\zeta)$, where it is named $\hat{A}$ in Rel. (A.12).

[12] $\hat{S}^\dagger(\zeta)\hat{D}_2^\dagger(\alpha_2)\hat{D}_1^\dagger(\alpha_1)\hat{a}_1\hat{a}_2\hat{D}_1(\alpha_1)\hat{D}_2(\alpha_2)\hat{S}(\zeta)=\hat{S}^\dagger(\zeta)\hat{D}_1^\dagger(\alpha_1)\hat{a}_1\hat{D}_1(\alpha_1)(\hat{S}(\zeta)\hat{S}(\zeta)^\dagger)\hat{D}_2^\dagger(\alpha_2)\hat{a}_2\hat{D}_2(\alpha_2)\hat{S}(\zeta)$.

Setting ζ real with $\theta = 0$ and using (4.17) and (4.15), one obtains

$$\begin{aligned} \hat{X}_1 &= \hat{x}_1 \cosh r - \hat{x}_2 \sinh r \\ \hat{P}_1 &= \hat{p}_1 \cosh r + \hat{p}_2 \sinh r \end{aligned} \tag{4.21}$$

and similarly for $\hat{X}_2$ and $\hat{P}_2$ just by taking $1 \leftrightarrow 2$ in the previous expressions (4.21). Then, in these expressions the operators $\hat{X}_i$, $\hat{P}_i$, $\hat{x}_i$ and $\hat{p}_i$ can be replaced by the associated eigenvalues X_i, P_i, x_i and p_i, respectively[13]. Using these quantities in (4.19) and (4.20), for

$$\alpha_1 = \frac{1}{2\sqrt{2}} \left(v\, e^{-r} - u\, e^{r} \right) \qquad \alpha_2 = \frac{1}{2\sqrt{2}} \left(v\, e^{-r} + u\, e^{r} \right) \tag{4.22}$$

yields straightforwardly (4.12) and (4.13). Let us finally remark that for a single mode squeezing, i.e. $1 = 2$ in (4.15), by the same reasoning, the wave function of the displaced squeezed vacuum is given by

$$\psi(x) = \frac{e^r}{\sqrt{\pi}} \exp\left\{ -\frac{(x + \sqrt{2}\alpha)^2}{2} e^{2r} \right\} \underset{r \to \infty}{\longrightarrow} \delta(x + \sqrt{2}\alpha) \tag{4.23}$$

for α real, thus describing in the limit of infinite squeezing the displaced zero position eigenstate and having an infinite mean photon number $n = {}_a\langle 0| A^\dagger A |0\rangle_a = |\alpha|^2 + \sinh^2 r$ diverging as $\sinh^2 r$ when $r \to \infty$.

It is easily shown from (4.117) with $\hat{\rho} = |\psi\rangle\langle\psi|$ that the Wigner function (see 4.3.1) of state (4.11), considered as being the limiting case of a physical and normalizable two-mode squeezed state with squeezzing parameter r (see (4.12) or (4.13), is given by

$$W(\mathbf{q}, \mathbf{p}) \propto \exp\left\{ -\frac{e^{-2r}}{2} \left[(x_1 + x_2 + v)^2 + (p_1 + p_2)^2 \right] - \frac{e^{2r}}{2} \left[(x_1 - x_2 - u)^2 + (p_1 - p_2)^2 \right] \right\} \tag{4.24}$$

with $\mathbf{q} = x_1, x_2$ and $\mathbf{p} = p_1, p_2$. The Wigner function links the Schrödinger's wave function (or more generically the quantum density operator) to a quasi-probability distribution in phase space $(\mathbf{q}, \mathbf{p})$, the term *quasi* referring to the fact that the Wigner function is not always positive semi-definite since it can have negative values. An always positive Wigner function, as is the one of state (4.11), can be interpreted as a classical probability distribution, thus allowing a hidden-variable interpretation of the correlations exhibited by this entangled state. This is true as long as Gaussian measurements, i.e. linear combinations of position and momentum measurements, are considered [14].

Here we can see that the Wigner function (4.24) of the EPR state is Gaussian and therefore positive semi-definite. This means that the state can be represented by a classical probability distribution. As a consequence, for a Gaussian measurement , this EPR state **cannot** violate Bell's inequalities [8, 113][15]. In other words, **as long as Gaussian measurements are concerned, the EPR state** (4.11) **displays a non-locality that can be mimicked by a classical probability distribution, viz. by a hidden variable theory**. However, the non-locality of Gaussian states such as (4.11) can be revealed by non-Gaussian measurements. Hence, non-locality is revealed not only by the quantum structure of the considered state (that must in any case be entangled in order to possibly violate locality constraints), but also by the type of measurement performed and hence on the observables chosen to build a Bell-type inequality [8].

[13] Using (4.15) with $\theta = 0$ and (4.21) it is easily checked that $S^\dagger \hat{x}_i S = \hat{X}_i$, implying that $\hat{X}_1 |X_1, X_2\rangle = S^\dagger \hat{x}_i S |X_1, X_2\rangle = S^\dagger \hat{x}_i S (S^\dagger S) |X_1, X_2\rangle = X_i |X_1, X_2\rangle$. Multiplying from the left the last equality by S yields $\hat{x}_i (S |X_1, X_2\rangle) = X_i (S |X_1, X_2\rangle)$. Then, $\hat{X}_1 |x_1, x_2\rangle = S^\dagger \hat{x}_i (S |x_1, x_2\rangle) = X_i S^\dagger (S |x_1, x_2\rangle) = X_1 |x_1, x_2\rangle$. Therefore, applying $|x_1, x_2\rangle$ to the first line of (4.21) yields $X_1 = x_1 \cosh r - x_2 \sinh r$. The same argument holds for the X_2, P_1 and P_2.

[14] For any given input Gaussian state, a Gaussian measurement is defined as a measurement yielding a Gaussian probability distribution for the output : it is therefore an operation that projects Gaussian states onto Gaussian states [113].

[15] In a paper dated 1986 [114] Bell himself remarked that the EPR state could not violate his inequality because of the Gaussianity of the Wigner function of the EPR state but this remark has proven to be true only for Gaussian measurements.

For the unphysical state given in (4.10) and (4.11), the two particles are in an entangled state exhibiting perfect correlations in their positions and momenta [8]. Then, for such a state, EPR argument reads as follows. For state (4.11), measuring particle 1 to be in state x_0 immediately yields state $|x_0\rangle_1 \langle x_0|\psi\rangle = |x_0, x_0 - u\rangle$ implying that particle 2 is *with certainty* in position state $x_0 - u$. But since there should not be, according to special relativity, any immediate action at a distance, the measurement made on particle 1 should not have *disturbed* the state of particle 2 : hence, the two particle being space-like separated, the position of particle 2 must have been *predetermined*, i.e. particle 2 should have been in position $x_0 - u$ even before the measurement performed on particle 1. The same argument apply to momenta : *locality* implies that particle 2 should have been in momentum $-p_0$ even before the measurement performed on particle 1 had yielded momentum p_0. Then, not only the outcome of the measurement on particle 1 should not be *random* but also particle 2 should be in a state with *preditermined position* $x_0 - u$ ***and*** *momentum* $-p_0$ since its state should not depend on the choice of measurement (position or momentum) made on particle 1. **But** quantum mechanics forbids to be in a state where position and momentum are both predetermined with infinte precision, i.e. with certainty. Therefore, according to the EPR argument, quantum mechanics is inconsistent and thus incomplete as long as locality of interaction, i.e. no action at a distance, and/or realism are/is preserved. Since local realism implies incompleteness of quantum mechanics [8] it is then essential to be able to test whether a more complete hidden-variable theory can account for quantum correlations : Bell inequalities provide such a test.

4.1.3 . The 1964 Bell and 1969 CHSH inequalities : mathematical constraints on local realism

Nonlocality can be revealed through the violation of the constraints that local realism imposes on the joint probability distribution of two physically separable systems [8]. These constraints, known as *Bell inequalities*, can be violated by quantum mechanics and when these inequalities imposed by local realism are violated then the correlations of the relevant quantum state contradict (1) locality or (2) realism or (3) both (locality and realism). The term *nonlocality* loosely refers to any of these alternatives [8]. In order to be able to violate Bell inequalities, measurements must resort to *non-commuting observables* [16] and must apply to *entangled* states[17].

Let us say [95] that Alice and Bob can perform independently a measurement of an observable on two apparently different systems[18]. The measurement by Alice is defined as some random variable A yielding outcome a and is considered to be conditioned by some variable X freely set to the value x. Similarly the measurement by Bob is defined as some random variable B yielding outcome b and is considered to be conditioned by some variable Y freely set to the value y. Generically the two measurements may not be statistically independent and one could have[19]

$$P_{AB|XY}(ab|xy) \neq P_{A|X}(a|x)P_{B|Y}(b|y) \tag{4.25}$$

Considering A and B to be space-like events, i.e. causally disconnected events, one may account for the correlations resulting in the non-factorability of (4.25) by invoking some set of (possibly random) past factors Λ related to some local interaction between the two (sub-)systems [20]. In this *local theory* the common past explains the correlations by resorting to a common cause. In this case, despite (4.25), one can factorize the probability distribution of the outcomes as

$$P_{AB|XY\Lambda}(ab|xy\lambda) = P_{A|X\Lambda}(a|x\lambda)P_{B|Y\Lambda}(b|y\lambda) \tag{4.26}$$

[16] See for example (A.72) in the computation of the upper bound or Cirel'son bound for the CHSH inequality in Appendix A.3.

[17] In other words, violation of local realism is related to the quantum, i.e. non classical, correlations exhibited by conjugate variables.

[18] In reality two subsystems of one unique system as one must consider quantum mechanically two particles propagating in opposite directions after interacting.

[19] Setting, accordingly to what has been said, $P_{A|XY}(a|xy) = P_{A|X}(a|x)$ and $P_{B|XY}(b|xy) = P_{B|Y}(b|y)$.

[20] "Let this more complete specification [of the system] be effected by means of parameters λ. It is a matter of indifference in the following whether λ denotes a single variable or a set, or even a set of functions, and whether the variables are discrete or continuous"[7].

It can be noticed that the reasoning followed to obtain (4.26) is actually a three-step reasoning implying three assumptions : *realism*, *free-will* and *no-signaling* [21]. It is then worth to clarify them.
The *realism* assumption states that any correlation between A and B is determined by some unobserved or unobservable reality - a set of past factors - which is encoded, as we said, in the possibly random variable Λ. Since the variable Λ is possibly random it can be described by a probability distribution $P_\Lambda(\lambda)$. This assumption is written[22]

$$P_{AB|XY}(ab|xy) = \int_\Lambda d\lambda\, P_{AB\Lambda|XY}(ab\lambda|xy) = \int_\Lambda d\lambda\, P_{AB|\Lambda XY}(ab|\lambda xy) P_{\Lambda|XY}(\lambda|xy) \tag{4.27}$$

The *free-will* assumption guarantees that the observers of A and B can freely choose (free-choice) which measurement they are performing. This implies not only that A and B are independent of either Y or X respectively but also that X and Y are independent of each other and therefore independent of Λ. The independence from Λ of X and Y is written[23]

$$P_{\Lambda|XY}(\lambda|xy) = P_\Lambda(\lambda) \quad \Leftrightarrow \quad P_{XY|\Lambda}(xy|\lambda) = P_{XY}(xy) = P_X(x) P_Y(y) \tag{4.28}$$

where the last equality states also the mutual independence of X and Y. These relations constitute the free-will assumption. Finally, the *no-signaling* assumption assumes that A and B are spacelike events, i.e. measurements that are causally disconnected. This assumption is written[24]

$$P_{AB|\Lambda XY}(ab|\lambda xy) = P_{A|\Lambda XY}(a|\lambda xy) P_{B|\Lambda XY}(b|\lambda xy) = P_{A|\Lambda X}(a|\lambda x) P_{B|\Lambda Y}(b|\lambda y) \tag{4.29}$$

where we can see[25] that the correlations between A and B have been taken such to be generated exclusively by the set of hidden variables Λ, i.e. A neither depends on B and Y nor B on A and X. The three previous conditions (4.27), (4.28) and (4.29) lead to the *locality* constraint

$$P_{AB|XY}(ab|xy) = \int_\Lambda d\lambda\, P_{A|\Lambda X}(a|\lambda x) P_{B|\Lambda Y}(b|\lambda y) P_\Lambda(\lambda) \tag{4.30}$$

It is now possible to define the average quantity

$$\langle AB\rangle(x,y) = \int_A da \int_B db\, ab\, P_{AB|XY}(ab|xy) \tag{4.31}$$

and

$$S(x,x',y,y') = \langle AB\rangle(x,y) + \langle AB\rangle(x,y') + \langle AB\rangle(x',y) - \langle AB\rangle(x',y') \tag{4.32}$$

Applying the locality constraint (4.30) in (4.32) one obtains

$$S_{\text{local}}(x,x',y,y') = \int_\Lambda d\lambda\, P_\Lambda(\lambda) \Big\{ \langle A\rangle(\lambda,x) \left[\langle B\rangle(\lambda,y) + \langle B\rangle(\lambda,y')\right] + \langle A\rangle(\lambda,x') \left[\langle B\rangle(\lambda,y) - \langle B\rangle(\lambda,y')\right] \Big\} \tag{4.33}$$

with

$$\langle A\rangle(\lambda,x) = \int_A da\, a P_{A|\Lambda X}(a|\lambda x) \qquad \langle B\rangle(\lambda,y) = \int_B db\, b P_{B|\Lambda Y}(b|\lambda y) \tag{4.34}$$

[21] We are following here the line of reasoning given by A. Smerzi in his course "Quantum Interferometry" during the second week of the *Cold Atom Predoc School* (Les Houches, Sept. 26th - Oct. 7th 2022).
[22] If the variable Λ is considered to be discrete then one has $\int_\Lambda d\lambda \to \sum_\Lambda$.
[23] This relation is also known as *Reichenbach's Common Cause Principle* (1956).
[24] Using $P(AB|C) = P(A|BC)P(B|C)$ and the independence relation $P(A|B) = P(A)$.
[25] Under the free-will conditions, i.e. if Y is independent from A, X and Λ, one has both

$$P_{A\Lambda XY}(a\lambda xy) = P_{A\Lambda X}(a\lambda x) P_Y(y) = P_{A|\Lambda X}(a|\lambda x) P_{\Lambda X}(\lambda x) P_Y(y)$$
$$P_{A\Lambda XY}(a\lambda xy) = P_{A|\Lambda XY}(a|\lambda xy) P_{\Lambda XY}(\lambda xy) = P_{A|\Lambda XY}(a|\lambda xy) P_{\Lambda X}(\lambda x) P_Y(y)$$

Therefore, equating the two previous relations, one obtains $P_{A|\Lambda XY}(a|\lambda xy) = P_{A|\Lambda X}(a|\lambda x)$. Similarly if X is independent from B, Y and Λ, one gets $P_{B|\Lambda XY}(b|\lambda xy) = P_{B|\Lambda Y}(b|\lambda y)$.

It can clearly be seen that if

$$a \in [-1, 1] \qquad b \in [-1, 1] \tag{4.35}$$

then every average of the form $\langle A\rangle(\lambda, x)$ appearing in (4.33) will be bounded by ± 1. Hence one obtains for S under locality constraint, i.e. S_{local}, the inequality

$$|S_{\text{local}}(x, x', y, y')| \leq 2 \tag{4.36}$$

The previous expression, consisting in the mathematical formulation of a locality constraint, is referred to as *Bell's inequality* [7] in its *CHSH* (Clauser-Horne-Shimony-Holt) formulation [105]. As it is, the inequality is conditioned by the locality constraint (4.30), i.e. by the factorability of the probability distribution $P_{AB|\lambda XY}$ as expressed in the no-signaling assumption formulated in (4.29) (A and B are causally disconnected) after taking into account realism (4.27), i.e. the existence of Λ, and free-will, i.e. the independence of X,Y and Λ. It is then either this very same factorability, leading to the *locality* constraint, or the very existence of a set of hidden variables yielded by realism that is questioned by the so-called *non-locality* of quantum mechanics.

4.1.4 . Measures of Genuine Bipartite and Tripartite Entanglement and Non-locality

Non-locality is related to entanglement since only entangled states can violate locality [8]. In this section we shortly review different measures of entanglement in order to motivate, in our study, the choice of the "PPT-measure" for bipartite entanglement (see 4.3.6) and of the Mermin's nonlocality parameter (see 4.6.4) as a witness of the GHZ nature of our low-energy tripartite state.

Bipartite Entanglement and Nonlocality

By singular value decomposition (SVD), any $m \times n$ matrix A can be written as $A = UDV^\dagger$ with D a $m \times n$ diagonal matrix with non-negative real components and U and V two unitary matrices of dimension $m \times m$ and $n \times n$ respectively. Then for any pure bipartite state one has

$$|\psi\rangle = \sum_{p,q} A_{pq} |p\rangle |q\rangle = \sum_k D_{kk} \left(\sum_p U_{pk} |p\rangle\right) \left(\sum_q V^*_{qk} |q\rangle\right) = \sum_k D_{kk} |u_k\rangle |v_k\rangle \tag{4.37}$$

with $\{|p\rangle\}$, $\{|q\rangle\}$, $\{|u_k\rangle\}$ and $\{|v_k\rangle\}$ orthogonal bases and the sum over k has $d = \min(m, n)$ terms. The $D_{kk} = \sqrt{d_k}$ are called the *Schmidt coefficients* and the last expression in (4.37) a *Schmidt decomposition*. By definition of the density matrix $\hat{\rho} = |\psi\rangle \langle\psi|$ whose trace must equal one, the Schmidt coefficients must fulfill $\sum_k d_k = 1$. Any bipartite state can therefore be written as a convex combination of product states[26]. The state will be *maximally entangled* if all its Schmidt coefficients are equal and separable or *factorizable* if the number of nonzero coefficients, i.e. its *Schmidt rank*, is one [8][27]. Then, the the two reduced density operators obtained by partial tracing are given by

$$\begin{aligned} \hat{\rho}_1 &= \text{Tr}_2 \hat{\rho} = \sum_k d_k |u_k\rangle \langle u_k| \\ \hat{\rho}_2 &= \text{Tr}_1 \hat{\rho} = \sum_k d_k |v_k\rangle \langle v_k| \end{aligned} \tag{4.38}$$

and it can be seen that the partial tracing of one subsystem in a maximally entangled pure state leaves the other one in the *maximally mixed state* of uniform distribution $1/d$. Given the von Neumann entropy

$$S(\hat{\rho}) = -\text{Tr}\{\hat{\rho} \log_d \hat{\rho}\} \tag{4.39}$$

a unique measure $E_{v.N.}$ of bipartite entanglement for pure states is given by

$$E_{v.N.}(\hat{\rho}) = S(\hat{\rho}_1) = S(\hat{\rho}_2) = -\sum_k d_k \log_d d_k \tag{4.40}$$

[26] A convex combination for the x_i defined in a real or complex vector space is given by $\sum_i \alpha_i x_i$ with α_i real and $\sum_i \alpha_i = 1$ and $\alpha_i \geq 0$.

[27] There is then only one non-vanishing coefficient which is by definition equal to one.

From a continuous variable perspective, for a two-mode squeezed state, such as the EPR state in the limit of infinite squeezing, which can always be written as

$$|\psi\rangle = \hat{S}(\zeta)\,|0\rangle\,|0\rangle = \sqrt{1-\lambda}\sum_{n=0}^{\infty}\lambda^{n/2}\,|n\rangle\,|n\rangle \tag{4.41}$$

with $\hat{S}(\zeta = r)$ given in (4.15) and $\lambda = \tanh^2 r$, the *partial von Neumann entropy* will give

$$\begin{aligned} E_{v.N.}(\hat{\rho}) = S(\hat{\rho}_1) = S(\hat{\rho}_2) &= -\ln(1-\lambda) - \frac{\lambda}{1-\lambda}\ln(\lambda) \\ &= (\cosh^2 r)\ln(\cosh^2 r) - (\sinh^2 r)\ln(\sinh^2 r) \\ &= \ln(\cosh^2 r) - (\sinh^2 r)\ln(\tanh^2 r) \end{aligned} \tag{4.42}$$

which goes as $2r - \ln(4) + 1$ for very large r and is zero for $r = 0$. Any pure bipartite Gaussian state can be transformed to a two-mode squeezed state via a Local Linear Unitary BOgoliubov transformation (LLUBO) which does not modify the entanglement properties of the state[28] : its entanglement can then be measured by (4.42) [8]. Even if pure bipartite Gaussian states have a positive semi-definite Wigner function, they do violate Bell inequalities due to the non-Gaussianity of the measurements involved in the non-locality tests. Local realism can only be violated by entangled states since the tests for non-locality are sensitive to quantum, i.e. non classical, correlations : but if not all entangle states do violate locality, any entangled *pure bipartite state* does violate local realism [8].

The entanglement entropy $E_{v.N}$ generalizes to the *entanglement of formation* E_f [115] when bipartite mixed states are considered, with

$$E_f(\hat{\rho}) = \inf\left\{\sum_i p_i E_{v.N}(\hat{\rho}_i)\right\} \tag{4.43}$$

with a the infimum taken over all the possible ways of decomposing the bipartite mixed state $\hat{\rho}$ in a convex sum of bipartite (possibly entangled and not necessarily orthogonal) pure states $\hat{\rho}_i = |\psi_i\rangle\langle\psi_i|$, i.e. with $\hat{\rho} = \sum_i p_i\,\hat{\rho}_i$. But as argued in section 4.3.6 the entanglement of formation is not not easily determined in non symmetric two-mode Gaussian mixed states such as the ones we consider, since in general the mixedness A_i and A_j (defined in (4.197)) for modes i and j respectively, are not equal. This criterion is therefore unpractical in the study of our system.

Let us here recall that a mixed bipartite state is separable or factorizable if its density operator is given by a convex sum ($\sum_i p_i = 1$ with $p_i \geq 0$ for all i) of product states, i.e.[29]

$$\hat{\rho} = \sum_i p_i\,\hat{\rho}_1^i \otimes \hat{\rho}_2^i \tag{4.44}$$

Then, the *Perez-Horodecki criterion* or *Partial Positive Transpose* (PPT) criterion states that a bipartite density operator, i.e. any bipartition $(N \times M)$ of a system of $N + M$ modes each mode being a discrete variable with d degrees of freedom or a continuous variable described by its position and momentum, is separable if its partially transposed density matrix yields a legitimate density operator and has therefore only non-negative eigenvalues [8, 86]. The matrix is said to be partially transposed since one of the two modes is transposed. Thus the partial transposed of a generic two-mode density operator

$$\hat{\rho} = \sum_{i,j,l,m} A_{ijlm}\,|i,l\rangle\langle j,m| \tag{4.45}$$

will be given by[30]

$$\hat{\rho}^{(PT)} = (\mathcal{T}_1 \otimes \mathbb{1}_2)\,\hat{\rho} = \sum_{i,j,l,m} A_{ijlm}\;|j,l\rangle\langle i,m| = \sum_{i,j,l,m} A_{jilm}\,|i,l\rangle\langle j,m| \tag{4.46}$$

[28] A local transformation does not mix different modes.

[29] If only one $p_k = 1$ then $\hat{\rho} = \hat{\rho}_1 \otimes \hat{\rho}_2$ is a simply separable state or product state and one has the von Neumann entropy $S(\hat{\rho}) = S(\hat{\rho}_1) + S(\hat{\rho}_2)$.

[30] Any of the two modes can be transposed. Here we have transposed the first one.

with $\mathcal{T}_1$ the transposition operator in subspace 1[31]. If at least one eigenvalue of $\hat{\rho}^{(PT)}$ is negative we will say that $\rho^{(PT)}$ has a negative partial transpose (npt) and is therefore inseparable, i.e. npt is a sufficient condition for inseparability since a positive partial transpose is a necessary condition for separability. For bipartitions (2×2) and (2×3) for finite-dimensional systems and $(1 \times N)$-Gaussian systems [32], all inseparable bipartite states show also npt and the criterion is necessary but for higher dimensions not all inseparable bipartite states show npt and the criterion is only sufficient for inseparability, i.e. "if npt then inseparable" [8]. It is then clear that the PPT criterion is a "yes or no" condition for inseparability : in the general case, if the system shows npt then it is inseparable but if it does not one cannot tell if it is separable or inseparable.

Similarly, with the norm $||\hat{O}||_1 = \text{Tr}\{\sqrt{\hat{O}^\dagger \hat{O}}\}$, the *negativity* is defined as[33]

$$\mathcal{N}(\hat{\rho}^{(PT)}) = \frac{||\hat{\rho}^{PT}||_1 - 1}{2} \tag{4.47}$$

Since $||\hat{\rho}||_1 = 1$ by definition of the density operator, the more $\rho^{(PT)}$ has negative eigenvalues the less it is semi-positive definite and hence the more $||\hat{\rho}^{PT}||_1$ goes to zero[34]. Therefore $\mathcal{N}(\hat{\rho}^{(PT)})$ varies between 0 and -0.5. Equivalently, from $||.||_1$, the *logarithmic negativity* is defined as

$$E_N(\hat{\rho}) = \log_2 ||\hat{\rho}^{(PT)}||_1 \tag{4.48}$$

If the *entanglement entropy*, its generalization to mixed states, i.e. the *entanglement of formation*, and the *logarithmic negativity*, are monotonous measures of entanglement, they possibly violate monogamy inequalities for tripartite systems [116]. Hence these measures are problematic in the tripartite case.

The "PPT measure" for bipartite Gaussian systems [86] adopted in this work is a generalization of the PPT criterion, without any of the previously mentioned drawbacks. This measure is monotonic with entanglement : at one the state is maximally entangled and below zero it is no longer entangled (see section 4.3.6). The "PPT measure" mimics many features of the Gaussian contangle that we will introduce in (4.53) as a proper measure for the monogamy inequality but is much easier to compute. The allows therefore to easily characterize the degree of entanglement of any bipartite system.

Williamson's theorem states that any covariance matrix σ[35] can be put in a diagonal form by a symplectic[36] matrix S through the transformation $S\sigma S^T$. A 2-mode Gaussian state will have a 4×4 covariance matrix whose partial transpose $\sigma^{(PT)}$ will have twice-degenerated symplectic eigenvalues $\nu_\pm^{(PT)}$[37]. The PPT-criterion [90, 86] states that if $\nu_\pm^{(PT)} \geq 1$ then the state is separable. Therefore, since $\nu_+^{(PT)} \geq 1$, the positiveness of the parameter

$$\Lambda = 1 - \nu_-^{(PT)} \tag{4.49}$$

[31] The density operator is hermitian. Therefore transposition is equivalent to complex conjugation. Furthermore, complex conjugation of the Schrödinger equation gives $i\hbar\partial_t \to -i\hbar\partial_t$ and means therefore time reversal. Hence, in terms of continuous variables time reversal yields sign change in the momentum variables, i.e. $p_i \to -p_i$ [8].

[32] The first two cases correspond to discrete systems of $2+2$ and $2+3$ modes respectively, each mode with a finite number of degrees of freedom, whereas the last one is a continuous-variable $N+1$ Gaussian-mode system. Let us remark here that there exists other criteria that witness, at least in principle, separability of all bipartitions of $N \times M$ Gaussian-mode systems (see [8]).

[33] With $\log_2$ for qubits and $\ln$ for continuous variable states.

[34] Since the density operator $\hat{\rho}$ is hermitian, $\hat{\rho}^T = \rho^*$. Then, if $\rho^{(PT)}$ is a well-defined density operator its norm $||.||_1$ will be one.

[35] For a definition of the covariance matrix see section 4.3.3.

[36] A matrix M is symplectic if $MJM^T = J$ with

$$J = \begin{pmatrix} 0 & \mathbb{1}_n \\ -\mathbb{1}_n & 0 \end{pmatrix}$$

a skew-symmetric $2n \times 2n$ block matrix such that $\det J = 1$, $J^2 = -\mathbb{1}$, $J^T = -J$ and hence $J^T = J^{-1}$ Multiplying $MJM^T = J$ from the left by J and from the right by M^{-1} one obtains the inverse $M^{-1} = -JM^TJ$ of the symplectic matrix M. Applying our definition of a sympltectic matrix with $M = J$ proves that J is also a symplectic matrix. See section 4.3.3.

[37] The symplectic eigenvalues associated to the covariance matrix σ are the eigenvalues of $|i\Omega\sigma|$ with Ω defined in Eq. (4.126) of section 4.3.3 [90].

will quantify the degree of entanglement of the system[38]: this is the PPT measure. Let us finally signal the DGCZ criterion [117] also obtained from the covariance matrix. In the case of our system [90][39] this criterion reduces to

$$\begin{aligned} |\langle \hat{c}_i \hat{c}_2 \rangle|^2 &> \langle \hat{c}_i^\dagger \hat{c}_i \rangle \langle \hat{c}_2^\dagger \hat{c}_2 \rangle \\ |\langle \hat{c}_0 \hat{c}_1^\dagger \rangle|^2 &> \langle \hat{c}_0^\dagger \hat{c}_0 \rangle \langle \hat{c}_1^\dagger \hat{c}_1 \rangle \end{aligned} \tag{4.50}$$

with $i = 0, 1$ and which is nothing else than a violation (in the case of inseparable states) of the Cauchy-Schwarz inequality $|\langle u|v\rangle|^2 < |\langle u|u\rangle||\langle v|v\rangle|$. Contrarily to measures such as the **Cauchy-Schwarz criterion**, the PPT measure has the advantage of being an entanglement monotone.

Genuine Tripartite Entanglement and Mermin's Nonlocality Test

The term *genuine tripartite state* refers to a tripartite state where none of the parties can be separated from the two other parties in a mixture of product states, i.e. the state is not such that $\sum_i p_i \hat{\rho}_j^i \otimes \hat{\rho}_{kl}^i$ with $p_i \geq 0$ and $\sum_i p_i = 1$ [8].

A proper measure of bipartite entanglement $E^{(A|B)}$, i.e. a nonnegative measure which is zero for separable states and which is monotonic, must satisfy monogamy inequalities when multipartite systems are considered. In the case of a tripartite systems such a monogamy inequality reads [86]

$$E^{(i|jk)} - E^{(i|j)} - E^{(i|k)} \geq 0 \tag{4.51}$$

where bipartition $(i|jk)$ means that the subsystem jk is taken as a whole. This monogamy inequality provides a measure of genuine tripartite entanglement. The logarithmic negativity (4.47) can be made a proper measure by squaring it. It is then called, in the case of Gaussian pure states $\hat{\rho} = |\psi\rangle\langle\psi|$, *contangle* (from "continuous entanglement") and reads

$$E_\tau(\sigma^p) = \left(\ln_2 ||\hat{\rho}^{(PT)}||_1\right)^2 \tag{4.52}$$

with σ the covariance matrix of the pure (p) the system. Its generalization to mixed stated is called the *Gaussian contangle* and reads

$$G_\tau(\sigma) = \inf_{\sigma^p \leq \sigma} E_\tau(\sigma^p) \tag{4.53}$$

with $\sigma^p \leq \sigma$ meaning that $\sigma - \sigma^p$ is positive semi-definite. This measure constitute an upper-bound to the measure with no restriction $\sigma^p \leq \sigma$ [86]. The monogamy measure 4.51 performed with contangle (4.52) and its generalization (4.53) is symmetric for tripartie qubits but is no longer symmetric for tripartite continuous modes. Nevertheless minimizing G_τ over all permutations of the modes makes it symmetric. This minimization is called the *residual contangle* and reads

$$G_\tau^{\text{res}} = \min_{i,j,k} \left(G_\tau^{(i|jk)} - G_\tau^{(i|j)} - G_\tau^{(i|k)}\right) \tag{4.54}$$

This residual contangle was computed for our state in Ref. [86]. Since it is not of very practical use and that it cannot be used at finite temperature, we will resort in this work to the Mermin's parameter as a witness of nonlocality for the GKMR pseudo-spins measurements (see section 4.4) on our tripartite state.

A straightforward tripartite generalization of the bipartite CHSH inequality is given by the Svetlichny parameter given in Eq. (4.215) of section 4.6.1.

In the Zero Temperature and Zero Energy Limit, the GHZ nature of out tripartite pure state is shown in section 4.6.3. In section 4.6.4, the persistence of this feature at finite energy is inquired through the computation of Mermin paramater [111] given in Eq. (4.232), which relates to the Svetlichny three-mode Bell operator given in (4.215), as shown in Eq. (4.234).

[38] See section 4.3.6

[39] See section 4.3.5 for the definition of $\langle \hat{c}_i \hat{c}_2 \rangle$ and $\langle \hat{c}_0 \hat{c}_1^\dagger \rangle$.

We will therefore here introduce Mermin's nonlocality test for tripartite systems. We recall that the GHZ state[40], written in the basis of the $\hat{\sigma}_z \otimes \hat{\sigma}_z \otimes \hat{\sigma}_z$ spin operator, is given by

$$|\psi_{\text{GHZ}}\rangle = \frac{1}{\sqrt{2}}(|+++\rangle + |---\rangle) \tag{4.55}$$

It is easily checked that this state is an eigenvector of the operators $(\hat{\sigma}_x \otimes \hat{\sigma}_y \otimes \hat{\sigma}_y)$, $(\hat{\sigma}_y \otimes \hat{\sigma}_x \otimes \hat{\sigma}_y)$ and $(\hat{\sigma}_y \otimes \hat{\sigma}_y \otimes \hat{\sigma}_x)$ for eigenvalue -1 and eigenvector of $\hat{\sigma}_x \otimes \hat{\sigma}_x \otimes \hat{\sigma}_x$ with eigenvalue $+1$. Because of the previous properties one must then have

$$\begin{aligned}\langle(\hat{\sigma}_x \otimes \hat{\sigma}_y \otimes \hat{\sigma}_y)(\hat{\sigma}_y \otimes \hat{\sigma}_x \otimes \hat{\sigma}_y)(\hat{\sigma}_y \otimes \hat{\sigma}_y \otimes \hat{\sigma}_x)\rangle &= \langle\hat{\sigma}_x \otimes \hat{\sigma}_y \otimes \hat{\sigma}_y\rangle\langle\hat{\sigma}_y \otimes \hat{\sigma}_x \otimes \hat{\sigma}_y\rangle\langle\hat{\sigma}_y \otimes \hat{\sigma}_y \otimes \hat{\sigma}_x\rangle \\ &= -\langle\hat{\sigma}_x \otimes \hat{\sigma}_x \otimes \hat{\sigma}_x\rangle \\ &= -1\end{aligned} \tag{4.56}$$

with the averages $\langle . \rangle$ taken on the GHZ state[41]. Consequently, knowing any two measurements, each one being either ± 1, the last outcome is known with certainty. According to the EPR reasoning the outcomes should then have been predetermined since the prediction on the last measurement can in principle be made at any arbitrary distance. Then, in order to explain the previous results, not only the outcome of one detector should be predetermined by some hidden variable λ such that $s_{x,i}(\lambda)$ (outcome of a measure of particle i if $\hat{\sigma}_x$ is measured) and $s_{y,i}(\lambda)$ (outcome of a measure of particle i if $\hat{\sigma}_y$ is measured) have a definite value (either $+1$ or -1) for each particle i but also the correlations between the three particles (encoded in λ) should yield the previous statistics (4.56) obtained for the $|\psi_{\text{GHZ}}\rangle$. But, setting λ to fulfill the results obtained for the measurements of one $\hat{\sigma}_x$ and two $\hat{\sigma}_y$, yields

$$(\sigma_{x,1}\,\sigma_{y,2}\,\sigma_{y,3})\,(\sigma_{y,1}\,\sigma_{x,2}\,\sigma_{y,3})\,(\sigma_{y,1}\,\sigma_{y,2}\,\sigma_{x,3}) = -1 \quad \Rightarrow \quad \sigma_{x,1}\,\sigma_{x,2}\,\sigma_{x,3} = -1 \tag{4.57}$$

since $(\sigma_{y,i})^2 = 1$. Hence the prediction (with certainty) of local realism is -1 for the measurement $\hat{\sigma}_x \otimes \hat{\sigma}_x \otimes \hat{\sigma}_x$. But, as can be seen from (4.56), prediction (with certainty) of quantum mechanics for the same observable is $+1$. Therefore, the EPR reality criterion predicts $\sigma_x \otimes \hat{\sigma}_x \otimes \hat{\sigma}_x$ with the wrong eigenvalue : in Mermin's words, "[i]n this sense the GHZ experiment provides the strongest possible contradiction between quantum mechanics and the EPR reality criterion" [112]. Not surprisingly, the non-local prediction of quantum mechanics results from the non-commutativity of the Pauli algebra operators. Finally, and strikingly, the EPR local realism is here refuted not by a statistics (as in Bell inequalities) but by the inconsistent predictions of one single outcome.

4.2 . BOGOLIUBOV TRANSFORMATION AND SQUEEZED VACUUM IN THE ANALOG BLACK HOLE SYSTEM

4.2.1 . The Three-mode Pure State

For describing analog black holes physics one should consider observables operating in the Fock space of the outgoing modes, as would an observer located outside the horizon of a gravitational black hole. However, the physical implementation of the analog black hole configurations presented in 3.1 is realized in the vacuum of the incoming modes. This mismatch is the origin of the quantum evaporation process, as first presented by Hawking [11]. An ingoing vacuum mode of frequency ω (which we denote as $|0_\omega\rangle^{\text{in}}$) relates to an outgoing vacuum mode $|0_\omega\rangle^{\text{out}}$ through, as we will see, a Bogoliubov transformation. In our system we therefore define the $\hat{b}_i(\omega)$ and $\hat{c}_i(\omega)$ bosonic annihilation operators for *ingoing* and

[40] "Although there is no rigorous definition of maximally entangled multiparty state due to the lack of a general Schmidt decomposition, the form of the GHZ state with all Schmidt coefficients equal suggests that it exhibits maximum multipartite entanglement" [8].

[41] Indeed, using $\hat{\sigma}_i^2 = \mathbb{1}$ and the non-commutativity of the Pauli algebra, one has

$$(\hat{\sigma}_x \otimes \hat{\sigma}_y \otimes \hat{\sigma}_y)(\hat{\sigma}_y \otimes \hat{\sigma}_x \otimes \hat{\sigma}_y)(\hat{\sigma}_y \otimes \hat{\sigma}_y \otimes \hat{\sigma}_x) = (\hat{\sigma}_x\hat{\sigma}_y\hat{\sigma}_y) \otimes (\hat{\sigma}_y\hat{\sigma}_x\hat{\sigma}_y) \otimes (\hat{\sigma}_y\hat{\sigma}_y\hat{\sigma}_x) = -\hat{\sigma}_x \otimes \hat{\sigma}_x \otimes \hat{\sigma}_x$$

Furtheremore, $|\psi_{GHZ}\rangle$ being eigenvector of each one of the three operators appearing on the left-hand-side of the first line, this expression is indeed equivalent to the right-hand-side of the first line.

outgoing i-th mode, with $\hat{q}_i(\omega)$ and $\hat{p}_i(\omega)$ being, as we will see, the dimensionless position and momentum operator of the i-th mode, respectively. In the Fock space the two vacua are defined as

$$|0_\omega\rangle^{\text{in}} = |0_\omega\rangle^{\text{in}}_{(0)} \otimes |0_\omega\rangle^{\text{in}}_{(1)} \otimes |0_\omega\rangle^{\text{in}}_{(2)} \tag{4.58a}$$

$$|0_\omega\rangle^{\text{out}} = |0_\omega\rangle^{\text{out}}_{(0)} \otimes |0_\omega\rangle^{\text{out}}_{(1)} \otimes |0_\omega\rangle^{\text{out}}_{(2)} \tag{4.58b}$$

where $|0_\omega\rangle^{\text{in}}_{(i)}$ is the vacuum of operator $\hat{b}_i(\omega)$ and $|0_\omega\rangle^{\text{out}}_{(i)}$ the vacuum of operator $\hat{c}_i(\omega)$, with $i \in \{0,1,2\}$. The $\hat{c}_i(\omega)$ *out-going* mode operators are related to *ingoing* mode operators $\hat{b}_i(\omega)$ by the Bogoliubov transformation

$$\hat{\mathbf{c}}_S(\omega) = S(\omega)\,\hat{\mathbf{b}}_S(\omega) \tag{4.59}$$

with

$$\begin{aligned}\hat{\mathbf{c}}_S(\omega) &= (\hat{c}_0(\omega), \hat{c}_1(\omega), \hat{c}_2^\dagger(\omega))^T \\ \hat{\mathbf{b}}_S(\omega) &= (\hat{b}_0(\omega), \hat{b}_1(\omega), \hat{b}_2^\dagger(\omega))^T\end{aligned} \tag{4.60}$$

and $S(\omega)$ the 3×3 scattering matrix[42] defined as

$$\begin{aligned}S\eta S^\dagger &= S^\dagger \eta S = \eta \\ \eta &= \text{diag}(1,1,-1)\end{aligned} \tag{4.61}$$

where the explicit ω-dependence as been dropped, as it will often be the case below, for legibility. One can rewrite (4.61) explicitly as

$$\begin{aligned}\left(S\eta S^\dagger\right)_{00} &= |S_{00}|^2 + |S_{01}|^2 - |S_{02}|^2 = 1 \\ \left(S\eta S^\dagger\right)_{11} &= |S_{10}|^2 + |S_{11}|^2 - |S_{12}|^2 = 1 \\ \left(S\eta S^\dagger\right)_{22} &= |S_{20}|^2 + |S_{21}|^2 - |S_{22}|^2 = -1 \\ \left(S\eta S^\dagger\right)_{kl} &= S_{k0}(S_{l0})^* + S_{k1}(S_{l1})^* - S_{k2}(S_{l2})^* \underset{k\neq l}{=} 0\end{aligned} \tag{4.62}$$

and as

$$\begin{aligned}\left(S^\dagger\eta S\right)_{00} &= |S_{00}|^2 + |S_{10}|^2 - |S_{20}|^2 = 1 \\ \left(S^\dagger\eta S\right)_{11} &= |S_{01}|^2 + |S_{11}|^2 - |S_{21}|^2 = 1 \\ \left(S^\dagger\eta S\right)_{22} &= |S_{02}|^2 + |S_{12}|^2 - |S_{22}|^2 = -1 \\ \left(S^\dagger\eta S\right)_{kl} &= (S_{0k})^* S_{0l} + (S_{1k})^* S_{1l} - (S_{2k})^* S_{2l} \underset{k\neq l}{=} 0\end{aligned} \tag{4.63}$$

Defining any scattering matrix component as

$$S_{ij} = |S_{ij}| e^{i\varphi_{ij}} \tag{4.64}$$

the last line of (4.62) can then be rewritten as

$$|S_{k0}||S_{l0}| e^{i(\varphi_{k0}-\varphi_{l0})} + |S_{k1}||S_{l1}| e^{i(\varphi_{k1}-\varphi_{l1})} - |S_{k2}||S_{l2}| e^{i(\varphi_{k2}-\varphi_{l2})} \underset{k\neq l}{=} 0 \tag{4.65}$$

The Bogoliubov transformation in (4.59) is a linear transformation that preserves the commutation relations: if the $\hat{b}_i$ are well-defined bosonic annihilation operators then the $\hat{c}_i$ are also well-defined annihilation operators. With respect to the vectors $\hat{\mathbf{c}}$ and $\hat{\mathbf{b}}$ defined as a generic $\hat{\mathbf{a}}$ will be in (4.129), i.e. as

$$\hat{\mathbf{a}} = (\hat{a}_0, \hat{a}_1, \hat{a}_2, \hat{a}_0^\dagger, \hat{a}_1^\dagger, \hat{a}_2^\dagger)^T \tag{4.66}$$

[42] The index S for $\hat{\mathbf{c}}_S$ and $\hat{\mathbf{b}}_S$ indicates that these two vectors are related by the scattering matrix S through the relation given in (4.60). They should not be confused with $\hat{\mathbf{c}}$ and $\hat{\mathbf{b}}$ appearing in (4.67) and which are defined in the same way as $\hat{\mathbf{a}}$ in (4.129).

the Bogoliubov transformation is written

$$\hat{\mathbf{c}}(\omega) = T(\omega)\,\hat{\mathbf{b}}(\omega) \tag{4.67}$$

with

$$T(\omega) = \begin{pmatrix} S_{00} & S_{01} & 0 & 0 & 0 & S_{02} \\ S_{10} & S_{11} & 0 & 0 & 0 & S_{12} \\ 0 & 0 & S^*_{22} & S^*_{20} & S^*_{21} & 0 \\ 0 & 0 & S^*_{02} & S^*_{00} & S^*_{01} & 0 \\ 0 & 0 & S^*_{12} & S^*_{10} & S^*_{11} & 0 \\ S_{20} & S_{21} & 0 & 0 & 0 & S_{22} \end{pmatrix} \tag{4.68}$$

The matrix T encodes a non-local Bogoliubov transformation, where "non-local" means that the different modes are mixed in the operation. One can immediately see that T has the block structure

$$T = \begin{pmatrix} \alpha^* & -\beta^* \\ -\beta & \alpha \end{pmatrix} \tag{4.69}$$

with α and β two $N \times N$ matrices. We wish here to define the *outgoing* covariance matrix σ_c. Since

$$\boldsymbol{\xi}_c = \sqrt{2}\,U\,\mathbf{c} = \sqrt{2}\,U\,T\,\mathbf{b} = \sqrt{2}\,U\,T\,U^\dagger\,U\,\mathbf{b} = U\,T\,U^\dagger\,\boldsymbol{\xi}_b \tag{4.70}$$

In order for $\mathbf{c}$ and $\boldsymbol{\xi}_c$ to fulfill as $\mathbf{b}$ and $\boldsymbol{\xi}_b$ respectively the commutation relations (4.132) and (4.125) one must have

$$\begin{aligned} T\,J\,T^T &= J \\ (U\,T\,U^\dagger)\,\Omega(U^*\,T^T\,U^T) &= \Omega \end{aligned} \tag{4.71}$$

A transformation S_{Sp} acting in a $2N$-dimensional complex vector space, as the ones in (4.71), i.e. such that $S_{\mathrm{Sp}} X S_{\mathrm{Sp}}^T = X$ with X skew-symmetric ($X^T = -X$), is said to belong to the symplectic group $\mathrm{Sp}(2N, \mathbb{C})$. We define the symplectic transformation

$$S_T = U\,T\,U^\dagger \tag{4.72}$$

Multiplying the first relation in (4.71) by J on the right and by T^{-1} on the left one obtains

$$T^{-1} = -J\,T^T J = \begin{pmatrix} \alpha^T & \beta^\dagger \\ \beta^T & \alpha^\dagger \end{pmatrix} \tag{4.73}$$

Then the relations $T^{-1}T = \mathbb{1}_{2N}$ and $T\,T^{-1} = \mathbb{1}_{2N}$ impose four relations if written in terms of the $N \times N$ matrices α and β, that is to say

$$\begin{aligned} -\beta\beta^\dagger + \alpha\alpha^\dagger &= \mathbb{1}_N & -\beta\alpha^T + \alpha\beta^T &= 0 \\ -\beta^T\beta^* + \alpha^\dagger\alpha &= \mathbb{1}_N & -\alpha^T\beta^* + \beta^\dagger\alpha &= 0 \end{aligned} \tag{4.74}$$

Relations (4.74) are equivalent to (4.62) and (4.63). Furthermore relation (4.67) can be restated as

$$c_i = V^\dagger b_i V \tag{4.75}$$

with V a unitary operator[43]. Then the vacua $|0_\omega\rangle^{\mathrm{in}}$ and $|0_\omega\rangle^{\mathrm{out}}$ defined as

$$\hat{b}_i\,|0_\omega\rangle^{\mathrm{in}} = 0 \qquad \hat{c}_i\,|0_\omega\rangle^{\mathrm{out}} = 0 \tag{4.76}$$

[43] Relation

$$c_i = V^\dagger b_i V = \sum_j T_{ij} b_j$$

allows, as we will see, to express the operator V in terms of the components of the matrix T.Let us recall that in the previous relation one has $c_n = \hat{c}_n$ and $c_{2n} = \hat{c}_n^\dagger$ accordingly to (4.66), and similarly for $\mathbf{b}$.

can be related by

$$\hat{c}_i \left|0_\omega\right\rangle^{\text{out}} = 0 \quad \Rightarrow \quad V^\dagger b_i V \left|0_\omega\right\rangle^{\text{out}} = 0 \tag{4.77}$$

which yields

$$\left|0_\omega\right\rangle^{\text{in}} = V \left|0_\omega\right\rangle^{\text{out}} \tag{4.78}$$

For

$$X = -\beta^* \alpha^{-1} \tag{4.79}$$

a $N \times N$ matrix, the unitary operator V is then defined[44] by

$$\left|0_\omega\right\rangle^{\text{in}} = V \left|0_\omega\right\rangle^{\text{out}} = \left[\frac{1}{\sqrt{|\det \alpha|}} e^{\frac{1}{2}\sum_{i,j} X_{ij} \hat{c}_i^\dagger \hat{c}_j^\dagger}\right] \left|0_\omega\right\rangle^{\text{out}} \tag{4.80}$$

Since X is a symmetric matrix[45] one has

$$X = \begin{pmatrix} 0 & 0 & \frac{S_{02}}{S_{22}} \\ 0 & 0 & \frac{S_{12}}{S_{22}} \\ \frac{S_{02}}{S_{22}} & \frac{S_{12}}{S_{22}} & 0 \end{pmatrix} \tag{4.81}$$

where the X_{20} and X_{21} components are simplified using the symmetry of the X matrix. Therefore since $\hat{c}_i^\dagger$ and $\hat{c}_j^\dagger$ commute, one is left[46] with

$$\left|0_\omega\right\rangle^{\text{in}} = \left[\frac{1}{|S_{22}|} e^{\left(X_{02}\hat{c}_0^\dagger + X_{12} c_1^\dagger\right)\hat{c}_2^\dagger}\right] \left|0_\omega\right\rangle^{\text{out}} = \left[\frac{1}{|S_{22}|} e^{X_{02}\hat{c}_0^\dagger \hat{c}_2^\dagger} e^{X_{12} c_1^\dagger \hat{c}_2^\dagger}\right] \left|0_\omega\right\rangle^{\text{out}} \tag{4.82}$$

where, as seen in (4.81), $X_{i2}(\omega) = S_{i2}(\omega)/S_{22}(\omega)$. Defining, as we did in (4.58), the full Fock space as the tensor product of the Fock spaces of each mode i, we can define in the outgoing basis

$$\left|n\right\rangle_{(i)} = \left|n_\omega\right\rangle_{(i)} = \frac{1}{\sqrt{n!}} (c_i^\dagger)^n \left|0_\omega\right\rangle_{(i)}^{\text{out}} \tag{4.83}$$

with $i = 0, 1, 2$. Then, one obtains, after a Taylor expansion of the two exponentials in (4.82),

$$\left|0_\omega\right\rangle^{\text{in}} = \frac{1}{|S_{22}|} \sum_{m=0}^{+\infty} \sum_{n=0}^{+\infty} \sqrt{C_{n+m}^m} [X_{02}]^m [X_{12}]^n \left|m\right\rangle_{(0)} \left|n\right\rangle_{(1)} \left|n+m\right\rangle_{(2)} \tag{4.84}$$

with

$$C_n^k = \binom{n}{k} = \frac{n!}{k!(n-k)!} \tag{4.85}$$

the binomial coefficient[47]. One can see that $\left|0_\omega\right\rangle^{\text{in}}$ is a three-mode pure state.

---

[44] See Appendix A.1 for details.

[45] X is symmetric if $X^T = X$, i.e. if $[\alpha^{-1}]^T \beta^\dagger = \beta^* \alpha^{-1}$. Since $[\alpha^{-1}]^T = [\alpha^T]^{-1}$, multiplying the previous equality from the left by α^T and from the right by α one obtains $\beta^\dagger \alpha = \alpha^T \beta^*$ which is the last relation in (4.74). Hence X is symmetric.

[46] The prefactor $|S_{22}|^{-1}$ comes from the normalization of (4.84). Comparing this normalization with the general expression (4.80) imposes the relation

$$\det \alpha = S_{22} S_{00}^* S_{11}^* - S_{22} S_{01}^* S_{10}^* = |S_{22}|^2 \Rightarrow S_{00}^* S_{11}^* - S_{01}^* S_{10}^* = S_{22}^*$$

in the same way as the symmetry of the matrix X imposes relations

$$X_{2i} \underset{i\neq 2}{=} S_{20}^* S_{1i}^* - S_{21}^* S_{0i}^* \underset{i\neq 2}{=} \frac{S_{i2} S_{22}^*}{S_{22}}$$

These three relations seem to be difficult to demonstrate from (4.63) but can be checked numerically.

[47] The normalization gives

$$\sum_{n,m} C_{n+m}^m [|X_{02}|^2]^m [|X_{12}|^2]^n = \sum_{N=0}^{\infty} \sum_{m=0}^{N} C_N^m [|X_{02}|^2]^m [|X_{12}|^2]^{N-m} = \sum_{N=0}^{\infty} \left(|X_{02}|^2 + |X_{12}|^2\right)^N = \frac{1}{1 - |X_{02}|^2 - |X_{12}|^2}$$

which is just, using the definition of the X_{i2} components given in (4.81) and the third relation of (4.63), $|S_{22}|^2$.

4.2.2 . Reduced Densisty Matrices

Tracing out modes 0 and 1, one obtains in the outgoing basis of the $\hat{c}_2$ operators

$$\hat{\rho}_{(2)} = \frac{1}{|S_{22}|^2} \sum_{n=0}^{+\infty} \left(\frac{\sqrt{|S_{22}|^2 - 1}}{|S_{22}|} \right)^{2n} |n\rangle_{(2)\,(2)} \langle n| \tag{4.86}$$

where the third relation in (4.63) has been used. Similarly[48] one obtains

$$\hat{\rho}_{(1)} = \frac{1}{1 + |S_{12}|^2} \sum_{n=0}^{+\infty} \left(\frac{|S_{12}|}{1 + |S_{12}|} \right)^{2n} |n\rangle_{(1)\,(1)} \langle n| \tag{4.87}$$

when tracing out modes 0 and 2, and

$$\hat{\rho}_{(0)} = \frac{1}{1 + |S_{02}|^2} \sum_{n=0}^{+\infty} \left(\frac{|S_{02}|}{1 + |S_{02}|} \right)^{2n} |n\rangle_{(0)\,(0)} \langle n| \tag{4.88}$$

when tracing out modes 1 and 2. Finally, defining the positive parameter r_i as

$$\begin{aligned} \sinh r_i &= \sqrt{|S_{i2}|^2 - \delta_{i2}} = \sqrt{\langle \hat{c}_i^\dagger \hat{c}_i \rangle_0} = \sqrt{\mathcal{N}_i} \\ \cosh r_2 &= |S_{22}| \end{aligned} \tag{4.89}$$

with $\langle ... \rangle_0$ the vacuum of the ingoing modes $\hat{b}_i$, one can write all the previous formulae as

$$\hat{\rho}_{(i)} = \frac{1}{\cosh^2 r_i} \sum_{n=0}^{+\infty} (\tanh r_i)^{2n} |n\rangle_{(i)\,(i)} \langle n| \tag{4.90}$$

with $i = 0, 1, 2$, or analagously,

$$\hat{\rho}_{(i)} = \frac{1}{1 + \mathcal{N}_i} \sum_{n=0}^{+\infty} \left(\frac{\mathcal{N}_i}{1 + \mathcal{N}_i} \right)^{n} |n\rangle_{(i)\,(i)} \langle n| \tag{4.91}$$

This is the expression of a thermal state and one has

$$\mathcal{N}_i(\omega) = \langle \hat{c}_i^\dagger(\omega) \hat{c}_i(\omega) \rangle_0 = \mathsf{Tr} \left\{ c_i^\dagger \hat{c}_i \hat{\rho}_{(i)} \right\} = \frac{1}{e^{\frac{\hbar\omega}{k_B T_i}} - 1} \tag{4.92}$$

which implies[49]

$$\sinh^2 r_i = \frac{1}{e^{\frac{\hbar\omega}{k_B T_i}} - 1} \tag{4.93}$$

and therefore

$$T_i(\omega) = \frac{\hbar\omega}{2 k_B \ln[\coth r_i(\omega)]} \tag{4.94}$$

Then T_0 is an effective temperature : but contrary to the Hawking temperature of a gravitational black-hole, which is the effective temperature of a black-body radiation, T_0 is energy dependent. Nevertheless, the analog Hawking temperature T_H can be obtained from (4.89) since one can define T_H as the energy-independent fitting parameter of

$$\mathcal{N}_0(\omega) = \langle \hat{c}_0^\dagger(\omega) \hat{c}_0(\omega) \rangle_0 = |S_{02}(\omega)|^2 = \frac{1}{e^{\frac{\hbar\omega}{k_B T_H}} - 1} \tag{4.95}$$

Then, even if this radiation at temperature T_0 is not purely thermal, one can retrieve an energy-independent effective temperature $T_0 \to T_H$ when $\omega \to 0$ [90].

[48] Using, after a change of variable,

$$\sum_q C_{n+q}^n X^q = \frac{(1 - X)^{-n}}{1 - X}$$

and then again applying the definition of the X_{i2} component given in (4.81) and the third relation of (4.63).

[49] One has indeed

$$\sum_{n=0}^{+\infty} n \, (\tanh r_i)^{2n} = \cosh^2 r_i \sinh^2 r_i$$

when computing the previous trace.

4.2.3 . Optical Analog of the Acoustic Analog : the $\{\hat{e}\}$ and $\{\hat{f}\}$ Bases

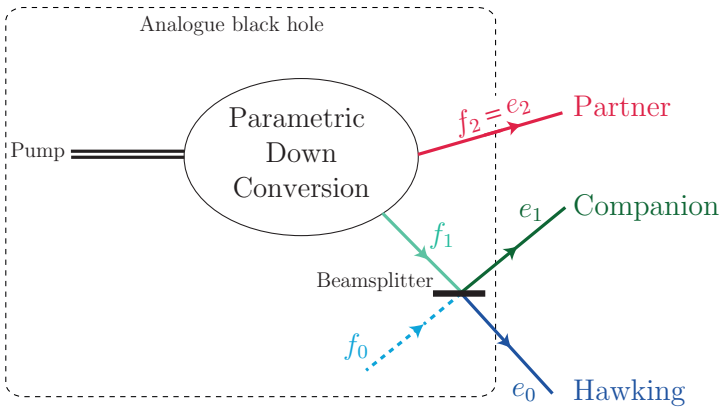

Figure 4.1: Optical analog of the acoustic analog of a black hole [86]. The effective modes f_i and e_i ($i = 0, 1$ and 2) are related to the physical outgoing modes c_i through Eqs. (4.103) and (4.97). The f_0 mode is represented with a dashed line because, contrarily to modes f_1 and f_2, it is not occupied at zero temperature, as can be seen in Eqs. (4.180). The long wavelength transmission coefficient of the beam-splitter plays the role of the greybody factor Γ_0 of the analogous black hole and is defined in (4.208) for the waterfall configuration [38].

Considering (4.89) and the third line of (4.63) one has

$$\sinh^2 r_0 + \sinh^2 r_1 = \sinh^2 r_2 \tag{4.96}$$

Then defining

$$\hat{e}_0 = e^{-i\varphi_{02}}\hat{c}_0 \quad \hat{e}_1 = e^{-i\varphi_{12}}\hat{c}_1 \quad \hat{e}_2 = e^{i\varphi_{22}}\hat{c}_2 \tag{4.97}$$

with the phases defined in (4.64), one can write the expression in the exponential in (4.82) as

$$\left(X_{02}\hat{c}_0^\dagger + X_{12}c_1^\dagger\right)\hat{c}_2^\dagger = \tanh r_2 \left(\frac{\sinh r_0}{\sinh r_2}\hat{e}_0^\dagger + \frac{\sinh r_1}{\sinh r_2}e_1^\dagger\right)\hat{e}_2^\dagger = \tanh r_2 \left(\cos\theta\hat{e}_0^\dagger + \sin\theta e_1^\dagger\right)\hat{e}_2^\dagger \tag{4.98}$$

with, by virtue of (4.96),

$$\cos\theta = \frac{\sinh r_0}{\sinh r_2} \quad \sin\theta = \frac{\sinh r_1}{\sinh r_2} \tag{4.99}$$

for $\theta \in [0, \pi/2]$ since the r_i are positive parameters [50] . The transformation (4.97) can be written as

$$\boldsymbol{e} = W^\dagger \boldsymbol{c} W = T'\,\boldsymbol{c} \qquad \Rightarrow \qquad \boldsymbol{e} = W^\dagger V^\dagger \boldsymbol{b} V W = T'T\,\boldsymbol{b} \tag{4.100}$$

with $\boldsymbol{e}$ and $\boldsymbol{c}$ defined as $\hat{\mathbf{a}}$ in (4.129)[51]. Contrary to T which is non-local, one can see that T', which is defined as

$$T' = \text{diag}(e^{-i\varphi_{02}}, e^{-i\varphi_{12}}, e^{i\varphi_{22}}, e^{i\varphi_{02}}, e^{i\varphi_{12}}, e^{-i\varphi_{22}}) \tag{4.101}$$

is a Local Linear Unitary BOgoliubov transformation (LLUBO) since there is no mixing of different modes. Then one obtains[52] for $V' = VW$

$$|0_\omega\rangle^{\text{in}} = V'\,|0_\omega\rangle^e = \left[\frac{1}{\cosh r_2} e^{\tanh r_2\left(\cos\theta\hat{e}_0^\dagger + \sin\theta e_1^\dagger\right)\hat{e}_2^\dagger}\right]|0_\omega\rangle^e \tag{4.102}$$

with $|0_\omega\rangle^e$ the vacuum of operators $\hat{e}_i$. Finally, as discussed in Ref. [86], a final change of basis can be performed towards the effective modes $\hat{f}_0, \hat{f}_1, \hat{f}_2$ schematically represented in Fig. 4.1. These modes are related to the physical outgoing modes by

$$\hat{f}_0 = -\sin\theta\,\hat{e}_0 + \cos\theta\,\hat{e}_1 \tag{4.103a}$$

$$\hat{f}_1 = \cos\theta\,\hat{e}_0 + \sin\theta\,\hat{e}_1 \tag{4.103b}$$

$$\hat{f}_2 = \hat{e}_2 \tag{4.103c}$$

[50] One can also write $|X_{02}| = \tanh r_2 \cos\theta$ and $|X_{12}| = \tanh r_2 \sin\theta$.
[51] One has therefore straightforwardly $\boldsymbol{e} = W^\dagger V^\dagger \boldsymbol{b} V W = T'T\,\boldsymbol{b}$.
[52] See Appendix A.1 for details.

that one can also encode as

$$\boldsymbol{f} = Z^\dagger \boldsymbol{e}\, Z = T''\, \boldsymbol{e} \qquad \Rightarrow \qquad \boldsymbol{f} = Z^\dagger W^\dagger V^\dagger \boldsymbol{b}\, V W Z = T'' T' T\, \boldsymbol{b} \tag{4.104}$$

with

$$T'' = \begin{pmatrix} -\sin\theta & \cos\theta & 0 & 0 & 0 & 0 \\ \cos\theta & \sin\theta & 0 & 0 & 0 & 0 \\ 0 & 0 & 1 & 0 & 0 & 0 \\ 0 & 0 & 0 & -\sin\theta & \cos\theta & 0 \\ 0 & 0 & 0 & \cos\theta & \sin\theta & 0 \\ 0 & 0 & 0 & 0 & 0 & 1 \end{pmatrix} \tag{4.105}$$

Then[53] $V'' = VWZ$ is defined by

$$|0_\omega\rangle^{\text{in}} = V''\,|0_\omega\rangle^f = \left[\frac{1}{\cosh r_2} e^{\tanh r_2 \hat{f}_1^\dagger \hat{f}_2^\dagger}\right] |0_\omega\rangle^f \tag{4.106}$$

or[54] equivalently

$$|0_\omega\rangle^{\text{in}} = \left[e^{r_2\left(\hat{f}_1^\dagger \hat{f}_2^\dagger - \hat{f}_1 \hat{f}_2\right)}\right] |0_\omega\rangle^f \tag{4.107}$$

Furthermore the mode $\hat{f}_0$ does not appear in the previous expression and, since the transformation (4.103) preserves the commutation relations, it is straightforward to see from (4.106) that $\langle f_0^\dagger f_0\rangle_0 = 0$ with the mean value $\langle\,.\,\rangle_0 = {}^{\text{in}}\langle 0_\omega|\,.\,|0_\omega\rangle^{\text{in}}$ taken over the vacuum of the incoming $\hat{b}_i$ operators[55]. We recall that in (4.107) the parameter

$$r_2(\omega) = \operatorname{arsinh}\sqrt{|S_{22}|^2 - 1} \tag{4.108}$$

is called the **squeezing parameter**[56]. Therefore, expression (4.107) indicates that the $T = 0$ state of the system is, as far as the f_1 and f_2 modes are concerned, a two-mode squeezed vacuum with squeezing parameter $r_2(\omega)$. The f_1 and f_2 modes are mixed by a beamsplitter (see Fig. 4.1) of transmission and reflection coefficients $\cos^2\theta$ and $\sin^2\theta$, respectively. It has been argued in Ref. [86] that the long wavelength limit of the transmission coefficient, $\Gamma_0 = \lim_{\omega\to 0}\cos^2\theta$, plays the role of the greybody factor of the analog black hole.

Entanglement is localized in the two-mode squeezed state $f_1|f_2$ (see section 4.5.3). It is then dispatched by mean of a beam splitter which performs a non local transformation from the effective modes (f_0, f_1, f_2) onto other effective modes (e_0, e_1, e_2) which connect to the physical outgoing modes (c_0, c_1, c_2) by a simple local linear unitary Bogoliubov transformation (LLUBO), see details in Appendix 4.2.3. We stress that the configuration depicted in Fig. 4.1 captures the essence of the analog black hole configuration and is generic : a similar model has been used in Ref. [118] for describing an optical system containing a pair white-black hole analog and then studied on general grounds in [119]. Albeit the fact that we allow the down-conversion process to violate Lorentz invariance (since we enforce the Bogoliubov dispersion relation) the two-mode squeezed state built on $\hat{f}_1$ and $\hat{f}_2$ is the closest possible analog to an ideal black hole. The additional beam splitter is inherent to any analog model, with the transmission coefficient of this beam splitter playing the role of the greybody factor in the gravitational context [86].

[53] See Appendix A.1 for details.

[54] See Appendix A.1 for justification.

[55] Using (4.103) as well as the previous transformations and noticing that $\langle e_i^\dagger e_i\rangle_0 = \langle c_i^\dagger c_i\rangle_0 = |S_{i2}|^2 - \delta_{i2} = \sinh^2 r_i$ and $\langle e_1^\dagger e_0\rangle_0 = |\langle c_1^\dagger c_0\rangle_0| = |S_{02}||S_{12}| = \sinh r_0 \sinh r_1$, one can indeed easily check that

$$\langle f_0^\dagger f_0\rangle_0 = \sin^2\theta \sinh^2 r_0 + \cos^2\theta \sinh^2 r_1 - 2\cos\theta \sin\theta \sinh r_0 \sinh r_1 = 0$$

by applying the definitions of $\cos\theta$ and $\sin\theta$ given in (4.99).

[56] See also (4.89) for the definition of r_2.

4.3 . WIGNER FUNCTION AND COVARIANCE MATRIX OF THE ANALOG BLACK HOLE SYSTEM

4.3.1 . Computing expectation values of observables with the Wigner function

The use of the technique of Wigner transform (see, e.g., Refs. [120, 121]) is particularly well suited for determining the different averaged contributions of the pseudo-spin operator to the bipartite (4.211) and tripatite (4.216) measures of genuine non-locality and to the Mermin parameter (4.232). There are two main reasons for this : first, we consider a Gaussian state and we thus just need to evaluate Gaussian integrals weighted by the Wigner transforms of the spin operators and secondly, the Wigner transforms of the pseudo-spins (4.191) are simple enough that the relevant integrals can be evaluated analytically.

The Wigner characteristic function (see Ref. [90]) of any N-mode quantum (pure or mixed) state $\hat{\rho}$ is defined as

$$\chi_a^{(\hat{\rho})}(\boldsymbol{\lambda}) = \langle \hat{D}_{\hat{\boldsymbol{a}}}(\boldsymbol{\lambda}) \rangle = \mathrm{Tr}\{\hat{\rho}\hat{D}_{\hat{\boldsymbol{a}}}(\boldsymbol{\lambda})\} \tag{4.109}$$

with

$$\begin{aligned} \hat{D}_{\hat{\boldsymbol{a}}}(\boldsymbol{\lambda}) &= e^{\boldsymbol{\lambda}^T \hat{\boldsymbol{a}}} \\ \boldsymbol{\lambda} &= (\lambda_0, \lambda_{N-1}, -\lambda_0^*, ..., -\lambda_{N-1}^*)^T \quad , \lambda_i \in \mathbb{C} \\ \hat{\boldsymbol{a}} &= (\hat{a}_0, ..., \hat{a}_{N-1}, \hat{a}_0^\dagger, ..., \hat{a}_{N-1}^\dagger)^T \end{aligned} \tag{4.110}$$

the displacement operator. From (4.110) it is easy to check that the displacement operator can equivalently be written as

$$\hat{D}_{\hat{\boldsymbol{a}}}(\boldsymbol{r}) = e^{i\boldsymbol{\xi}_a^T \Omega \boldsymbol{r}} \tag{4.111}$$

with $\boldsymbol{r}$ a $2N$ real vector [90] and

$$\hat{\boldsymbol{\xi}}_a = (\hat{\xi}_0, \hat{\xi}_1, ..., \hat{\xi}_{2N-1})^T = \sqrt{2}(\hat{q}_0, \hat{p}_0, ..., \hat{q}_{N-1}, \hat{p}_{N-1})^T \tag{4.112}$$

for a N-mode system, with $\hat{q}_i$ and $\hat{p}_i$ respectively the position operator and the momentum operator of the i-th mode. Here both $\hat{q}_j$ and $\hat{p}_j$ are *dimensionless* [57] and are defined as

$$\hat{q}_j = \frac{1}{\sqrt{2}}(\hat{a}_j + \hat{a}_j^\dagger) \qquad \text{and} \qquad \hat{p}_j = \frac{1}{i\sqrt{2}}(\hat{a}_j - \hat{a}_j^\dagger) \tag{4.113}$$

with $\hat{a}_j$ and $\hat{a}_j^\dagger$ bosonic creation and annihilation operators. Then it can be shown [113] that for Gaussian states

$$\chi_a^{(\hat{\rho})}(\boldsymbol{r}) = \langle \hat{D}_{\hat{\boldsymbol{a}}}(\boldsymbol{r}) \rangle = \exp\left\{ -\frac{1}{2}\boldsymbol{r}^T \Omega \sigma_a \Omega^T \boldsymbol{r} - i\langle \boldsymbol{\xi}_{\hat{\boldsymbol{a}}} \rangle^T \Omega^T \boldsymbol{r} \right\} \tag{4.114}$$

with σ_a the covariance matrix of the system that will be defined in (4.124). The Wigner function of the density operator $\hat{\rho}$ is defined as the Fourier transform of the characteristic function, i.e.

$$W_\rho(\boldsymbol{\xi_a}) = \int_{-\infty}^{+\infty} \frac{d^{2N}\boldsymbol{r}}{2^N \pi^{2N}} e^{-i\boldsymbol{\xi}_{\boldsymbol{a}}^T \Omega \boldsymbol{r}} \chi_a^{(\hat{\rho})}(\boldsymbol{r}) \tag{4.115}$$

which[58] straightforwardly gives

$$W_{\hat{\rho}}(\boldsymbol{\xi_a}) = \frac{1}{\pi^N \sqrt{\det \sigma}} \exp\left\{ -\frac{1}{2} \left(\boldsymbol{\xi_a} - \langle \boldsymbol{\xi}_{\hat{\boldsymbol{a}}} \rangle\right)^T \sigma_a^{-1} \left(\boldsymbol{\xi_a} - \langle \boldsymbol{\xi}_{\hat{\boldsymbol{a}}} \rangle\right) \right\} \tag{4.116}$$

Using (4.115) and (4.109) it is easy to show[59] that one has also generically, i.e. for any (Gaussian or non Gaussian) state,

$$W_{\hat{\rho}}(\boldsymbol{q}, \boldsymbol{p}) = \frac{1}{\pi^N 2^N} \int_{-\infty}^{+\infty} d^N \boldsymbol{z}\, e^{i\boldsymbol{p}.\boldsymbol{z}} \left\langle \boldsymbol{q} - \frac{1}{2}\boldsymbol{z} \right| \hat{\rho} \left| \boldsymbol{q} + \frac{1}{2}\boldsymbol{z} \right\rangle \tag{4.117}$$

[57] In analogy with the quantum harmonic oscillator one can write $\hat{X}\hat{P}/\hbar = [\sqrt{m\omega/\hbar}\hat{X}][\sqrt{1/\hbar m\omega}\hat{P}] = \hat{q}\hat{p}$ with $\hat{q}$ and $\hat{p}$ being dimensionless.

[58] Let us remark that here the normalization is $1/(2^N\pi^{2N})$ and not $1/(2\pi)^{2N}$ as usually written (see Ref. [113]) since there is here a $\sqrt{2}$ factor in the definition of $\boldsymbol{\xi}_a$. Then the obtained expression of the Wigner function is appropriately normalized.

[59] One just need to take the trace in position space, use $e^{-ix\hat{p}}\left|q\right\rangle = \left|q + x\right\rangle$ after applying the Baker-Campell-Hausdorff formula.

where N is the dimension of position $\boldsymbol{q}$ space and $\boldsymbol{z}$ a N real vector corresponding to the odd components of the $2N$ real vector $\boldsymbol{r}$. The Wigner function of the density matrix $\hat{\rho}$ should obey the normalization condition

$$\int_{-\infty}^{+\infty} d^N\boldsymbol{q}\, d^N\boldsymbol{p}\, W_{\hat{\rho}}(\boldsymbol{q},\boldsymbol{p}) = \mathrm{Tr}\{\hat{\rho}\} = 1 \tag{4.118}$$

The Wigner function is a quasi-probability distribution (*quasi* since it is not always positive-definite[60]) and can be used to compute expectation values for continuous variables. The expectation value of an observable $\hat{A}$ can, in an abstract dimensional phase space, indeed be expressed as

$$\langle\hat{A}\rangle = \mathrm{Tr}\{\hat{\rho}\hat{A}\} = \int_{-\infty}^{+\infty} d^N\boldsymbol{q} \int_{-\infty}^{+\infty} d^N\boldsymbol{p}\, W_{\hat{\rho}}(\boldsymbol{q},\boldsymbol{p})\, W_{\hat{A}}(\boldsymbol{q},\boldsymbol{p}) \tag{4.119}$$

with $W_{\hat{\rho}}(\boldsymbol{q},\boldsymbol{p})$ the Wigner distribution, i.e. the Wigner transform of the density operator $\hat{\rho}$, and $W_{\hat{A}}(\boldsymbol{q},\boldsymbol{p})$ the Wigner transform of the operator $\hat{A}$, that is to say[61]

$$W_{\hat{A}}(\boldsymbol{q},\boldsymbol{p}) = \int_{-\infty}^{+\infty} d^N\boldsymbol{z}\, \exp\{i\boldsymbol{p}.\boldsymbol{z}\}\, \langle \boldsymbol{q} - \frac{1}{2}\boldsymbol{z}|\, \hat{A}\, |\boldsymbol{q} + \frac{1}{2}\boldsymbol{z}\rangle \tag{4.120}$$

In this expression $\boldsymbol{q}$ (as well as $\boldsymbol{z}$ and $\boldsymbol{p}$) is a vector in an abstract $n = 3$ dimensional space (with basis $\boldsymbol{e}_0, \boldsymbol{e}_1, \boldsymbol{e}_2$). The kets involved in (4.120) are of the type $|\boldsymbol{Q}\rangle = |Q_0\rangle_0 \otimes |Q_1\rangle_1 \otimes |Q_2\rangle_2$ where $\boldsymbol{Q} = Q_0\boldsymbol{e}_0 + Q_1\boldsymbol{e}_1 + Q_2\boldsymbol{e}_2$ and $|Q\rangle_j$ is the eigenstate of operator $\hat{q}_j$ associated to the eigenvalue Q ($j = 0$, 1 or 2). In the case of a reduced two modes Gaussian state $n = 2$ and the vector $\boldsymbol{Q}$ is two-dimensional: the component associated to the traced mode disappears, as it also does in $|\boldsymbol{Q}\rangle$.

For *Gaussian states*, as is our two-mode or three-mode state, the Wigner function of the density matrix $\hat{\rho}$ (see Ref. [113]) is given by (4.116) where σ_a is the total (or reduced, as appropriate) covariance matrix defined in Eq. (4.140). In (4.116) then, $N = 3$ and $\boldsymbol{\xi}_a = \sqrt{2}\,(q_0, p_0, q_1, p_1, q_2, p_2)^{\mathrm{T}}$ in the three-mode case. In the reduced two-mode case, $N = 2$ and one should remove from the expression of $\boldsymbol{\xi}$ the entries corresponding to the subscript of the traced mode[62]. The Wigner transform (4.116) of a Gaussian state is non-negative, and it was originally considered impossible to violate Bell's inequality under such conditions [114]. This was latter proven incorrect [122, 123]. In particular, Revzen *et al.* [124] proved that observables can be associated to the violation of Bell inequality over a Gaussian state provided their Wigner transform takes values different from the eigenvalues of the associated quantal (i.e. discrete) operator. We will see that two of the pseudo-spins (4.191) we consider, namely $\hat{\Pi}_y$ and $\hat{\Pi}_z$ belong to this class of observables, denoted as "improper" in Ref. [124]. Still, since we work with Gaussian states, all we need to know in order to compute the averaged value of any of our pseudo-spins (4.191) is the covariance matrix of our system.

Let us conclude this section by proving that if a basis $\{\mathbf{b}\}$ and a basis $\{\mathbf{c}\}$ are related by a Linear Unitary BOgoliubov (LUBO) transformation such as (4.67) or equivalently (4.75), then if $\chi_b^{(\hat{\rho}_b)}$ is Gaussian so is $\chi_c^{(\hat{\rho}_b)}$. By definitions (4.109) and (4.110), one has indeed

$$\chi_c^{(\hat{\rho}_b)}(\boldsymbol{\lambda}) = \mathrm{Tr}\{\hat{\rho}_b \hat{D}_{\hat{\boldsymbol{c}}}(\boldsymbol{\lambda})\} = \mathrm{Tr}\{\hat{\rho}_b e^{\boldsymbol{\lambda}^T T\hat{\boldsymbol{b}}}\} = \mathrm{Tr}\{\hat{\rho}_b e^{(T^T\boldsymbol{\lambda})^T\hat{\boldsymbol{b}}}\} = \mathrm{Tr}\{\hat{\rho}_b \hat{D}_{\hat{\boldsymbol{b}}}(T^T\boldsymbol{\lambda})\} = \chi_b^{(\hat{\rho}_b)}(T^T\boldsymbol{\lambda}) \tag{4.121}$$

Then, since $\chi_b^{(\hat{\rho}_b)}$ is Gaussian so is $\chi_b^{(\hat{\rho}_c)}$. Alternatively, one can prove that if a state is related by a squeezing operator (yielded by a LUBO) to another state which is Gaussian then this state is Gaussian (see [90]). Our vacuum state $|0_\omega\rangle^{\mathrm{in}}$ for the $\hat{b}_i$ operators is by definition a Gaussian state whose density matrix is given by $\hat{\rho}_b = |0_\omega\rangle^{\mathrm{in}\,\mathrm{in}}\langle 0_\omega|$. This means that the Wigner characteristic function $\chi_b^{(\hat{\rho}_b)}(\lambda)$ of this state is Gaussian. Defining, as we did in (4.78), $|0_\omega\rangle^{\mathrm{out}} = V^\dagger |0_\omega\rangle^{\mathrm{in}}$ one has $\rho_c = V^\dagger|0_\omega\rangle^{\mathrm{in}\,\mathrm{in}}\langle 0_\omega|V = V^\dagger\hat{\rho}_b V$ and then, by definitions (4.109), (4.110), (4.75) and (4.67), one obtains

$$\chi_b^{(\hat{\rho}_b)}(\boldsymbol{\lambda}) = \mathrm{Tr}\{\hat{\rho}_b \hat{D}_{\hat{\boldsymbol{b}}}(\boldsymbol{\lambda})\} = \mathrm{Tr}\{\hat{\rho}_c V^\dagger \hat{D}_{\hat{\boldsymbol{b}}}(\boldsymbol{\lambda}) V\} = \mathrm{Tr}\{\hat{\rho}_c \hat{D}_{\hat{\boldsymbol{c}}}(\boldsymbol{\lambda})\} = \mathrm{Tr}\{\hat{\rho}_c \hat{D}_{\hat{\boldsymbol{b}}}(T^T\boldsymbol{\lambda})\} = \chi_b^{(\hat{\rho}_c)}(T^T\lambda) \tag{4.122}$$

[60] For a Gaussian state it is always positive-definite since it is a Gaussian.

[61] It can be easily shown (taking first the integral over $\boldsymbol{p}$ and then changing variables) that for any two observables $\hat{A}$ and $\hat{B}$ one has $\int_{-\infty}^{+\infty} d^N\boldsymbol{q} \int_{-\infty}^{+\infty} d^N\boldsymbol{p}\, W_{\hat{A}}(\boldsymbol{q},\boldsymbol{p})\, W_{\hat{B}}(\boldsymbol{q},\boldsymbol{p}) = \mathrm{Tr}\{\hat{A}\hat{B}\}$. Then taking $\hat{B} = \hat{\rho}$ one obtains (4.119).

[62] The Wigner functions of the density matrices representing our different subsystems as well as the one of the full system are given in Appendix A.9.

where we have used[63]

$$V^\dagger \hat{D}_{\hat{\boldsymbol{b}}}(\boldsymbol{\lambda}) V = V^\dagger e^{\boldsymbol{\lambda}^T \hat{\boldsymbol{b}}} V = e^{\boldsymbol{\lambda}^T V^\dagger \hat{\boldsymbol{b}} V} = e^{\boldsymbol{\lambda}^T \hat{\boldsymbol{c}}} = e^{\boldsymbol{\lambda}^T T \hat{\boldsymbol{b}}} = e^{(T\boldsymbol{\lambda})^T \hat{\boldsymbol{b}}} = \hat{D}_{\hat{\boldsymbol{b}}}(T^T \boldsymbol{\lambda}) \tag{4.123}$$

and the cyclic property of the trace. Then, since $\chi_b^{(\hat{\rho}_b)}$ is Gaussian so is $\chi_b^{(\hat{\rho}_c)}$. One can therefore use any basis to compute the covariance matrix of the system as long as this basis is related by a LUBO to the basis of a Gaussian state since the LUBO preserves the gaussianity of the Wigner characteristic function.

4.3.2 . The Covariance Matrix : General Formalism

From (4.112) and (4.113), the covariance matrix of a state is defined as

$$\sigma_{kl} \equiv \frac{1}{2}\langle\{(\hat{\xi}_k - \langle\hat{\xi}_k\rangle), (\hat{\xi}_l - \langle\hat{\xi}_l\rangle)\}\rangle = \frac{1}{2}\langle\hat{\xi}_k\hat{\xi}_l + \hat{\xi}_l\hat{\xi}_k\rangle - \langle\hat{\xi}_k\rangle\langle\hat{\xi}_l\rangle \tag{4.124}$$

The usual commutation relations between the canonical conjugated variables $\hat{q}_k$ and $\hat{p}_l$ can be written as

$$[\hat{\xi}_k, \hat{\xi}_l] = 2i\,\Omega_{kl} \tag{4.125}$$

where[64]

$$\Omega = \oplus_{n=0}^{N-1} \omega_n \underset{N=3}{=} \begin{pmatrix} \omega_0 & 0_2 & 0_2 \\ 0_2 & \omega_1 & 0_2 \\ 0_2 & 0_2 & \omega_2 \end{pmatrix} \tag{4.126}$$

the symplectic form defined by

$$\omega_n = \begin{pmatrix} 0 & 1 \\ -1 & 0 \end{pmatrix} \tag{4.127}$$

In other terms, Ω is here a $2N \times 2N$ matrix with components $\Omega_{2n,2n+1} = 1$, $\Omega_{2n+1,2n} = -1$ and 0 otherwise. By definition one has

$$\begin{aligned} &\Omega^T = -\Omega \\ &\Omega^T\Omega = \Omega\Omega^T = \mathbb{1}_{2N} \\ &\Omega^2 = -\mathbb{1}_{2N} \end{aligned} \tag{4.128}$$

with the first relation encoding Ω as a skew-symmetric form. Defining

$$\hat{\mathbf{a}} = (\hat{a}_0, \hat{a}_1, ..., \hat{a}_{N-1}, \hat{a}_0^\dagger, \hat{a}_1^\dagger, ..., \hat{a}_{N-1}^\dagger)^T \tag{4.129}$$

one can then write

$$\hat{\boldsymbol{\xi}}_a = \sqrt{2}\, U\, \hat{\mathbf{a}} \tag{4.130}$$

with U a $2N \times 2N$ unitary matrix given (for a 3-mode state) by

$$U = \begin{pmatrix} \frac{1}{\sqrt{2}} & 0 & 0 & \frac{1}{\sqrt{2}} & 0 & 0 \\ \frac{1}{i\sqrt{2}} & 0 & 0 & \frac{-1}{i\sqrt{2}} & 0 & 0 \\ 0 & \frac{1}{\sqrt{2}} & 0 & 0 & \frac{1}{\sqrt{2}} & 0 \\ 0 & \frac{1}{i\sqrt{2}} & 0 & 0 & \frac{-1}{i\sqrt{2}} & 0 \\ 0 & 0 & \frac{1}{\sqrt{2}} & 0 & 0 & \frac{1}{\sqrt{2}} \\ 0 & 0 & \frac{1}{i\sqrt{2}} & 0 & 0 & \frac{-1}{i\sqrt{2}} \end{pmatrix} \tag{4.131}$$

Then since one has

$$[\hat{a}_k, \hat{a}_l] = J_{kl} \tag{4.132}$$

[63] Let the matrix A be a diagonalizable matrix, i.e. $A = PDP^{-1}$ with D diagonal, then $e^A = Pe^D P^{-1}$ by simple Taylor expansion of the exponential.

[64] In the block structure of Ω, 0_2 is the 2×2 null matrix.

with[65]

$$J = \begin{pmatrix} 0_N & \mathbb{1}_N \\ -\mathbb{1}_N & 0_N \end{pmatrix} \tag{4.133}$$

the symplectic form

$$\begin{aligned} J^T &= -J \\ J^T J &= J J^T = \mathbb{1}_{2N} \\ J^2 &= -\mathbb{1}_{2N} \end{aligned} \tag{4.134}$$

the fulfillment of (4.132) and (4.125) leads through definition (4.130) to

$$J = i\, U^\dagger \Omega\, U^* \tag{4.135}$$

One can see that this last definition fulfill immediately all the relations in (4.134) because of (4.128) as long as one has not only $UU^\dagger = U^\dagger U = \mathbb{1}_N$ (unitarity) but also

$$U^* U^\dagger = \Omega\, U\, U^T \Omega \tag{4.136}$$

One can check that this is indeed the case. Inverting (4.135) one has also

$$\Omega = -i\, U J\, U^T \tag{4.137}$$

Even if $\langle \hat{\xi}_k \rangle$ is not always zero (for example, it is not zero when the average is taken over a coherent state), by a local unitary (LU) transformation[66] $\langle \hat{\xi}_k \rangle \xrightarrow{\text{LU}} \langle \hat{\xi}'_k \rangle$ which by definition does not modify the entanglement properties of a quantum state, it can always be brought to $\langle \hat{\xi}'_k \rangle = 0$ for all k. Therefore, taking $\langle \hat{\xi}_k \rangle$ to $\langle \hat{\xi}'_k \rangle$ such as $\langle \hat{\xi}'_k \rangle = 0$ and renaming $\langle \hat{\xi}'_k \rangle$, the covariance matrix in (4.138) can be written without loss of generality as

$$\sigma_{kl} = \frac{1}{2} \langle \hat{\xi}_k \hat{\xi}_l + \hat{\xi}_l \hat{\xi}_k \rangle \tag{4.138}$$

Finally, a well-defined covariance matrix σ must satisfy the relation

$$\sigma + i\, \Omega \geq 0 \tag{4.139}$$

which asserts the positiveness of the covariance matrix as implied by the canonical commutation relations [90, 86, 125].

4.3.3 . The Covariance Matrix of a Three-Mode Gaussian State

Relationships (4.82) and (4.84) ensure that the system is in a pure three-mode Gaussian state and is therefore fully characterized by its 6×6 covariance matrix $\sigma(\omega)$ with entries

$$\sigma_{\ell m}(\omega) \equiv \frac{1}{2} \langle \hat{\xi}_\ell\, \hat{\xi}_m + \hat{\xi}_m\, \hat{\xi}_\ell \rangle \tag{4.140}$$

Defined as in the generic (4.113) and (4.112), the operator $\hat{\xi}_\ell(\omega)$ or $\hat{\xi}_m(\omega)$ is here one of the 6 components of the column vector

$$\hat{\boldsymbol{\xi}}_a = (\hat{\xi}_0, \hat{\xi}_1, ..., \hat{\xi}_5)^T = \sqrt{2}(\hat{q}_0, \hat{p}_0, \hat{q}_1, \hat{p}_1, \hat{q}_2, \hat{p}_2)^T \tag{4.141}$$

where

$$\hat{q}_j(\omega) = \frac{1}{\sqrt{2}}(\hat{a}_j + \hat{a}_j^\dagger) \quad \text{and} \quad \hat{p}_j(\omega) = \frac{1}{i\sqrt{2}}(\hat{a}_j - \hat{a}_j^\dagger) \tag{4.142}$$

with $\hat{a}_j(\omega)$ being, for $j \in \{0, 1, 2\}$, any kind of *ingoing* or *outgoing* operators such as our $\hat{b}_j(\omega)$ or $\hat{c}_j(\omega)$ or any generic $\hat{e}_j(\omega)$ that will be defined later on. In expression (4.140) and in all the following, the averages $\langle \cdots \rangle$ are performed over the density matrix of the system. This density matrix is simply $\rho = |0\rangle^{\text{in}\,\text{in}}\langle 0|$ in

[65] In the block structure of J, 0_N is the $N \times N$ null matrix.
[66] A *local* transformation does not mix different modes.

the ideal case of the pure vacuum state.

We also consider more realistic situations where some incoherent excitations are present and the system is not in a pure state. A simple manner to account for this situation would be to assume that the system is in a thermal state. This is however impossible because the analog configurations depicted in 3.1 are thermodynamically unstable. A way to circumvent this problem has been proposed in Refs. [93, 94]. It consists in postulating that the system was initially in a Gaussian thermal state[67], i.e. in thermal equilibrium at temperature T with a constant density and velocity (n_u and V_u, respectively) and that the flow has been adiabatically modified by slowly ramping the appropriate external potential, eventually reaching the black hole configuration of interest. This situation, although idealized, is less schematic than the zero excitation regime. It emulates the experimental situation of Refs. [34, 35] if the system is considered to have been initially in equilibrium in the frame attached to the flowing condensate. In this case one has (for $j \in \{0,1,2\}$)

$$\bar{n}_j(\omega) \equiv \langle \hat{b}_j^\dagger(\omega)\hat{b}_j(\omega)\rangle = n_{\rm th}\big[\omega_{{\rm B},\alpha}\big(q_{j|{\rm in}}(\omega)\big)\big] \tag{4.143}$$

where $n_{\rm th}(\omega)$ is the thermal Bose occupation distribution at temperature T and energy $\hbar\omega$, whereas $\omega_{{\rm B},\alpha}(q_{j|{\rm in}})$ is the Bogoliubov dispersion relation (3.25), with $\alpha = u$ if $j = 0$ and $\alpha = d$ if $j = 1$ or 2. The functions $q_{j|{\rm in}}(\omega)$ appearing in expression (4.143) are pictorially defined in Fig. 3.2. For instance $q_{2|{\rm in}}(\omega)$ is the function that, to a given angular frequency $\omega \in [0,\Omega]$, associates a wave-vector along the $2|{\rm in}$ dispersion branch[68]. We loosely refer to the cases where $\bar{n}_j$ ($j \in \{0,1,2\}$) is equal to the right-hand side (r.h.s.) of (4.143) as "finite temperature" situations. In the simplest configuration, denoted as "zero temperature" the system is in the pure state $|0\rangle^{\rm in}$ and the $\bar{n}_j$'s are all equal to zero. We will not specify the values of the $\bar{n}_j$'s in the following, so that the formulas we give are generally valid, even in situations where the occupation numbers should not be given by formulas of the type of Eq. (4.143). However, for illustrative purposes, all the finite temperature figures of this work are plotted in specific temperature cases with the $\bar{n}_j$ given by formula (4.143).

Thus, we will consider in the following, the system as being either in the Gaussian vacuum state or in the Gaussian state at finite temperature T, with the vacuum defined with respect to the *ingoing* annihilation operators $\hat{b}_j(\omega)$. Therefore we will consider $\langle \hat{b}_j^\dagger \hat{b}_j\rangle$ as being either $\langle \hat{b}_j^\dagger \hat{b}_j\rangle_{th} = \bar{n}_j(\omega)$ or $\langle \hat{b}_j^\dagger \hat{b}_j\rangle_0 = 0$ with $\bar{n}_j(\omega)$ the "thermal occupation number" of mode j at energy $\hbar\omega$ computed through the formula (4.143). Then, as can be seen from (4.59) and (4.60), the vacuum $|0_\omega\rangle^{\rm in}$ of operators $\hat{b}_j$, i.e. $\hat{b}_j\,|0_\omega\rangle^{\rm in} = 0$, is not the vacuum $|0_\omega\rangle^{\rm out}$ of operators $\hat{c}_j$.
We will refer to the covariance matrix in (4.140) as $\sigma_b(\omega)$ when it is defined through $\boldsymbol{\xi}_b(\omega)$ given in (4.112) with the $\hat{q}_k$ and $\hat{p}_l$ defined in terms of the $\hat{b}_j(\omega)$ and $\hat{b}_j^\dagger(\omega)$ operators. The average, as we said, will always be taken over a 3-mode Gaussian pure or GAUSSIAN "thermal state" defined with respect to these same operators. Therefore the *ingoing* covariance matrix $\sigma_b(\omega)$ evaluated for the vacuum of $\hat{b}_j(\omega)$ is by definition

$$\sigma_b|_{\langle\ldots\rangle_0} = \mathbb{1}_6 \tag{4.144}$$

Plugging $\boldsymbol{\xi}_b = UT^{-1}U^\dagger\boldsymbol{\xi}_c = -UJT^TJU^\dagger\boldsymbol{\xi}_c$, obtained from (4.70) with (4.73), in the definition of the covariance matrix (4.138), it is straightforward to show that

$$\sigma_c = S_T\sigma_b S_T^T \tag{4.145}$$

[67] The set of Gaussian states can indeed be defined (see [125]) as the set of all ground and thermal states of second-order semi-positive Hamiltonians $H > 0$

$$\hat{\rho}_G = \frac{e^{-\beta\hat{H}}}{{\rm Tr}\{e^{-\beta\hat{H}}\}}$$

with $\beta = 1/k_BT$ where k_B is Boltzmann constant and $\hat{H} = (\xi^T H\,\xi)/2$.The pure Gaussian states are obtained for $\beta \to \infty$. After the Bogoliubov linearization of the field operator, the Hamiltonian of our system is a **quadratic** Hamiltonian but it has negative-norm modes with positive energy in the supersonic regime and is therefore thermodynamically unstable in the frame where the condensate is moving. Hence the schematic procedure adopted here.

[68] $q_{2|{\rm in}}(\omega) \in [q^*, q_0]$ with $q^* = q_{2|{\rm in}}(\Omega)$ and $q_0 = q_{2|{\rm in}}(0)$, see Fig. 3.2.

with S_T the symplectic transformation defined in (4.72). One can also simply use relation (4.59) to expand the components of the covariance matrix (4.138) written in the $\boldsymbol{c}$ basis. Indeed the 6×6 covariance matrix σ defined in Eq. (4.140) can be written in terms of 2×2 submatrices σ_i and ε_{ij}:

$$\sigma_c = \begin{pmatrix} [\sigma_0]_c & [\epsilon_{01}]_c & [\epsilon_{02}]_c \\ [\epsilon_{01}^T]_c & [\sigma_1]_c & [\epsilon_{12}]_c \\ [\epsilon_{02}^T]_c & [\epsilon_{12}^T]_c & [\sigma_2]_c \end{pmatrix} \tag{4.146}$$

where $[\sigma_i]_c = [\epsilon_{ii}]_c$ and[69]

$$[\epsilon_{ij}]_c = 2\begin{pmatrix} Re\langle \hat{q}_i\hat{q}_j\rangle & Re\langle \hat{q}_i\hat{p}_j\rangle \\ Re\langle \hat{p}_i\hat{q}_j\rangle & Re\langle \hat{p}_i\hat{p}_j\rangle \end{pmatrix} \tag{4.147}$$

$$[\epsilon_{ij}^T]_c = 2\begin{pmatrix} Re\langle \hat{q}_j\hat{q}_i\rangle & Re\langle \hat{q}_j\hat{p}_i\rangle \\ Re\langle \hat{p}_j\hat{q}_i\rangle & Re\langle \hat{p}_j\hat{p}_i\rangle \end{pmatrix} \tag{4.148}$$

Remembering that the Bogoliubov transformation preserves commutation relations, one gets

$$[\epsilon_{ij}]_c \underset{i<j}{=} 2\begin{pmatrix} Re\langle \hat{c}_i\hat{c}_j\rangle + Re\langle \hat{c}_i\hat{c}_j^\dagger\rangle & Im\langle \hat{c}_i\hat{c}_j\rangle - Im\langle \hat{c}_i\hat{c}_j^\dagger\rangle \\ Im\langle \hat{c}_i\hat{c}_j\rangle + Im\langle \hat{c}_i\hat{c}_j^\dagger\rangle & -Re\langle \hat{c}_i\hat{c}_j\rangle + Re\langle \hat{c}_i\hat{c}_j^\dagger\rangle\rangle \end{pmatrix} \tag{4.149}$$

$$\begin{aligned} [\epsilon_{ij}]_c^T &\underset{i<j}{=} 2\begin{pmatrix} Re\langle \hat{c}_j\hat{c}_i\rangle + Re\langle \hat{c}_j\hat{c}_i^\dagger\rangle & Im\langle \hat{c}_j\hat{c}_i\rangle - Im\langle \hat{c}_j\hat{c}_i^\dagger\rangle \\ Im\langle \hat{c}_j\hat{c}_i\rangle + Im\langle \hat{c}_j\hat{c}_i^\dagger\rangle & -Re\langle \hat{c}_j\hat{c}_i\rangle + Re\langle \hat{c}_j\hat{c}_i^\dagger\rangle\rangle \end{pmatrix} \\ &\underset{i<j}{=} 2\begin{pmatrix} Re\langle \hat{c}_i\hat{c}_j\rangle + Re\langle \hat{c}_i\hat{c}_j^\dagger\rangle & Im\langle \hat{c}_i\hat{c}_j\rangle + Im\langle \hat{c}_i\hat{c}_j^\dagger\rangle \\ Im\langle \hat{c}_i\hat{c}_j\rangle - Im\langle \hat{c}_i\hat{c}_j^\dagger\rangle & -Re\langle \hat{c}_i\hat{c}_j\rangle + Re\langle \hat{c}_i\hat{c}_j^\dagger\rangle\rangle \end{pmatrix} \end{aligned} \tag{4.150}$$

and for $i = j$

$$[\sigma_i]_c = [\epsilon_{ii}]_c = \begin{pmatrix} 1+2\langle \hat{c}_i^\dagger\hat{c}_i\rangle & 0 \\ 0 & 1+2\langle \hat{c}_i^\dagger\hat{c}_i\rangle \end{pmatrix} = \left(1+2\langle \hat{c}_i^\dagger\hat{c}_i\rangle\right)\mathbb{1}_2 \tag{4.151}$$

Up to here, even if we have been referring to our *outgoing* basis, the expressions of the block components of the covariance matrix apply generally to any operator fulfilling the bosonic commutation relations (which, as we said, are indeed preserved by a Bogoliubov transformation). Then, considering specifically our *outgoing* operators defined accordingly to our previous definitions (4.59) and (4.60), one obtains

$$\begin{aligned} &\langle \hat{c}_0\hat{c}_1\rangle = \langle \hat{c}_1\hat{c}_0\rangle = \langle \hat{c}_0^\dagger\hat{c}_1^\dagger\rangle = \langle \hat{c}_1^\dagger\hat{c}_0^\dagger\rangle = 0 \\ &\langle \hat{c}_0\hat{c}_2^\dagger\rangle = \langle \hat{c}_0^\dagger\hat{c}_2\rangle = \langle \hat{c}_1\hat{c}_2^\dagger\rangle = \langle \hat{c}_1^\dagger\hat{c}_2\rangle = 0 \\ &\langle \hat{c}_2\hat{c}_0^\dagger\rangle = \langle \hat{c}_2^\dagger\hat{c}_0\rangle = \langle \hat{c}_2\hat{c}_1^\dagger\rangle = \langle \hat{c}_2^\dagger\hat{c}_1\rangle = 0 \end{aligned} \tag{4.152}$$

that is to say

$$[\epsilon_{01}]_c = 2\begin{pmatrix} Re\langle \hat{c}_0\hat{c}_1^\dagger\rangle & -Im\langle \hat{c}_0\hat{c}_1^\dagger\rangle \\ Im\langle \hat{c}_0\hat{c}_1^\dagger\rangle & Re\langle \hat{c}_0\hat{c}_1^\dagger\rangle \end{pmatrix} \tag{4.153}$$

$$[\epsilon_{01}^T]_c = 2\begin{pmatrix} Re\langle \hat{c}_1\hat{c}_0^\dagger\rangle & -Im\langle \hat{c}_1\hat{c}_0^\dagger\rangle \\ Im\langle \hat{c}_1\hat{c}_0^\dagger\rangle & Re\langle \hat{c}_1\hat{c}_0^\dagger\rangle \end{pmatrix} = 2\begin{pmatrix} Re\langle \hat{c}_0\hat{c}_1^\dagger\rangle & Im\langle \hat{c}_0\hat{c}_1^\dagger\rangle \\ -Im\langle \hat{c}_0\hat{c}_1^\dagger\rangle & Re\langle \hat{c}_0\hat{c}_1^\dagger\rangle \end{pmatrix} \tag{4.154}$$

[69] In relation (4.147) and (4.148) the specifcations of the real part are relevant only for $i = j$ since otherwise the operators commute.

and, for $i \neq 2$,

$$[\epsilon_{i2}]_c \underset{i\neq 2}{=} 2 \begin{pmatrix} Re\langle \hat{c}_i \hat{c}_2 \rangle & Im\langle \hat{c}_i \hat{c}_2 \rangle \\ Im\langle \hat{c}_i \hat{c}_2 \rangle & -Re\langle \hat{c}_i \hat{c}_2 \rangle \end{pmatrix} \tag{4.155}$$

$$[\epsilon_{i2}^T]_c \underset{i\neq 2}{=} 2 \begin{pmatrix} Re\langle \hat{c}_2^\dagger \hat{c}_i^\dagger \rangle & -Im\langle \hat{c}_2^\dagger \hat{c}_i^\dagger \rangle \\ -Im\langle \hat{c}_2^\dagger \hat{c}_i^\dagger \rangle & -Re\langle \hat{c}_2^\dagger \hat{c}_i^\dagger \rangle \end{pmatrix} = 2 \begin{pmatrix} Re\langle \hat{c}_i \hat{c}_2 \rangle & Im\langle \hat{c}_i \hat{c}_2 \rangle \\ Im\langle \hat{c}_i \hat{c}_2 \rangle & -Re\langle \hat{c}_i \hat{c}_2 \rangle \end{pmatrix} \tag{4.156}$$

Let us remark that all the previous relations (4.152), (4.153), (4.154), (4.155) and (4.156), are true for $\langle ... \rangle$ being generically $\langle ... \rangle_{th}$ or specifically $\langle ... \rangle_0$.

4.3.4 . Generic Rotation and Standard Form of the Covariance Matrix

We rotate our covariance matrix σ_c according to

$$\begin{aligned} \sigma_e &= S_R \sigma_c S_R^T \\ S_R &= \text{diag}\{R(\Phi_{02}), R(\Phi_{12}), R(\Phi_{22})\} \\ R(\Phi_{ij}) &= \begin{pmatrix} \cos\Phi_{ij} & \sin\Phi_{ij} \\ -\sin\Phi_{ij} & \cos\Phi_{ij} \end{pmatrix} \end{aligned} \tag{4.157}$$

and each 2x2 matrix ϵ_{ij} of the covariance matrix is rotated according to

$$\begin{aligned} [\epsilon_{ij}]_e &= R(\Phi_{i2})[\epsilon_{ij}]_c R^T(\Phi_{j2}) \\ [\epsilon_{ij}]_e^T &= R(\Phi_{j2})[\epsilon_{ij}]_c^T R^T(\Phi_{i2}) \end{aligned} \tag{4.158}$$

where we have denoted

$$\begin{aligned} \epsilon_{ij} &\underset{i>j}{=} \epsilon_{ji}^T \\ \epsilon_{ii} &= \sigma_i \end{aligned} \tag{4.159}$$

For the diagonal 2×2 matrix $[\sigma_i]_e$ one obtains simply

$$[\sigma_i]_e = [\sigma_i]_c \tag{4.160}$$

For the 2×2 matrix $[\epsilon_{01}]_e$ one obtains the following components

$$\begin{aligned} [[\epsilon_{01}]_e]_{00} &= 2[Re\langle \hat{c}_0 \hat{c}_1^\dagger \rangle] \cos(\Phi_{02} - \Phi_{12}) + 2[Im\langle \hat{c}_0 \hat{c}_1^\dagger \rangle] \sin(\Phi_{02} - \Phi_{12}) \\ [[\epsilon_{01}]_e]_{01} &= 2[Re\langle \hat{c}_0 \hat{c}_1^\dagger \rangle] \sin(\Phi_{02} - \Phi_{12}) - 2[Im\langle \hat{c}_0 \hat{c}_1^\dagger \rangle] \cos(\Phi_{02} - \Phi_{12}) \\ [[\epsilon_{01}]_e]_{10} &= -2[Re\langle \hat{c}_0 \hat{c}_1^\dagger \rangle] \sin(\Phi_{02} - \Phi_{12}) + 2[Im\langle \hat{c}_0 \hat{c}_1^\dagger \rangle] \cos(\Phi_{02} - \Phi_{12}) \\ [[\epsilon_{01}]_e]_{11} &= 2[Re\langle \hat{c}_0 \hat{c}_1^\dagger \rangle] \cos(\Phi_{02} - \Phi_{12}) + 2[Im\langle \hat{c}_0 \hat{c}_1^\dagger \rangle] \sin(\Phi_{02} - \Phi_{12}) \end{aligned} \tag{4.161}$$

whereas for the 2×2 matrices $[\epsilon_{i2}]_e$ with $i \neq 2$ one obtains

$$\begin{aligned} [[\epsilon_{i2}]_e]_{00} &\underset{i\neq 2}{=} 2[Re\langle \hat{c}_i \hat{c}_2 \rangle] \cos(\Phi_{i2} + \Phi_{22}) + 2[Im\langle \hat{c}_i \hat{c}_2 \rangle] \sin(\Phi_{i2} + \Phi_{22}) \\ [[\epsilon_{i2}]_e]_{01} &\underset{i\neq 2}{=} -2[Re\langle \hat{c}_i \hat{c}_2 \rangle] \sin(\Phi_{i2} + \Phi_{22}) + 2[Im\langle \hat{c}_i \hat{c}_2 \rangle] \cos(\Phi_{i2} + \Phi_{22}) \\ [[\epsilon_{i2}]_e]_{10} &\underset{i\neq 2}{=} -2[Re\langle \hat{c}_i \hat{c}_2 \rangle] \sin(\Phi_{i2} + \Phi_{22}) + 2[Im\langle \hat{c}_i \hat{c}_2 \rangle] \cos(\Phi_{i2} + \Phi_{22}) \\ [[\epsilon_{i2}]_e]_{11} &\underset{i\neq 2}{=} -2[Re\langle \hat{c}_i \hat{c}_2 \rangle] \cos(\Phi_{i2} + \Phi_{22}) - 2[Im\langle \hat{c}_i \hat{c}_2 \rangle] \sin(\Phi_{i2} + \Phi_{22}) \end{aligned} \tag{4.162}$$

Let us write

$$\begin{aligned} Re\langle \hat{c}_0 \hat{c}_1^\dagger \rangle &= |\langle \hat{c}_0 \hat{c}_1^\dagger \rangle| \cos\theta_{01} \\ Im\langle \hat{c}_0 \hat{c}_1^\dagger \rangle &= |\langle \hat{c}_0 \hat{c}_1^\dagger \rangle| \sin\theta_{01} \\ Re\langle \hat{c}_i \hat{c}_2 \rangle &\underset{i\neq 2}{=} |\langle \hat{c}_i \hat{c}_2 \rangle| \cos\theta_{i2} \\ Im\langle \hat{c}_i \hat{c}_2 \rangle &\underset{i\neq 2}{=} |\langle \hat{c}_i \hat{c}_2 \rangle| \sin\theta_{i2} \end{aligned} \tag{4.163}$$

with

$$\begin{aligned} |\langle \hat{c}_0 \hat{c}_1^\dagger \rangle|^2 &= [Re\langle \hat{c}_0 \hat{c}_1^\dagger \rangle]^2 + [Im\langle \hat{c}_0 \hat{c}_1^\dagger \rangle]^2 \\ |\langle \hat{c}_i \hat{c}_2 \rangle|^2 &\underset{i\neq 2}{=} [Re\langle \hat{c}_i \hat{c}_2 \rangle]^2 + [Im\langle \hat{c}_i \hat{c}_2 \rangle]^2 \end{aligned} \tag{4.164}$$

Applying these last definitions in (4.166) and (4.167) after defining

$$\begin{aligned} \Theta_{01} &= (\Phi_{02} - \Phi_{12}) - \theta_{01} \\ \Theta_{i2} &\underset{i\neq j}{=} (\Phi_{i2} + \Phi_{22}) - \theta_{i2} \end{aligned} \tag{4.165}$$

one obtains

$$\begin{aligned} [[\epsilon_{01}]_e]_{00} &= +2|\langle \hat{c}_0 \hat{c}_1^\dagger \rangle| \cos\Theta_{01} \\ [[\epsilon_{01}]_e]_{01} &= +2|\langle \hat{c}_0 \hat{c}_1^\dagger \rangle| \sin\Theta_{01} \\ [[\epsilon_{01}]_e]_{10} &= -2|\langle \hat{c}_0 \hat{c}_1^\dagger \rangle| \sin\Theta_{01} \\ [[\epsilon_{01}]_e]_{11} &= +2|\langle \hat{c}_0 \hat{c}_1^\dagger \rangle| \cos\Theta_{01} \end{aligned} \tag{4.166}$$

whereas for the 2×2 matrices $[\epsilon_{i2}]_e$ with $i \neq 2$ one obtains

$$\begin{aligned} [[\epsilon_{i2}]_e]_{00} &\underset{i\neq 2}{=} +2|\langle \hat{c}_i \hat{c}_2 \rangle| \cos\Theta_{i2} \\ [[\epsilon_{i2}]_e]_{01} &\underset{i\neq 2}{=} -2|\langle \hat{c}_i \hat{c}_2 \rangle| \sin\Theta_{i2} \\ [[\epsilon_{i2}]_e]_{10} &\underset{i\neq 2}{=} -2|\langle \hat{c}_i \hat{c}_2 \rangle| \sin\Theta_{i2} \\ [[\epsilon_{i2}]_e]_{11} &\underset{i\neq 2}{=} -2|\langle \hat{c}_i \hat{c}_2 \rangle| \cos\Theta_{i2} \end{aligned} \tag{4.167}$$

Then one sees from (4.165), (4.166) and (4.167) that taking

$$\begin{aligned} \Phi_{02} - \Phi_{12} &= \theta_{01} + m_0\pi \\ \Phi_{i2} + \Phi_{22} &\underset{i\neq 2}{=} \theta_{i2} + m_i\pi \end{aligned} \tag{4.168}$$

with the m_i some integers, immediately diagonalizes the $[\epsilon_{ij}]_e$ matrices as long as, for $m = m_2 - m_1 - m_0$, the constraint

$$\theta_{01} + \theta_{12} = \theta_{02} + m\pi \tag{4.169}$$

is fulfilled. If this is so, one therefore obtains

$$\begin{aligned} [\sigma_i]_e &= (1 + 2\langle \hat{c}_i^\dagger \hat{c}_i \rangle)\mathbb{1}_2 \\ [\epsilon_{01}]_e &= (-1)^{m_0} 2|\langle \hat{c}_0 \hat{c}_1^\dagger \rangle| \mathbb{1}_2 \\ [\epsilon_{i2}]_e &\underset{i\neq 2}{=} (-1)^{m_i} 2|\langle \hat{c}_i \hat{c}_2 \rangle| \sigma_z \end{aligned} \tag{4.170}$$

with $\mathbb{1}_2$ the 2x2 identity matrix and σ_z the Pauli matrix [70]. In this case one has

$$[\epsilon_{ij}]_e \underset{i<j}{=} [\epsilon_{ij}]_e^T \tag{4.171}$$

If the constraint (4.169) is fulfilled, the obtained form of the covariance matrix (4.170) is called the *standard form* of the covariance matrix. It is important to note that the rotation is energy dependent since the θ_{ij} are energy dependent : in other words, the rotation is not the same at each energy. Furthermore, the previous rotation is a local transformation (no mixing of different modes) : it therefore does not change the entanglement properties of our system. Nevertheless a nonlocality measure is basis dependent.

[70] The previous relations are true for $\langle ... \rangle$ being generically $\langle ... \rangle_{th}$ or more specifically $\langle ... \rangle_0$.

According to our results, rotations to the standard form of the covariance matrices seem to maximize the nonlocality measure of our two-mode Bell operator. Setting generically

$$\begin{aligned} A_i &= 1 + 2\langle \hat{c}_i^\dagger \hat{c}_i \rangle \\ F_{01} &= 2|\langle \hat{c}_0 \hat{c}_1^\dagger \rangle| \cos\Theta_{01} \\ F_{i2} &\underset{i\neq 2}{=} 2|\langle \hat{c}_i \hat{c}_2 \rangle| \cos\Theta_{i2} \\ G_{01} &= 2|\langle \hat{c}_0 \hat{c}_1^\dagger \rangle| \sin\Theta_{01} \\ G_{i2} &\underset{i\neq 2}{=} 2|\langle \hat{c}_i \hat{c}_2 \rangle| \sin\Theta_{i2} \end{aligned} \tag{4.172}$$

one can finally write

$$[\sigma_i]_e = \begin{pmatrix} A_i & 0 \\ 0 & A_i \end{pmatrix} \quad [\epsilon_{01}]_e = \begin{pmatrix} F_{01} & G_{01} \\ -G_{01} & F_{01} \end{pmatrix} \quad [\epsilon_{i2}]_e = \begin{pmatrix} F_{i2} & -G_{i2} \\ -G_{i2} & -F_{i2} \end{pmatrix} \tag{4.173}$$

Let us remark that when tracing out one mode it is always possible to bring the covariance matrix to the standard form both at zero and at finite temperature. On the contrary, for the three-mode state the standard form can be obtained only at zero temperature since at finite temperature the constraint (4.169) cannot generically be fulfilled.

To sum up, in the limit of zero temperature the system is in a three mode pure Gaussian state. Its covariance matrix (4.146) can accordingly be brought by a Local Linear Unitary BOgoliubov transformation (LLUBO) to a "standard form" in which matrices σ_i are proportional to the identity (as they already are, cf. (4.151)) and matrices ε_{ij} are diagonal [117, 126]. After this operation the matrices ε_{ij} take the following form [86]

$$\varepsilon_{01} = 2\,|\langle \hat{c}_0\, \hat{c}_1^\dagger \rangle| \mathbb{1}_2\ , \quad \varepsilon_{i2} = 2\,|\langle \hat{c}_i\, \hat{c}_2 \rangle|\, \sigma_z, \tag{4.174}$$

where $i \in \{0, 1\}$ and σ_z is the third Pauli matrix.

The situation at finite temperature is less simple. The system is in a Gaussian mixed state with no special symmetry, and the covariance matrix (4.146) cannot be put in a standard form where the matrices ε_{ij} are all diagonal [126]. However, the situation simplifies again if one is interested in bipartite entanglement only (say, between modes i and j). In this case one should trace out the third mode (let's denote it by k) which simply amounts to remove from the total covariance matrix (4.146) the two rows and two columns where index k appears. The remaining 4×4 covariance matrix associated with the reduced two-mode state reads

$$\sigma^{(i|j)} = \begin{pmatrix} \sigma_i & \varepsilon_{ij} \\ \varepsilon_{ij}^{\mathrm{T}} & \sigma_j \end{pmatrix}, \tag{4.175}$$

where the 2×2 blocks are the same as the ones in (4.146). This reduced covariance matrix can always be brought by a LLUBO to its standard form [117], in which the matrix ε_{ij} takes again the form (4.174) with here an average taken over the finite temperature state.

4.3.5 . Zero and finite temperature averages

As clear from the above expressions (4.151), (4.153) and (4.155), the theoretical evaluation of the components of the covariance matrix relies on the computation of averages of two creation or annihilation operators of the outgoing modes. For a generic a generic GAUSSIAN "thermal state" one has

$$\begin{aligned} \langle \hat{c}_i^\dagger \hat{c}_i \rangle &\underset{i\neq 2}{=} |S_{i0}|^2 \langle \hat{b}_0^\dagger \hat{b}_0 \rangle + |S_{i1}|^2 \langle \hat{b}_1^\dagger \hat{b}_1 \rangle + |S_{i2}|^2 (1 + \langle \hat{b}_2^\dagger \hat{b}_2 \rangle) \\ &\underset{i\neq 2}{=} |S_{i2}|^2 + |S_{i0}|^2 \bar{n}_0 + |S_{i1}|^2 \bar{n}_1 + |S_{i2}|^2 \bar{n}_2 \end{aligned} \tag{4.176}$$

and for $i = 2$

$$\begin{aligned} \langle \hat{c}_2^\dagger \hat{c}_2 \rangle &= |S_{20}|^2 (1 + \langle \hat{b}_0^\dagger \hat{b}_0 \rangle) + |S_{21}|^2 (1 + \langle \hat{b}_1^\dagger \hat{b}_1 \rangle) + |S_{22}|^2 \langle \hat{b}_2^\dagger \hat{b}_2 \rangle \\ &= |S_{20}|^2 + |S_{21}|^2 + |S_{20}|^2 \bar{n}_0 + |S_{21}|^2 \bar{n}_1 + |S_{22}|^2 \bar{n}_2 \\ &= -1 + |S_{22}|^2 + |S_{20}|^2 \bar{n}_0 + |S_{21}|^2 \bar{n}_1 + |S_{22}|^2 \bar{n}_2 \end{aligned} \tag{4.177}$$

Furthermore one has

$$\begin{aligned}\langle \hat{c}_0 \hat{c}_1^\dagger \rangle &= S_{00}S_{10}^*(1+\langle \hat{b}_0^\dagger \hat{b}_0 \rangle) + S_{01}S_{11}^*(1+\langle \hat{b}_1^\dagger \hat{b}_1 \rangle) + S_{02}S_{12}^* \langle \hat{b}_2^\dagger \hat{b}_2 \rangle \\ &= S_{00}S_{10}^* + S_{01}S_{11}^* + S_{00}S_{10}^* \bar{n}_0 + S_{01}S_{11}^* \bar{n}_1 + S_{02}S_{12}^* \bar{n}_2 \\ &= |S_{02}||S_{12}| e^{i(\varphi_{02}-\varphi_{12})} + |S_{00}||S_{10}| e^{i(\varphi_{00}-\varphi_{10})} \bar{n}_0 \\ &\quad + |S_{01}||S_{11}| e^{i(\varphi_{01}-\varphi_{11})} \bar{n}_1 + |S_{02}||S_{12}| e^{i(\varphi_{02}-\varphi_{12})} \bar{n}_2 \end{aligned} \tag{4.178}$$

$$\begin{aligned}\langle \hat{c}_i \hat{c}_2 \rangle &\underset{i\neq 2}{=} S_{i0}S_{20}^*(1+\langle \hat{b}_0^\dagger \hat{b}_0 \rangle) + S_{i1}S_{21}^*(1+\langle \hat{b}_1^\dagger \hat{b}_1 \rangle) + S_{i2}S_{22}^* \langle \hat{b}_2^\dagger \hat{b}_2 \rangle \\ &\underset{i\neq 2}{=} S_{i0}S_{20}^* + S_{i1}S_{21}^* + S_{i0}S_{20}^* \bar{n}_0 + S_{i1}S_{21}^* \bar{n}_1 + S_{i2}S_{22}^* \bar{n}_2 \\ &\underset{i\neq 2}{=} |S_{i2}||S_{22}| e^{i(\varphi_{i2}-\varphi_{22})} + |S_{i0}||S_{20}| e^{i(\varphi_{i0}-\varphi_{20})} \bar{n}_0 \\ &\quad + |S_{i1}||S_{21}| e^{i(\varphi_{i1}-\varphi_{21})} \bar{n}_1 + |S_{i2}||S_{22}| e^{i(\varphi_{i2}-\varphi_{22})} \bar{n}_2 \end{aligned} \tag{4.179}$$

Let us recall that in order to obtain all the previous relations we have been using relations (4.59), (4.62), (4.64) and (4.65), and that the $\bar{n}_j$'s ($j = 0$, 1 or 2) are the occupation numbers of the incoming modes (see Eq. (4.143)). When the average is taken at zero temperature, all the occupation numbers $\bar{n}_j$ are zero in the previous expressions. Furthermore, the coefficients of the S matrix appearing in the above formulae can be determined numerically as explained in Ref. [38]. The different basis dependent expressions of the covariance matrix used in this work are given in Appendix A.7.

It is also possible to evaluate the previous averages in the $\{\mathbf{f}\}$ basis of the optical model. The shape of the covariance matrix in this case is given in Appendix A.7.3. From definitions (4.103) and (4.97) and expressions (4.176)-(4.179), it is a simple matter to evaluate these averages, at all zero and finite temperatures. One obtains :

$$\begin{aligned}\langle \hat{f}_0^\dagger \hat{f}_0 \rangle &= \frac{1}{\sinh^2 r_2} \sum_{i=0}^{1} |S_{12}S_{0i} - S_{02}S_{1i}|^2 \, \bar{n}_i \\ \langle \hat{f}_1^\dagger \hat{f}_1 \rangle &= \bar{n}_{01} \cosh^2 r_2 + (1+\bar{n}_2) \sinh^2 r_2 \\ \langle \hat{f}_2^\dagger \hat{f}_2 \rangle &= \bar{n}_{01} \sinh^2 r_2 + (1+\bar{n}_2) \cosh^2 r_2 - 1 \\ \langle \hat{f}_0 \hat{f}_1^\dagger \rangle &= \frac{S_{22}}{\sinh^2 r_2} \sum_{i=0}^{1} S_{2i}^* \left(\frac{|S_{02}|}{|S_{12}|} S_{12}^* S_{1i} - \frac{|S_{12}|}{|S_{02}|} S_{02}^* S_{0i} \right) \bar{n}_i \\ \langle \hat{f}_1 \hat{f}_2 \rangle &= (\bar{n}_{01} + \bar{n}_2 + 1) \cosh r_2 \sinh r_2 \\ \langle \hat{f}_0 \hat{f}_2 \rangle &= \langle \hat{f}_0 \hat{f}_1^\dagger \rangle \tanh r_2 \end{aligned} \tag{4.180}$$

The occupation numbers $\bar{n}_j$ ($j = 0$, 1 or 2) in the above expressions are defined in (4.143) and use has been made of the shorthand notation

$$\bar{n}_{01} \equiv \frac{|S_{20}|^2}{\sinh^2 r_2} \bar{n}_0 + \frac{|S_{21}|^2}{\sinh^2 r_2} \bar{n}_1. \tag{4.181}$$

Let us remark that one has also

$$\begin{gathered} \langle \hat{f}_0 \hat{f}_1 \rangle = 0 \\ \langle \hat{f}_0 \hat{f}_0 \rangle = \langle \hat{f}_1 \hat{f}_1 \rangle = \langle \hat{f}_2 \hat{f}_2 \rangle = 0 \\ \langle \hat{f}_0 \hat{f}_2^\dagger \rangle = \langle \hat{f}_1 \hat{f}_2^\dagger \rangle = 0 \end{gathered} \tag{4.182}$$

As clear from the previous considerations about the covariance matrix of our system in 4.3.3 and 4.3.4, it is important, in order to characterize the correlations in our system, and, as we will see, entanglement and nonlocality, to be able to determine the average values of different combination of two creation or annihilation operators of the outgoing modes. At the experimental level, this determination could reveal difficult for quantities such as $\langle \hat{c}_0 \, \hat{c}_2 \rangle$ for instance. Steinhauer proposed a possible way to extract this information from the knowledge of the density-density correlation function [54]. As stressed in Refs. [39, 90] this method needs to be used with more care than initially thought, but is indeed a possible manner to obtain the information. At the theoretical level, it is a straightforward matter to compute

the expectation values of products of the ingoing creation and annihilation operator (quantities such as (4.143) for instance). From there, expression (3.50) makes it possible to compute the equivalent expressions for the outgoing operators, which are the quantities of interest. The relevant formulae are given in 4.3.3, Eqs. (4.176)-(4.179).

4.3.6 . A Measure of Bipartite Entanglement from the Two-mode Covariance Matrix : the "PPT Measure"

Several observables have been proposed to theoretically evaluate the bipartite entanglement in the context of analog gravity, such as the Cauchy-Schwarz criterion [127, 128, 129, 130, 54, 131], the generalized Peres-Horodecki parameter [132, 133], the logarithmic negativity [134, 135, 136, 137], the entanglement entropy [138, 137], the entanglement of formation [139], the Gaussian contangle [86][71].

In the present work, we chose as in Ref. [86], to evaluate the bipartite entanglement between modes i and j by means of a quantity $\Lambda^{(i|j)}(\omega) \in]-\infty, 1]$ which is a monotonous measure of entanglement that we denote as the Positive Partial Transpose or "**PPT measure**". It has indeed been argued in [86] that an efficient measure of bipartite entanglement was given by the "PPT measure'

$$\Lambda^{(i|j)} \equiv 1 - \nu^{-}_{(i|j)} \tag{4.183}$$

where $\nu^{-}_{(i|j)}$ is the lowest simplectic eigenvalue of the partial transpose $[\sigma^{(i|j)}]^{\mathrm{PT}}$ of the two-mode covariance matrix $\sigma^{(i|j)}$, and is defined as [86]

$$2\,(\nu^{-}_{(i|j)})^2 = \Delta^{PT}_{ij} - \sqrt{(\Delta^{PT}_{ij})^2 - 4\det\sigma^{(i|j)}} \tag{4.184}$$

with

$$\Delta^{PT}_{ij} = \det\sigma_i + \det\sigma_j - \det\epsilon_{ij} \tag{4.185}$$

The partial transposition corresponds to a mirror reflection in phase space which inverts the p_j coordinate, leaving q_i, p_i and q_j unchanged [140]. The resulting transposed covariance matrix can be brought by means of a symplectic transform to a diagonal form [141]. The corresponding diagonal elements are the simplectic eigenvalues. They are twice degenerate, and in our 4×4 case there are thus two such eigenvalues: $\nu^{-}_{(i|j)}$ and $\nu^{+}_{(i|j)}$, with $\nu^{\pm}_{(i|j)} \in \mathbb{R}^{+}$ and $\nu^{-}_{(i|j)} \leq \nu^{+}_{(ij)}$.The largest entanglement corresponds to $\Lambda^{(i|j)} = 1$ while separability is reached when $\Lambda^{(i|j)} < 0$. Therefore, states i and j are separable when $\Lambda^{(i|j)} < 0$. We we will see in 4.5.1 that this is always the case when $(i|j) = (0|1)$: the companion and the Hawking modes are not entangled. The two other couples of modes, $(0|2)$ and $(1|2)$, are always entangled at $T = 0$ for all ω. Their entanglement decreases with increasing temperature by an amount specified by the PPT measure.

The separability condition of the chosen "PPT measure" can be shown to be equivalent to the **Peres-Horodecki criterion** [142, 143]. Contrarily to other observables, such as the **Cauchy-Schwarz criterion** or the **generalized Peres-Horodecki parameter** which have been often used in the domain, the PPT measure has the advantage of being an entanglement monotone. Other observables have been used in the context of analog gravity, which are monotonous measures of entanglement, such as the **entanglement entropy**, the **entanglement of formation** or the **logarithmic negativity**, but they all have some drawbacks. First of all the state of our system is mixed in a finite temperature situation, which discards the entanglement entropy as a possible measure. Secondly, even if the entanglement entropy generalizes for mixed states to the entanglement of formation [115], this quantity is not easily determined in non symmetric two-mode Gaussian states such as the ones we consider, where the reduced state is nonsymmetric, since in general the mixedness A_i and A_j (defined in (4.197)) for modes i and j respectively, are not equal. Thirdly, the logarithmic negativity shares with the entanglement of formation the drawback of possibly violating monogamy inequalities [116]. This is a relatively mild drawback in the context of evaluating bipartite entanglement, but becomes prohibitive in the tripartite context. Finally, the **Gaussian contangle** was introduced in Ref. [116] as a quantity which has none of the previous deficiencies. It has been studied in the gravitational context [144] and also in analog gravity [86], but it is

[71] See section 4.1.4

not of very practical use as its determination requires numerical minimisation of a complex expression. Nevertheless, since none of these measures are of practical use at finite temperature in the case tripartite systems, in our study we resorted to the Mermin's nonlocality test in order to investigate genuine tripartite entanglement (see sections 4.1.4 and 4.6.4).

The **PPT measure** we use in the present study was introduced in Ref. [86] as a measure which mimics many aspects of the Gaussian contangle but is much simpler to evaluate. Its evaluation is as simple as the one of the above quoted quantities albeit it shares none of their drawbacks. Applying the definitions of the covariance matrices for the different subsystems here considered one obtains straightforwardly (see notations in (4.172))

$$\begin{aligned}
\Delta_{01}^{PT} &= A_0^2 + A_1^2 - 8|\langle \hat{c}_0 \hat{c}_1^\dagger \rangle|^2 \\
\det \sigma^{(0|1)} &= A_{01}^2 = (A_0 A_1 - 4|\langle \hat{c}_0 \hat{c}_1^\dagger \rangle|^2)^2 \\
\Delta_{i2}^{PT} &\underset{i<2}{=} A_i^2 + A_2^2 + 8|\langle \hat{c}_i \hat{c}_2 \rangle|^2 \\
\det \sigma^{(i|2)} &\underset{i<2}{=} A_{i2}^2 = (A_i A_2 - 4|\langle \hat{c}_i \hat{c}_2 \rangle|^2)^2
\end{aligned} \tag{4.186}$$

The previous expressions (4.186) are just the same when computed in the $\{\hat{\mathbf{e}}\}$ basis and $\{\hat{\mathbf{f}}\}$, with the $\hat{\mathbf{e}}$ and $\hat{\mathbf{f}}$ replacing the $\hat{\mathbf{c}}$[72]. Considering the positiveness of $\det \sigma^{(i|j)}$ one can write $\det \sigma^{(i|j)} = \sqrt{\det \sigma^{(i|j)}}^2$ and therefore factorize expression (4.187) as

$$\begin{aligned}
2\,(\nu_{(i|j)}^-)^2 &= \Delta_{ij}^{PT} - \sqrt{\Delta_{ij}^{PT} + 2\sqrt{\det \sigma^{(i|j)}}}\sqrt{\Delta_{ij}^{PT} - 2\sqrt{\det \sigma^{(i|j)}}} \\
&= \left(\sqrt{\frac{\Delta_{ij}^{PT} + 2\sqrt{\det \sigma^{(i|j)}}}{2}} - \sqrt{\frac{\Delta_{ij}^{PT} - 2\sqrt{\det \sigma^{(i|j)}}}{2}} \right)^2
\end{aligned} \tag{4.187}$$

which yields for partition $(0|1)$

$$(\nu_{(0|1)}^-)^2 = \left(\frac{|A_0 - A_1|}{2} - \sqrt{\left(\frac{A_i + A_2}{2} \right)^2 - 4|\langle \hat{c}_0\, \hat{c}_1^\dagger \rangle|^2} \right)^2 \tag{4.188}$$

and for partition $(i|2)$

$$(\nu_{(i|2)}^-)^2 = \left(\frac{A_i + A_2}{2} - \sqrt{\left(\frac{A_i - A_2}{2} \right)^2 + 4|\langle \hat{c}_i\, \hat{c}_2 \rangle|^2} \right)^2 \tag{4.189}$$

Since all $\nu_{(i|j)}^-$ ore positive, one must choose the positive root. The "PPT measure" shows that these two modes of the partition $(0|1)$ are never entangled in our system. We therefore give here only the explicit expression of $\Lambda^{(i|2)}(\omega)$ characterizing the coupling between mode $i = 0$ or 1 and mode $j = 2$, which reads

$$\Lambda^{(i|2)}(\omega) = -\langle \hat{c}_i^\dagger\, \hat{c}_i \rangle - \langle \hat{c}_2^\dagger\, \hat{c}_2 \rangle + \sqrt{\left(\langle \hat{c}_i^\dagger\, \hat{c}_i \rangle - \langle \hat{c}_2^\dagger\, \hat{c}_2 \rangle \right)^2 + 4|\langle \hat{c}_i\, \hat{c}_2 \rangle|^2} \tag{4.190}$$

This last expression (4.186) is straightforwardly adapted to the $\{\mathbf{e}\}$ and $\{\mathbf{f}\}$ bases, just by replacing the $\mathbf{c}$ by the $\mathbf{e}$ or $\mathbf{f}$ operators.

4.4 . BELL INEQUALITIES IN AN ANALOG BLACK HOLE THROUGH GKMR PSEUDO-SPINS

The CHSH Bell operator [105] has been originally thought for discrete variables with finite outcomes[73]. From a continuous variable perspective, it seems *a priori* difficult to derive an upper and lower bound of the expectation value of a Bell-type observable whose set of outcomes is typically unbounded. Even

[72] This can be checked using the explicit expressions of the covariance matrices given in Appendices A.7.3 and A.8.
[73] See Appendix A.3 for a classical derivation of Bell inequality violation with discrete Bell states.

if the authors of Refs. [145, 146] were able, through Fine–Abramsky–Brandenburger theorem [147, 148], to derive continuous Bell inequalities for continuous and unbounded observables, no practical (theoretical or experimental) use of such fully continuous approaches has been, to our knowledge, successfully implemented so far. Indeed, most Bell-like inequalities proposed in the context of continuous variables rely on a **discretization process** [149, 150, 151, 152, 153, 154]. Using a binning of the outcome results, observables defined from continuous measurements can be mapped to observables which can only take a finite number of outcomes. From an observable with bounded expectation value, one can then construct a Bell inequality similar to those derived for discrete variables. A well-known *bichotomic* binning of such continuos observables are the so-called **pseudo-spin operators**. These operators live in an infinite-dimensional Hilbert space but the outcome of their measurement is either -1 or $+1$.
Due to its practicability, we chose to follow this discretization approach to derive Bell-like inequalities in the context of BEC analog black holes. In this work we use the GKMR (Gour, Khanna, Mann and Revzen) pseudo-spins introduced in Ref. [106]. To an outgoing mode j ($j \in \{0,1,2\}$) of energy ω is associated a Hermitian vectorial operator $\hat{\mathbf{\Pi}}^{(j)}(\omega)$ whose expression in Cartesian coordinates is given by

$$\hat{\Pi}_x^{(j)}(\omega) = \int_0^{+\infty} \mathrm{d}q \left(|q\rangle_j \, {}_j\langle q| - |-q\rangle_j \, {}_j\langle -q| \right), \tag{4.191a}$$

$$\hat{\Pi}_y^{(j)}(\omega) = i \int_0^{+\infty} \mathrm{d}q \left(|q\rangle_j \, {}_j\langle -q| - |-q\rangle_j \, {}_j\langle q| \right), \tag{4.191b}$$

$$\hat{\Pi}_z^{(j)}(\omega) = \int_{-\infty}^{+\infty} \mathrm{d}q \, |q\rangle_j \, {}_j\langle -q| \tag{4.191c}$$

where $|q\rangle_j$ is the eigenstate associated to the eigenvalue q of the position operator $\hat{q}_j(\omega)$ (4.142). The operators (4.191) anti-commute with each others and all square to unity. They verify the Pauli algebra, i.e. the expected spin (anti)commutation relations

$$\left[\hat{\Pi}_r^{(j)}, \hat{\Pi}_s^{(j)}\right] = 2\, i\, \varepsilon_{rst} \hat{\Pi}_t^{(j)} \tag{4.192a}$$

$$\left\{\hat{\Pi}_r^{(j)}, \hat{\Pi}_s^{(j)}\right\} = 2\, \delta_{rs} \tag{4.192b}$$

with δ_{rs} the Kronecker-delta and ε_{rst} the Levi-Civita symbol[74]. In Appendix A.2 we recall the properties of the pseudo-spin operator (4.191) and of its eigenvectors we will be referring to in the following, and we will show in Sec. 4.6.3 how these very same properties helped us to understand an unforeseen characteristic of our system, i.e. that the structure of the zero temperature ground state of the analog system, i.e. the vacuum $|0\rangle^{\mathrm{in}}$, is most easily analyzed in terms of a combination of eigenstates of operator $\hat{\Pi}_x$.

As a final remark, we note here that the GKMR spins operators have been studied in contexts similar to ours in Refs. [154, 155, 156]. Compared with other pseudo-spin operators such as for instance those introduced by Banaszek and Wodkiewicz [157, 158], the GKMR spins (4.191) have the advantage of having simple Wigner transforms, which makes the computation of their expectation values over Gaussian states relatively easy, as detailed in Appendix 4.3.1. Nevertheless, it is important to stress (see [106]) that different choices of spin representation lead to different values of averages of the observables (4.211), (4.216) and (4.232) we are interested in. Therefore these observables must be considered as **witnesses of nonlocality**, their violation of Bell-type inequalities being a sufficient but not necessary test of nonlocal behavior.

For evaluating expectation values such as those appearing in Eqs.(4.211), (4.216) and (4.232), we need to compute the Wigner transforms of the components of the pseudo-spin operators. These are to be evaluated in a 2 dimensional phase space, since operator $\hat{\mathbf{\Pi}}^{(j)}$ concerns a single mode (mode j). The

[74] Usual $1/2$-spin operators trace also to zero and have determinant -1. The pseudo-spins (4.191) operate in infinite space where the trace and determinant are not well defined : see [106] for discussion. Still, the Pauli algebra defining the (anti)commutation relations (4.192) is fulfilled by pseudospins (4.191).

result is independent of j and reads :

$$\begin{aligned} W_{\hat{\Pi}_x}(q,p) &= \mathrm{sgn}\,(q) \\ W_{\hat{\Pi}_y}(q,p) &= i\,\delta(q)\int_{-\infty}^{\infty}\mathrm{d}x\,\mathrm{sgn}\,(x)\exp\{-2ipx\} = \delta(q)\mathcal{P}(1/q) \\ W_{\hat{\Pi}_z}(q,p) &= \pi\delta(q)\delta(p) \end{aligned} \tag{4.193}$$

where $\mathcal{P}$ denotes the principal value[75]. Since the eigenvalues of the projections along a given axis of the pseudo-spin operator $\hat{\mathbf{\Pi}}$ are ± 1, the above expressions of the Wigner transforms thus demonstrate that, contrarily to $\hat{\Pi}_x$, which has indeed a two-valued Wigner function able to mimic "classicaly" the two-valued quantum observable, operators $\hat{\Pi}_y$ and $\hat{\Pi}_z$ are "improper" in the sense of Ref. [124]: they may be involved in violation of Bell inequality even for a state with a non-negative Wigner transform, such as the Gaussian state we consider.

For evaluating the expectation values appearing in (4.211) we need to compute the two-mode integrals

$$\mathcal{T}_{rs}^{(ij)}(\omega) \equiv \langle \hat{\Pi}_r^{(i)} \otimes \hat{\Pi}_s^{(j)} \rangle = \mathrm{Tr}\{\hat{\rho}_{(ij)}\,\hat{\Pi}_r^{(i)} \otimes \hat{\Pi}_s^{(j)}\} = \int \mathrm{d}^2\boldsymbol{q}\mathrm{d}^2\boldsymbol{p}\, W_{\hat{\Pi}_r}(q_i,p_i) W_{\hat{\Pi}_s}(q_j,p_j) W_{\hat{\rho}}(\boldsymbol{q},\boldsymbol{p}) \tag{4.194}$$

with $r,s \in \{x,y,z\}$, the density matrix $\hat{\rho}_{(ij)}$ of the two-particle system composed by particles i and j, the pseudo-spin operator $\hat{\Pi}$ acting in the space of particle i or j and $\boldsymbol{q} = (q_i, q_j)$ and $\boldsymbol{p} = (p_i, p_j)$ where $(i,j) = (0,1)$, $(i,j) = (0,2)$ or $(i,j) = (1,2)$.Similarly for evaluating the expectation values appearing in (4.216) and (4.232), we need to compute the three-mode integrals

$$\begin{aligned} \mathcal{T}_{rst}(\omega) \equiv \langle \hat{\Pi}_r^{(0)} \otimes \hat{\Pi}_s^{(1)} \otimes \hat{\Pi}_t^{(2)} \rangle &= \mathrm{Tr}\{\hat{\rho}_{(012)}\,\hat{\Pi}_r^{(0)} \otimes \hat{\Pi}_s^{(1)} \otimes \hat{\Pi}_t^{(2)}\} \\ &= \int \mathrm{d}^3\boldsymbol{q}\mathrm{d}^3\boldsymbol{p}\, W_{\hat{\Pi}_r}(q_0,p_0) W_{\hat{\Pi}_s}(q_1,p_1) W_{\hat{\Pi}_t}(q_2,p_2) W_{\hat{\rho}}(\boldsymbol{q},\boldsymbol{p}) \end{aligned} \tag{4.195}$$

with $r,s,t \in \{x,y,z\}$ $\boldsymbol{q} = (q_0,q_1,q_2)$ and $\boldsymbol{p} = (p_0,p_1,p_2)$. The explicit calculation of the terms $\mathcal{T}_{rs}^{(i2)}$ involved in the determination of the CHSH parameter (4.211) is similar to the one figuring in the Appendix of Ref. [154]. First of all, one finds

$$\mathcal{T}_{zz}^{(i2)} = \frac{1}{A_i A_2 - 4|\langle \hat{c}_i \hat{c}_2 \rangle|^2}, \tag{4.196}$$

where

$$A_j = 1 + 2\langle \hat{c}_j^\dagger \hat{c}_j \rangle \tag{4.197}$$

is known (see Ref. [39]) as the **local mixedness** of mode j ($j = 0, 1$ or 2)[76]. Then one finds that all expectation values for which the index z appears a single time cancel at all temperatures. The values of the other non-zero averages are ($i = 0$ or 1):

$$\begin{aligned} \mathcal{T}_{xx}^{(i2)} &= \frac{2}{\pi}\arctan\frac{2\,\mathrm{Re}\,\langle \hat{c}_i \hat{c}_2 \rangle}{\sqrt{A_i A_2 - 4(\mathrm{Re}\,\langle \hat{c}_i \hat{c}_2 \rangle)^2}} \\ \mathcal{T}_{yy}^{(i2)} &= \frac{-1}{A_{i2}}\mathcal{T}_{xx}^{(i2)} \\ \mathcal{T}_{xy}^{(i2)} &= \frac{2}{\pi\,A_2}\,\mathrm{arsinh}\,\frac{2\,\mathrm{Im}\,\langle \hat{c}_i \hat{c}_2 \rangle}{\sqrt{A_{i2}}} \\ \mathcal{T}_{yx}^{(i2)} &= \frac{2}{\pi\,A_i}\,\mathrm{arsinh}\,\frac{2\,\mathrm{Im}\,\langle \hat{c}_i \hat{c}_2 \rangle}{\sqrt{A_{i2}}} \end{aligned} \tag{4.198}$$

where A_{i2} is defined in Eq. (4.199) below, and we recall that the expression of the quantity $\langle \hat{c}_i \hat{c}_2 \rangle$ is given in (4.179)[77].

[75] The details of the computations can be found in Appendix A.10.1.

[76] In this work we have chosen the convention of writing generically the terms containing finite temperature components in upper case letters and the ones referring only at the zero temperature pure state in lower case letters. In the published article given in section 6.3.7 the local mixedness are always referred to in lower case letters, as it is often the case in the literature.

[77] All the details of the computations are to be found in Appendix A.10.2. In the same Appendix will also be found the expressions $\mathcal{T}_{rs}^{(01)}$ which are not given here since modes 0 and 1 are not entangled and therefore the pair never violates Bell's inequalities.

For studying the Svetlichny observable (4.216) and the related Mermin parameter (4.232), it is necessary to evaluate the averages $\mathcal{T}_{rst}(\omega)$ given in Eq. (4.195) and involving the Cartesian coordinates of three pseudo-spins, where r, s and $t \in \{x, y, z\}$. These quantities are zero if z is not one of the indices or appears exactly twice. In order to write down tractable expressions in the other cases, it is convenient to introduce new compact notations

$$\begin{aligned} A_{01} =& A_0 A_1 - 4\,|\langle \hat{c}_0 \hat{c}_1^\dagger \rangle|^2 \\ A_{i2} \underset{i<2}{=}& A_i A_2 - 4\,|\langle \hat{c}_i \hat{c}_2 \rangle|^2 \end{aligned} \tag{4.199}$$

$$\begin{aligned} Z_0 &= -2A_0 \langle \hat{c}_1 \hat{c}_2 \rangle^* + 4 \langle \hat{c}_0 \hat{c}_1^\dagger \rangle \langle \hat{c}_0 \hat{c}_2 \rangle^* \\ Z_1 &= -2A_1 \langle \hat{c}_0 \hat{c}_2 \rangle^* + 4 \langle \hat{c}_0 \hat{c}_1^\dagger \rangle^* \langle \hat{c}_1 \hat{c}_2 \rangle^* \\ Z_2 &= -2A_2 \langle \hat{c}_0 \hat{c}_1^\dagger \rangle^* + 4 \langle \hat{c}_1 \hat{c}_2 \rangle \langle \hat{c}_0 \hat{c}_2 \rangle^* \end{aligned} \tag{4.200}$$

and

$$\begin{aligned} D =& A_0 A_1 A_2 + 16\,\mathrm{Re}\left\{ \langle \hat{c}_0 \hat{c}_1^\dagger \rangle \langle \hat{c}_1 \hat{c}_2 \rangle \langle \hat{c}_0 \hat{c}_2 \rangle^* \right\} \\ & - 4A_0 |\langle \hat{c}_1 \hat{c}_2 \rangle|^2 - 4A_1 |\langle \hat{c}_0 \hat{c}_2 \rangle|^2 - 4A_2 |\langle \hat{c}_0 \hat{c}_1^\dagger \rangle|^2 \end{aligned} \tag{4.201}$$

D is the square root of the determinant of the 6×6 covariance matrix (4.146). At $T = 0$ the system is in a pure state and $D = 1$ for all values of ω [78] , whereas $D = \mathcal{O}(1/\omega)$ at finite temperature, as can be shown on the basis of the low energy expansion of the matrix elements of the S-matrix given in Ref. [38].

The explicit theoretical evaluation of the quantities (4.197), (4.199), (4.200) and (4.201) is easily done from Eqs. (4.176)-(4.179). A long computation[79] shows that the averages (4.195) which are non zero can be expressed in terms of these quantities :

$$\begin{aligned} \mathcal{T}_{zxx} &= -\frac{2}{\pi A_0} \arctan \frac{\mathrm{Re}\, Z_0}{\sqrt{A_{01} A_{02} - (\mathrm{Re}\, Z_0)^2}} \\ \mathcal{T}_{xzx} &= -\frac{2}{\pi A_1} \arctan \frac{\mathrm{Re}\, Z_1}{\sqrt{A_{01} A_{12} - (\mathrm{Re}\, Z_1)^2}} \\ \mathcal{T}_{xxz} &= -\frac{2}{\pi A_2} \arctan \frac{\mathrm{Re}\, Z_2}{\sqrt{A_{02} A_{12} - (\mathrm{Re}\, Z_2)^2}} \end{aligned} \tag{4.202}$$

$$\begin{aligned} \mathcal{T}_{zyy} &= -\frac{A_0}{D} \mathcal{T}_{zxx} \quad \mathcal{T}_{yzy} = -\frac{A_1}{D} \mathcal{T}_{xzx} \\ \mathcal{T}_{yyz} &= +\frac{A_2}{D} \mathcal{T}_{xxz} \end{aligned} \tag{4.203}$$

$$\begin{aligned} A_{02} \mathcal{T}_{zxy} = A_{01} \mathcal{T}_{zyx} &= \mathrm{arsinh} \left(\frac{\mathrm{Im}\, Z_0}{\sqrt{A_0 D}} \right) \\ A_{01} \mathcal{T}_{yzx} = A_{12} \mathcal{T}_{xzy} &= \mathrm{arsinh} \left(\frac{\mathrm{Im}\, Z_1}{\sqrt{A_1 D}} \right) \\ -A_{12} \mathcal{T}_{xyz} = A_{02} \mathcal{T}_{yxz} &= \mathrm{arsinh} \left(\frac{\mathrm{Im}\, Z_2}{\sqrt{A_2 D}} \right) \end{aligned} \tag{4.204}$$

and

$$\mathcal{T}_{zzz} = \frac{1}{D}. \tag{4.205}$$

[78] The c-modes are related to the b-modes by a Bogoliubov transformation, see (3.50). In this case the covariance matrix σ of the c-modes relates to the one of the b-modes by a symplectic transform which conserves the determinant (see, e.g., [86] and references therein). At $T = 0$ the b-modes are all empty and their covariance matrix is the identity $\mathbb{1}_6$. It thus follows that in this case $\delta = (\det \sigma)^2 = 1$.

[79] Some details are given in Appendix A.10.3.

4.5 . GENUINE BIPARTITE VIOLATION

4.5.1 . Bipartite Entanglement

Expressions (4.176)-(4.179) are useful for computing the PPT measure of entanglement (4.190) and the CHSH (4.211) and Svetlichny (4.216) parameters that will be defined later on as witnesses of bipartite and tripartite nonlocality, respectively. As an illustration we now indicate how to compute the PPT measure $\Lambda^{(i|2)}$ at zero temperature. Using here the definition (4.108) as a short hand notation one gets from (4.190)

$$\Lambda^{(i|2)}(\omega) \underset{T=0}{=} -|S_{i2}|^2 - \sinh^2(r_2) + \sqrt{[|S_{i2}|^2 + \sinh^2(r_2)]^2 + 4|S_{i2}|^2} \tag{4.206}$$

It was shown in Ref. [38] that the ratio $|S_{i2}|^2/\sinh^2(r_2)$ tends to a constant when $\omega \to 0$. Let's denote Γ_i the value of this constant ($i = 0$ or 1) [80]. A simple expansion of (4.206) with $\sinh r_2 \to \infty$ when $\omega \to 0$ shows that

$$\lim_{\omega\to 0} \Lambda^{(i|2)} \underset{T=0}{=} \frac{2\Gamma_i}{1+\Gamma_i}. \tag{4.207}$$

In the waterfall configuration [38] one has

$$\Gamma_0 = \frac{4m_u}{(1+m_u)^2}, \tag{4.208}$$

Furthermore from relation (3.48) it follows that $\Gamma_0 + \Gamma_1 = 1$. Hence, for the waterfall configuration

$$\lim_{\omega\to 0} \Lambda^{(0|2)} \underset{T=0}{=} \frac{8m_u}{1+6m_u+m_u^2}, \tag{4.209a}$$

$$\lim_{\omega\to 0} \Lambda^{(1|2)} \underset{T=0}{=} \frac{(1-m_u)^2}{1+m_u^2}. \tag{4.209b}$$

The maximum value of $\Lambda^{(0|2)}$ is always reached at $\omega = 0$, thus the $T = 0$ numerically determined value $\max_\omega \Lambda^{(0|2)}$ plotted in Fig. 4.3 is identical to (4.209a). The maximum value of the PPT measure of entanglement between modes 1 and 2 is reached at $\omega = 0$ only for $m_u \lesssim 0.18$: the numerically determined value $\max_\omega \Lambda^{(1|2)}$ plotted in Fig. 4.3 is thus identical to (4.209b) in this range of values of m_u.

4.5.2 . Bipartite Nonlocality

Equipped with the pseudo-spin operators (4.191) we can define a CHSH Bell operator [105] measuring the correlations between the emitted quasi-particles of type i and j as

$$\hat{\mathscr{B}}^{(i|j)}(\omega) = (\boldsymbol{a}+\boldsymbol{a}')\cdot\hat{\boldsymbol{\Pi}}^{(i)} \otimes \boldsymbol{b}\cdot\hat{\boldsymbol{\Pi}}^{(j)} + (\boldsymbol{a}-\boldsymbol{a}')\cdot\hat{\boldsymbol{\Pi}}^{(i)} \otimes \boldsymbol{b}'\cdot\hat{\boldsymbol{\Pi}}^{(j)} \tag{4.210}$$

where $\boldsymbol{a}$, $\boldsymbol{a}'$, $\boldsymbol{b}$ and $\boldsymbol{b}'$ are unit vectors. Given a unit vector $\boldsymbol{n}$ it is easily checked that $(\boldsymbol{n}\cdot\hat{\boldsymbol{\Pi}}^{(j)})^2 = \mathbb{1}$, meaning that the Hermitian operator $\boldsymbol{n}\cdot\hat{\boldsymbol{\Pi}}^{(j)}$ has eigenvalues ± 1. It then follows from direct inspection that, local realism imposes that a measure of the operator $\hat{\mathscr{B}}^{(i|j)}$ yields a result ± 2[81]. Thus, local realism is violated when $\langle\hat{\mathscr{B}}^{(i|j)}\rangle > 2$, whereas Cirel'son bound [159] imposes $\langle\hat{\mathscr{B}}^{(i|j)}\rangle \leq 2\sqrt{2}$. Since the modes 0 and 1 are not entangled the quantity $\langle\hat{\mathscr{B}}^{(0|1)}\rangle$ is always lower than 2 and its computation is of no interest to us. For attempting to violate as much as possible Bell inequality one should consider the modes 0 and 2 (or 1 and 2) and look for an arrangement of the four measurement directions $\boldsymbol{a}$, $\boldsymbol{a}'$, $\boldsymbol{b}$ and $\boldsymbol{b}'$ which maximizes $\langle\hat{\mathscr{B}}^{(i|2)}\rangle$ ($i = 0$ or 1). This procedure is explained in Appendix A.4 and makes it possible to analytically compute the quantity

$$B^{(i|2)}(\omega) \equiv \max_{\boldsymbol{a},\boldsymbol{a}',\boldsymbol{b},\boldsymbol{b}'} \left\langle \hat{\mathscr{B}}^{(i|2)}(\omega) \right\rangle \tag{4.211}$$

[80] Γ_0 and Γ_1 are the low energy limits of the transmission and reflection coefficients (γ_0 and γ_1, respectively) of the beam splitter involved in the effective optical model depicted in Fig. 4.1, see Appendix 4.2.3. In the notations of Appendix 4.2.3, $\Gamma_0 = \lim_{\omega\to 0}\cos^2\theta$.

[81] From local realism is follows that the measurement of an observable of the type $\boldsymbol{a}\cdot\hat{\boldsymbol{\Pi}}^{(i)} \otimes \boldsymbol{b}\cdot\hat{\boldsymbol{\Pi}}^{(j)}$ is the product $\Pi^{(i)}(\lambda,\boldsymbol{a})\cdot\Pi^{(j)}(\lambda,\boldsymbol{b})$ of the result $\Pi^{(i)}(\lambda,\boldsymbol{a}) = \pm 1$ of measurement of the pseudo-spin $\hat{\boldsymbol{\Pi}}^{(i)}$ along direction $\boldsymbol{a}$ with the result $\Pi^{(i)}(\lambda,\boldsymbol{b}) = \pm 1$ of measurement of the pseudo-spin $\hat{\boldsymbol{\Pi}}^{(j)}$ along direction $\boldsymbol{b}$, where λ is the hidden variable. Within this approach, there are only two possible cases: either $\Pi^{(i)}(\lambda,\boldsymbol{a})$ and $\Pi^{(i)}(\lambda,\boldsymbol{a}')$ are equal (their difference cancels and they sum to ± 2) either they are opposite (their sum cancels and their difference is ± 2). From expression (4.210) directly follows that such a measurement of $\hat{\mathscr{B}}^{(i|j)}$ yields a result ± 2.

The corresponding explicit expression is given in Eq. (A.91b). The values of $B^{(0|2)}$ and $B^{(1|2)}$ are plotted as functions of ω for different temperatures in Fig. 4.2 for a waterfall configuration with a downstream Mach number[82] $m_d \equiv V_d/c_d = 2.9$, the same as in the Technion 2019 experiment [34]. We also plot for comparison the values of the corresponding PPT measures $\Lambda^{(0|2)}$ and $\Lambda^{(1|2)}$, as defined by (4.190).

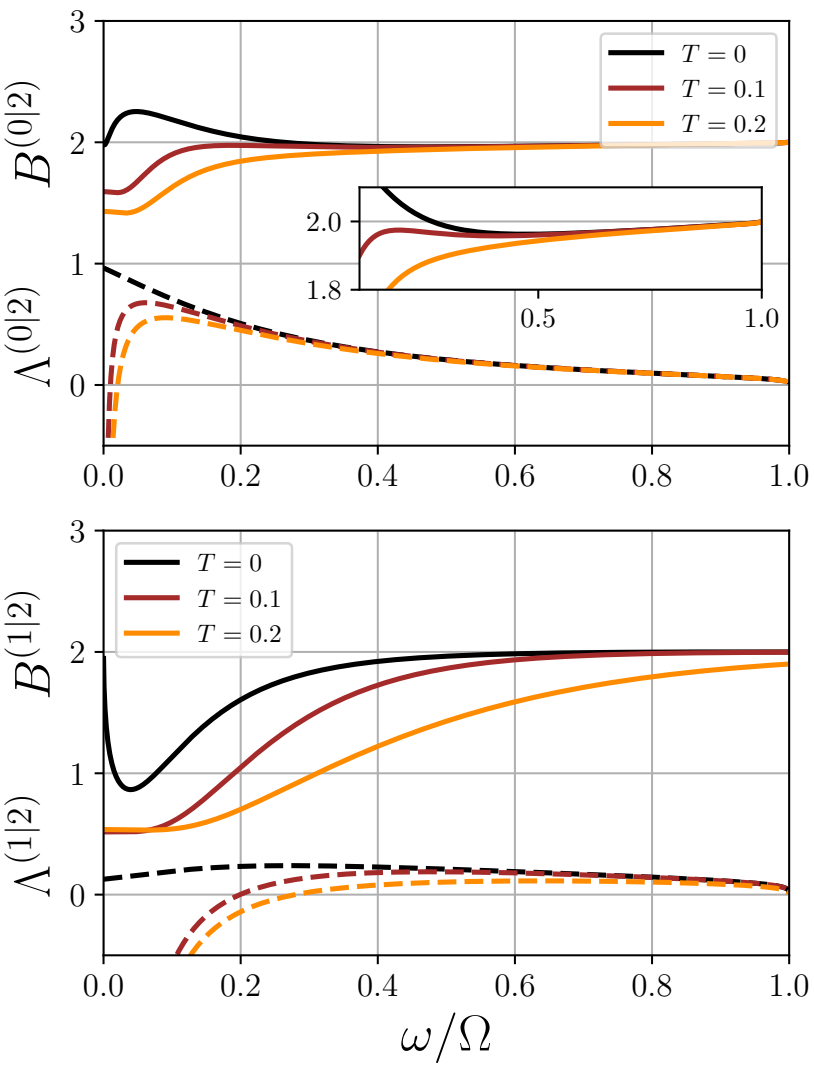

Figure 4.2: Plot of $B^{(i|2)}$ (solid lines) and $\Lambda^{(i|2)}$ (dashed lines) as functions of ω for the waterfall configuration with $m_d = 2.9$ and different temperatures. We only consider the range of frequencies $\omega < \Omega$ for which the vacua of the outgoing and ingoing modes do not coincide. The value of the temperature is indicated in units of $g\,n_u = mc_u^2$. Upper plot: $i = 0$. Lower plot $i = 1$. Non separability of modes i and 2 is achieved when $\Lambda^{(i|2)} > 0$. Bell inequality is violated when $B^{(i|2)} > 2$. The inset in the upper plot is a blow-up of the region $1.8 \leq B^{(0|2)} \leq 2.1$ and $0.1 \leq \omega/\Omega \leq 1$ showing that the reduced state $(0|2)$ does not violate Bell inequality at temperatures $T = 0.1$ and 0.2.

The figure illustrates that, as well known, entanglement is necessary but not sufficient for violating Bell inequality. Also, the amount by which the Bell inequality is violated is not proportional to the amount of entanglement. This is clearly seen, for instance, by comparing the values of $B^{(0|2)}$ and $\Lambda^{(0|2)}$ at $T = 0$: the maximum violation of Bell inequality is not achieved for the maximal entanglement. One can also notice that the violation of Bell inequality is much less resilient to temperature than is the entanglement. These features can be most easily understood in the framework of the optical model represented in Fig. 4.1. They originate from the dilution of entanglement between the three modes caused by the beam splitter, as discussed in 4.2.3.

Fig. 4.2 indicates that, in the waterfall configuration we consider (with $m_d = 2.9$), the entanglement is lower and the violation of Bell inequality less significant for the correlations among modes 1 and 2 than for the correlations among modes 0 and 2. However, this is not always the case. This point is illustrated in Fig. 4.3 which displays, for all waterfall configurations, the zero temperature values of $\max_\omega B^{(i|2)}$ and $\max_\omega \Lambda^{(i|2)}$ (for $i = 0$ and 1) as functions of the upper Mach number m_u (the maximisation is performed at fixed m_u, for $\omega \in [0, \Omega]$). All the possible waterfall configurations are considered since m_u spans the whole interval $[0, 1]$. In this figure we aim at evaluating the largest amount of entanglement and nonlocality reached in each configuration. This is the reason why we plot the maximal values taken by

[82] In this theoretical model configuration, fixing the value of m_d determines all the other dimensionless parameters: $m_d = m_u^{-2} = n_u/n_d = V_d/V_u$, see Ref. [38].

the quantities $\Lambda^{(i|2)}$ and $B^{(i|2)}$ over the energy interval $[0, \Omega]$ [where Ω is defined by Relation (3.26)] since it is only for energies in this interval that spontaneous emission of quasi-particles occurs.

For instance, the situation depicted in Fig. 4.2 ($m_d = 2.9$) corresponds in Fig. 4.3 to the point $m_u = 0.587$ since for waterfall configurations m_u and m_d are related by (3.19). And indeed, Fig. 4.3 shows that for this value of m_u the maximum over ω of $B^{(0|2)}$ is 2.25, and the one of $B^{(1|2)}$ is 2, as observed in Fig. 4.2.

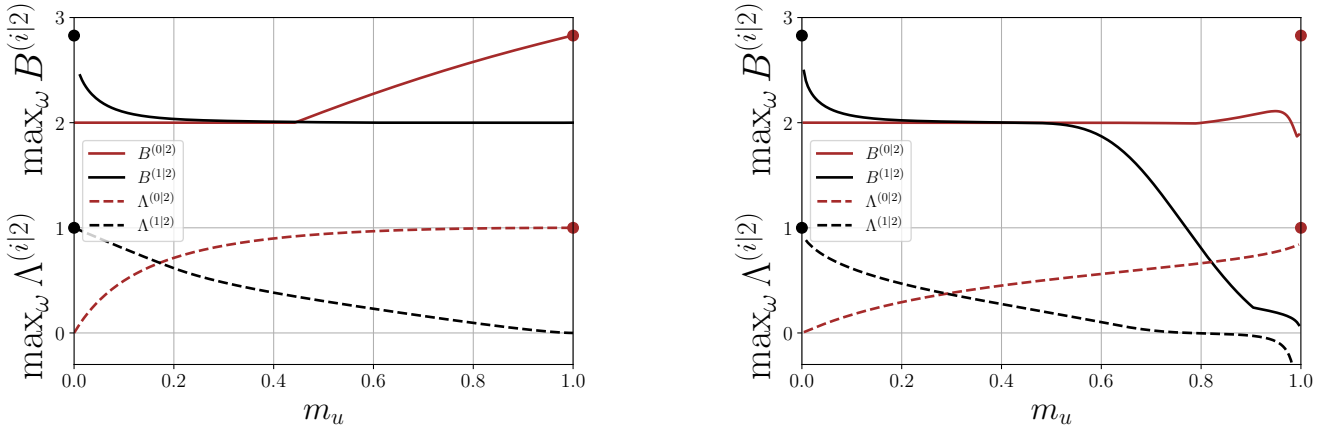

Figure 4.3: LEFT PLOT: Zero temperature value of the CHSH parameter and of the PPT measure characterizing non separability of modes i ($= 0$ and 1) and 2 for the waterfall configuration. The maximal value reached by these quantities over the interval $\omega \in [0, \Omega]$ is plotted as a function of the upper Mach number m_u which (as explained in Appendix 3.1) characterizes a given configuration. The values of $B^{(1|2)}$ for $m_u \leq 0.01$ are not indicated because of lack of numerical precision. The upper bounds of $B^{(i|2)}$ and $\Lambda^{(i|2)}$ ($\sqrt{8}$ and 1, respectively) are indicated with filled dots. RIGHT PLOT: Same as left plot but for a temperature $T = 0.2\, g n_u$. Contrarily to what is observed in the zero temperature case displayed in left plot, the maxima of Λ and B (1 and $2\sqrt{2}$, respectively) are never reached.

Fig. 4.3 shows that for values of m_u larger than 0.6, the entanglement is mainly concentrated between modes 2 and 0, i.e., between the Hawking quantum and the partner. This is indicated by the fact that both the PPT measure and the CHSH parameter significantly point to nonseparability and nonlocality between these two modes. For $m_u \leq 0.2$ instead, the figure shows that entanglement is concentrated between the partner and the companion (modes 2 and 1, respectively). A plot similar to the one of Fig. 4.3, but where the quantities are evaluated at finite temperature, enables to evaluate the resilience of entanglement and non-separability to an increase of temperature. This check is performed in Fig. 4.3 which shows that, whereas at $T = 0.2\, g n_u$ the PPT measure is not dramatically affected, the CHSH parameters $B^{(0|2)}$ and $B^{(1|2)}$ no longer show evidences of violation of Bell inequality, except in the $(1|2)$ sector for waterfall configurations with $m_u \lesssim 0.15$ and, in a lesser extent, in the $(0|2)$ sector for $m_u \gtrsim 0.85$.

Figs. 4.3 and 4.3 illustrate a specific feature of analog models : there is no reason for qualifying one of the positive norm modes (in our specific case, mode 0 or 1) as unessential. For instance, it is incorrect to study the system discarding *a priori* the companion (mode 1) from the analysis. Fig. 4.3 shows that, at zero temperature, this is allowed in some regions of parameters, but incorrect in others. Fig. 4.3 even shows that only the companion-partner correlations display violation of Bell inequality above a certain temperature. In this case it is the Hawking mode which is unessential. It is therefore important to give a proper account of all the modes involved in our analog system without *a priori* neglecting any of them.

4.5.3 . Bipartite Entanglement and Nonlocality in the $\{\mathrm{f}\}$ Basis of the Optical Analog

Another way to consider the same problem is to use the equivalent model depicted in Fig. 4.1. It is well known that a nondegenerate optical parametric amplifier generates an EPR state when the squeezing parameter tends to infinity (see, e.g., Ref. [160]). As discussed in section 4.2.3 this is the case for the two mode squeezed state (4.107) when $\omega \to 0$. The zero energy transmission coefficient Γ_0 of the effective beam splitter (pictorially defined in Fig. 4.1) tends to 0 or 1 when the upper Mach number m_u tends

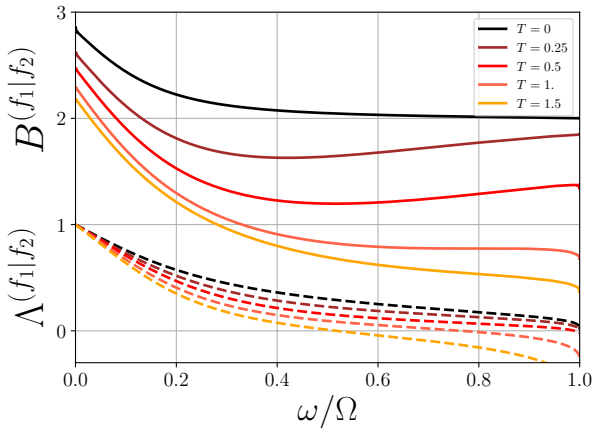

Figure 4.4: $B^{(f_1|f_2)}$ (solid lines) and $\Lambda^{(f_1|f_2)}$ (dashed lines) plotted as functions of ω for the two-mode squeeze state emulating the waterfall configuration with $m_d = 2.9$. The values of the different temperatures are indicated in units of $g\, n_u$.

to 0 or 1, respectively (see e.g., Eq. (4.208) which holds for the waterfall configuration)[83]. In these two limits the system forms an EPR state between two of the three outgoing modes : **in these two limiting cases, i.e. $m_u \to 0$ or $m_u \to 1$, and only in these, the third mode of the system can then be omitted since for j the omitted mode one has $\langle \hat{c}_j^\dagger c_j \rangle_0 \to 0$.** This EPR state involves, either the Hawking quantum and the partner (when $m_u \to 1$) or the companion and the partner (when $m_u \to 0$). This is the reason why the entanglement and nonlocality bounds are reached in this two limits in Fig. 4.3, and similarly in Figs. 4.7 of section 4.7 for the delta peak and flat profile configurations, respectively. It is quite informative to quantify the entanglement between the two effective modes f_1 and f_2 and the amount by which the corresponding squeezed state violates Bell inequality. At $T = 0$ all the relevant quantities can be expressed in terms of the squeezing parameter (4.108) involved in the transformation (4.107). For instance, the analogs for the the modes $\hat{f}_1$ and $\hat{f}_2$, of the PPT measure of entanglement and of the CHSH parameter defined for the modes $\hat{c}_i$ and $\hat{c}_2$ by Eqs. (4.190) and (4.211), respectively, read[84]

$$\Lambda^{(f_1|f_2)} \underset{T=0}{=} 1 - \exp(-2r_2), \tag{4.212}$$

and [106]

$$B^{(f_1|f_2)} \underset{T=0}{=} 2\sqrt{1 + \frac{4}{\pi^2} \arctan^2 \left[\sinh(2r_2)\right]}. \tag{4.213}$$

The finite temperature values of these quantities can be obtained by replacing the $\hat{c}$ operators by the $\hat{f}$'s in expressions (4.190) and (A.91b) and using formulae (4.180). They are represented in Fig. 4.4 as functions of ω for a specific black hole configuration (waterfall with $m_d = 2.9$). As anticipated, it appears that the violation of Bell inequality is here much more resilient to temperature than for the true Hawking-partner pair or the companion-partner pair (compare with Fig. 4.2). This is explained by the fact that the beam splitter distributes and, so to say, dilutes the entanglement. This is clear at $T = 0$: in this case the f_0 mode is empty (cf. (4.180)) and the system is, as far as the f modes are concerned, in a pure two-mode squeezed vacuum state. At $\omega = 0$ for instance, the system is maximally entangled (the squeezing parameter $r_2 \to \infty$) and both $\Lambda^{(f_1|f_2)}$ and $B^{(f_1|f_2)}$ reach their upper bounds (1 and $2\sqrt{2}$ respectively). At variance, if working with the true outgoing modes described by the $\hat{c}$ (or equivalently the $\hat{e}$) operators,

[83] Thinking about the gravitational analogy, when in the long-wavelength limit the greybody factor $\Gamma_0 \to 1$, there is no back-scattering of Hawking particles. On the contrary when $\Gamma_0 \to 0$ all Hawking particles are scattered back by the gravitational potential. In the waterfall configuration, $\Gamma_0 \to 1$ when $m_u \to 1$, and since $m_d = m_u^{-2}$ the two asymptotic Mach numbers are in this case very close to each other : this then would mimic an horizon for which the gradient of the gravitational potential is not very steep at the horizon (the steeper the potential, the stronger the back-scattering), for example with a very massive black-hole (the heavier the black hole, the larger its Schwarzschild radius, which is proportional to the mass).

[84] Relation (4.212) is just the expansion of (4.190) in the $\{\mathbf{f}\}$ basis (the $\hat{f}_i$ need just to replace the $\hat{c}_i$ in the given expression) with $r_2 \to \infty$ at zero temperature and zero energy.

for studying two-mode entanglement it is necessary to trace the (occupied) third one. **Indeed, when m_u is not approaching the two limiting cases $m_u \to 0$ or $m_u \to 1$, the omitted (traced out) third mode has an occupation number $\langle \hat{c}_j^\dagger c_j \rangle_0$ which is significantly not zero. The resulting density matrix is mixed**, and in this case, entanglement and violation of Bell inequality are two different things, as clear from Fig. 4.2.

Another way to tackle this issue consists in expressing the PPT measure of entanglement (4.190) between the partner (mode 2) and mode i ($i = 0$ or 1) in terms of the parameters of the equivalent optical system. Denoting as $\gamma_0(\omega) = \cos^2\theta$ and $\gamma_1(\omega) = \sin^2\theta$ the transmission and reflection coefficient of the beam splitter makes it possible to write the PPT measure (4.190) at zero temperature (see (4.206)) under the form

$$\Lambda^{(i|2)}(\omega) \underset{T=0}{=} (1+\gamma_i)(\sinh r_2) \times \left\{ \sqrt{\cosh^2 r_2 - \left(\frac{1-\gamma_i}{1+\gamma_i}\right)^2} - \sinh r_2 \right\} \tag{4.214}$$

Algebraic manipulations[85] then show that, because $\gamma_i \leq 1$, $\Lambda^{(i|2)}$ is always lower than $\Lambda^{(f_1|f_2)}$. This means that the entanglement between modes i and 2 is always lower than the entanglement between the modes issued from the parametric down conversion represented in Fig. 4.1. The equality is reached when $\gamma_i = 1$, and, since $\gamma_0 + \gamma_1 = 1$, in this case the other channel (let's denote it as $\bar{\imath} = 1 - i$) is not entangled with mode 2 since $\Lambda^{(\bar{\imath}|2)} = 0$. So, indeed, the effect of the beam splitter is, so to say, to dispatch the entanglement of the effective squeezed modes f_1 and f_2 between modes c_0, c_1 and c_2.

We conclude this section by noticing that, from a quantum information perspective, the fact that reduced bipartite states of a tripartite system are entangled is of no particular significance *per se*. It is however important for future experimental studies of analog systems to determine for which configurations, and to quantify to which extent, the three-mode acoustic Hawking emission is bipartite entangled and nonlocal. Besides, we will see in the next section that this resilience of entanglement to partial tracing acquires a particular significance when examining the exact nature of the long wavelength components of the three-mode state $|0\rangle^{\text{in}}$ (the ground state of the system).

4.6 . GENUINE TRIPARTITE VIOLATION

4.6.1 . The Svetlichny Parameter

Equipped with the same pseudo-spin operators as the ones defined in Sec. 4.5 one can define a three-mode Bell operator of a type similar to the two-mode one (4.210). This operator measures the correlations between the outgoing quasi-particles of type i, j and k. It is defined as (see [161, 162])

$$\hat{\mathscr{S}}^{(i|j|k)}(\omega) = \tfrac{1}{2}\hat{\mathscr{B}}^{(i|j)} \otimes \boldsymbol{c}' \cdot \hat{\boldsymbol{\Pi}}^{(k)} + \tfrac{1}{2}\hat{\mathscr{B}}'^{(i|j)} \otimes \boldsymbol{c} \cdot \hat{\boldsymbol{\Pi}}^{(k)} \tag{4.215}$$

where $\hat{\mathscr{B}}'^{(j|k)}(\omega)$ is the same as $\hat{\mathscr{B}}^{(j|k)}(\omega)$ defined in (4.210) with the primes reversed, and $\boldsymbol{c}$ and $\boldsymbol{c}'$ are normalized vectors as are $\boldsymbol{a}$, $\boldsymbol{a}'$, $\boldsymbol{b}$, and $\boldsymbol{b}'$ involved in the definition of $\hat{\mathscr{B}}^{(j|k)}$). Expanding expression (4.215) shows that $\hat{\mathscr{S}}^{(i|j|k)}$ is invariant upon a permutation of its indices, provided the names of the unit vectors $(\boldsymbol{a}, \boldsymbol{b}, \boldsymbol{c})$ and $(\boldsymbol{a}', \boldsymbol{b}', \boldsymbol{c}')$ undergo the same permutation. In the following we arbitrarily chose the order $(i, j, k) = (0, 1, 2)$.

Similarly to what occurs for the two-mode operator, the principle of local realism, if correct, should predict that the statistical average $\langle \hat{\mathscr{S}}^{(0|1|2)} \rangle$ be bounded by ± 2. The system violates this principle when the average of the previous average is larger than two. This is often referred to as violation of Svetlichny inequality. It is important to note that the observable $\hat{\mathscr{S}}^{(0|1|2)}$ is specially designed in order to be sensitive to *genuine tripartite nonlocality* (see discussions in Refs. [161, 163, 162, 95] and references therein): a

[85] Indeed at zero temperature, when $\gamma_i = 1$, the expression in $\{.\}$ of (4.214) is just equal to $\cosh r_2 - \sinh r_2 = e^{-r_2}$ and therefore $\Lambda^{(i|2)}(\omega)$ equals $\Lambda^{(f_1|f_2)}(\omega)$ of (4.212). On the contrary when $\gamma_i = 0$ the measure $\Lambda^{(i|2)}(\omega)$ vanishes. Then, since $\Lambda^{(i|2)}(\omega)$ is at zero temperature a monotonically increasing function of $\gamma_1 \in [0, 1]$, one has $\Lambda^{(i|2)}(\omega)$ always smaller than $\Lambda^{(f_1|f_2)}(\omega)$.

tripartite system can involve nonlocal correlations between any of its bipartitions and still not violate the Svetlichny inequality $\langle \hat{\mathscr{S}}^{(0|1|2)} \rangle < 2$. A simple example of a system which displays two mode nonlocality but does not pass the Svetlichny test is our optical analog presented in 4.2.3. This can be seen below in Eq. (4.238). We will further comment on this last result when proving it.

In order to reach a maximum violation of Svetlichny (i.e., three-mode Bell) inequality it is necessary to choose a particular arrangement of the vectors $\boldsymbol{a}$, $\boldsymbol{a}'$, $\boldsymbol{b}$, $\boldsymbol{b}'$, $\boldsymbol{c}$ and $\boldsymbol{c}'$ which maximizes the expectation value $\langle \hat{\mathscr{S}}^{(0|1|2)} \rangle$. To do so, we resort to a genetic algorithm which is presented in Appendix A.6, i.e. we numerically determines the quantity

$$S^{(0|1|2)}(\omega) \equiv \max_{\boldsymbol{a},\boldsymbol{a}',\boldsymbol{b},\boldsymbol{b}',\boldsymbol{c},\boldsymbol{c}'} \left\langle \hat{\mathscr{S}}^{(0|1|2)}(\omega) \right\rangle \tag{4.216}$$

It is shown in Appendix A.5 that the tripartite parameter $S^{(0|1|2)}(\omega)$ is bounded from above by $2\sqrt{2}$ (this is Eq. (A.96)) and that this bound is reached at $\omega = 0$ and $T = 0$([see Eq. (A.108)).

The behavior of $S^{(0|1|2)}(\omega)$ at zero temperature is displayed in Fig. 4.5 for different realizations of the waterfall configuration. Although the bound $2\sqrt{2}$ is reached in the long wave length limit for all the realizations, even a weak temperature is able to destroy the signal of nonlocality as illustrated in Fig. 4.5. This weakness of the signal is connected to the loss of purity of the finite temperature system and can be understood analytically, again in the long wave length limit, as discussed in Appendix A.5. This sensitivity to a small finite temperature probably precludes the experimental observation of tripartite nonlocality by means of the observable (4.216). However, although the zero temperature behavior is certainly difficult to observe, it is rich of fundamental insight on the nature of the state of the system, as we now discuss.

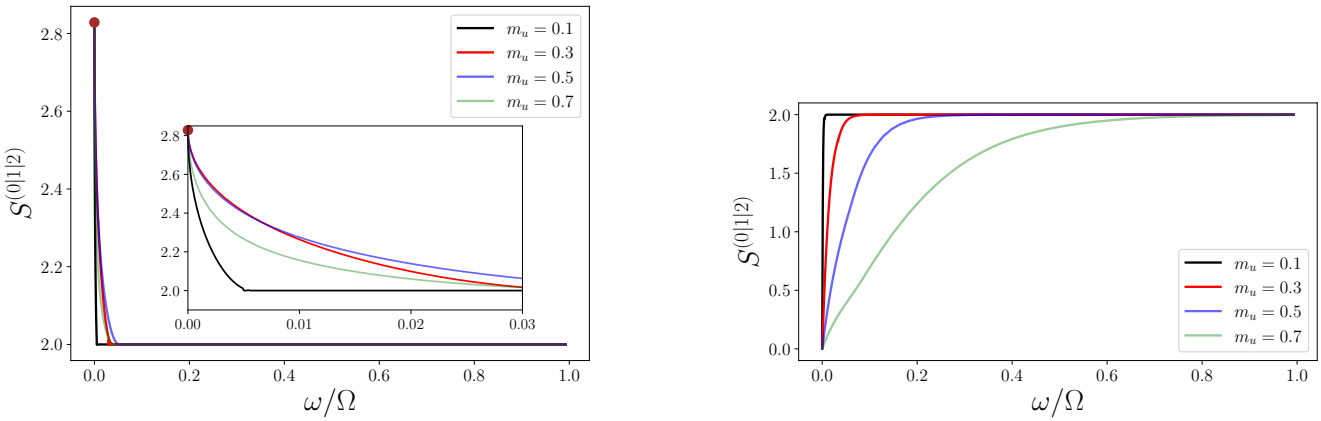

Figure 4.5: LEFT PLOT : Zero temperature value of the tripartite parameter $S^{(0|1|2)}$ plotted as a function of energy for different realization of the waterfall configuration, each being characterized by the upstream Mach number m_u. The inset displays a blow up of the figure at low energy. The upper bound $2\sqrt{2}$ is marked by a brown dot. It is reached at $\omega = 0$ in all configurations. RIGHT PLOT : Same as left plot for a temperature $T = 0.05\, g n_u$. At variance with the zero temperature situation the tripartite measure (4.216) is here always less than or equal to 2.

4.6.2 . The GKMR Pseudo-spins in the Zero Temperature and Zero Energy Limit

The low energy behavior of the quantities (4.202) is dictated by the one of the local mixednesses a_0, a_1 and a_2 which diverge as $1/\omega$ for all temperature. As a result

$$\lim_{\omega\to 0} \mathcal{T}_{zxx} = \lim_{\omega\to 0} \mathcal{T}_{xzx} = \lim_{\omega\to 0} \mathcal{T}_{xxz} \underset{\forall T}{=} 0. \tag{4.217}$$

On the other hand, the behavior of the quantities (4.203) depends on the behavior of the square root D of the determinant of the covariance matrix which is unity at $T = 0$ [78]. In this case

$$\mathcal{T}_{zzz}(\omega) \underset{T=0}{=} 1, \tag{4.218}$$

and, in the waterfall configuration,

$$-\lim_{\omega\to 0}\mathcal{T}_{zyy}=\lim_{\omega\to 0}\mathcal{T}_{yzy}=\lim_{\omega\to 0}\mathcal{T}_{yyz}\underset{T=0}{=}1. \tag{4.219}$$

The reason for this behavior is that, at $T=0$, $D=1$ whereas the arguments of all the $\arctan$ terms in (4.202) diverge as $\omega^{-1/2}$, as shown by detailed inspection based on Eqs. (4.199), (4.200), (4.176)-(4.179) and the asymptotic expression of the coefficients of the S matrix given in [38].

Alternatively, at finite temperature D diverges at low energy (as $1/\omega$) and the limits (4.219) all cancel

$$\lim_{\omega\to 0}\mathcal{T}_{zyy}=\lim_{\omega\to 0}\mathcal{T}_{yzy}=\lim_{\omega\to 0}\mathcal{T}_{yyz}\underset{T\neq 0}{=}0, \tag{4.220}$$

as also does $\lim_{\omega\to 0}\mathcal{T}_{zzz}\underset{T\neq 0}{=}0$.

As argued in Appendix 4.3.1, the fact that, at zero temperature and $\omega=0$ the system reaches the tripartite upper bound ($S^{(0|1|2)}=2\sqrt{2}$, see Fig. 4.5) mathematically stems from the fact that, under these conditions the system is in a pure state and displays perfect correlations in the following expectation values (see Eqs. (4.218), (4.219) and (4.195)) :

$$\langle\hat{\Pi}_y^{(0)}\otimes\hat{\Pi}_y^{(1)}\otimes\hat{\Pi}_z^{(2)}\rangle=\langle\hat{\Pi}_y^{(0)}\otimes\hat{\Pi}_z^{(1)}\otimes\hat{\Pi}_y^{(2)}\rangle=-\langle\hat{\Pi}_z^{(0)}\otimes\hat{\Pi}_y^{(1)}\otimes\hat{\Pi}_y^{(2)}\rangle=\langle\hat{\Pi}_z^{(0)}\otimes\hat{\Pi}_z^{(1)}\otimes\hat{\Pi}_z^{(2)}\rangle=1 \tag{4.221}$$

All the other expectation values of tensor products of three components of the $\hat{\mathbf{\Pi}}$ operator are zero. The precise values ±1 for the non vanishing averages are here given for the waterfall configuration. The situation is identical for the delt peak configuration but slightly different in the case of a flat profile configuration, where $\mathcal{T}_{yyz}=-1$ and $\mathcal{T}_{zzz}=\mathcal{T}_{zyy}=\mathcal{T}_{yzy}=1$, with all other coefficients also vanishing. Then, since all the operators in (4.221) have only ±1 as eigenvalues, each term must reach its extremal value and the vacuum mode of zero frequency $|0_{\omega=0}\rangle^{\text{in}}$ must therefore be an eigenstate of the operators appearing in (4.221), i.e.

$$\hat{\Pi}_y^{(0)}\otimes\hat{\Pi}_y^{(1)}\otimes\hat{\Pi}_z^{(2)}|0_{\omega=0}\rangle^{\text{in}}=+|0_{\omega=0}\rangle^{\text{in}} \tag{4.222a}$$
$$\hat{\Pi}_y^{(0)}\otimes\hat{\Pi}_z^{(1)}\otimes\hat{\Pi}_y^{(2)}|0_{\omega=0}\rangle^{\text{in}}=+|0_{\omega=0}\rangle^{\text{in}} \tag{4.222b}$$
$$\hat{\Pi}_z^{(0)}\otimes\hat{\Pi}_y^{(1)}\otimes\hat{\Pi}_y^{(2)}|0_{\omega=0}\rangle^{\text{in}}=-|0_{\omega=0}\rangle^{\text{in}} \tag{4.222c}$$
$$\hat{\Pi}_z^{(0)}\otimes\hat{\Pi}_z^{(1)}\otimes\hat{\Pi}_z^{(2)}|0_{\omega=0}\rangle^{\text{in}}=+|0_{\omega=0}\rangle^{\text{in}} \tag{4.222d}$$

Relations (4.222) define a state which exhibits the GHZ paradox, contradicting local hidden variable theories by means of a single measurement; cf. e.g., the discussion in [112].

4.6.3 . Superposition of Degenerate GHZ States in the Zero Temperature and Zero Energy Limit

We show here that the state we consider is, at finite temperature and in the long wavelength limit, an infinite sum of degenerate GHZ states of a continuous variable system. To this end it is convenient to expand the state $|0_{\omega=0}\rangle^{\text{in}}$ over the eigenstates of the operators $\hat{\Pi}_x^{(j)}$ ($j=0$, 1 or 2). As discussed in Appendix A.2 these eigenstates can be written as $|x_n^{\pm}\rangle_j$: they are labeled by their eigenvalue (±1) plus another integer index (n in the above expression) associated to the infinite degeneracy of both eigenvalues.

Indeed, at variance with what occurs for a regular spin operator, the projection of the pseudo-spin (4.191) over a given axis (here $\hat{\Pi}_x$) has infinitely degenerate eigenvalues. The existence of such an infinitely degenerate subspace for each eigenvalue implies the existence of an infinite number of mutually orthogonal eigenstates with the same eigenvalue ($+1$ or -1), i.e.

$$\forall n\in\mathbb{N},\quad \hat{\Pi}_x^{(j)}|x_n^{\pm}\rangle_j=\pm|x_n^{\pm}\rangle_j \tag{4.223}$$

whereas

$$\forall(n,m)\in\mathbb{N}^2,\quad {}_j\langle x_n^{\pm}|x_m^{\pm}\rangle_j=\delta_{n,m}. \tag{4.224}$$

This can be shown (see Eqs. (A.39) and (A.48)) by directly constructing the eigenstates of $\hat{\Pi}_x$ from the number states. The expansion of $|0_{\omega=0}\rangle^{\text{in}}$ over the complete basis $\{|x_l^{\sigma_0}, x_m^{\sigma_1}, x_n^{\sigma_2}\rangle\}$ is given by

$$|0_{\omega=0}\rangle^{\text{in}} = \sum_{\substack{\sigma_0,\sigma_1,\sigma_2 \\ l,m,n}} C_{l,m,n}^{\sigma_0,\sigma_1,\sigma_2} |x_l^{\sigma_0}, x_m^{\sigma_1}, x_n^{\sigma_2}\rangle. \tag{4.225}$$

where σ_0, σ_1 and $\sigma_2 = \pm$ and $(l,m,n) \in \mathbb{N}^3$ whereas the indices $j = 0$, 1 or 2 of the kets have been dropped for legibility. It follows from relations (4.222) and (A.52a)[86] that:

$$-\sigma_0\sigma_1\, C_{l,m,n}^{-\sigma_0,-\sigma_1,-\sigma_2} = -\sigma_0\sigma_2\, C_{l,m,n}^{-\sigma_0,-\sigma_1,-\sigma_2} = \sigma_1\sigma_2\, C_{l,m,n}^{-\sigma_0,-\sigma_1,-\sigma_2} = C_{l,m,n}^{-\sigma_0,-\sigma_1,-\sigma 2} \tag{4.226}$$

This imposes that the only nonzero coefficients in expansion (4.225) are those for which

$$\sigma_1 = \sigma_2 = -\sigma_0 \tag{4.227}$$

The two previous relations (4.226) and (4.227) imply finally

$$C_{l,m,n}^{+--} = C_{l,m,n}^{-++} \equiv C_{l,m,n}. \tag{4.228}$$

Expansion (4.225) thus simplifies to

$$|0_{\omega=0}\rangle^{\text{in}} = \sum_{l,m,n} C_{l,m,n} \Big(|x_l^+, x_m^-, x_n^-\rangle + |x_l^-, x_m^+, x_n^+\rangle \Big) \tag{4.229}$$

which shows that the vacuum $|0_{\omega=0}\rangle^{\text{in}}$ of the $\hat{b}_j(\omega = 0)$ operators (the ingoing ground state) is an infinite sum of degenerate GHZ states. It is easily checked that this definition of $|0_{\omega=0}\rangle^{\text{in}}$ is indeed an eigenstate of the operators appearing in (4.222). Most significantly, the structure of $|0_{\omega=0}\rangle^{\text{in}}$ given in (4.229) enables the reduced state obtained after partial tracing over one mode to remain entangled despite the GHZ nature of the system. Indeed, tracing over mode 0 for instance leads to a reduced density matrix

$$\text{Tr}_{(0)}\Big(|0_{\omega=0}\rangle^{\text{in}}\, {}^{\text{in}}\langle 0_{\omega=0}| \Big) = \sum_{m,n,\mu,\nu} \mathcal{C}_{m,n,\mu,\nu}^{(0)} \Big(|x_m^- x_n^-\rangle \langle x_\mu^- x_\nu^-| + |x_m^+ x_n^+\rangle \langle x_\mu^+ x_\nu^+| \Big) \tag{4.230}$$

In this expression, where the kets and bras concern modes 1 and 2 since mode 0 has been traced out,

$$\mathcal{C}_{m,n,\mu,\nu}^{(0)} = \sum_{l=0}^{\infty} C_{l,\mu,\nu}^* C_{l,m,n} \tag{4.231}$$

If the eigenvalues $+1$ and -1 of operator $\hat{\Pi}_x$ were non-degenerate, this would impose $m = \mu$ and $n = \nu$ in expression (4.230) and the corresponding reduced state would be clearly separable. Nothing similar occurs in our situation when either mode 0 or mode 1 is traced out, and indeed the corresponding reduced states are typically entangled, as shown in Sec. 4.5. But when mode 2 is traced out the reduced state clearly appears to be not entangled, as can again be seen in Sec. 4.5. This may suggest that the structure of the vacuum $|0_{\omega=0}\rangle^{\text{in}}$ given in (4.229) may be further simplified.

4.6.4 . Mermin Parameter : Weak Resilience to Temperature of the GHZ State

Since we now understand the exact GHZ nature of the zero temperature and $\omega = 0$ state of the system, it is of interest to quantify to what extent this feature persists at finite temperature and finite energy. To this aim, we use the genetic algorithm presented in Appendix A.6 to compute the optimum of the Mermin parameter [111, 164]

$$M^{(0|1|2)}(\omega) \equiv \max_{\boldsymbol{a},\boldsymbol{a}',\boldsymbol{b},\boldsymbol{b}',\boldsymbol{c},\boldsymbol{c}'} \left| \left\langle \hat{\mathscr{M}}^{(0|1|2)}(\omega) \right\rangle \right| \tag{4.232}$$

where

$$\begin{aligned} \hat{\mathscr{M}}^{(0|1|2)}(\omega) = &- \boldsymbol{a}\cdot\hat{\boldsymbol{\Pi}}^{(0)} \otimes \boldsymbol{b}\cdot\hat{\boldsymbol{\Pi}}^{(1)} \otimes \boldsymbol{c}\cdot\hat{\boldsymbol{\Pi}}^{(2)} + \boldsymbol{a}\cdot\hat{\boldsymbol{\Pi}}^{(0)} \otimes \boldsymbol{b}'\cdot\hat{\boldsymbol{\Pi}}^{(1)} \otimes \boldsymbol{c}'\cdot\hat{\boldsymbol{\Pi}}^{(2)} \\ &+ \boldsymbol{a}'\cdot\hat{\boldsymbol{\Pi}}^{(0)} \otimes \boldsymbol{b}\cdot\hat{\boldsymbol{\Pi}}^{(1)} \otimes \boldsymbol{c}'\cdot\hat{\boldsymbol{\Pi}}^{(2)} + \boldsymbol{a}'\cdot\hat{\boldsymbol{\Pi}}^{(0)} \otimes \boldsymbol{b}'\cdot\hat{\boldsymbol{\Pi}}^{(1)} \otimes \boldsymbol{c}\cdot\hat{\boldsymbol{\Pi}}^{(2)} \end{aligned} \tag{4.233}$$

[86] Rewriting them as $\hat{\Pi}_y|x_n^{\sigma_0}\rangle = -i\,\sigma_0|x_n^{-\sigma_0}\rangle$ and $\hat{\Pi}_z|x_n^{\sigma_0}\rangle = |x_n^{-\sigma_0}\rangle$ respectively.

We note here $\hat{\mathscr{M}}^{(0|1|2)}(\omega)$ that relates to the three-mode Bell operator given in (4.215) since one has

$$\hat{\mathscr{S}}^{(0|1|2)} = \tfrac{1}{2}\hat{\mathscr{M}}^{(0|1|2)} + \tfrac{1}{2}\hat{\mathscr{M}}'^{(0|1|2)} \tag{4.234}$$

where $\hat{\mathscr{M}}'^{(0|1|2)}$ is the same as $\hat{\mathscr{M}}^{(0|1|2)}$ with the prime reversed [163].

The largest possible value of the Mermin parameter (4.232) is 4. This upper bound is reached for a state verifying relations (4.221), such as a GHZ state or the low wavelength component of the ground state of our system as just discussed[87]. Indeed, at $T = 0$, $M^{(0|1|2)}(0) = 4$ for all black hole configurations. This is illustrated in Fig. 4.6 in which $M^{(0|1|2)}$ is plotted as a function of ω for different values of m_u, at

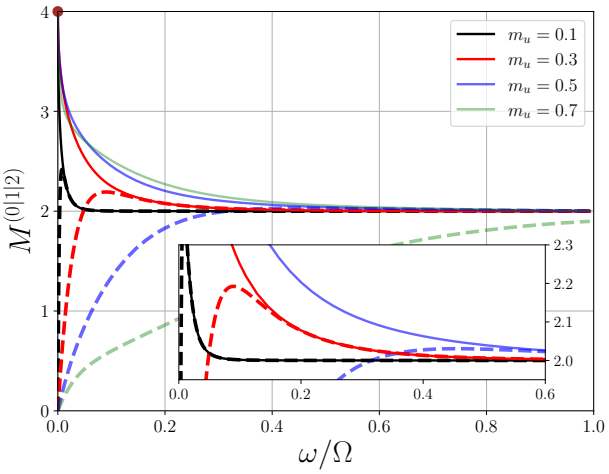

Figure 4.6: Mermin parameter $M^{(0|1|2)}(\omega)$ plotted for different waterfall configurations. The continuous lines starting from $M^{(0|1|2)} = 4$ at $\omega = 0$ are zero temperature results and the thick dashed ones (with $M^{(0|1|2)}(0) = 0$) correspond to $T = 0.1\, gn_u$. The inset is a blow up of the figure around the region $M^{(0|1|2)} = 2$ for $\omega/\Omega \leq 0.6$.

zero and finite temperature ($T = 0$ and $T = 0.1\, gn_u$). If the departure of $M^{(0|1|2)}$ from its upper bound is taken as an indication of how much the system differs from a GHZ state, this suggests that the GHZ character of the state is restricted to the low energy and low temperature sector. We stress however that such a criterion is only indicative: the Svetlichny and Mermin parameters provide useful bounds, but not proper measures. This is illustrated by their poor effectiveness for evaluating genuine tripartite entanglement. It is known [163] that if

$$M^{(0|1|2)} > 2\sqrt{2} \qquad \text{or} \qquad S^{(0|1|2)} > 2 \tag{4.235}$$

the system exhibits genuine three-mode entanglement. Figs. 4.5 and 4.6 show that this type of entanglement is certainly reached at $T = 0$ for low energy. However, the criteria (4.235) are here too restrictive, since the computation of the residual contangle done in Ref. [86] demonstrates that at $T = 0$ the system is genuinely tripartite entangled for *all* energies and *all* configurations. This general conclusion certainly cannot be reached by inspecting, in Figs. 4.5 and 4.6, in which domain of energy and for which value of m_u the criteria (4.235) are met. However, these criteria are valid and can be useful, for instance at finite temperature. In this case the state of the system is not pure, the evaluation of the residual contangle appears to be very difficult, and the criterion (4.235) is the only way we know to demonstrate genuine tripartite entanglement, which, as can be inferred from the tendency displayed in Fig. 4.6, is reached at low T, low ω and small values of m_u.

Finally, the Mermin parameter (4.232) is also an interesting witness of nonlocality. A local hidden variable theory predicts that it should verify the Mermin-Klyshko inequality $M^{(0|1|2)} \leq 2$. It can be seen from Fig. 4.6 that this inequality is violated at zero temperature for all waterfall configurations. For $T > 0$ instead, $M^{(0|1|2)}(0) = 0$. Therefore, the Mermin parameter has the same behaviour as the Svetlichny

[87] From (4.221) it is clear that at zero temperature and $\omega = 0$ the maximum (4.232) is obtained when $\boldsymbol{a} = \boldsymbol{b}' = \boldsymbol{c}' = \boldsymbol{e}_z$ and $\boldsymbol{a}' = \boldsymbol{b} = \boldsymbol{c} = \boldsymbol{e}_y$, reaching the upper bound 4.

parameter and for the same reason : at finite temperature the state of the system is no longer pure, and in this case all the expectation values of products of three components of the pseudo-spin tend to zero in the long wavelength limit as can been seen from discussion in Appendix 4.3.1. However, contrary to what occurs for the Svetlichny parameter, there are accessible finite temperature situations where the Mermin parameter is larger that the nonlocality threshold $M^{(0|1|2)} = 2$ (compare Figs. 4.6 and 4.5). In that respect, the Mermin parameter may even reveal more useful that the CHSH parameter (4.211). For instance, at $T = 0.1gn_u$, for $m_u = 0.3$ the largest value of $M^{(0|1|2)}$ is 2.19 (as seen from Fig. 4.6), higher than the largest values reached by both CHSH parameters $B^{(0|2)}$ and $B^{(0|1)}$ in the same situation (2 and 2.017, respectively).

4.6.5 . No Genuine Tripartite Entanglement and Nonlocality in the $\{\mathbf{f}\}$ Basis of the Optical Analog

After discussing two modes entanglement (see section 4.5.3) it is also interesting to briefly consider tripartite entanglement in the effective optical system depicted in Fig. 4.1. As already said in section 4.5.3, this system has been designed (by means of a procedure called entanglement localization [165]) in such a way that it concentrates entanglement between the effective squeezed modes f_1 and f_2. Therefore, it should be expected that, in the $\{\mathbf{f}\}$ basis, the quantity $\langle \hat{\mathscr{S}}^{(f_0|f_1|f_2)} \rangle$, which is sensible to a genuine tripartite nonlocality, will never reach values above two. Indeed, in this basis, at zero temperature one has

$$\langle \hat{\Pi}_r^{(f_0)} \otimes \hat{\Pi}_s^{(f_1)} \otimes \hat{\Pi}_t^{(f_2)} \rangle \underset{T=0}{=} \langle \hat{\Pi}_r^{(f_0)} \rangle \langle \hat{\Pi}_s^{(f_1)} \otimes \hat{\Pi}_t^{(f_2)} \rangle. \tag{4.236}$$

with

$$\langle \hat{\Pi}_z^{(f0)} \rangle = 1 \qquad \langle \hat{\Pi}_y^{(f0)} \rangle = 0 \qquad \langle \hat{\Pi}_x^{(f0)} \rangle = 0 \tag{4.237}$$

As it is shown at the end of Appendix A.5, one then obtains straightforwardly that

$$S^{(f_0|f_1|f_2)}(\omega) \underset{T=0}{=} 2. \tag{4.238}$$

Of course the value of $S^{(f_0|f_1|f_2)}$ decreases when the temperature increases. This quantity is thus always lower than 2, indicating, as expected, that **there is no genuine tripartite nonlocality between the effective $\{\mathbf{f}\}$ modes**.

Furthermore, from Eqs. (A.110) and (A.111), and also from the facts that $\langle \hat{\Pi}_s^{(f_1)} \otimes \hat{\Pi}_t^{(f_2)} \rangle = 0$ if $s \neq t$ and that, at $\omega = 0$ and $T = 0$,

$$\langle \hat{\Pi}_x^{(f_1)} \otimes \hat{\Pi}_x^{(f_2)} \rangle = -\langle \hat{\Pi}_y^{(f_1)} \otimes \hat{\Pi}_y^{(f_2)} \rangle = 1, \tag{4.239}$$

it is easily found that, at $\omega = 0$, the optimized Mermin parameter (4.232) of the f modes is

$$M^{(f_0|f_1|f_2)}(0) \underset{T=0}{=} 2. \tag{4.240}$$

This shows that, at variance with the $\{\mathbf{c}\}$ modes, the effective $\{\mathbf{f}\}$ modes do not violate the Mermin-Klyshko inequality and certainly do not exhibit the GHZ paradox. Results (4.238) and (4.240) were expected: since the $\{\mathbf{f}\}$ modes do not exhibit tripartite entanglement they should fulfill none of the inequalities (4.235) and therefore should never violate locality.

Finally, it follows from (4.208) that when $m_u = 0$ or 1, at $\omega = 0$, $\cos\theta = 0$ or 1, respectively. In this case Eqs. (4.103), (4.97) and (4.99) indicate that the $\{\mathbf{f}\}$ modes are connected to the $\{\mathbf{c}\}$ modes not by a Non-Local Linear Unitary BOgoliubov (NLLUBO) transformation, as they generically are, but by a local one (LLUBO): then, the tripartite character of the true system thus disappears in these two limiting cases, even when $T = 0$. However our results indicate that these two limits are singular, since the GHZ character of the system is observed (at $\omega = 0$ and $T = 0$) for all $m_u \in]0, 1[$.

4.7 . RESULTS FOR TWO OTHER ANALOG BLACK HOLE CONFIGURATIONS

4.7.1 . Bipartite Results

The only configuration which has been realized experimentally so far is the waterfall configuration [34, 35]. At least theoretically there are two other configurations : the delta peak and the flat profile

configurations, which are defined in 3.1. It is interesting to note that, to some respects, the obtained results are configuration independent. The equivalents of Fig. 4.3 for these alternative configurations are plotted in Fig. 4.7. In the flat profile configuration the value of m_d is a free parameter. Thus, in order to compare the results of the flat profile configuration with Fig. 4.3 we impose $m_d = 1/m_u^2$, as is the case for the waterfall configuration defined in Eq. (3.19). Such a procedure is not required (nor possible) for the delta peak configuration where fixing m_u unambiguously determines m_d, as can be seen from (3.16).

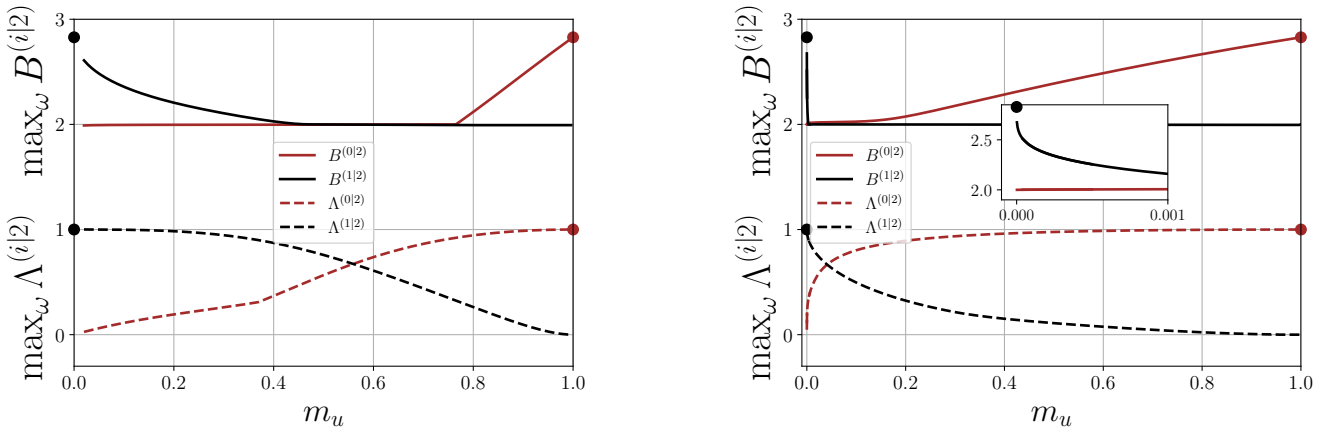

Figure 4.7: Same as Fig. 4.3 for a zero temperature flat profile configuration with $m_d = 1/m_u^2$ (left plot) and for a zero temperature delta peak configuration (right plot). The inset is a blow up at low m_u.

Fig. 4.7 shows that the delta peak configuration has a special feature: the EPR state formed by the companion and the partner (see Sec. 4.5) is only reached at extremely low values of the upstream mach number m_u, whereas bipartite nonseparability between the Hawking quantum and the partner (modes o and 2, respectively) is significant in a wide range of values of m_u (roughly speaking, for $m_u \gtrsim 0.2$). Despite this peculiarity, it is fair to say that Figs. 4.7 both display the **same general trend** as Fig. 4.3, thus supporting the idea that the behavior already discussed for the waterfall configuration is generic. We do not produce finite temperature figures equivalent to Fig. 4.3 since, as expected, the delta peak and the flat profile configurations behave similarly to the waterfall configuration when the temperature is increased. There is however a quantitative change which is worth noticing: in these two alternative configurations the violation of bipartite Bell inequality does not persist as much as for the waterfall configuration when T is increased.

4.7.2 . Tripartite Results

Regarding the study of genuine tripartite nonlocality, the zero and finite temperature values of the Svetlichny parameter $S^{(0|1|2)}(\omega)$ can be computed as well in the delta peak and flat profile configurations. We present in Figs. 4.8 the results for zero temperature which are the equivalents of Fig. 4.5. Again, results at finite temperature are not displayed since the trend is the same as for the waterfall configuration but with a weaker resilience to temperature. For the zero temperature case, the phenomenology is indeed the same as the one discussed for the waterfall configuration. There is a clear signal of nonlocality at $T = 0$, in a domain of energy typically more extended than for the waterfall configuration, but as is the case for the waterfall configuration this signal does not persist at small finite temperature.

As a further (and final) confirmation of the generality of the obtained results, it is worth noticing that the he GHZ character of the long wave length modes also appears in the delta peak and flat profile configurations. As argued in Sec. 4.6, at zero temperature both configurations display the GHZ paradox at $\omega = 0$ and verify $M^{(0|1|2)}(0) = 4$. The behavior of the optimized Mermin parameter $M^{(0|1|2)}(\omega)$ given (4.232) is represented at finite and zero temperature in Figs. 4.9 and 4.9 which correspond to the delta peak and flat profile configuration, respectively. At zero temperature the signal (4.235) of genuine tripartite entanglement is more pronounced for the delta peak and flat profile configurations than for the waterfall. This was also the case for the signal (4.235) of genuine tripartite nonlocality. However, this signal, although more noticeable at $T = 0$, is less resilient to an increase of temperature than for

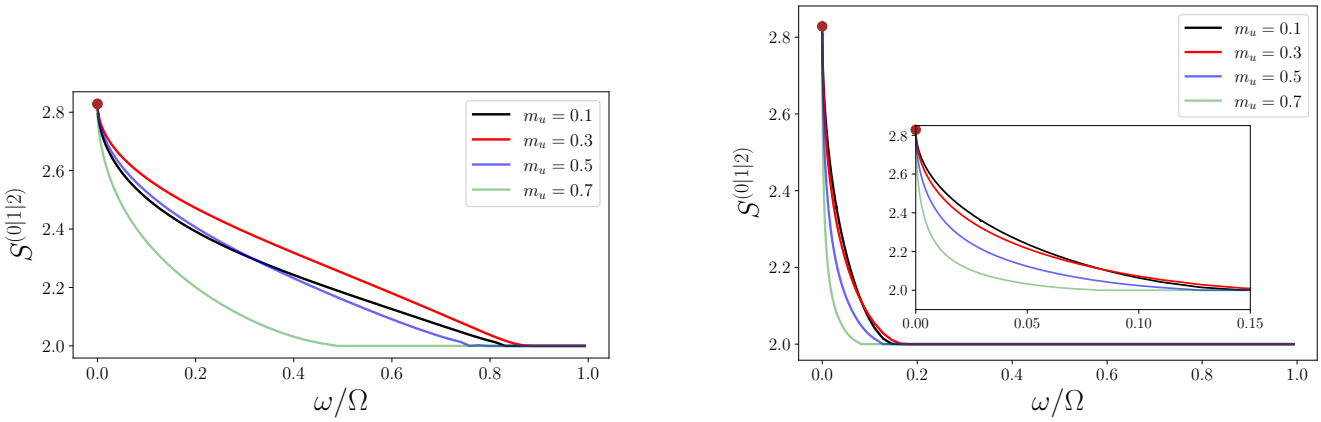

Figure 4.8: Same as Fig. 4.5 for zero temperature flat profile configurations (left plot) and for zero temperature delta peak configurations (right plot). The inset displays a blow up of the figure at low energy.

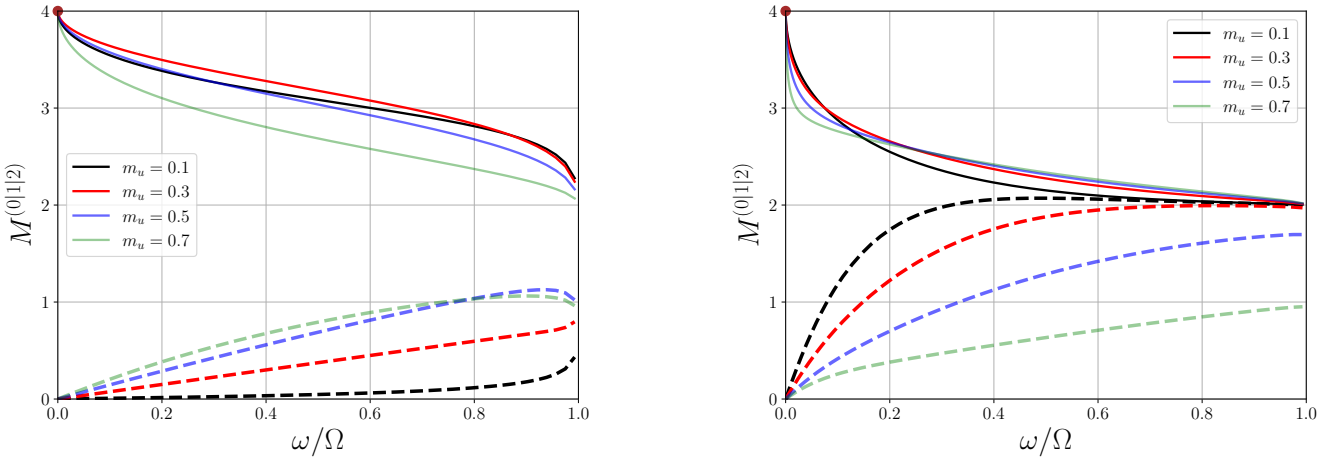

Figure 4.9: Same as Fig. 4.6 for (left plot) flat profile configurations at $T = 0$ (thin solid lines) and $T = 0.1gn_u$ (thick dashed lines) and for (right plot) for delta peak configurations at $T = 0$ (thin solid lines) and $T = 0.1gn_u$ (thick dashed lines).

the waterfall configuration, especially for the flat profile configuration as can be seen in Fig. 4.9. Once again, despite some specificities, the general trend is the same as for the waterfall configuration : the departure from the GHZ signal $M^{(0|1|2)}(0) = 4$ increases at high energy. At finite temperature, the GHZ behavior is lost but since the Mermin parameter is larger than 2 the signal of nonlocality persists at zero temperature and is more pronounced at $T \neq 0$ for the waterfall configuration than for the two others.

4.8 . MAIN RESULTS

4.8.1 . About Bipartite and Tripartite Nonlocality

In our acoustic black hole a simple pair production process induces (and this is far from being intuitive) *genuine* tripartite entanglement and *genuine* tripartite non-locality, as it has been shown in Ref. [86] and in the present study respectively. Once a quasi-particle of our tripartite system is traced out, the remaining bipartite system may exhibit *genuine* bipartite entanglement and *genuine* bipartite non-locality in the case of the Hawking-partner and companion-partner pairs. If the **violation of Bell inequality** is a signature of **genuine bipartite nonlocality**, the **violation of Svetlichny inequality** is a signature of **genuine tripartite nonlocality**. According to our results, there is reasonable hope to witness genuine bipartite nonlocality in an acoustic analog of a black hole whereas the observation of signatures of genuine tripartite nonlocality appears to be presumably more difficult. It seems indeed (see Fig. 4.6 and

Figs. (4.9)) that tripartite signatures only weakly resist to an increase in temperature [88].

Since we assumed our system to be in a **Gaussian state** the full information about the correlations exhibited by the system can be extracted from the **covariance matrix**. The only quantities that need to be measured are $\langle \hat{c}_i^\dagger \, \hat{c}_i \rangle$, $|\langle \hat{c}_0 \, \hat{c}_1^\dagger \rangle|$ $|\langle \hat{c}_0 \, \hat{c}_2 \rangle|$ and $|\langle \hat{c}_1 \, \hat{c}_2 \rangle|$. In BEC physics indirect techniques have been used for measuring some of the entries of this matrix potentially difficult to determine experimentally, such as $\langle \hat{c}_0 \, \hat{c}_2 \rangle$, for example by carefully extracting information from the knowledge of the density-density correlation function [54, 39, 90], but others techniques have to be devised for measuring some other entries where an access to the the phases of the averaged quadratures is needed. It is here worth noticing that our approach can be adapted with little modification to other systems, such as exciton-polaritons in microcavities, or more generally setups involving nonlinear light, in which all the entries of the covariance matrix could possibly be measured with more direct procedures. For the quantities we are interested in, the long wavelength behavior of the modes, and therefore of the dispersion relation and of the corresponding S matrix components, is of major interest.
Indeed, if the breaking of Lorentz invariance due to dispersive effects (non-linearity of the dispersion relation) could appear as a flaw in the analogy, it is this very same apparent shortcoming, common to all analog physics [166, 167, 168, 169], that causes the existence not only of a Hawking and a partner mode but also of a third mode here denoted as the companion. It is then a main result of our work to have shown that our three-quasi-particle system not only exhibits tripartite entanglement [86] but also **tripartite nonlocality**. This peculiar nonlocal tripartite configuration, together with the continuous nature of the degrees of freedom, translates into a system whose long wavelength quantum modes are surprisingly described by a **superposition of degenerate GHZ states** which, at variance with GHZ states built on qubits, remains **entangled after partial tracing**.
This result is likely to be generic in any system with a sonic-like low energy dispersion relation, thus suggesting that condensed matter analogs may be considered in the future not only as empirical analogies but also on their own as valuable systems for inquiring into the flow of multipartite quantum information for a continuous variable regime. Finally, since the **Gaussian assumption** that has been made stems from our **Bogoliubov linearization of the Gross-Pitaevskii equation** for the field operator, i.e. from the reduction of a quartic (interaction) Hamiltonian to a **quadratic Hamiltonian**, it is important to recall that nonlinear effects might significantly affect quantum emission processes in the context of analog physics [170, 171, 172, 173]. It would then be of great interest to precisely characterize how these nonlinear back reaction effects reshape the radiation processes in the black hole analogs we consider.

4.8.2 . Article : Violation of Bell Inequalities in an Analog Black Hole

G. Ciliberto , S. Emig , N. Pavloff , M. Isoard, Physical Review A **109**, 063325 (2024)

doi : https://doi.org/10.1103/PhysRevA.109.063325

Signals of entanglement and nonlocality are quantitatively evaluated at zero and finite temperature in an analog black hole realized in the flow of a quasi-one-dimensional Bose-Einstein condensate. The violation of Lorentz invariance inherent to this analog system opens the prospect to observe three-mode quantum correlations and we study the corresponding violation of bipartite and tripartite Bell inequalities. It is shown that the long-wavelength modes of the system are maximally entangled, in the sense that they realize a superposition of continuous variable versions of Greenberger-Horne-Zeilinger states the entanglement of which resists partial tracing.

[88] It is worth noticing that, among the three black hole configurations here considered, the waterfall configuration appears to be less sensitive to increased temperature Fig. 4.6 and Figs. (4.9).

5 - BACK-REACTION IN AN ANALOG BLACK HOLE

In this chapter we derive the back-reaction equations for an analog black hole in a one-dimensional weakly-interacting quasicondensate. This is done by expanding the field operator $\hat{\Psi}(x,t)$ of the system up to second order. The averaged second-order terms will then constitute the source terms in the dynamical equations describing the corrections to the zeroth order classical meanfield approximation of the field operator[1]. Stationary solutions will be considered and preliminary asymptotic results will be derived.

5.1 . BACK-REACTION : A short overview

An analog black hole is an out-of-equilibrium quantum system. This is revealed by the presence of excitations of negative energy in the supersonic region. At zeroth order, in a naive approach, one could state that the systems tries (hopelessly) to reach equilibrium by emitting Hawking radiation. In the analog configuration we consider equilibrium is never reached : since energy is constantly injected by the external potential, the system remains in an out-of-equilibrium stationary state and never relaxes to equilibrium. It then radiates permanently. In order to study the *relaxation*, higher-order quantum contributions have to be taken into account : the effects of these contributions on the flow constitute the *back-reaction* phenomenon. Then, what is at stake is to understand how Hawking radiation perturbs the flow and by this means to gain a hint on how the system eventually reaches an equilibrium state no longer containing any negative energy modes.

It is in analogy with this relaxation phenomenon that a gravitational black hole radiates thermally at temperature T_H in order to reach its equilibrium state, which is in Hawking's theory [10, 11] the vanishing of the black hole, i.e. its total evaporation. Contrary to the general relativity case, where there is no tested theory of quantum gravity, the back-reaction effects of the quantized excitations can be treated in our BEC analog setup in the framework of a unified quantum nonlinear theory[2]. The averaged quantum fluctuations of higher-order will therefore in our system constitute the quantum correction terms to the zeroth order effective metric parametrized by the mean-field wavefunction. In this perspective, they can be seen in analogy to the modification of the space-time metric yielded by the loss of energy, i.e. mass, in the radiating black hole.

Another incentive for studying back-reaction has been put forward: the derivation by Hawking of its thermal radiation does not contemplate back-reaction. The existence of these higher-order terms in the dynamics could alter the thermal character of the quantum emission. Some researchers advocate that this could be a possible solution of the "information paradox" [9]. This paradox, first noticed by Hawking himself [174], appears only after full evaporation of a black hole through Hawking radiation. Quantum mechanically, if the initial state before the formation of the black-hole was a pure state, the unitary evolution of this state must lead to a pure final state. But the final state of the Hawking process, after total evaporation, is a thermal bath in flat space-time [9]. As long as the black-hole is still there, the thermality of the radiation is justified by the presence of a causally disconnected region. The outgoing flux is *entangled* with the degrees of freedom of the interior region over which an exterior observer must trace out. Because of this unknown information the state of the system appears as thermal to this observer (as discussed in Chapter 4). Hence, the inconsistency lies in the thermality of the final state which suggest an irreversible process which is not authorized by the unitarity of quantum mechanics. The back-reaction phenomenon may reveal, at higher-orders, correlations of the outgoing flux not only to the interior matter but also with the degrees of freedom of quantized space-time.

[1] The reasoning here adopted follows closely the results obtained by C. Mora and Y. Castin for a static quasicondensate [89] and generalizes it to a flowing quasicondensate. The present work is indebted to some preliminary notes by A. Fabbri (University of Valencia) and R. Balbinot (University of Bologna) on the previous paper by C. Mora and Y. Castin.

[2] The back-reaction source term is hard to compute in the gravitational framework. For an account of the gravitational backreaction phenonmenon and for a derivation of a 2D, i.e. (1+1), backreaction see [82].

According to the previous remarks, it is then sound to consider, for future inquiries, the analog hydrodynamic setups as valuable systems to test possible models beyond classical general relativity and suggest how quantum gravity effects could be incorporated in a gravitational framework [9]. The back-reaction phenomenon we consider in this work may be regarded then as part of such an attempt.

5.2 . THE BACK-REACTION EQUATIONS

In this section we derive the back-reaction equations by expanding, in the Gross-Pitaevskii equation, the field operator $\hat{\Psi}(\mathbf{x},t)$ to second order in the density-phase representation (5.6).

5.2.1 . From the Lagrangian to the Gross-Pitaevskii quantum field equation

Let us first define an hermitian Lagrangian density $\mathscr{L}(\hat{\Psi},\partial_\mu\hat{\Psi},\hat{\Psi}^\dagger,\partial_\mu\hat{\Psi}^\dagger)$ with $\mu = t,\mathbf{x}$ and $\mathbf{x} = (x,y,z)^T$ for a non-hermitian bosonic field operator $\hat{\Psi}(t,\mathbf{x})$ as

$$\mathscr{L} = \frac{i\hbar}{2}\left(\hat{\Psi}^\dagger\partial_t\hat{\Psi} - (\partial_t\hat{\Psi}^\dagger)\hat{\Psi}\right) - \frac{\hbar^2}{2m}(\nabla\hat{\Psi}^\dagger).(\nabla\hat{\Psi}) - V\hat{\Psi}^\dagger\hat{\Psi} - \frac{g}{2}\hat{\Psi}^\dagger\hat{\Psi}^\dagger\hat{\Psi}\hat{\Psi} \tag{5.1}$$

with V an external potential and g a repulsion coefficient that can be both taken as functions of t and $\mathbf{x}$ in the most general case[3]. The Lagrangian is then defined as

$$L = \int d\mathbf{x}\,\mathscr{L} \tag{5.2}$$

The two equations of motion for the bosonic field operator and its hermitian conjugate are then given by

$$\begin{aligned}\partial_\mu\frac{\delta L}{\delta\partial_\mu\hat{\Psi}} - \frac{\delta L}{\delta\hat{\Psi}} = 0\\ \partial_\mu\frac{\delta L}{\delta\partial_\mu\hat{\Psi}^\dagger} - \frac{\delta L}{\delta\hat{\Psi}^\dagger} = 0\end{aligned} \tag{5.3}$$

with implicit summation on repeated indices, i.e. Einstein's convention [4]. The second relation yields the evolution equation for the field operator

$$i\hbar\partial_t\hat{\Psi} = \left[-\frac{\hbar^2}{2m}\nabla^2 + V + g\hat{\Psi}^\dagger\hat{\Psi}\right]\hat{\Psi} \tag{5.4}$$

and the first one gives its hermitian conjugate[5] :

$$-i\hbar\partial_t\hat{\Psi}^\dagger = \hat{\Psi}^\dagger\left[-\frac{\hbar^2}{2m}\nabla^2 + V + g\hat{\Psi}^\dagger\hat{\Psi}\right] \tag{5.5}$$

Equation (5.4) is the Gross-Pitaevskii field equation.

---

[3] In the previous relation we have dropped the time and spatial dependence of the operator for convenience. We will do so every time this doesn't lead to confusion. For the same reason we have dropped the possible time and spatial dependence of $V(t,\mathbf{x})$ and $g(t,\mathbf{x})$ since them varying or being constant doesn't modify the equations of motion that we will obtain in the following.

[4] We also recall that $\partial_\mu = (\partial_t,\partial_i)^T$ with $i = x,y,z$. Therefore

$$\partial_\mu\frac{\delta}{\delta\partial_\mu\,.} = \partial_t\frac{\delta}{\delta\partial_t\,.} + \sum_i\partial_i\frac{\delta}{\delta\partial_i\,.}$$

Furthermore for any field (operator) $\phi(\mathbf{x},t)$ we recall that

$$\frac{\delta\phi(\mathbf{x},t)}{\delta\phi(\mathbf{x}',t)} = \delta(\mathbf{x}-\mathbf{x}')$$

[5] The equation is written with the spatial derivatives acting on the left.

5.2.2 . Bosonic commutation relations in the density-phase representation

We now define the bosonic field operator in the density-phase representation as

$$\hat{\Psi}(t,\mathbf{x}) = e^{i\left(\theta(t,\mathbf{x})+\delta\hat{\theta}(t,\mathbf{x})\right)}\sqrt{\rho(t,\mathbf{x})+\delta\hat{\rho}(t,\mathbf{x})} \tag{5.6}$$

by introducing a classical contribution, i.e. the phase $\theta(t,\mathbf{x})$ and the density $\rho(t,\mathbf{x})$, and a quantum correction, i.e. the hermitian phase operator $\delta\hat{\theta}(t,\mathbf{x})$ and the hermitian density operator $\delta\hat{\rho}(t,\mathbf{x})$ respectively for phase and density fluctuations. This definition yields

$$\hat{\Psi}^\dagger(t,\mathbf{x})\hat{\Psi}(t,\mathbf{x}) = \rho(t,\mathbf{x}) + \delta\hat{\rho}(t,\mathbf{x}) \tag{5.7}$$

Since the field operator $\hat{\Psi}$ is a bosonic operator it obeys the bosonic equal time commutation relations

$$\begin{aligned}\left[\hat{\Psi}(t,\mathbf{x}),\hat{\Psi}^\dagger(t,\mathbf{x}')\right] &= \delta(\mathbf{x}-\mathbf{x}')\\ \left[\hat{\Psi}(t,\mathbf{x}),\hat{\Psi}(t,\mathbf{x}')\right] &= \left[\hat{\Psi}^\dagger(t,\mathbf{x}),\hat{\Psi}^\dagger(t,\mathbf{x}')\right] = 0\end{aligned} \tag{5.8}$$

If we consider the expansion up to second order in $\delta\hat{\rho}$ and $\delta\hat{\theta}$ of $\hat{\Psi}$ or equivalently the one for $\hat{\Phi} = e^{-i\theta}\hat{\Psi}$ given in relation (5.17), one can check that for $\mathbf{x}=\mathbf{x}'$: the order zero terms give $\hat{\Psi}^\dagger\hat{\Psi} = \rho$ and $\hat{\Psi}\hat{\Psi}^\dagger = \rho$, hence $[\hat{\Psi},\hat{\Psi}^\dagger] = 0$; the first order terms give $\hat{\Psi}^\dagger\hat{\Psi} = \delta\hat{\rho}$ and $\hat{\Psi}\hat{\Psi}^\dagger = \delta\hat{\rho}$, hence $[\hat{\Psi},\hat{\Psi}^\dagger] = 0$; the second order terms give $\hat{\Psi}^\dagger\hat{\Psi} = 0$ and $\hat{\Psi}\hat{\Psi}^\dagger = -i[\delta\hat{\rho},\delta\hat{\theta}]$, hence $[\hat{\Psi},\hat{\Psi}^\dagger] = -i[\delta\hat{\rho},\delta\hat{\theta}]$. It can be checked that the third order terms give $\hat{\Psi}^\dagger\hat{\Psi} = 0$ and $\hat{\Psi}\hat{\Psi}^\dagger = 0$, hence $[\hat{\Psi},\hat{\Psi}^\dagger] = 0$. Therefore one sees that (5.7) is indeed verified up to third order as it should be up to all orders since it is an exact relation.
Furthermore, repeating the very same reasoning for $\mathbf{x}\neq\mathbf{x}'$, one can check that the zeroth and first order terms in the commutators given in (5.8) add up to zero. But in order for the three commutator relations in (5.8) to be verified at second order as they should be, one can prove after some algebra that $\delta\hat{\rho}(t,\mathbf{x})$ and $\delta\hat{\theta}(t,\mathbf{x})$ must obey the following commutation relations :

$$\begin{aligned}\left[\delta\hat{\rho}(t,\mathbf{x}),\delta\hat{\theta}(t,\mathbf{x}')\right] &= i\delta(\mathbf{x}-\mathbf{x}')\\ [\delta\hat{\rho}(t,\mathbf{x}),\delta\hat{\rho}(t,\mathbf{x}')] &= \left[\delta\hat{\theta}(t,\mathbf{x}),\delta\hat{\theta}(t,\mathbf{x}')\right] = 0\end{aligned} \tag{5.9}$$

From the commutation relation given in the first relation of (5.9), it can be inferred that $\delta(\mathbf{x}-\mathbf{x}')$ is here a second order term : we will have to keep this in mind. Finally, it can also be checked that, with the second order relations (5.9) holding, the third order terms in all the three commutators for the field operator given in (5.8) also add up to zero.
In the Lagrangian and in the equations of motion we will need the equal position commutator

$$\left[\hat{\Psi}(t,\mathbf{x}),\hat{\Psi}^\dagger(t,\mathbf{x})\right] = -i\left[\delta\hat{\rho}(t,\mathbf{x}),\delta\hat{\theta}(t,\mathbf{x})\right] = \delta(\mathbf{0}) \tag{5.10}$$

The quantity $\delta(\mathbf{0})$ is ill defined. However, in all the following it will either be involved in expressions in which it regularizes an ultra-violet divergence or as a (diverging) constant contribution to a term of which we take the gradient.

Finally, we also define for any (spatial or temporal) variable α and for any operator $\hat{\varphi}$ the commutator $[\hat{\varphi}(...,\alpha,...),\partial_\alpha\hat{\varphi}(...,\alpha,...)]$ through the coincidence limit

$$[\hat{\varphi}(...,\alpha,...),\partial_\alpha\hat{\varphi}(...,\alpha,...)] = \lim_{\alpha'\to\alpha}\partial_{\alpha'}[\hat{\varphi}(...,\alpha,...),\hat{\varphi}(...,\alpha',...)] \tag{5.11}$$

The same definition applies to the anticommutator $\{\hat{\varphi}(...,\alpha,...),\partial_\alpha\hat{\varphi}(...,\alpha,...)\}$. Therefore, the partial derivatives appearing in the (anti)commutators we will operate with in the Lagrangian and in our equations of motions are to be understood as defined in (5.11). This means that $\delta\hat{\rho}(t,\mathbf{x})$ and $\delta\hat{\theta}(t,\mathbf{x})$ commute *respectively* with their own spatial derivatives $\nabla\delta\hat{\rho}(t,\mathbf{x})$ and $\nabla\delta\hat{\theta}(t,\mathbf{x})$ since the coincidence limit (5.11) applied to the equal time commutation relations in the second line of (5.9) gives zero.

5.2.3 . Second-order expansion of the field operator in the Gross-Pitaevskii equation

Let us start directly from the Gross-Pitaevskii equation (5.4) for the field operator $\hat{\Psi}$, that is to say :

$$i\hbar\partial_t\hat{\Psi} = \left[-\frac{\hbar^2}{2m}\nabla^2 + V + g\hat{\Psi}^\dagger\hat{\Psi}\right]\hat{\Psi} \tag{5.12}$$

Shifting the phase of the field operator we define

$$\hat{\Phi}(t,\mathbf{x}) = e^{-i\theta(t,\mathbf{x})}\hat{\Psi}(t,\mathbf{x}) \tag{5.13}$$

Then, substituting $\hat{\Psi}(t,\mathbf{x})$ with $e^{i\theta(t,\mathbf{x})}\hat{\Phi}(t,\mathbf{x})$ in (5.12) and defininig

$$\begin{aligned}\mathbf{v} &= \frac{\hbar}{m}\nabla\theta \\ \mu &= -\hbar\partial_t\theta\end{aligned} \tag{5.14}$$

with $\mathbf{v}$ the velocity and μ the chemical potential, we can restate equation (5.12) as

$$i\hbar\partial_t\hat{\Phi} = \left[-\frac{\hbar^2}{2m}\nabla^2 - i\hbar\mathbf{v}.\nabla + \frac{m\mathbf{v}^2}{2} - i\hbar\frac{(\nabla.\mathbf{v})}{2} + V + g\hat{\Phi}^\dagger\hat{\Phi} - \mu\right]\hat{\Phi} \tag{5.15}$$

Taking the hermitian conjugate of the Gross-Pitaevskii equation for the field, that is to say equation (5.5), yields the hermitian conjugate of the previous equation[6] :

$$-i\hbar\partial_t\hat{\Phi}^\dagger = \hat{\Phi}^\dagger\left[-\frac{\hbar^2}{2m}\nabla^2 + i\hbar\mathbf{v}.\nabla + \frac{m\mathbf{v}^2}{2} + i\hbar\frac{(\nabla.\mathbf{v})}{2} + V + g\hat{\Phi}^\dagger\hat{\Phi} - \mu\right] \tag{5.16}$$

Now we expand the field operator $\hat{\Phi}$ up to second order :

$$\hat{\Phi} \approx \sqrt{\rho} + \frac{\delta\hat{\rho}}{2\sqrt{\rho}} + i\sqrt{\rho}\delta\hat{\theta} - \frac{\delta\hat{\rho}^2}{8\rho^{3/2}} - \frac{\sqrt{\rho}\delta\hat{\theta}^2}{2} + i\frac{\delta\hat{\theta}\delta\hat{\rho}}{2\sqrt{\rho}} \tag{5.17}$$

Subtracting or adding to equation (5.15) its hermitian conjugate (5.16) one gets two equations. In order to state these equations in a concise way let us define

$$\begin{aligned}\hat{L}_{GP} &= -\frac{\hbar^2}{2m}\nabla^2 + \frac{m\mathbf{v}^2}{2} + V + g\rho - \mu \\ \hat{L}_t &= \partial_t + (\nabla.\mathbf{v}) + \mathbf{v}.\nabla\end{aligned} \tag{5.18}$$

After some algebra, taking all the terms to the left-hand-side of equations (5.15) and (5.16), up to second order the first equation of motion (obtained by adding (5.15) and its hermitian conjugate (5.16)) is given by :

$$\begin{aligned}&-2\hat{L}_{GP}\sqrt{\rho} - 2\sqrt{\rho}\hbar\left(\hat{L}_t - (\nabla.\mathbf{v})\right)\delta\hat{\theta} - \left(\hat{L}_{GP} + 2g\rho\right)\frac{\delta\hat{\rho}}{\sqrt{\rho}} - \frac{\hbar}{\sqrt{\rho}}(\hat{L}_t\rho)\delta\hat{\theta} \\ &-\frac{\hbar}{2\sqrt{\rho}}\hat{L}_t\{\delta\hat{\rho},\delta\hat{\theta}\} + \hat{L}_{GP}\sqrt{\rho}\delta\hat{\theta}^2 + i\left(\hat{L}_{GP} - 2g\rho\right)\frac{[\delta\hat{\rho},\delta\hat{\theta}]}{2\sqrt{\rho}} + \left(\hat{L}_{GP} - 4g\rho\right)\frac{\delta\hat{\rho}^2}{4\rho^{3/2}} \\ &+\frac{\hbar}{2\rho}(\hat{L}_t\rho)\frac{\{\delta\hat{\rho},\delta\hat{\theta}\}}{2\sqrt{\rho}} = 0\end{aligned} \tag{5.19}$$

In the same way, taking all the terms to the left-hand-side of equations (5.15) and (5.16), up to second order the second equation of motion (obtained by subtracting to (5.15) its hermitian conjugate (5.16)) is given, after multiplication by i, by :

$$\begin{aligned}&-\frac{\hbar}{\sqrt{\rho}}\hat{L}_t\rho - \frac{\hbar}{\sqrt{\rho}}\hat{L}_t\delta\hat{\rho} + 2\hat{L}_{GP}\sqrt{\rho}\delta\hat{\theta} + \frac{\hbar}{2\rho}(\hat{L}_t\rho)\frac{\delta\hat{\rho}}{\sqrt{\rho}} \\ &+\hbar\sqrt{\rho}\left(\hat{L}_t - (\nabla.\mathbf{v})\right)\delta\hat{\theta}^2 + \frac{\hbar}{4\rho^{3/2}}\left(\hat{L}_t + (\nabla.\mathbf{v})\right)\delta\hat{\rho}^2 + i\frac{\hbar}{2\sqrt{\rho}}\hat{L}_t[\delta\hat{\rho},\delta\hat{\theta}] + \left(\hat{L}_{GP} + 2g\rho\right)\frac{\{\delta\hat{\rho},\delta\hat{\theta}\}}{2\sqrt{\rho}} \\ &+\frac{\hbar}{2\rho}(\hat{L}_t\rho)\left(\sqrt{\rho}\delta\hat{\theta}^2 - \frac{3\delta\hat{\rho}^2}{4\rho^{3/2}} - i\frac{[\delta\hat{\rho},\delta\hat{\theta}]}{2\sqrt{\rho}}\right) = 0\end{aligned} \tag{5.20}$$

[6] As previously in (5.5), the equation is written with the spatial derivatives acting on the left.

In these two equations, the first terms are the zeroth order terms, the second to the fourth terms are the first order terms and the remaining ones the second order terms. Defining $\rho_0(t,\mathbf{x})$ and $\theta_0(t,\mathbf{x})$ as the solutions of the zeroth order equations and setting

$$\begin{aligned}\hat{L}^{(0)}_{GP} &= -\frac{\hbar^2}{2m}\nabla^2 + \frac{m\mathbf{v_0}^2}{2} + V + g\rho_0 - \mu_0 \\ \hat{L}^{(0)}_{t} &= \partial_t + (\nabla.\mathbf{v_0}) + \mathbf{v_0}.\nabla\end{aligned} \tag{5.21}$$

one obtains

$$\hat{L}^{(0)}_{GP}\sqrt{\rho_0} = 0 \tag{5.22}$$

$$\hat{L}^{(0)}_{t}\rho_0 = 0 \tag{5.23}$$

where $\hat{L}^{(0)}_{GP}$ and $\hat{L}^{(0)}_{t}$ mean simply that in the definition (5.18) of L_{GP} and L_t, we have set $\rho(t,\mathbf{x})$ to $\rho_0(t,\mathbf{x})$ and $\mathbf{v}(t,\mathbf{x})$ to $\mathbf{v}_0(t,\mathbf{x})$ with $\theta(t,\mathbf{x})$ set to $\theta_0(t,\mathbf{x})$ in definitions (5.14). The first equation is just the *Gross-Pitaevskii equation* and the second one just the *continuity equation*. With the zeroth order holding, i.e. with $\rho(t,\mathbf{x}) \to \rho_0(t,\mathbf{x})$ and $\theta(t,\mathbf{x}) \to \theta_0(t,\mathbf{x})$ one can define $\delta\hat{\rho}_0(\mathbf{x},t)$ and $\delta\hat{\theta}_0(\mathbf{x},t)$ as being the solutions of the first order equations

$$\hbar\left(\hat{L}^{(0)}_{t} - (\nabla.\mathbf{v}_0)\right)\delta\hat{\theta}_0 = -\frac{1}{2\sqrt{\rho_0}}\left(\hat{L}^{(0)}_{GP} + 2g\rho_0\right)\frac{\delta\hat{\rho}_0}{\sqrt{\rho_0}} \tag{5.24}$$

$$\hbar\hat{L}^{(0)}_{t}\delta\hat{\rho}_0 = 2\sqrt{\rho_0}\hat{L}^{(0)}_{GP}\sqrt{\rho_0}\delta\hat{\theta}_0 \tag{5.25}$$

These two equations are just the (first order) Bogoliubov-de Gennes equations in the density-phase representation. Even if $\delta\hat{\rho}_0(\mathbf{x},t)$ and $\delta\hat{\theta}_0(\mathbf{x},t)$ are first order terms the lower index refers to the fact that they are determined by equations parametrized with the zeroth order terms $\rho_0(t,\mathbf{x})$ and $\theta_0(t,\mathbf{x})$. Let us know understand how equations (5.19) and (5.20) can be turned into back-reaction equations and explain how the presence of second order terms is crucial to the back-reaction dynamics.

5.2.4 . The two Back-Reaction equations

The back-reaction problematics can be summed up in these terms : how do the quantum fluctuations, generated by the presence of an acoustic horizon in the condensate, act (or more precisely *back-react*) upon the configuration of the condensate that has generated them ?
In order to obtain the back-reaction equations from equations (5.19) and (5.20), one expands in these equations $\rho(\mathbf{x},t)$ and $\theta(\mathbf{x},t)$ respectively as

$$\begin{aligned}\rho(\mathbf{x},t) &\to \rho_0(\mathbf{x},t) + \rho_{BR}(\mathbf{x},t) \\ \theta(\mathbf{x},t) &\to \theta_0(\mathbf{x},t) + \theta_{BR}(\mathbf{x},t)\end{aligned} \tag{5.26}$$

with $\rho_0(\mathbf{x},t)$ and $\theta_0(\mathbf{x},t)$ solutions of the zeroth order equations, i.e. of the Gross-Pitaevskii equation (5.22) and the continuity equation (5.23). This implies expanding $\hat{L}_{GP}$ and $\hat{L}_t$ given in (5.18)[7] as

$$\begin{aligned}\hat{L}_{GP} &= \hat{L}^{(0)}_{GP} + m\mathbf{v}_0.\mathbf{v}_{BR} + g\rho_{BR} + \hbar\partial_t\theta_{BR} \\ \hat{L}_{t} &= \hat{L}^{(0)}_{t} + (\nabla.\mathbf{v}_{BR}) + \mathbf{v}_{BR}.\nabla\end{aligned} \tag{5.27}$$

The terms $\rho_{BR}(\mathbf{x},t)$ and $\theta_{BR}(\mathbf{x},t)$ are small fluctuations terms (of second order as we will see) that encode the back-reaction dynamics. More precisely, $\rho_{BR}(\mathbf{x},t)$ and $\theta_{BR}(\mathbf{x},t)$ are to be considered as average fluctuations, respectively in the density and phase of the condensate, generated by the quantum fluctuations arising due to the presence of the acoustic horizon. Furthermore, in order to turn (5.19) and (5.20) into back-reaction equations, the quantum fluctuations in the density $\delta\hat{\rho}(\mathbf{x},t)$ and in the phase $\delta\hat{\theta}(\mathbf{x},t)$ must be defined as determined as first order solutions of the Bogoliubov-de Gennes equations

[7] Definition (5.14) must not be forgotten.

parametrized by the zeroth order terms $\rho_0(\mathbf{x},t)$ and $\theta_0(\mathbf{x},t)$, as it has just been described at the end of section (5.2.3). Therefore all the $\delta\hat{\rho}(\mathbf{x},t)$ and $\delta\hat{\theta}(\mathbf{x},t)$ appearing in equations (5.19) and (5.20) will be denoted respectively as $\delta\hat{\rho}_0(\mathbf{x},t)$ and $\delta\hat{\theta}_0(\mathbf{x},t)$, keeping in mind that they are first order terms, the lower index referring at them being solutions of first order equations parametrized by $\rho_0(\mathbf{x},t)$ and $\theta_0(\mathbf{x},t)$. The back reaction equations are then given by averaging equations (5.19) and (5.20) over the system state. This amounts to adding or subtracting the two *averaged* equations of motion (5.3) for the bosonic operator and its hermitian conjugate, that is to say to take the average of equations (5.16) + (5.15) and (5.16) − (5.15) after performing the second order expansion (5.17) of the field $\hat{\Phi}$ defined in (5.13), i.e.

$$\begin{aligned}\left\langle \partial_\mu \frac{\delta L}{\delta \partial_\mu \hat{\Psi}^\dagger} - \frac{\delta L}{\delta \hat{\Psi}^\dagger} \right\rangle + \left\langle \partial_\mu \frac{\delta L}{\delta \partial_\mu \hat{\Psi}} - \frac{\delta L}{\delta \hat{\Psi}} \right\rangle = 0 \\ \left\langle \partial_\mu \frac{\delta L}{\delta \partial_\mu \hat{\Psi}^\dagger} - \frac{\delta L}{\delta \hat{\Psi}^\dagger} \right\rangle - \left\langle \partial_\mu \frac{\delta L}{\delta \partial_\mu \hat{\Psi}} - \frac{\delta L}{\delta \hat{\Psi}} \right\rangle = 0\end{aligned} \tag{5.28}$$

When taking the average of equations (5.19) and (5.20) one has $\langle\delta\hat{\rho}_0(t,\mathbf{x})\rangle = \langle\delta\hat{\theta}_0(t,\mathbf{x})\rangle = 0$ and therefore all the first order terms disappear from our equations. This is why one needs second order terms to describe the back-reaction dynamics. Furthermore since $\rho_{BR}(\mathbf{x},t)$ and $\theta_{BR}(\mathbf{x},t)$ are determined by the mean values of second order quantum fluctuation terms they are also second order terms. Since one wants to keep the equations at second order, when multiplying second order (and even first order) quantum fluctuation terms $\rho \to \rho_0 + \rho_{BR}$ and $\theta \to \theta_0 + \theta_{BR}$ must necessarily reduce to ρ_0 and θ_0 respectively.

The details of the computations can be found in Appendix B.1. After some algebra, the *first back-reaction equation* reads

$$\begin{aligned}&\hbar\partial_t\theta_{BR} + m\mathbf{v}_0.\mathbf{v}_{BR} + \frac{\hbar}{2\rho_0}(\partial_t + (\nabla.\mathbf{v}_0) + \mathbf{v}_0.\nabla)Re\langle\delta\hat{\rho}_0\delta\hat{\theta}_0\rangle \\ &+g\rho_0\left(\frac{\rho_{BR}}{\rho_0} + \frac{\langle\delta\hat{\rho}_0^2\rangle}{2\rho_0^2} - \frac{\delta(\mathbf{0})}{2\rho_0}\right) - \frac{\hbar^2}{4m\rho_0}\nabla\left(\rho_0\nabla\left(\frac{\rho_{BR}}{\rho_0} - \left(\frac{\langle\delta\hat{\rho}_0^2\rangle}{4\rho_0^2} + \langle\delta\hat{\theta}_0^2\rangle - \frac{\delta(\mathbf{0})}{2\rho_0}\right)\right)\right) = 0\end{aligned} \tag{5.29}$$

where we have written $\langle\{\delta\hat{\rho}_0, \delta\hat{\theta}_0\}\rangle = 2Re\langle\delta\hat{\rho}_0\delta\hat{\theta}_0\rangle$ and $\langle[\delta\hat{\rho}_0, \delta\hat{\theta}_0]\rangle = \langle i\delta(\mathbf{0})\rangle = i\delta(\mathbf{0})$. Dividing this equation by m, one can introduce the coefficients $c(t,\mathbf{x})\xi(t,\mathbf{x}) = \hbar/m$ and $c^2(t,\mathbf{x}) = g(t,\mathbf{x})\rho_0(t,\mathbf{x})/m$ with c the velocity of sound in the fluid and ξ the healing length. On the other hand, the *second back-reaction equation* reads

$$\partial_t\rho_{BR} + \nabla\Big(\rho_{BR}\mathbf{v}_0 + \rho_0\mathbf{v}_{BR} + Re\langle\delta\hat{\rho}_0\delta\hat{\mathbf{v}}_0\rangle\Big) = 0 \tag{5.30}$$

where we have written $\langle\{\delta\hat{\rho}_0, \nabla\delta\hat{\theta}_0\}\rangle = 2Re\langle\delta\hat{\rho}_0\nabla\delta\hat{\theta}_0\rangle$ and $\delta\hat{\mathbf{v}}_0 = (\hbar/m)\nabla\delta\hat{\theta}_0$. These two equations correspond to the two equations (B.14) and (B.15) obtained at the end of Appendix B.1. The expression of the source terms is given in Appendix (B.2).

5.3 . STATIONARY 1D BACK-REACTION EQUATIONS

This section presents the stationary version of the back-reaction equations (5.29) and (5.30). The idea is to look, as often done in the Gross-Pitaevskii approach, for a stationary flow solution in the presence of a sonic horizon. The results presented in this section are preliminary in the sense that they do not provide a full solution of the exact equations (5.41) obtained below. We only consider the stationary modifications of the asymptotic flows (away from the horizon). Several tracks are investigated and discussed, corresponding in particular to different possible choices of boundary conditions.

5.3.1 . Stationary equations

We consider (see Chapter 3) a stationary solution of the Gross-Pitaevskii equation for a 1-D quasi-consensate. In this configuration, it is sound to look for solutions of the back-reaction equations that be

stationary as well, since back-reaction is expected to be there. This approach appears to be a better one with respect to one where the time evolution of the solutions whould be "switched on" at some arbitrary time t_0.

In order to find such stationary solutions let us first remark that all the source terms, i.e. the quantum average terms, are time-independent when a stationary zeroth order solution to the Gross-Pitaevskii equation is considered. Secondly, it can be shown, just by applying (B.19), that in the first back-reaction equation

$$\frac{\langle\delta\hat{\rho}_0^2\rangle}{4\rho_0^2}+\langle\delta\hat{\theta}_0^2\rangle-\frac{\delta(0)}{2\rho_0}=\frac{1}{2}\left[\frac{\langle\delta\hat{\rho}_0^2\rangle}{2\rho_0^2}-\frac{\delta(0)}{2\rho_0}\right]+\left[\langle\delta\hat{\theta}_0^2\rangle-\frac{\delta(0)}{4\rho_0}\right]=\frac{\langle\delta\hat{\Psi}^\dagger\delta\hat{\Psi}\rangle}{\rho_0} \tag{5.31}$$

with $\langle\delta\hat{\Psi}^\dagger(x,t)\delta\hat{\Psi}(x,t)\rangle$ the depletion of the condensate. Then, defining

$$\begin{aligned}\frac{g^{(2)}}{2} &= \frac{\langle\delta\hat{\rho}_0^2\rangle}{2\rho_0^2}-\frac{\delta(0)}{2\rho_0}\\ C_\infty &= \langle\delta\hat{\theta}_0^2\rangle-\frac{\delta(0)}{4\rho_0}\end{aligned} \tag{5.32}$$

with[8]

$$g^{(2)}(x)=\frac{\langle:\hat{n}(x,t)\hat{n}(x,t):\rangle-\langle\hat{n}(x,t)\rangle\langle\hat{n}(x,t)\rangle}{\rho_0^2(x)} \tag{5.33}$$

it can be shown [175] that C_∞ is a diverging term in ω but that this divergence in energy is x-independent. Hence

$$\partial_x C_\infty=0 \tag{5.34}$$

We then look for solutions of the 1-D back-reaction equations (5.29) and (5.30) with

$$\partial_t\rho_{BR}=0 \qquad \partial_t v_{BR}=0 \tag{5.35}$$

Recalling from (5.14) the definition of the chemical potential

$$\mu=-\hbar\partial_t\theta \qquad \Rightarrow \qquad \mu=\mu_0+\mu_{BR}=-\hbar\partial_t\theta_0-\hbar\partial_t\theta_{BR} \tag{5.36}$$

and of the velocity

$$v=\frac{\hbar}{m}\partial_x\theta \qquad \Rightarrow \qquad v=v_0+v_{BR}=\frac{\hbar}{m}\partial_x\theta_0+\frac{\hbar}{m}\partial_x\theta_{BR} \tag{5.37}$$

it can be seen from the two previous relations (5.36) and (5.37) that

$$\partial_x\mu=-m\partial_t v \tag{5.38}$$

Hence

$$\partial_x\mu_{BR}=-m\partial_t v_{BR} \tag{5.39}$$

Therefore if we are looking for a stationary configuration where v_{BR} is time-independent, μ_{BR} must be x-independent, i.e.

$$\partial_x\mu_{BR}\underset{\text{stat.}}{=}0 \tag{5.40}$$

With all the previous considerations in mind, the two 1-D back-reaction equations (5.29) and (5.30) reduce

[8] The term $:\ .\ :$ denotes normal ordering and $\hat{n}(x,t)=\hat{\Psi}^\dagger(x,t)\hat{\Psi}(x,t)$. Clearly $g^{(2)}(x)$ is the two-point density-correlation function $G^{(2)}(x,x')=\langle:\hat{n}(x,t)\hat{n}(x',t):\rangle-\langle\hat{n}(x,t)\rangle\langle\hat{n}(x',t)\rangle$ computed in $x=x'$ and divided by $\rho_0^2(x)$.

to the stationary relations

$$\begin{aligned}\mu_{BR} &= mv_0v_{BR} + g\rho_{BR} - \frac{\hbar^2}{4m\rho_0}\partial_x^2\rho_{BR} \\ &+ \frac{\hbar^2(\partial_x\rho_0)}{4m\rho_0^2}\partial_x\rho_{BR} + \frac{\hbar^2(\partial_x^2\rho_0)}{4m\rho_0^2}\rho_{BR} - \frac{\hbar^2(\partial_x\rho_0)^2}{4m\rho_0^3}\rho_{BR} \\ &+ \frac{\hbar(\partial_x v_0)}{2\rho_0}Re\langle\delta\hat\rho_0\delta\hat\theta_0\rangle + \frac{\hbar v_0}{2\rho_0}\partial_x Re\langle\delta\hat\rho_0\delta\hat\theta_0\rangle + g\rho_0\frac{g^{(2)}}{2} + \frac{\hbar^2(\partial_x\rho_0)}{8m\rho_0}\partial_x\frac{g^{(2)}}{2} + \frac{\hbar^2}{8m}\partial_x^2\frac{g^{(2)}}{2} \\ J_{BR} &= \rho_{BR}v_0 + \rho_0 v_{BR} + Re\langle\delta\hat\rho_0\delta\hat v_0\rangle\end{aligned} \tag{5.41}$$

with μ_{BR} and J_{BR} being the second-order corrections to the chemical potential and to the current respectively : they are here both constant in space and time. The second equation of (5.41) can be inverted to obtain a definition of v_{BR}, i.e.

$$\rho_0 v_{BR} = J_{BR} - \rho_{BR}v_0 - Re\langle\delta\hat\rho_0\delta\hat v_0\rangle \tag{5.42}$$

which can be used in the first equation of (5.41) in order to obtain an equation for ρ_{BR}, i.e.

$$\left(g\rho_0 - mv_0^2\right)\rho_{BR} - \frac{\hbar^2}{4m}\partial_x^2\rho_{BR} + \frac{\hbar^2(\partial_x)}{4m\rho_0^2}\partial_x\rho_{BR} + \frac{\hbar^2(\partial_x^2\rho_0)}{4m\rho_0}\rho_{BR} - \frac{\hbar^2(\partial_x\rho_0)^2}{4m\rho_0^2}\rho_{BR} = S(x) \tag{5.43}$$

with $S(x)$ the source term given by

$$\begin{aligned}S(x) =& \rho_0\mu_{BR} - mv_0J_{BR} + mv_0Re\langle\delta\hat\rho_0\delta\hat v_0\rangle \\ &- \frac{\hbar(\partial_x v_0)}{2}Re\langle\delta\hat\rho_0\delta\hat\theta_0\rangle - \frac{\hbar v_0}{2}\partial_x Re\langle\delta\hat\rho_0\delta\hat\theta_0\rangle - g\rho_0^2\frac{g^{(2)}}{2} - \frac{\hbar^2(\partial_x\rho_0)}{8m}\partial_x\frac{g^{(2)}}{2} - \frac{\hbar^2}{8m}\rho_0\partial_x^2\frac{g^{(2)}}{2}\end{aligned} \tag{5.44}$$

5.3.2 . Homogeneous and stationary condensate

If one takes $v_0(x) = 0$ and $\rho_0(x) = c^{\rm st}$, then $Re\langle\delta\hat\rho_0\delta\hat v_0\rangle = 0$ and $g^{(2)} = -2/(\pi\rho_0\xi_0)$ where $\hbar^2/(m\xi_0^2) = g\rho_0$. In this case the solutions of the back reaction equations (5.41) are, $v_{BR} = 0 = J_{BR}$ and

$$\rho_{BR} = \frac{\mu_{BR}}{g} + \frac{1}{\pi\xi_0} \tag{5.45}$$

One can choose either to fix $\rho_{BR} = 0$ or $\mu_{BR} = 0$. At the order of approximation we consider, this yields the same expression for the speed of sound. Let's first impose $\rho_{BR} = 0$. Then (5.45) yields $\mu = \mu_0 + \mu_{BR} = g\rho_0 - g/(\pi\xi_0)$. Since now $\rho_0 = \rho$, one obtains

$$\mu = g\rho - \frac{g\sqrt{gm}}{\pi\hbar}\sqrt{\rho} \tag{5.46}$$

From the thermodynamic relation $mc^2(T=0) = \rho(\partial\mu(T=0)/\partial\rho)$ one gets

$$c = \frac{1}{m}\sqrt{g\rho - \frac{g}{2\pi\xi}} \tag{5.47}$$

Formula (5.47) defines the expression of the speed of sound in terms of the density. It has been derived imposing $\rho_{BR} = 0$, but it can be reasonably taken to be valid for any ρ, with $\xi = \xi_0 + \xi_{BR}$ taken to be ξ_0 for an expression linear in the back-reaction terms[9], since the same expression is obtained by taking $\mu_{BR} = 0$[10]. Indeed, when we will use (5.47) below, the total density will be of the form $\rho = \rho_0 + \rho_{BR}$ with $\rho_{BR} \ll \rho_0$ and the term $g/(2\pi\xi_0)$ will also be small. It will thus be legitimate to make in (5.47) the approximation

$$c \simeq \frac{1}{m}\sqrt{g(\rho_0+\rho_{BR}) - g/(2\pi\xi_0)} \simeq c_0\left[1 + \frac{\rho_{BR}}{2\rho_0} - \frac{1}{4\pi\rho_0\xi_0}\right] \tag{5.48}$$

[9] The term $1/\pi\xi_0$ is already a back-reaction term.

[10] Taking $\mu_{BR} = 0$ implies $\mu = \mu_0 = g\rho_0 = g(\rho - \rho_{BR}) = g\rho - g\sqrt{m\mu}/(\pi\hbar)$ since now $\rho_{BR} = 1/(\pi\xi_0) = \sqrt{m\mu}/(\pi\hbar)$. One has therefore

$$\left[1 + \frac{g\sqrt{m}}{2\pi\hbar\sqrt{\mu}}\right]d\mu = gd\rho$$

Since $g\sqrt{m}/(2\pi\hbar\sqrt{\mu}) = 1/(2\pi\rho_0\xi_0)$ one then obtains, for an expression linear in the back-reaction terms, exactly (5.47).

5.3.3 . Asymptotic stationary 1-D solutions to the back-reaction equations

In the two asymptotic upstream ($x \to -\infty$) and downstream ($x \to +\infty$) regions, i.e. $\alpha = u$ or $\alpha = d$ respectively, setting $A_\alpha = A(x \to \pm\infty)$ for any quantity A, the stationary equations (5.43) and (5.42) for ρ_{BR} and v_{BR} become

$$\begin{aligned} \frac{4m^2}{\hbar^2}\left(c_\alpha^2 - v_\alpha^2\right)\rho_{BR} - \partial_x^2\rho_{BR} &= \frac{4m}{\hbar^2}S_\alpha \\ n_\alpha v_{BR} &= J_{BR} - \rho_{BR}v_\alpha - Re\langle\delta\hat{\rho}_0\delta\hat{v}_0\rangle_\alpha \end{aligned} \tag{5.49}$$

with the source term being the constant

$$S_\alpha = n_\alpha\mu_{BR} - mv_\alpha J_{BR} + mv_\alpha Re\langle\delta\hat{\rho}_0\delta\hat{v}_0\rangle_\alpha - g_\alpha n_\alpha^2\frac{g_\alpha^{(2)}}{2} \tag{5.50}$$

We recall that μ_{BR} and J_{BR} are constant in a stationary configuration. Then, defining

$$\kappa_\alpha = \frac{2m}{\hbar}|c_\alpha^2 - v_\alpha^2|^{1/2} \tag{5.51}$$

and recalling that $c_u > v_u$ and $c_d < v_d$, one obtains for the first equation in (5.49) :

$$\begin{aligned} \kappa_u^2\,\rho_{BR} - \partial_x^2\rho_{BR} &= \frac{4m}{\hbar^2}S_u \qquad \text{if } x \to -\infty \\ -\kappa_d^2\,\rho_{BR} - \partial_x^2\rho_{BR} &= \frac{4m}{\hbar^2}S_d \quad \text{if } x \to +\infty \end{aligned} \tag{5.52}$$

The previous equations give straightforwardly the two solutions

$$\rho_{BR} = \begin{cases} \dfrac{4m}{\hbar^2\kappa_u^2}S_u + \mathcal{A}_u e^{\kappa_u x} & \text{if} \quad x \to -\infty \\ -\dfrac{4m}{\hbar^2\kappa_d^2}S_d + \mathcal{A}_d\sin(k_d x + \delta) & \text{if} \quad x \to +\infty \end{cases} \tag{5.53}$$

5.3.4 . Constant asymptotic solutions

In all the following, for simplicity we ignore the x dependence in the above formula and assume that in both asymptotic regions

$$\rho_{BR}(x) \to \rho_{BR}^\alpha = \frac{S_\alpha}{m(c_\alpha^2 - v_\alpha^2)} \tag{5.54}$$

This is clearly an uncontrolled assumption, but it is also clear that it will give sensible orders of magnitude.

The following procedure then naturally arises: one chooses for instance to impose $\rho_{BR}^u = 0 = v_{BR}^u$[11], then the second of Eqs. (5.49) fixes J_{BR} and (5.54) fixes $S_u = 0$ and thus μ_{BR} (through Eq. (5.50)). Explicitly:

$$J_{BR} = \mathrm{Re}\langle\delta\hat{\rho}_0\delta\hat{v}_0\rangle_u \qquad \mu_{BR} = mc_u^2\frac{g_u^{(2)}}{2} \tag{5.55}$$

Equation (5.54) for $\alpha = d$ and Eq. (5.50) then yield

$$(c_d^2 - v_d^2)\rho_{BR}^d = \frac{S_d}{m} = v_d\left(\mathrm{Re}\langle\delta\hat{\rho}_0\delta\hat{v}_0\rangle_d - \mathrm{Re}\langle\delta\hat{\rho}_0\delta\hat{v}_0\rangle_u\right) + \tfrac{1}{2}n_d(c_u^2 g_u^{(2)} - c_d^2 g_d^{(2)}), \tag{5.56}$$

and the second of Eqs. (5.49) yields

$$\frac{v_{BR}^d}{v_d} = \frac{\mathrm{Re}\langle\delta\hat{\rho}_0\delta\hat{v}_0\rangle_u}{n_u v_u} - \frac{\mathrm{Re}\langle\delta\hat{\rho}_0\delta\hat{v}_0\rangle_d}{n_d v_d} - \frac{\rho_{BR}^d}{n_d} \tag{5.57}$$

[11] One could equally well impose $\rho_{BR}^d = 0 = v_{BR}^d$, and indeed the results for this choice of boundary condition will also be presented.

Expressions (5.56) and (5.57) unambiguously determine ρ^d_{BR} and v^d_{BR}. The last quantities we need to evaluate are the new asymptotic velocities of sound. Eq. (5.48) yields here[12]

$$\frac{c^\alpha_{BR}}{c_\alpha} = \frac{\rho^\alpha_{BR}}{2n_\alpha} - \frac{1}{4\pi n_\alpha \xi_\alpha} \tag{5.58}$$

In the far upstream region ($\alpha = u$), this quantity should be evaluated with $\rho^u_{BR} = 0$. In the far downstream region instead, one should use the value of ρ^d_{BR} given by expression (5.56). Eventually the new Mach number are

$$\frac{v_\alpha + v^\alpha_{BR}}{c_\alpha + c^\alpha_{BR}} = m_\alpha + m^\alpha_{BR} \quad \text{with} \quad m^\alpha_{BR} = m_\alpha \left(\frac{v^\alpha_{BR}}{v_\alpha} - \frac{c^\alpha_{BR}}{c_\alpha} \right) \tag{5.59}$$

For instance, our prescription ($\rho^u_{BR} = 0 = v^u_{BR}$) yields $m^u_{BR}/m_u = 1/4\pi n_u \xi_u$. Fig. 5.1 presents the results of the quantities m^α_{BR}/m_α for waterfall configurations with m_u ranging from 0 to 1. Instead of imposing $\rho^u_{BR} = 0 = v^u_{BR}$ one may impose equivalent conditions downstream: $\rho^d_{BR} = 0 = v^d_{BR}$. The corresponding results are also displayed in Fig. 5.1.

5.3.5 . Practical implementation

To evaluate ρ^d_{BR} and v^d_{BR} at best it is appropriate to introduce dimensionless variables by writing:

$$g^{(2)}_\alpha = \frac{1}{n_\alpha \xi_\alpha} \left(-\frac{2}{\pi} + \mathcal{G}^{(H)}_\alpha \right) \qquad \frac{\mathrm{Re}\langle \delta\hat{\rho}_0 \delta\hat{v}_0 \rangle_\alpha}{n_\alpha v_\alpha} = \frac{1}{n_\alpha \xi_\alpha} \mathcal{J}^{(H)}_\alpha . \tag{5.60}$$

The dimensionless quantities $\mathcal{G}^{(H)}_\alpha$ and $\mathcal{J}^{(H)}_\alpha$ originate from Hawking radiation. Their explicit expressions are

$$\mathcal{G}^{(H)}_u = \int_0^{\Omega_u} \frac{\mathrm{d}\varepsilon_u}{\pi} |S_{02}|^2 N(-Q_{0|\mathrm{out}}, m_u), \tag{5.61}$$

$$\mathcal{G}^{(H)}_d = \int_0^{\Omega_d} \frac{\mathrm{d}\varepsilon_d}{\pi} \Big\{ |S_{12}|^2 N(Q_{1|\mathrm{out}}, -m_d) - (|S_{22}|^2 - 1) N(Q_{2|\mathrm{out}}, m_d) \Big\}, \tag{5.62}$$

where the Q_ℓ are the dimensionless wave vectors, $\varepsilon_\alpha = \hbar\omega/(mc^2_\alpha)$, $\Omega_\alpha = \hbar\Omega_{\max}/(mc^2_\alpha)$ and

$$N(Q, m_\alpha) = \frac{Q/2}{1 + Q^2/2 - m_\alpha \sqrt{1 + Q^2/4}}. \tag{5.63}$$

As for the currents:

$$\mathcal{J}^{(H)}_u = \frac{1}{m_u} \int_0^{\Omega_u} \frac{\mathrm{d}\varepsilon_u}{\pi} |S_{02}|^2 T(-Q_{0|\mathrm{out}}, m_u), \tag{5.64}$$

$$\mathcal{J}^{(H)}_d = \frac{1}{m_d} \int_0^{\Omega_d} \frac{\mathrm{d}\varepsilon_d}{\pi} \Big\{ |S_{12}|^2 T(Q_{1|\mathrm{out}}, -m_d) + (|S_{22}|^2 - 1) T(Q_{2|\mathrm{out}}, m_d) \Big\}, \tag{5.65}$$

where

$$T(Q, m_\alpha) = \frac{Q/2}{\frac{1+Q^2/2}{\sqrt{1+Q^2/4}} - m_\alpha}. \tag{5.66}$$

Eqs. (5.56) and (5.57) can be adimensionalized by the use of the quantities $\mathcal{G}^{(H)}_\alpha$ and $\mathcal{J}^{(H)}_\alpha$ and then read

$$(1 - m_d^2)\, n_d \xi_d \frac{\rho^d_{BR}}{\rho_d} = m_d^2 \left(\mathcal{J}^{(H)}_d - \frac{c_d}{c_u} \mathcal{J}^{(H)}_u \right) + \frac{1}{2} \frac{c_u}{c_d} \left(-\frac{2}{\pi} + \mathcal{G}^{(H)}_u \right) + \frac{1}{2} \left(\frac{2}{\pi} - \mathcal{G}^{(H)}_u \right), \tag{5.67}$$

(where $m_d = v_d/c_d$ is the asymptotic downstream Mach number) and

$$n_d \xi_d \frac{v^d_{BR}}{v_d} = \frac{c_d}{c_u} \mathcal{J}^{(H)}_u - \mathcal{J}^{(H)}_d - n_d \xi_d \frac{\rho^d_{BR}}{n_d}. \tag{5.68}$$

[12] In order to comply with the convention used everywhere in the present manuscript we denote as n_α the asymptotic value of $\rho_0(x)$, with $\alpha = u$ or d when $x \to \pm\infty$.

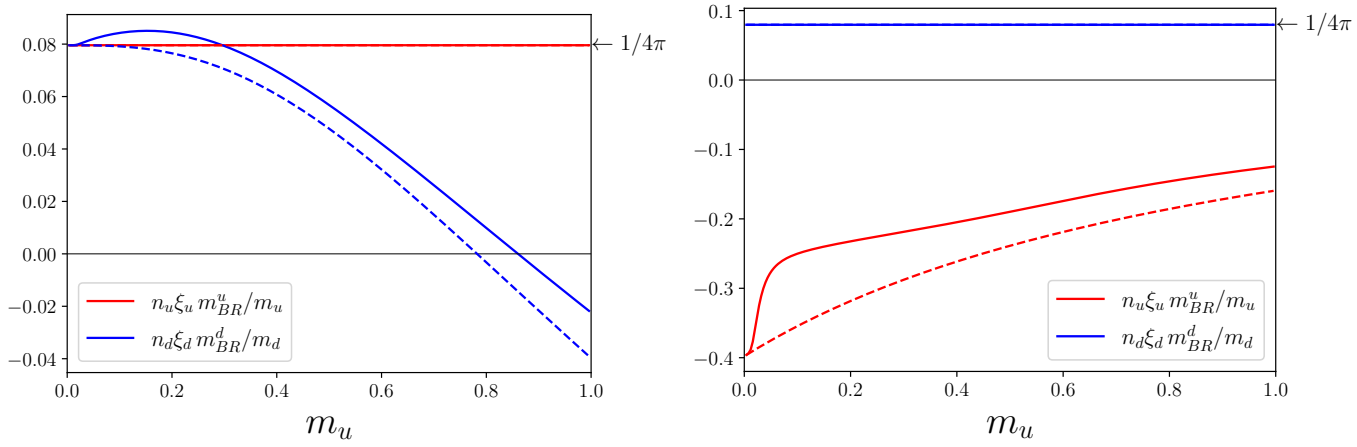

Figure 5.1: Modification of the asymptotic Mach numbers induced by the back-reaction effects. We consider here all possible waterfall configurations, a given configuration being specified by a given value of m_u, see Sec. 3.1.4. As explained in the text we plot the quantities $n_\alpha\xi_\alpha m^\alpha_{BR}/m_\alpha$ for $\alpha = u$ (blue solid line) and $\alpha = d$ (red solid line). The dashed line is obtained by removing the Hawking contribution and only accounts for the departure of the expression of the sound velocity from the Gross-Pitaevskii result (3.7). The left plot displays the results corresponding to the boundary conditions $\rho^u_{BR} = 0 = v^u_{BR}$, the right one to the boundary conditions $\rho^d_{BR} = 0 = v^d_{BR}$.

Expressions (5.68) and (5.67) are then inserted in (5.58) and (5.59) to compute the modification of the asymptotic Mach numbers induced by the back-reaction effects.

A remark is in order here. In the above expressions (5.68) and (5.67) one needs to use an experimental input : the value of the experimental parameter $n_u\xi_u$. Once this parameter is known, the equivalent downstream quantity $n_d\xi_d = n_u\xi_u c_d/c_u$ is unambiguously fixed by the value of the ratio c_d/c_u corresponding to the configuration we consider (flat profile, waterfall or delta peak). A realistic choice is $n_u\xi_u = 70$, which corresponds to the value in Steinhauer's experiment [34]. In order to present results relevant to possibly different experimental setups we plot in Fig. 5.1 the quantities $n_\alpha\xi_\alpha m^\alpha_{BR}/m_\alpha$ for $\alpha = u$ and $\alpha = d$.

In Figure 5.1 we present two plots, corresponding to two different boundary conditions. The left plot is obtained by imposing $\rho^u_{BR} = 0 = v^u_{BR}$, meaning that the density and velocity of the upstream flow are considered as fixed by the experimental setup. Back reaction effects then modify the downstream profile and velocity compared to the values predicted by the (zeroth order) Gross-Pitaevskii equation. This, in turn, induces a modification of the downstream Mach number by an amount m^d_{BR}, represented with a blue solid line in the figure. Note that the upstream Mach number is also modified in this case. Not by the back reaction effect, but by the fact that the sound velocity is not exactly given by the Gross-Pitaevskii formula (3.7), but rather by expression (5.47). In this case one simply gets $m^u_{BR}/m_u = 1/(4\pi n_u\xi_u)$ which corresponds to the horizontal red line in the left plot of Fig. 5.1. In order to separate, in the modification of the downstream Mach number, what is due to the Hawking effect from what is due to the modification of the speed of sound with respect to the Gross-Pitaevskii result (3.7), we plot as a dashed blue line, the results obtained if all the Hawking terms are set equal to zero: $\mathcal{G}^{(H)}_\alpha = 0 = \mathcal{J}^{(H)}_\alpha$ for $\alpha = u$ and d in Eqs. (5.67) and (5.68).

The right plot in Figure 5.1 displays the results corresponding to boundary conditions where the downstream density and velocity are considered as fixed: $\rho^d_{BR} = 0 = v^d_{BR}$. The choice of a given set of boundary conditions (fixed upstream asymptotic flow as in the left plot or fixed downstream asymptotic flow as in the right plot) depends on the experimental setup. It appears that Steinhauer's experiment corresponds to a given asymptotic downstream flow, i.e., to the right plot in Figure 5.1. In this plot the back reaction effects appear more significant than in the left one. As demonstrated by the order of magnitude fixed by the results obtained by artificially killing the Hawking radiation (dashed lines) this effect is simply associated to the dependence of the asymptotic flow on the conditions imposed in the other side (which is larger in the right plot than in the left one). In the experimentally relevant situation of the right plot, the back-reaction effect appears to decrease the difference between the upstream and

downstream Mach numbers with respect to the value it would have according to the Gross-Pitaevskii approach. We expect that this will be associated to a decrease intensity of the Hawking signal, indeed corresponding to a tendency of the system to relax, the back-reaction profile being asymptotically closer to relaxation than the Gross-Pitaevskii one. However, the right plot displays configurations with an opposite tendency. It could be interesting to propose experimental setups corresponding to this type of boundary condition and to check if, indeed, instead of relaxing, the system would initially move to a more out-of-equilibrium configuration. However, it is important to note that the intensity of the Hawking signal is not really determined by the difference between the asymptotic downstream and upstream flows, contrarely to what is naively assumed in the few above lines. The intensity of the Hawking signal is determined by the surface gravity. A track more secure than the simple analysis of the asymptotic flows just presented would be to solve the stationary equations (5.41) not only in the asymptotic regions, but in the *whole space*. This would enable to evaluate the shift in position of the horizon with respect to the Gross-Pitaevskii prediction and, from Eqs. (2.105) and (2.106) , to determine the associated new (analog) surface gravity and Hawking temperature.

6 - TOPOLOGICAL CONSTRAINTS IN 2-D QUANTUM TURBULENCE

In this chapter, I will present some preliminary results of a combined experimental and theoretical investigation of the kinetics of vortices in two-dimensional, compressible quantum turbulence[1]. We follow the temporal evolution of a quantum fluid of exciton–polaritons, hybrid light–matter quasiparticles, and measure *both phase and modulus of the order parameter in the turbulent regime*.

In this work we explore the link between dynamical and topological properties in two-dimensional quantum turbulence. We propose to investigate the temporal properties of the quantum fluid velocity field by a novel strategy. The idea was to devise a minimal model for the quantum flow which complies with global topological constraints, without requiring local knowledge of the spatial dynamics of the system. To achieve this, we derive kinetic equations of formation and annihilation of critical points of the velocity field, and apply the approach to a non-equilibrium exciton-polariton fluid. We show that we can reproduce the experimentally observed rate of creation and annihilation of quantized vortices, thus identifying the elementary mechanisms responsible for the increase in the number of vortices – during the quantum turbulence growth – and for its reduction – during the quantum turbulence decay.

Indeed, fundamental topological constraints require that the formation and annihilation of vortices be guided by dynamical transitions involving velocity field critical points, namely *nodes* and *saddles*. Identifying the simplest mechanisms underlying these processes enables us to develop an effective kinetic model that closely aligns with the experimental observations, and show that two different dynamical processes are responsible for vortex number growth and decay. These findings underscore the crucial role played by topological conservation laws in shaping nonlinear, turbulent evolution of two-dimensional quantum fluids.

6.1 . QUANTUM HYDRODYNAMICS

A BEC is described by the non-linear Schrödinger equation (NLSE) or Gross-Piatevskii equation for the complex scalar field $\psi(\vec{r},t)$, also known as the order parameter of the BEC. This equation reads

$$i\hbar\partial_t\psi = -\frac{\hbar^2}{2m}\nabla^2\psi + U\psi + g|\psi|^2\psi \tag{6.1}$$

with $U(\vec{r},t)$ an external potential and $g(\vec{r},t)$ the interaction parameter. The order parameter can be written in the density-phase representation

$$\psi(\vec{r},t) = \sqrt{\rho(\vec{r},t)}\,\exp\left(i\,S(\vec{r},t)\right) \tag{6.2}$$

and accordingly the NLSE can be recast to the system of hydrodynamical equations

$$\begin{aligned} \partial_t\rho + \nabla.(\rho\vec{v}) &= 0 \\ \hbar\partial_t S = -\tfrac{\hbar^2}{2m}(\nabla S)^2 - \tfrac{\hbar^2}{2m}\tfrac{\nabla^2\sqrt{\rho}}{\sqrt{\rho}} - g\rho - U & \end{aligned} \tag{6.3}$$

where

$$\vec{v}(\vec{r},t) = \frac{\hbar}{m}\nabla S(\vec{r},t) \tag{6.4}$$

is the irrotational, i.e. $\nabla\times\vec{v}=0$, velocity of the condensate[2]. This is called the *Madelung* transformation[3]. In the NLSE equation (6.1) describing the hydrodynamics of quantum fluids, the term $g|\psi|^2$ can

[1]The experimental data has been provided by Riccardo Panico. The experiment was conducted, under the supervision of Dario Ballarini, at the Advanced Photonic Lab of the Institute of Nanotechnology (Lecce, IT). Alessandra Lanotte and Giovanni Martone of the same Institute of Nanotechnology as well as Thibault Congy of the Northumbria University also collaborated to the preliminary results presented here.

[2]The definition of $\vec{v}$ comes from the definition of the current $\vec{J} = (\hbar/m)Im(\psi^*\nabla\psi) = \rho\vec{v}$ with $\vec{v}$ defined as in (6.4).

[3]We already used this transformation when presenting Analog models in Chapter 2 and when deriving the back-reaction equations in Chapter 5. Indeed, equations (6.3) are the 3D version of the 1D equations (2.32).

be replaced by a more generic term $gf(\rho)$ describing non-linearities more complicated than $|\psi|^2$, with f a possibly complex function accounting for non-linear losses[4], whereas a complex potential U can account for linear losses such as absorption. This is the case in the non-equilibrium BEC of polaritons we consider in the following.

6.2 . VORTICITY IN 2D QUANTUM FLUIDS

6.2.1 . 2D Turbulence

In 3D turbulence, the energy dissipates to ever smaller scales. This is not the case in two dimensional systems. Denoting as $\vec{v}$ the velocity field and $\omega = (\vec{\nabla} \times \vec{v}) \cdot \vec{e}_z$ the vorticity, the kinetic energy E and enstrophy Ω of an incompressible fluid are

$$E = \frac{\rho}{2} \int \mathrm{d}^2 r \, v^2 \quad \Omega = \frac{1}{2} \int \mathrm{d}^2 r \, \omega^2 \tag{6.5}$$

where ρ is the fluid's density. In the absence of external forcing, finite viscosity results in the dissipation of E and Ω in a two-dimensional fluid according to the laws (see, e.g., Ref. [70])

$$\frac{\mathrm{d}E}{\mathrm{d}t} = -2\nu\rho\,\Omega \tag{6.6a}$$

$$\frac{\mathrm{d}\Omega}{\mathrm{d}t} = -2\nu \int \mathrm{d}^2 r \, |\vec{\nabla}\omega|^2 \tag{6.6b}$$

where ν is the viscosity. Eq. (6.6b) shows that enstrophy can only decrease and is thus bounded from above. Eq. (6.6a) then implies that $\mathrm{d}E/\mathrm{d}t \to 0$ in the limit $\nu \to 0$. This is the main difference with respect to 3D turbulence in which Ω can be amplified by vortex stretching, resulting in finite energy dissipation even in the limit of vanishing viscosity[5]. In 2D turbulence energy is not dissipated, it is dynamically transferred to large scales by an inverse cascade. Kraichnan [176] proposed an interpretation of the phenomenon according to which the inverse energy cascade is associated with the growth of patches of vorticity due to vortex merging and pushing energy toward larger length scales[6].

A scenario of this type was put forward by Onsager [47] who applied statistical mechanics to a model of point-like vortices relevant to quantum fluids: in a closed system vortices of the same vorticity tend to aggregate in clusters, forming a negative temperature equilibrium state that comprises more energy but less entropy as compared to a configuration of randomly distributed vortices[7]. Quantum vortex clustering and inverse energy cascade were indeed observed recently in two-dimensional atomic BECs [75, 76] and polariton condensates [79] demonstrating that classical and quantum two-dimensional turbulence bare important similarities. Nonetheless there exists a significant difference between the classical and quantum realm : quantum vortices carry topological charges and a description of vortex dynamics in a quantum fluid should account for the conservation of these charges. In the following we argue that a proper account of topological contraints in a 2D quantum fluid necessitates to consider not only vortices, but also other critical points such as nodes and saddles.

6.2.2 . Vorticity index I_V and Poincaré-Hopf index I_P

In the wave-mechanical and quantum context, while the importance of quantization of vorticity has been understood long ago in the physics of superfluid helium [47, 49], the relevance of another topological index, known as the Poincaré-Hopf index (see Eq. (6.11) below) has been stressed for stationary two-dimensional waves only in the 80's [178].

[4] This is, for example, relevant in non-linear optics, where one can have a term such as $g|\psi|^2/(1+|\psi|^2/I_{\mathrm{sat}})$ modeling the saturation of the non-linearity at high intensity in a non-linear medium.

[5] In 3D the r.h.s. of Eq. (6.6a) does not cancel when $\nu \to 0$ (more precisely at high Reynold number).

[6] As opposed to vorticity, vorticity gradients (the r.h.s. term of (6.6b) which is called "palinstrophy") are not bounded in two dimensions, and one expects a direct cascade of enstrophy associated with the stretching of patches of vorticity.

[7] Note however that the Kraichnan and Onsager scenarii are not exactly identical : clustering (Onsager) is not the same as merging (Kraichnan). Also, while in the initial Onsager model the number of vortices is conserved, it has been suggested [177] that the formation of high energy clusters is reached through annihilation of low energy vortex-antivortex pairs, a phenomenon which has been dubbed "evaporative heating".

We consider here a two-dimensional quantum fluid described by a scalar order parameter of the form $\psi(\vec{r},t) = \sqrt{\rho(\vec{r},t)}\exp\left(iS(\vec{r},t)\right)$. Here the real functions $\sqrt{\rho} \geq 0$ and S correspond to the amplitude and phase of the order parameter, respectively, and $\vec{r} = (x,y)$. The fluid's velocity field $\vec{v}$ [49] is defined in (6.4). In a two-dimensional setting, two topological indices are associated with any domain D delimited by a closed contour $\mathscr{C}$. The vorticity index $I_V(\mathscr{C})$ associated to the close contour $\mathscr{C}$ is defined as the circulation of the velocity $\vec{v}$ along the loop $\mathscr{C}$, i.e.

$$I_V(\mathscr{C}) = \frac{m}{2\pi\hbar}\oint_{\mathscr{C}} \vec{v}.d\vec{l} = \frac{1}{2\pi}\oint_{\mathscr{C}} (\nabla S).d\vec{l} = \oint_{\mathscr{C}} \frac{dS}{2\pi} \tag{6.7}$$

Defining an angle φ as the polar angle of $\vec{v}$, i.e.

$$\cos\varphi = \frac{\vec{v}.\vec{e}_x}{v} = v_x/v \qquad \sin\varphi = \frac{\vec{v}.\vec{e}_y}{v} = v_y/v \tag{6.8}$$

the Poincaré-Hopf index reads

$$I_P(\mathscr{C}) = \frac{1}{2\pi}\oint_{\mathscr{C}} (\nabla\varphi).d\vec{l} = \oint_{\mathscr{C}} \frac{d\varphi}{2\pi} \tag{6.9}$$

Definition (6.8) for the function $\varphi(v_x, v_y)$ implies that

$$\varphi = \arctan\frac{v_y}{v_x} \qquad \Rightarrow \qquad d\varphi = \frac{v_x dv_y - v_y dv_x}{v_x^2 + v_y^2} \tag{6.10}$$

Indices I_V and I_P assume (positive or negative) **integer** values because they simply relate to the variation along the close loop C of the phase of the order parameter and of the direction of the velocity, respectively.

6.2.3 . Critical points and topological constraints to quantum turbulence

In hydrodynamics a *critical point* is a point where the velocity vanishes, also called a *saturation point*. Here, by "critical points", we loosely refer to vortices, saddles and nodes. Theses "points" can be characterized by the respective values of the vorticity index I_V and the Poincaré-Hopf index I_C, i.e.

$$I_V = \frac{1}{2\pi}\oint_C \mathrm{d}S \qquad I_P = \frac{1}{2\pi}\oint_C \mathrm{d}\varphi \tag{6.11}$$

defined in the previous section 6.2.2. Both indices are zero if there are no singular nor stagnation point inside D. Nontrivial topological indices occur when the phase S displays extrema (local maxima or minima), saddles, or essential singularities. The corresponding points are nodes (attractive or repulsive), saddles, and quantum vortices, respectively (see Fig. 6.1 and Table 6.1). The indices I_P and I_V associated to a domain D are the sums of the indices of the critical points contained in D.

	node	saddle	vortex$_{(+)}$	vortex$_{(-)}$
I_P	+1	-1	+ 1	+ 1
I_V	0	0	+ 1	-1

Table 6.1: Values of the vorticity I_V and of the Poincaré-Hopf index I_P attached to non-degenerate critical points. Vortices with positive or negative vorticity are denoted as vortex$_{(+)}$ and vortex$_{(-)}$, respectively. The indices I_P and I_V associated to a domain D are the sums of the indices of the critical points contained in D.

Notably, the presence of nodes is a unique feature of compressible quantum fluids, such as polariton superfluids. These nodes are indeed observed in our experimental results, and we demonstrate that they play a crucial role in the onset of turbulence. Furthermore, it can be seen that the determination of the critical points through the streamlines of the flow requires the measurement of the phase of the scalar field : such a measurement is possible in the fluid of polaritons here considered. Through a phenomenological model based on topological charge conservation, our work provides new insights into the interplay of topology and quantum fluid dynamics, thus underscoring the crucial role played by topological conservation laws in both the growth and the decay of two dimensional quantum turbulence.

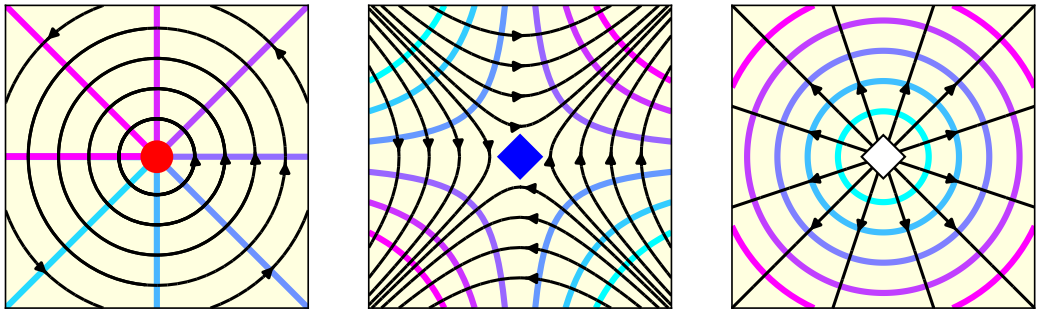

Figure 6.1: Tolopolical characterization of vortices, saddles and nodes with their respective vorticity index I_V and Poincaré-Hopf index I_P. The vorticity index I_V is the circulation of the velocity field $\vec{v}$, i.e. of the gradient ∇S of the phase field S, along the contour $\mathscr{C}$, whereas the Poincaré-Hopf index I_P is the circulation of the gradient $\nabla\varphi$ of the polar angle ϕ of $\vec{v}$ along the contour $\mathscr{C}$. The local velocity streamlines (oriented solid lines) and equiphase lines (thick colored lines) around a vortex, a saddle or a node, are reported. For a given domain D, I_V and I_P are the sums of the indices of all the critical points contained in D.

6.3 . A PHENOMENOLOGICAL MODEL FOR THE KINEMATICS

In the experiment a new generation of optical techniques that enables a precise measure of both the intensity and the phase of a light sheet [32,35,36,52–54] was used. This offers the possibility of an accurate and simple location not only of vortices but also of other critical points, such as saddles and nodes. This enabled us to obtain evidences of several (topologically constrained) mechanisms of formation of vortices and of associated singular points in the time domain, with an account of the evolution of the streamlines.

6.3.1 . The physical system

The physical system we examine here is an out-of-equilibrium Bose-Einstein condensate of exciton–polaritons. Exciton-polaritons are hybrid light–matter quasiparticles, resulting from the coupling of photons and excitons[8]. The experiment involves injecting a high-energy polariton superfluid, and allowing it to expand within a circular potential barrier [79].

Indeed, in the experiment, the polariton fluid is injected in a planar microcavity where a ring potential confines the polariton fluid by inducing a local energy blueshift in the polariton resonance. To inject the polariton fluid into the center of this potential, a pulsed laser (pulse duration of 2 ps) is focused into a Gaussian spot with a beam waist of approximately 17 $\mu\mathrm{m}$. The excitation energy is slightly blue-detuned from the ground state by 1.2 meV in the high-energy case and 0.21 meV ine the low-energy case. It provides the polaritons with an initial kinetic energy that allows for their rapid expansion within the potential and subsequent hydrodynamic vortex formation upon collision with the potential barrier. The time evolution of the polariton fluid is captured through the interference of the signal with a reference pulse (a sample of the excitation beam) with a variable time delay, enabling the retrieval of both the amplitude and phase of the fluid (Fig. 6.2). The temporal resolution is of around 1 ps and the spatial resolution is finer than the estimated healing length of the vortices. For each experimental condition and time frame, vortices and critical points are identified by computing the circulation around each point of the two-dimensional phase map and the corresponding velocity field, respectively, and searching for integer multiples of 2π. From a simple comparison, one can further distinguish which of the critical points are nodes.

The initial kinetic energy provided to the superfluid induces the creation not only of a dense vortex gas but also of a large number of saddles and nodes. The co-existence of these three types of points has

[8] A exciton is a bound state of an electron and an electron hole that attract each other through the Coulomb force.

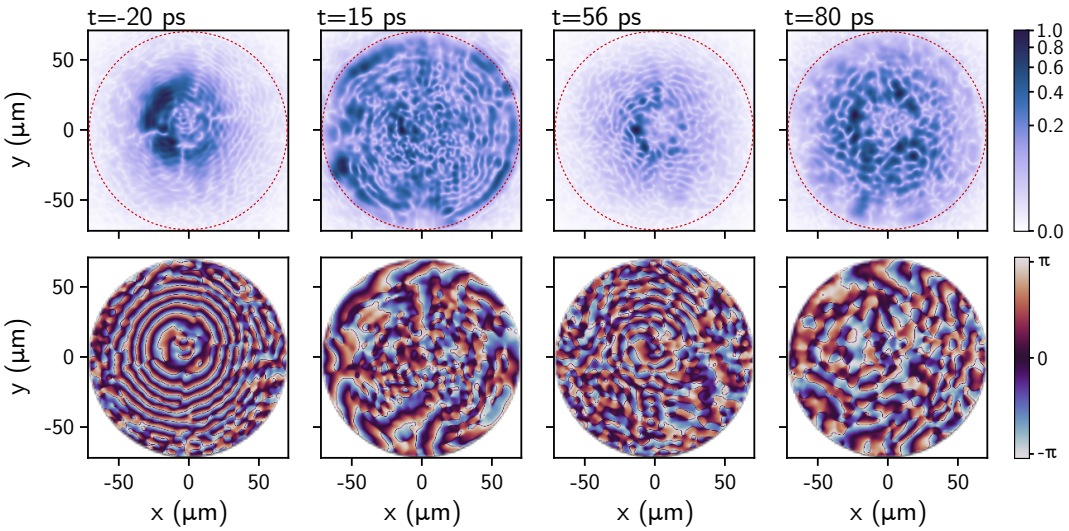

Figure 6.2: Measured density (top) and phase (bottom) of the polariton fluid for the high energy case. The dashed red circle represents the position of the confining potential. The time frames, from left to right, correspond to: the initial experimental condition (-20 ps), when the polariton fluid is still mostly localized in the center of the potential and has yet to fill all the available space; 15 ps after the sudden growth in the number of vortices, when the polariton fluid is flowing back after hitting the boundaries; the switching point at around 56 ps, when vortex growth stops and the Bristol mechanism becomes relevant; and finally, a snapshot near the end of the dynamics at around 80 ps.

been explicitly experimentally demonstrated in linear [179] and nonlinear [180] optics. The optical nature of polaritons makes it possible to measure both the phase and the modulus of the order parameter by interferometric techniques [181]. As shown in Fig. 6.3, by analyzing the velocity field, the evolution of hundreds of critical points can be tracked. In the enlarged region, the experimental phase portrait of the exciton-polariton fluid clearly reveals three saddles, two nodes, and a negative vortex. This method allows then to determine, at each time step, the number of vortices, saddles, and nodes present in the system.

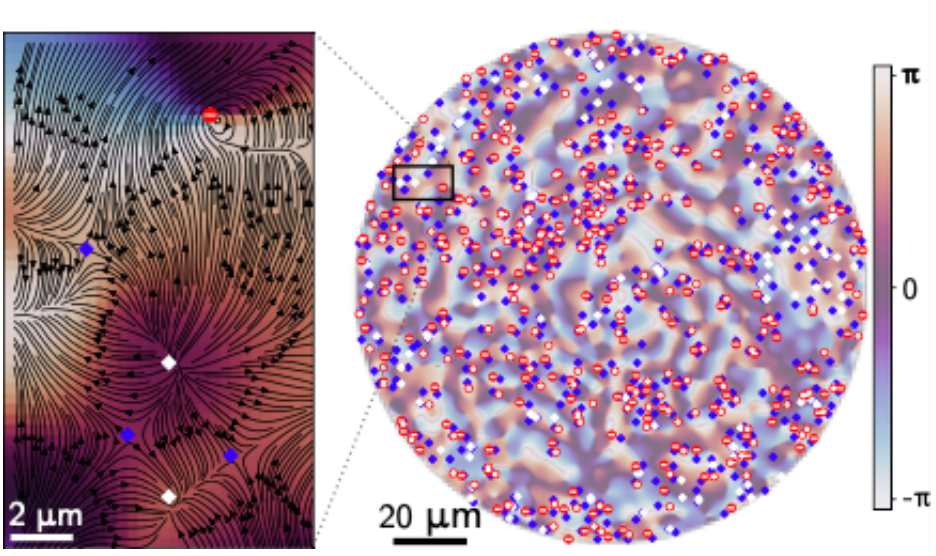

Figure 6.3: A snapshot of the polariton superfluid phase field, with the measured critical points. A zoom highlights the local flow organization.

6.3.2 . The model

We consider the following main mechanisms of creation (or annihilation) of critical points in the random flow field: (i) the nodes-to-vortices conversion in which two nodes coalesce and give birth to two vortices and (ii) the saddle-node bifurcation which creates one saddle and one node from scratch. These

two mechanisms conserve the vorticity and the Poincaré index; they correspond to well-identified bifurcations whose relevance for a two-dimensional quantum fluid has been validated in Ref. [180]. They can be schematically written as chemical reactions:

$$\text{node} + \text{node} \underset{b}{\overset{a}{\rightleftharpoons}} \text{vortex}_{(+)} + \text{vortex}_{(-)} \tag{6.12a}$$

$$\varnothing \underset{d}{\overset{c}{\rightleftharpoons}} \text{node} + \text{saddle} \tag{6.12b}$$

In the above formulae, the (positive) quantities a, b, c, and d are the reaction rates (see Eq. (6.13) below). Other mechanisms have been observed [180] which also conserve both the vorticity and the Poincaré-Hopf index: a saddle can transform into two saddles and one node in a pitchfork bifurcation, or also two vortices and two saddles can appear spontaneously (or coalesce) in what has been termed the "Bristol mechanism" in Ref. [180]. These reactions have been discarded for simplicity reasons (they involve collisions of a larger number of critical points) and also because much less often observed in a previous experiment and in numerical simulations [180][9]. From the modeling (6.12) we write a kinetic equation inspired by rate equations of elementary chemical reactions :

$$\begin{aligned} \frac{\mathrm{d}V_\pm}{\mathrm{d}t} &= aN^2 - bV_+V_- \qquad \frac{\mathrm{d}S}{\mathrm{d}t} = c - dNS \\ \frac{\mathrm{d}N}{\mathrm{d}t} &= -2aN^2 + 2bV_+V_- + c - dNS \end{aligned} \tag{6.13}$$

where $N(t)$ denotes the number of nodes, $S(t)$ the number of saddles, and $V_+(t)$ [$V_-(t)$] the number of vortices with positive [negative] vorticity. It results from the values of the topological indices listed in Fig. 6.3 that the total Poincaré-Hopf index of the system is $I_\mathrm{P} = N + V_+ + V_- - S$. It is easily verified that I_P is preserved by the system (6.13) : this comes as no surprise since the elementary processes in (6.12) conserve the Poincaré-Hopf index. Similarly, the conserved total vorticity of the system is $V_+ - V_-$. In the following we make the simplifying assumption that this difference is equal to zero: $V_+(t) = V_-(t) = V(t)/2$ where $V(t)$ is the total number of vortices. This hypothesis is confirmed by the experimental data (such as displayed in Fig. 6.4) and is certainly sound in the configuration we consider where typically $V(t) \gg 1$ while no external angular momentum is imparted to the system.

Defining the rescaled quantities $\tau = t/t_0$, $n = N/N_0$, $v = V/N_0$, and $s = S/N_0$, with $t_0 = 1/\sqrt{2ac}$ and $N_0 = \sqrt{c/2a}$, makes it possible to cast the system (6.13) under the following dimensionless form

$$\frac{\mathrm{d}v}{\mathrm{d}\tau} = n^2 - \alpha v^2 \qquad \frac{\mathrm{d}s}{\mathrm{d}\tau} = 1 - \gamma ns \qquad \frac{\mathrm{d}n}{\mathrm{d}\tau} = 1 - n^2 - \gamma ns + \alpha v^2 \tag{6.14}$$

where $\alpha = b/(4a)$ and $\gamma = d/(2a)$ [10].

[9] Let us remark that the "Bristol mechanisms" can be obtained from combining the two processes (6.12), with the second mechanism counted twice : the Bristol can then be considered as a higher order process.

[10] For completeness, note that in terms of the new parameters, the rates of reaction read $a = 1/2N_0t_0$, $b = 2\alpha/N_0t_0$, $c = N_0/t_0$, $d = \gamma/N_0t_0$.

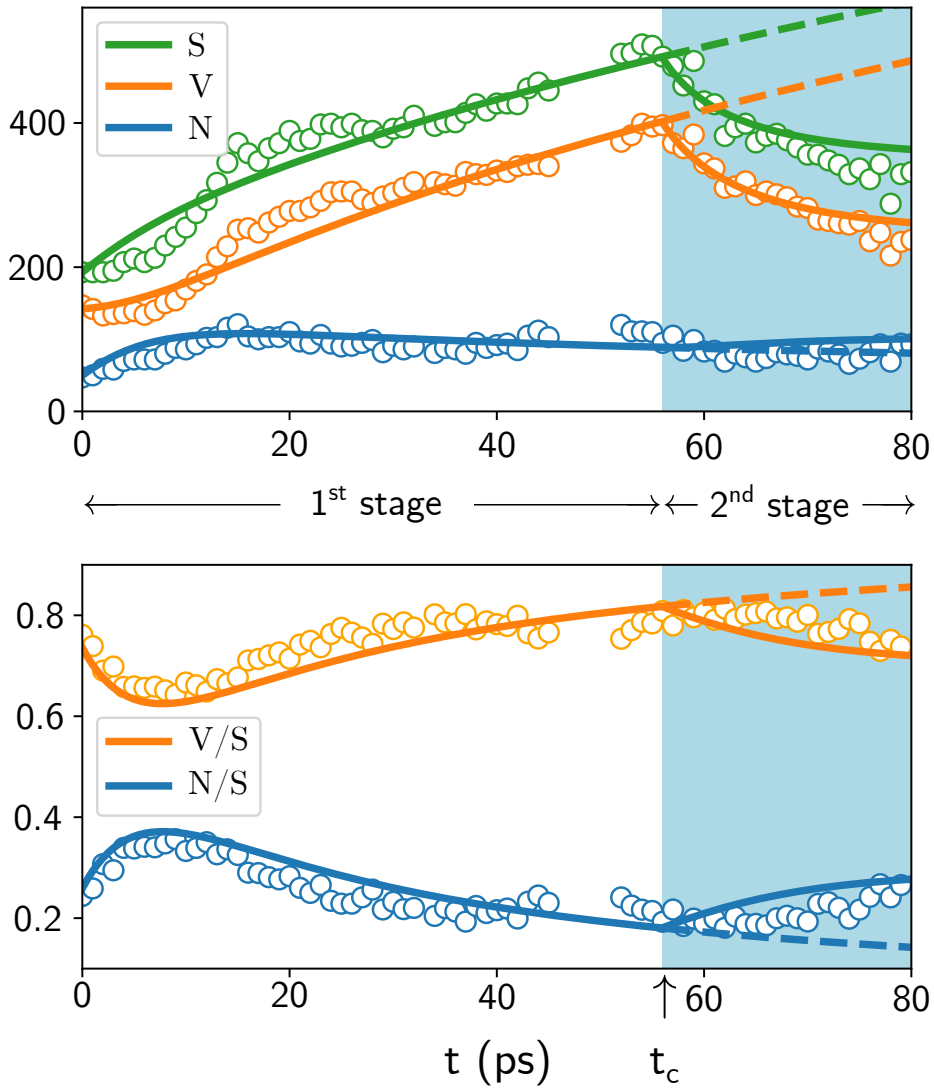

Figure 6.4: (Top) Comparison of the experimental results for $N(t)$, $V(t)$, and $S(t)$ (circles) with the theoretical predictions (lines). Experimental data are averages of four realisations of the same dynamical regime. For $t \leq t_c$, the solid lines have been obtained with the numerical integration of Eqs. (6.14); morevoer, $\gamma = 0.5 \pm 0.1$, $N_0 = 170 \pm 10$ and $t_0 = 12 \pm 1.5$ ps. For $t > t_c$, the dashed lines correspond to the results of (6.14), while the solid lines come from the numerical resolution of (6.16) with $\varepsilon = 0.05 \pm 0.01$. (Bottom) Same as above for the quantities $V(t)/S(t)$ and $N(t)/S(t)$. The value of t_c is 56 ps.

6.3.3 . Growth of turbulunce

We consider a turbulent regime of the polariton dynamics in which, after the fast expansion of the quantum fluid, the onset of vortex clustering and the emergence of the inverse kinetic energy cascade was evidenced on timescales of a few tens of picoseconds [79]. A low-energy data set, where the onset of turbulence is inhibited by dissipation, is shown in section 6.3.5. The numbers of vortices, saddles and nodes are displayed as circles in the upper part of Fig. 6.4. At $t = 0$, when the fluid encounters the barrier, some critical points are already present, having formed during the fluid's expansion. The turbulent dynamics is initiated at this moment, which we treat as the initial condition.

Let us first focus on the stage of turbulence growth, during which the numbers of vortices and saddles increase significantly (stage 1 in Fig. 6.4). In this time lag, the nucleation of many new vortices dominates the temporal evolution. This implies imposing $\alpha = 0$: indeed, when $\alpha \neq 0$ the system (6.14) has a fixed point and the numbers of vortices, saddles, and nodes tend to saturate, which is not what is observed in the experiment. We checked that a nonzero value of α always worsens the agreement of the theoretical curve with data: this confirms that in this stage the incompressible kinetic energy of the system is mostly increasing, as required for the establishment of the inverse kinetic energy cascade.

It is interesting to discuss the values of the rate of reactions in Eqs. (6.12). In particular $c/d = N_0^2/\gamma =$

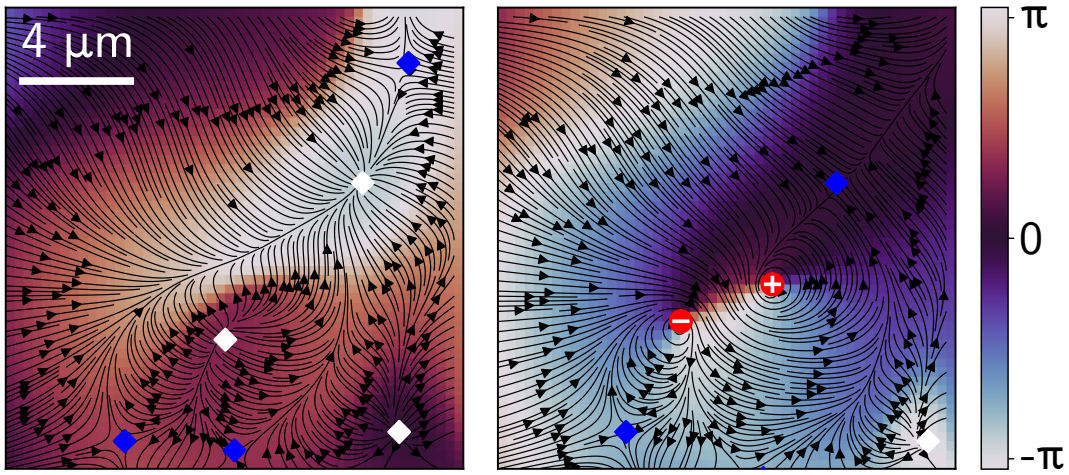

Figure 6.5: Experimental snapshots, taken at 15 and 16 ps, showing the formation of a vortex pair starting from two nearby nodes, as indicated by Eq. 6.12a. The streallines of the velocity field, $\vec{v} = (\hbar/m)\vec{\nabla}S$, are plotted on top of the color-coded phase field, $S(x, y)$.

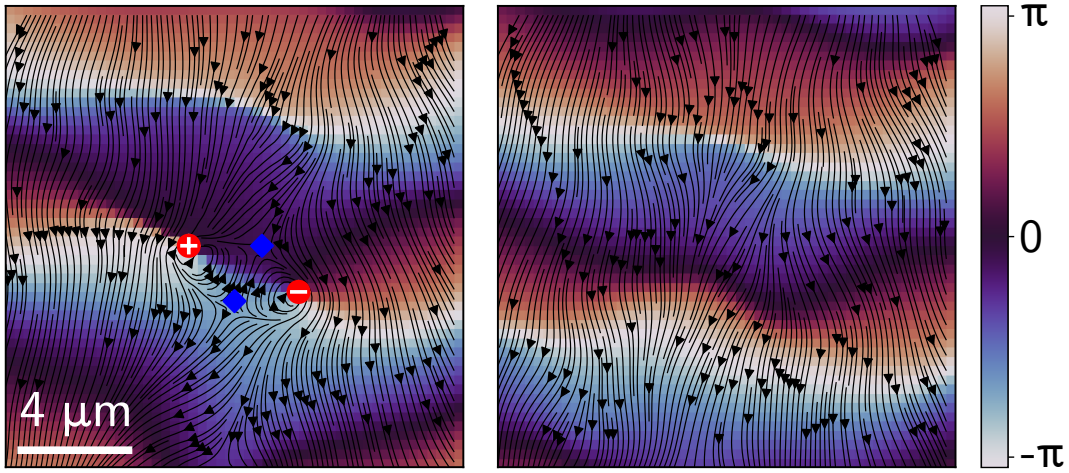

Figure 6.6: Experimental snapshots of the phase field $S(x, y)$ taken toward the end of the experiment (76 and 77 ps), showing the annihilation of a pair of saddles and vortices via the Bristol mechanism.

$6 \times 10^4 \gg 1$, implying that the saddle-node bifurcation is mainly unidirectional : the annihilation of a saddle with a node is much less frequent than their *creatio ex nihilo*. This indicates that the saddle-node formation mechanism (6.12b) is the real fuel of the whole process. The nodes-to-vortices reaction (6.12a) merely transmutes some of the nodes into vortices, but could not be effective on its own. This remark is of significance : the spontaneous creation of uniquely a vortex-antivortex pair being topologically forbidden (it would not conserve the Poincaré-Hopf index) we are in need of an explanation of the increase of the number $V(t)$ of vortices. In the system we consider, the formation of vortices arises from two saddle-nodes bifurcations (6.12a) followed by a nodes-to-vortices conversion (6.12b), ultimately resulting in the formation of two saddles and two vortices. This is the reason why the numbers of saddles and of vortices increase at the same pace, see the upper part of Fig. 6.4.

The results plotted in the lower panel of Fig. 6.4 indicate that the total Poincaré index is conserved and small. Indeed in this case $N+V = S$, the two quantities V/S and N/S sum to unity, and a minimum of one should correspond to a maximum of the other, as observed in the lower plot of Fig. 6.4. This property is model-independent: it is a prerequisite which should be embodied in any kinetic model, but its fulfillment is not a guarantee of accuracy of the model. Experimental results confirm the exact conservation of both I_V and I_P indices in every realization of the measurements.

It is intriguing to observe, during the time evolution of the experimental results, instances where two nodes transform into a vortex and an antivortex, respectively, as predicted by (6.12a). In Fig. 6.5, we present two consecutive time frames of the same spatial region, highlighting the phase field evolution from a configuration containing nodes and saddles to one where two nodes are transformed into a

vortex and an antivortex.

6.3.4 . Decay of turbulence

The results displayed in Fig. 6.4 show a stricking behavior, namely, a sharp temporal transition between stage 1, characterised by the nonlinear growth of the number of vortices/saddles, and stage 2, characterised by a dramatic decrease of the numbers of vortices (and saddles). However, the number of nodes is not experiencing a similar abrupt modification in the same period of time : this supports a scenario which does not involve nodes, still conserving both I_V and I_P. The so-called Bristol mechanism [178, 180], described by Eq. (6.15) below, is a perfect candidate :

$$\text{vortex}_{(+)} + \text{vortex}_{(-)} + \text{saddle} + \text{saddle} \underset{f}{\overset{e}{\rightleftharpoons}} \varnothing \tag{6.15}$$

In view of the significant decrease of the number of vortices and saddles during stage 2, we consider that the rate of reaction f is zero in Eq. (6.15). Hence, the process is assumed to be unidirectional [11]. The system (6.14) accordingly modifies to

$$\begin{aligned} \frac{\mathrm{d}v}{\mathrm{d}\tau} &= n^2 - \alpha v^2 - \varepsilon\, v^2 s^2, \quad \frac{\mathrm{d}s}{\mathrm{d}\tau} = 1 - \gamma n s - \varepsilon\, v^2 s^2 \\ \frac{\mathrm{d}n}{\mathrm{d}\tau} &= 1 - n^2 - \gamma n s + \alpha v^2 \end{aligned} \tag{6.16}$$

where $\varepsilon = \frac{1}{2} e N_0^3 t_0 = ec/(8a^2)$ is the rescaled rate of annihilation of saddles and vortices. We keep for all the other parameters the values previously determined, and during stage 2 we solve the system (6.16) with $\varepsilon \neq 0$. The corresponding results are displayed in Fig. 6.4. The agreement of the theoretical curve with the experimental observation supports the idea that at this time delay the system enters a new regime in which the annihilation mechanism (6.15) acquires an efficiency it previously did not have.

It is interesting to ask the question whether the mechanism of Eq. (6.15) could have been effective earlier, with a rate of reaction $f \neq 0$ explaining the rapid and concomitant increase of V and S during stage 1. The observation of the behavior of N in the same period makes this hypothesis rather unlikely, since N initially increases and then saturates. This advocates for a saddle-node creation process (6.12b) which then feeds the nodes-to-vortices one (6.12a). Only this process can explain (i) the occurrence of extrema of V/S and N/S at short times (lower plot of Fig. 6.4) and (ii) the saturation of N at a slightly later time (upper plot of the same figure). And indeed, it is not possible to fit the data on the basis of mechanisms (6.12a) and (6.15) only, or (6.12b) and (6.15) only.

In Fig. 6.6, the Bristol mechanism is observed in our experimental results during the second stage of the dynamics, when dissipation begins to dominate. Two consecutive frames illustrate the simultaneous annihilation of a pair of saddles and vortices within a laminar plane flow, marking the dissipation of incompressible kinetic energy from the system.

6.3.5 . Low-energy data set

The data presented in the previous sections 6.3.3 and 6.3.4 correspond to a turbulent regime in which a high-energy polariton superfluid is injected against a potential barrier. We consider in this section a data set obtained at relatively low injection energy ($E = 0.21$ meV here, instead of 1.20 meV in the high-energy case).

The experimental data, presented in Fig. 6.7, display a tendency to saturate: from $t = 60$ ps on, $V(t)$, $S(t)$, and $N(t)$ vary quite slowly. To emulate this behavior, the system (6.14) should have a fixed point and the value of the parameter α should thus be finite. In this case, if we denote as $n_\infty, v_\infty, s_\infty$ the coordinates of the fixed point, defining $\beta = 1/\sqrt{\alpha}$ we get $v_\infty = \beta n_\infty$, $s_\infty = 1/(\gamma n_\infty)$ and

$$n_\infty = \frac{I_{\mathrm{P}0} + \sqrt{I_{\mathrm{P}0}^2 + 4(1+\beta)/\gamma}}{2(1+\beta)} \tag{6.17}$$

[11] This unidirectional behavior was already observed in the experiment and the numerical simulations of [180]: In this reference the Bristol mechanism was always inducing the concomitant annihilation of two vortices and two saddles, and never their *creatio ex nihilo*.

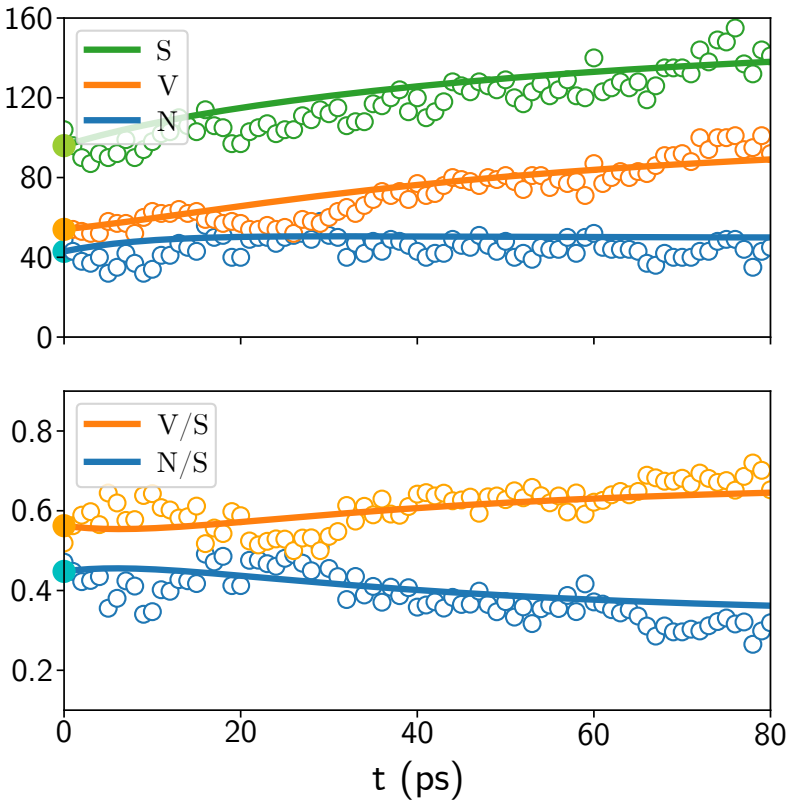

Figure 6.7: Comparison of the experimental results of the low-energy data set for the numbers $N(t)$ of nodes, $V(t)$ of vortices, and $S(t)$ of saddles (circles) with the numerical integration of Eqs. (6.14) (solid lines).

In this expression $I_{\mathrm{P}0} = n+v-s$ is the constant value of the rescaled Poincaré index of the whole system ($I_{\mathrm{P}0} = I_{\mathrm{P}}/N_0$). In the limit $I_{\mathrm{P}0}^2 \ll 4(1+\beta)/\gamma$ [12], formula (6.17) reads $n_\infty = [\gamma(1+\beta)]^{-1/2}$ and implies that $s_\infty = (1+\beta)n_\infty$. Comparing the values $v_\infty/n_\infty = \beta$ and $s_\infty/n_\infty = 1+\beta$ with the values $V/N \approx 2$ and $S/N \approx 3$ around $t = 60$ ps points to a value $\beta \approx 2$ (*i.e.*, $\alpha = 0.25$). We found that the choice $\gamma = 1 \pm 0.1$, $N_0 = 86 \pm 4$, $t_0 = 28 \pm 4$ ps and $\alpha = 0.25 \pm 0.05$ gives a good account of the data set, see Fig. 6.7.

The system is not here in a turbulent regime such as the one studied in the main text. The injection energy E is smaller, the number of vortices increases at a lower pace, and the stage of decay (stage 2 in Fig. 6.4) is not reached within the experimental time window. This interpretation of the different behaviors of the two data sets is corroborated by the following evaluation of orders of magnitude : a simple dimensional argument suggests that the characteristic time t_0 should scale as $t_0 \propto E^{-1/2}$. And indeed the characteristic times t_0 for the two sets of data are in a ratio $t_0^{\mathrm{low}}/t_0^{\mathrm{high}} = (28 \pm 4) : (12 \pm 1.5) = 2.33 \pm 0.6$ which is consistent with the value $\sqrt{E^{\mathrm{high}}/E^{\mathrm{low}}} = \sqrt{1.20\,\mathrm{meV}/0.21\,\mathrm{meV}} = 2.39$.

6.3.6 . Discussion

The onset of a turbulent inverse cascade of kinetic energy implies a temporal growth of the incompressible part of the total kinetic energy in the system. It was suggested in Ref. [79] that such energy input is at the expenses of the compressible kinetic energy in the quantum flow. This dynamical observation has its topological counterpart in the time window associated to the turbulence (and vortex clustering) growth, where the numbers of vortices and saddles increase, while nodes stay almost constant (stage 1 in Fig. 6.4). It is reasonable to think that not all vortices participate in the cascade, since they may not have time to correlate, nevertheless their increase reflects in the growth of the incompressible kinetic energy available for the cascade. When the ratio of compressible to incompressible kinetic energy stops growing, dissipation mechanisms prevail and turbulence starts decaying. This happens in our system with the simultaneous rapid decrease of both vortices and saddles. Interestingly, at the same time the clustering dynamics stops, as observed in Ref. [79]. Topological constraints also rule the mechanism of such a

[12] It can be checked *a posteriori* that this approximation is legitimate: the total experimental Poincaré-Hopf index is -1 ± 2 whereas N_0 is of order 10^2: $I_{\mathrm{P}0}^2 \approx 10^{-4}$. The term $4(1+\beta)/\gamma$ is instead of order unity.

decay; a process based on four vortices interactions [13], previously proposed in [182, 183, 184, 185, 186], here finds its origin in topological arguments. In the absence of a turbulent regime, the fate of vortices is different. Indeed in such a case, we physically expect a dynamical equilibrium between vortex creation and annihilation processes, in the presence of random, uncorrelated fluctuations. Our model faithfully describe this process by (6.12), although slower.

Our kinetic model is a minimal one : it is the simplest possible which complies with topological constraints. It provides a global description of the system based on phenomenological parameters (the rate coefficients) but is not meant to explain why these parameters assume different values in the turbulent or nonturbulent regimes, nor to predict when the growth of turbulence stops and why its decay (at $t \geq t_c$) is so abrupt. The description of this phenomenon implies to deal with spatial correlations in the system and goes beyond our global kinetic description.

Two-dimensional turbulence is an incredibly rich playground : after the pioneering contribution of Polyakov [187], it has been shown that the vorticity domains exhibit the same universal scaling arising in critical percolation theory, in both classical [188, 189] and quantum [190] fluids in the regime of inverse energy cascade. It would be of great interest to broaden the scope of our kinetic approach by developing a microscopic model able to integrate statistical properties and topological conservation laws. Such a model should account for the *interactions* of critical points (as in the vortex clustering) in a framework consistent with the conservation of topological indices.

6.3.7 . Article : Topological Pathways to Two-Dimensional Quantum Turbulence

R. Panico, G. Ciliberto, G. I. Martone, T. Congy, D. Ballarini, A. S. Lanotte, N. Pavloff, arXiv:2411.11671

doi : https://doi.org/10.48550/arXiv.2411.11671

We present a combined experimental and theoretical investigation of the formation and decay kinetics of vortices in two dimensional, compressible quantum turbulence. We follow the temporal evolution of a quantum fluid of exciton polaritons, hybrid light matter quasiparticles, and measure both phase and modulus of the order parameter in the turbulent regime. Fundamental topological conservation laws require that the formation and annihilation of vortices also involve critical points of the velocity field, namely nodes and saddles. Identifying the simplest mechanisms underlying these processes enables us to develop an effective kinetic model that closely aligns with the experimental observations, and shows that different processes are responsible for vortex number growth and decay. These findings underscore the crucial role played by topological constraints in shaping nonlinear, turbulent evolution of two dimensional quantum fluids.

[13] Note that since in the observed dynamics, saddles and vortices have similar temporal evolutions, the decay due to Bristol mechanism (6.15) is effectively equivalent to a four vortices decay process.

7 - CONCLUSIONS AND PERSPECTIVES

The domain of analog gravity aims to overcome the lack of theory and experiment in the field of quantum gravity by transposing some of its main issues and concerns to condensed matter systems. Following this strategy, we studied quantum non-separability, non-locality and back-reaction of the acoustic Hawking radiation emitted by an analog black hole implemented in the flow of a 1D quasi-condensate.

In chapter 4, our theoretical work sets the ground for future experimental studies by providing quantitative predictions of the degree of entanglement and of violation of Bell inequalities in a realistic analog configuration, both for bi- and tri-partite systems. Indeed, while the relativistic Hawking process involves, in the stationary case, only two modes, a third mode is present in the system under investigation : while not affecting the analogy with Hawking radiation in the considered regime, the third mode leads to a richer phenomenology. We therefore conducted a systematic study of the system, confirming the non-classical, i.e. nonseparable and nonlocal, character of analogous Hawking radiation thanks to experimentally relevant criteria. Furthermore, our study of different criteria of nonlocality demonstrates that the long wavelength quantum modes of the system consist in a superposition of continuous variable versions of degenerate GHZ states. Interestingly, the continuous nature of the degrees of freedom, at variance with GHZ states build on qbits, allows these modes to remain entangled after partial tracing. This confirms that continuous variable quantum information with analog black hole models opens new prospects of robust information processing in a variety of protocols, such as secret sharing or information scrambling.

In Chapter 5, we derived back-reaction equations that are generically valid for a inhomogeneous (flowing) condensate in any dimension. We specifically applied them to an analog black hole configuration in a 1D flowing quasi-condensate. We found asymptotic solutions and provided some preliminary results for consistent choices of parameters. Future work will be devoted to probe the exact dynamics of the horizon under the back-reaction effect and determine the consequent correction to the Hawking temperature of the system. Since in the gravitational framework, the quantum source of back-reaction has proven arduous to assess, the analog hydrodynamic setups appear to be valuable systems for testing models beyond (semi)classical gravity. In this perspective, since Hawking derivation of the Hawking effect does not take into account the back-reaction, a natural follow up of our study will be to write the modified Bogoliubov equations with a meanfield integrating the back-reaction. The effect of the back-reaction on Hawking radiation, the "back-back-reaction" so to say, could then be investigated and the *thermality* of the radiation reconsidered from this new perspective. This would again open new prospects on the nature of information carried by Hawking radiation.

Finally, in Chapter 6, we conducted a combined experimental and theoretical investigation of the kinetics of vortices in a 2D compressible quantum fluid of exciton–polaritons. Considering a minimal phenomenological model based on topological constraints we derived kinetic equations of formation and annihilation of critical points of the velocity field. These equations are able to reproduce the experimentally observed rate of creation and annihilation of quantized vortices both in the growing and decaying phases of quantum turbulence. These results will need to be further explored by refined numerical simulations. Furthermore, even if this final chapter is unrelated to analog gravity, one might think of future 2D models, with vorticity at play, that would exploit the constraints herein described : in this perspective, the topological charges considered in our effective phenomenological model of quantum turbulence, might also prove useful in investigating the physics of analog rotating black-holes and phenomena such as superradiance.

A - BELL INEQUALITIES : analytical computations

A.1 . Squeezing operator

As seen in 4.2.1, for $\mathbf{c} = T\mathbf{b} \Leftrightarrow c_i = V^\dagger b_i V$ with T a $2N \times 2N$ matrix, $\mathbf{c}$ and $\mathbf{b}$ defined as $\mathbf{a} = (\hat{a}_0, ..., \hat{a}_N, \hat{a}_0^\dagger, ..., \hat{a}_N^\dagger)^T$ and V a squeezing operator, one has by definition

$$c_i \left|0\right\rangle^c = V^\dagger b_i V \left|0\right\rangle^c \quad \Rightarrow \quad \left|0\right\rangle^b = V \left|0\right\rangle^c \tag{A.1}$$

Then it can be shown (see Refs. [90], [86], [87]) that

$$V = |\det \alpha^{-1/2} \exp\left[\frac{1}{2}\sum_{i,j=0}^{N-1} X_{ij}\hat{c}_i^\dagger \hat{c}_j^\dagger\right] \exp\left[\frac{1}{2}\sum_{i,j=0}^{N-1} Y_{ij}\hat{c}_i^\dagger \hat{c}_j\right] \exp\left[\frac{1}{2}\sum_{i,j=0}^{N-1} Z_{ij}\hat{c}_i \hat{c}_j\right] \tag{A.2}$$

with

$$X = -\beta^* \alpha^{-1} \qquad \exp\left(-Y^T\right) = \alpha \qquad Z = \alpha^{-1}\beta \tag{A.3}$$

and the $N \times N$ matrices α and β defined in 4.68. Since in (A.2) all the annihilation operators are on the right, when V is applied to the vacuum $\left|0\right\rangle^c$ it reduces to

$$V \left|0\right\rangle^c = (\det \alpha)^{-1/2} \exp\left[\frac{1}{2}\sum_{i,j=0}^{N-1} X_{ij}\hat{c}_i^\dagger \hat{c}_j^\dagger\right] \left|0\right\rangle^c \tag{A.4}$$

In this work we have defined $\left|0\right\rangle^b$ as being the incoming vacuum $\left|0\right\rangle^{\text{in}}$ and $\left|0\right\rangle^c$ as being the outgoing vacuum $\left|0\right\rangle^{\text{out}}$ with V given by (4.82). As V is characterize, through the matrices α, β and X given in (4.69) and (4.79), to be an operator squeezing the vacuum of the $\hat{c}_i$ to yield the vacuum of the $\hat{b}_i$, one can define similarly a V' or V'' operator to squeeze the vacuum of the $\hat{e}_i$ and $\hat{f}_i$ respectively in order to define the same vacuum of the $\hat{b}_i$. Using relations

$$\begin{aligned} &\boldsymbol{c} = V^\dagger \boldsymbol{b} V = T\,\boldsymbol{b} \\ &\boldsymbol{e} = W^\dagger \boldsymbol{c} W = T'\,\boldsymbol{c} \quad \Rightarrow \quad \boldsymbol{e} = W^\dagger V^\dagger \boldsymbol{b} V W = T'T\,\boldsymbol{b} \\ &\boldsymbol{f} = Z^\dagger \boldsymbol{e}\, Z = T''\,\boldsymbol{e} \quad \Rightarrow \quad \boldsymbol{f} = Z^\dagger W^\dagger V^\dagger \boldsymbol{b} V W Z = T''T'T\,\boldsymbol{b} \end{aligned} \tag{A.5}$$

one obtains

$$\alpha' = \begin{pmatrix} e^{i\varphi_{02}} S_{00}^* & e^{i\varphi_{12}} S_{01}^* & 0 \\ e^{i\varphi_{02}} S_{10}^* & e^{i\varphi_{12}} S_{11}^* & 0 \\ 0 & 0 & |S_{22}| \end{pmatrix} \quad \beta' = -\begin{pmatrix} 0 & 0 & |S_{02}| \\ 0 & 0 & |S_{12}| \\ e^{-i\varphi_{22}} S_{20} & e^{-i\varphi_{22}} S_{21} & 0 \end{pmatrix} \tag{A.6}$$

and

$$X' = \frac{1}{|S_{22}|}\begin{pmatrix} 0 & 0 & |S_{02}| \\ 0 & 0 & |S_{12}| \\ |S_{02}| & |S_{12}| & 0 \end{pmatrix} \qquad \det \alpha' = e^{i(\varphi_{02}+\varphi_{02}-\varphi_{22})} \det \alpha \tag{A.7}$$

where we have used the symmetry of the X' matrix. Furthermore one obtains

$$\alpha'' = \begin{pmatrix} e^{i\varphi_{12}} S_{10}^* \cos\theta - e^{i\varphi_{02}} S_{00}^* \sin\theta & e^{i\varphi_{12}} S_{11}^* \cos\theta - e^{i\varphi_{02}} S_{01}^* \sin\theta & 0 \\ e^{i\varphi_{02}} S_{00}^* \cos\theta + e^{i\varphi_{12}} S_{10}^* \sin\theta & e^{i\varphi_{02}} S_{01}^* \cos\theta + e^{i\varphi_{12}} S_{11}^* \sin\theta & 0 \\ 0 & 0 & |S_{22}| \end{pmatrix} \tag{A.8}$$

and

$$\beta'' = -\begin{pmatrix} 0 & 0 & 0 \\ 0 & 0 & \sinh r_2 \\ e^{-i\varphi_{22}} S_{20} & e^{-i\varphi_{22}} S_{21} & 0 \end{pmatrix} \tag{A.9}$$

Hence

$$X'' = \begin{pmatrix} 0 & 0 & 0 \\ 0 & 0 & \tanh r_2 \\ 0 & \tanh r_2 & 0 \end{pmatrix} \qquad \det \alpha'' = -\det \alpha' \tag{A.10}$$

where again the symmetry of X'' has been used to obtain the final expression given here. These relations yields straightforwardly relations (4.106) and (4.102) when considering (4.89) and (4.99).

Let us finally justify that

$$\frac{1}{\cosh r_2} e^{\tanh r_2 \hat{f}_1^\dagger \hat{f}_2^\dagger} |0_\omega\rangle^f = e^{r_2 \left(\hat{f}_1^\dagger \hat{f}_2^\dagger - \hat{f}_1 \hat{f}_2\right)} |0_\omega\rangle^f \tag{A.11}$$

One defines

$$\zeta = r e^{i\theta} \qquad \hat{A} = \zeta^* \hat{f}_1 \hat{f}_2 - \zeta \hat{f}_1^\dagger \hat{f}_2^\dagger \qquad \hat{B} = -e^{i\theta} \tanh r \hat{f}_1^\dagger \hat{f}_2^\dagger \tag{A.12}$$

and

$$\hat{F}_1(z) = e^{z\hat{A}} \hat{f}_1 \, e^{-z\hat{A}} = Z_A^{-1}(z) \hat{f}_1 Z_A(z) \tag{A.13}$$

with z real. One sees immediately that

$$Z_A^{-1}(z) = Z_A(-z) = Z_A^\dagger(z) \tag{A.14}$$

which means that Z_A is unitary. Considering the series expansion

$$\hat{F}_1(z) = \sum_{n=0} \frac{z^n}{n!} \hat{F}_1^{(n)}(0) \tag{A.15}$$

one has, by virtue of the commutation relation for the annihilation and creation operators $\hat{f}_i$ and $\hat{f}_i^\dagger$,

$$\hat{F}_1(z=-1) = \left(1 + \frac{|\zeta|^2}{2!} + \frac{|\zeta|^4}{4!} + ...\right) \hat{f}_1 - \frac{|\zeta|}{\zeta^*} \left(|\zeta| + \frac{|\zeta|^3}{3!} + ...\right) \hat{f}_2^\dagger = \cosh r \hat{f}_1 - e^{i\theta} \sinh r \hat{f}_2^\dagger \tag{A.16}$$

that is to say, setting $\mathbf{Z_A}(\mathbf{z} = -\mathbf{1}) = \mathbf{Z_A}$ as a shorthand notation,

$$\hat{F}_1(z=-1) = Z_A^{-1} \hat{f}_1 \, Z_A = \cosh r \hat{f}_1 - e^{i\theta} \sinh r \hat{f}_2^\dagger \tag{A.17}$$

Similarly, noticing that $Z_A(z=1) = Z_A^{-1}(z=-1)$ and therefore that $\hat{F}_1(z=1) = Z_A \hat{f}_1 Z_A^{-1}$, one can see, just by taking $\xi \to -\xi$ in (A.16), that one obtains

$$\hat{F}_1(z=1) = Z_A \hat{f}_1 \, Z_A^{-1} = \cosh r \hat{f}_1 + e^{i\theta} \sinh r \hat{f}_2^\dagger \tag{A.18}$$

Since $\hat{A}$ is symmetric by exchange $1 \leftrightarrow 2$, one obtains $Z_A^{-1} \hat{f}_2 \, Z_A$ and $Z_A \hat{f}_2 \, Z_A^{-1}$ just by taking $1 \leftrightarrow 2$ in (A.17) and (A.18). Then one has by definition

$$Z_A \hat{f}_1 \, Z_A^{-1} Z_A \, |0_\omega\rangle^f = Z_A \hat{f}_1 \, |0_\omega\rangle^f = 0 \quad \Rightarrow \quad (\cosh r \hat{f}_1 + e^{i\theta} \sinh r \hat{f}_2^\dagger)(Z_A \, |0_\omega\rangle^f) = 0 \tag{A.19}$$

where we have applied (A.17). Writing

$$|\xi\rangle = Z_A \, |0_\omega\rangle^f = \sum_{m,n} C_{m,n} \, |m,n\rangle^f \tag{A.20}$$

one obtains[1] from last relation in (A.19) that

$$\sum_{n=0}^{\infty} \sum_{q=-1}^{\infty} \left[\mu \, C_{n+q+1,n} \sqrt{n+q+1} + \nu \, C_{n+q,n-1} \sqrt{n}\right] |n+q, n\rangle^f = 0 \tag{A.21}$$

[1] Taking $m' = m+1$ in the first term and $n' = n+1$ in the second term, then renaming $m' \to m$ and $n' \to n$ and defining $m = n+q$.

with $\mu = \cosh r$ and $\nu = e^{i\theta}\sinh r$ and $C_{q,-1} = 0$. The expression in squared brackets must then vanish for all n and q. Writing the first terms in n one has

$$\begin{aligned} n=0 \quad & \mu\, C_{q+1,0}\sqrt{q+1} + 0 = 0 \\ n=1 \quad & \mu\, C_{q+2,1}\sqrt{q+2} + \nu\, C_{q+1,0} = 0 \\ n=2 \quad & \mu\, C_{q+3,2}\sqrt{q+3} + \nu\, C_{q+2,1}\sqrt{2} = 0 \end{aligned} \tag{A.22}$$

For $q \geq 0$ one can see that all the $C_{n+q+1,n}$ must vanish and that $q = -1$ makes the $C_{0,0}$ undetermined and implies

$$\mu\, C_{n,n} + \nu\, C_{n-1,n-1} = 0 \quad \Rightarrow \quad C_{n,m} = C_{0,0}\left(-\frac{\nu}{\mu}\right)^n \delta_{n,m} \tag{A.23}$$

Plugging this result in (A.20) one obtains[2]

$$|\xi\rangle = Z_A\,|0_\omega\rangle^f = C_{0,0}\left[\sum_n \left(-\frac{\nu}{\mu}\right)^n \frac{[f_1^\dagger]^n[f_2^\dagger]^n}{n!}\right]|0_\omega\rangle^f = C_{0,0}e^{-e^{i\theta}\tanh r\, \hat{f}_1^\dagger \hat{f}_2^\dagger}\,|0_\omega\rangle^f \tag{A.24}$$

which[3] implies here $\theta = \pi$ and $r = r_2$ in ζ, $\hat{A}$ and $\hat{B}$ of Eq. A.12. The normalization of (4.106) finally shows that $C_{0,0}^{-1} = \cosh r_2$.

A.2 . Eigenstates of the pseudo-spin operators

In this appendix we list the properties of the eigenstates of the pseudo-spin operators (4.191) which are useful in the main text. We will consider a given one of the three modes ($j = 0$, 1 or 2), always the same, and will omit the associated label (j) in order to lighten the notations. In a similar way, we do not write the ω-dependence which is implicit in all this appendix.
Let us define [106] the states

$$|\mathcal{E}\rangle = \frac{1}{\sqrt{2}}(|q\rangle + |-q\rangle) \qquad |\mathcal{O}\rangle = \frac{1}{\sqrt{2}}(|q\rangle - |-q\rangle) \tag{A.25}$$

with $|q\rangle$ the eigenstate of the position operator. Then one can define the operators

$$\hat{\mathbb{1}}_E = \int_0^\infty dq\,|\mathcal{E}\rangle\langle\mathcal{E}| \qquad \hat{\mathbb{1}}_O = \int_0^\infty dq\,|\mathcal{O}\rangle\langle\mathcal{O}| \tag{A.26}$$

One sees that for a generic state

$$|\psi_{e/o}\rangle = \int_{-\infty}^{+\infty} dq\,\psi_{e/o}(q)\,|q\rangle \tag{A.27}$$

with the wave function ψ_e even, i.e. $\psi_e(-q) = \psi_e(q)$, and the wave function ψ_o odd, i.e. $\psi_o(-q) = -\psi_o(q)$, one has

$$\hat{\mathbb{1}}_E\,|\psi_e\rangle = |\psi_e\rangle \qquad \hat{\mathbb{1}}_O\,|\psi_e\rangle = 0 \tag{A.28}$$

and

$$\hat{\mathbb{1}}_O\,|\psi_o\rangle = |\psi_o\rangle \qquad \hat{\mathbb{1}}_E\,|\psi_o\rangle = 0 \tag{A.29}$$

The parity operator or pseudo-spin operator (4.191c) is then defined as

$$\hat{\Pi}_z = \hat{\mathbb{1}}_E - \hat{\mathbb{1}}_O \qquad \hat{\Pi}_z\,|\psi_e\rangle = +\,|\psi_e\rangle \qquad \hat{\Pi}_z\,|\psi_o\rangle = -\,|\psi_o\rangle \tag{A.30}$$

The operators $\hat{\mathbb{1}}_E$ and $\hat{\mathbb{1}}_O$ can be expressed in the number representation basis. Indeed defining $|q\rangle = \sum_n C_n(q)\,|n\rangle$ and using $\hat{q} = (\hat{a} + \hat{a}^\dagger)/\sqrt{2}$ one obtains from $\langle n|\,\hat{q}\,|q\rangle = q\,\langle n|q\rangle$ with $\langle n|q\rangle = C_n(q)$ the recursive relation

$$\sqrt{n+1}\,C_{n+1}(q) + \sqrt{n}\,C_{n-1}(q) = \sqrt{2}\,q\,C_n(q) \tag{A.31}$$

[2] Applying $(a^\dagger)^n\,|0\rangle = \sqrt{n!}\,|n\rangle$.
[3] The same result would have been found if starting from $Z_A\hat{f}_2\,Z_A^{-1}$ instead by virtue of the symmetry $1 \leftrightarrow 2$ in (**??**) of the $f_i^\dagger$ operators.

Since

$$C_n(q) = \langle n|q\rangle = (2^n n!\sqrt{\pi}\,)^{-1/2}\exp(-q^2/2)H_n(q) \tag{A.32}$$

is a normalized Hermite function, relation (A.31) can be compared to the relation $H_{n+1}(q)+2nH_{n-1}(q) = 2q\,H_n(q)$ for the Hermite polynomials H_n. Then knowing that $H_n(-q) = (-1)^n H_n(q)$ one can see that $C_n(-q) = (-1)^n C_n(q)$. This last relation, since one has

$$\begin{aligned}\hat{\mathbb{1}}_{E/O} &= \frac{1}{2}\left[\int_0^{+\infty} dq\,|q\rangle\langle q| + \int_0^{+\infty} dq\,|-q\rangle\langle -q| \pm \int_0^{+\infty} dq\,|-q\rangle\langle q| \pm \int_0^{+\infty} dq\,|q\rangle\langle -q|\right]\\ &= \frac{1}{2}\left[\int_{-\infty}^{+\infty} dq\,|q\rangle\langle q| \pm \int_{-\infty}^{+\infty} dq\,|q\rangle\langle -q|\right]\\ &= \frac{1}{2}\left[1 \pm \int_{-\infty}^{+\infty} dq\,|q\rangle\langle -q|\right]\end{aligned} \tag{A.33}$$

and

$$\int_{-\infty}^{+\infty} dq\,|q\rangle\langle q| = 1 \Rightarrow \int_{-\infty}^{+\infty} C_n(q)C_m(q) = \delta_{nm} \tag{A.34}$$

where we used $\langle n|m\rangle = \delta_{nm}$, leads to

$$[\hat{\mathbb{1}}_{E/O}]_{nm} = \langle n|\,\hat{\mathbb{1}}_{E/O}\,|m\rangle = \frac{1}{2}\left(1 \pm (-1)^m\right)\delta_{nm} = \begin{cases}\delta_{nm} & \text{for } n \text{ even / odd}\\ 0 & \text{for } n \text{ odd / even}\end{cases} \tag{A.35}$$

that is to say

$$\begin{aligned}[\hat{\mathbb{1}}_E]_{nm} &= \sum_{n=0}^{\infty} |2n\rangle\langle 2n|\\ [\hat{\mathbb{1}}_O]_{nm} &= \sum_{n=0}^{\infty} |2n+1\rangle\langle 2n+1|\end{aligned} \tag{A.36}$$

and

$$\langle n|\,\hat{\Pi}_z\,|m\rangle = (-1)^m\delta_{nm} \tag{A.37}$$

Thus

$$\hat{\Pi}_z = \sum_{n=0}^{\infty}\Big(|2n\rangle\langle 2n| - |2n+1\rangle\langle 2n+1|\Big) \tag{A.38}$$

The eigenstates of $\hat{\Pi}_z$ are the number states and they have eigenvalue ± 1 depending on their parity. We denote them as

$$|z_n^+\rangle = |2n\rangle \quad \text{and} \quad |z_n^-\rangle = |2n+1\rangle \tag{A.39}$$

Contrarily to usual spins 1/2, the two eigenvalues (here $+1$ and -1) are infinitely degenerate[4] since every even function has eigenvalue $+1$ and every odd function has eigenvalue -1 : the **pseudo-spin** $\hat{\Pi}_z$ is nothing else than the **parity operator**. It is then worth noticing that this degeneracy property is shared by any projection of the pseudo-spin operator (4.191). Indeed, in the $|q\rangle$ basis, in addition to

$$\hat{\Pi}_z = \int_0^{\infty} dq\,|\mathcal{E}\rangle\langle\mathcal{E}| - \int_0^{\infty} dq\,|\mathcal{O}\rangle\langle\mathcal{O}| = \int_{-\infty}^{+\infty} dq\,|q\rangle\langle -q| \tag{A.40}$$

one has also

$$\begin{aligned}\hat{\Pi}_x &= \textstyle\int_0^{\infty} dq\,|\mathcal{E}\rangle\langle\mathcal{O}| + \int_0^{\infty} dq\,|\mathcal{O}\rangle\langle\mathcal{E}| = \int_0^{+\infty} dq\,|q\rangle\langle q| - \int_0^{+\infty} dq\,|-q\rangle\langle -q|\\ \hat{\Pi}_y &= i\textstyle\int_0^{\infty} dq\,|\mathcal{O}\rangle\langle\mathcal{E}| - i\int_0^{\infty} dq\,|\mathcal{E}\rangle\langle\mathcal{O}| = i\int_0^{+\infty} dq\,|q\rangle\langle -q| - i\int_0^{+\infty} dq\,|-q\rangle\langle q|\end{aligned} \tag{A.41}$$

Therefore, taking

$$\psi_o(q) = \begin{cases}\pm\,\psi_e(q) & \text{for } q \geq 0\\ \mp\,\psi_e(q) & \text{for } q < 0\end{cases} \tag{A.42}$$

[4]The two generic eigenfunction of the $\hat{\Pi}_z$ operator can be written as $|\psi_{e/o}\rangle = \sum_{n=0}^{+\infty} c_n^{\pm}|z_n^{\pm}\rangle$for the $+$ and $-$ eigenvalues, respectively.

one can write

$$\begin{aligned} |\psi_e\rangle &= \int_0^{+\infty} dq\, \psi_e(q)\, |q\rangle + \int_0^{+\infty} dq\, \psi_e(q)\, |-q\rangle \\ |\psi_o\rangle &= \int_0^{+\infty} dq\, [\pm\psi_e(q)]\, |q\rangle - \int_0^{+\infty} dq\, [\pm\psi_e(q)]\, |-q\rangle \end{aligned} \tag{A.43}$$

thus obtaining

$$\hat{\Pi}_x\, |\psi_e\rangle = \pm\, |\psi_o\rangle \qquad \hat{\Pi}_x\, |\psi_o\rangle = \pm\, |\psi_e\rangle \tag{A.44}$$

and

$$\hat{\Pi}_y\, |\psi_e\rangle = i \pm\, |\psi_o\rangle \qquad \hat{\Pi}_y\, |\psi_o\rangle = i \mp\, |\psi_e\rangle \tag{A.45}$$

The generic eigenstates of $\hat{\Pi}_x$ for eigenvalues ± 1 are then given by

$$|\psi_x^+\rangle = \frac{\pm}{\sqrt{2}}\Big(\, |\psi_e\rangle + |\psi_0\rangle\,\Big) \qquad |\psi_x^-\rangle = \frac{\pm}{\sqrt{2}}\Big(\, |\psi_e\rangle - |\psi_0\rangle\,\Big) \tag{A.46}$$

and those for $\hat{\Pi}_y$ for eigenvalues ± 1 by

$$|\psi_y^+\rangle = \frac{\pm}{\sqrt{2}}\Big(\, |\psi_e\rangle + i\, |\psi_0\rangle\,\Big) \qquad |\psi_y^-\rangle = \frac{\pm}{\sqrt{2}}\Big(\, |\psi_e\rangle - i\, |\psi_0\rangle\,\Big) \tag{A.47}$$

as long as the constraint (A.42) is verified.

The eigenstates $|x_n^\pm\rangle$ of $\hat{\Pi}_x$ associated to the eigenvalue ± 1 can also be constructed by rotating the eigenstates $|z_n^\pm\rangle$ of $\hat{\Pi}_z$ by angles $\pm\pi/2$ around the y axis, i.e.

$$|x_n^\pm\rangle = \hat{\mathcal{R}}_y\left(\pm\frac{\pi}{2}\right) |z_n^+\rangle = \frac{1}{\sqrt{2}}\left(\mathbb{1} \mp i\, \hat{\Pi}_y\right) |z_n^+\rangle \tag{A.48}$$

where $\hat{\mathcal{R}}_y(\theta) = \exp(-\frac{i}{2}\theta\, \hat{\Pi}_y)$ is the operator of rotation of angle θ around the y axis. The fact that $|x_n^\pm\rangle$ is an eigenstate of $\hat{\Pi}_x$ with eigenvalue ± 1 is easily checked by direct application of $\hat{\Pi}_x$ to the left of expression (A.48) and use of the relations

$$\hat{\Pi}_r \hat{\Pi}_s = i\, \varepsilon_{rst}\, \hat{\Pi}_t + \delta_{rs} \mathbb{1} \tag{A.49}$$

where ε_{rst} is the totally antisymmetric Levi-Civita symbol and $(r, s, t) = x$, y or z. Indeed

$$\hat{\Pi}_x |x_n^\pm\rangle = \frac{1}{\sqrt{2}}\left(\hat{\Pi}_x \pm \mathbb{1}\right) |z_n^+\rangle = \frac{1}{\sqrt{2}}\left(\hat{\Pi}_y^2 \hat{\Pi}_x \pm \mathbb{1}\right) |z_n^+\rangle = \frac{1}{\sqrt{2}}\left(-i\hat{\Pi}_y \hat{\Pi}_z \pm \mathbb{1}\right) |z_n^+\rangle = \pm |x_n^\pm\rangle \tag{A.50}$$

By the same token one obtains straightforwardly

$$|y_n^\pm\rangle = \hat{\mathcal{R}}_z\left(\pm\frac{\pi}{2}\right) |x_n^+\rangle \tag{A.51}$$

and

$$\hat{\Pi}_y |x_n^\pm\rangle = \mp i |x_n^\mp\rangle \qquad \hat{\Pi}_z |x_n^\pm\rangle = |x_n^\mp\rangle \tag{A.52a}$$

$$\hat{\Pi}_x |y_n^\pm\rangle = \pm i |y_n^\mp\rangle \qquad \hat{\Pi}_z |y_n^\pm\rangle = |y_n^\mp\rangle \tag{A.52b}$$

$$\hat{\Pi}_x |z_n^\pm\rangle = |z_n^\mp\rangle \qquad \hat{\Pi}_y |z_n^\pm\rangle = \pm i |z_n^\mp\rangle \tag{A.52c}$$

Applying (A.49) to the previous relations (A.52) gives the usual expressions of the $|z_n^\pm\rangle$ in terms of the $|x_n^\pm\rangle$ or $|y_n^\pm\rangle$. Then, through (A.38), these relations give straightforwardly the expression of $\hat{\Pi}_x$ and $\hat{\Pi}_y$ in the number representation basis, with[5]

$$\hat{\Pi}_x = \sum_{n=0}^{\infty} \Big(|x_n^+\rangle\langle x_n^+| - |x_n^-\rangle\langle x_n^-|\Big) = \sum_{n=0}^{\infty} \Big(|z_n^+\rangle\langle z_n^-| + |z_n^-\rangle\langle z_n^+|\Big) \tag{A.53}$$

and

$$\hat{\Pi}_y = \sum_{n=0}^{\infty} \Big(|y_n^+\rangle\langle y_n^+| - |y_n^-\rangle\langle y_n^-|\Big) = i \sum_{n=0}^{\infty} \Big(|z_n^-\rangle\langle z_n^+| - |z_n^+\rangle\langle z_n^-|\Big) \tag{A.54}$$

[5] Hence, any generic eigenfunction of the pseudo-spin operators can be written as $|\psi_s^\pm\rangle = \sum_{n=0}^{+\infty} (c_s^\pm)_n |s_n^\pm\rangle$ with $s = x, y, z$.

A.3 . The CHSH inequality

Let us say that Alice can measure two observables $\hat{A}$ and $\hat{A}'$ which yield respectively the outcomes $A = \{\pm 1\}$ and $A' = \{\pm 1\}$. Bob can also measure two observables $\hat{B}$ and $\hat{B}'$ which yield respectively the outcomes $B = \{\pm 1\}$ and $B' = \{\pm 1\}$. If Alice could perform two measurements at a time and so could Bob[6] then one would be able to define an observable $\hat{\mathscr{B}}$ and an outcome $\mathscr{B}$ such as

$$\mathscr{B} = (A + A')B + (A - A')B' = \pm 2 \tag{A.55}$$

It is then compulsory that

$$\hat{\mathscr{B}} = (\hat{A} + \hat{A}')\hat{B} + (\hat{A} - \hat{A}')\hat{B}' \qquad \Rightarrow \qquad |\langle\hat{\mathscr{B}}\rangle| \leq 2 \tag{A.56}$$

or, written explicitly,

$$|\langle\hat{A}\hat{B}\rangle + \langle\hat{A}'\hat{B}\rangle + \langle\hat{A}\hat{B}'\rangle - \langle\hat{A}'\hat{B}'\rangle| \leq 2 \tag{A.57}$$

This last relation (A.57) is called the *CHSH inequality* from Clauser-Horner-Shimony-Holt (see Ref. [105]). Since the averages $\langle . \rangle$ are statistical averages, the two measurements by Alice (and same for Bob) can now be not simultaneous, which means that Eq. (A.55) no longer holds but that Eqs. (A.56) and (A.57) still do. Referring to spin-$1/2$ measurements, one can define four unit vectors in a 3-dimensional real vector space, i.e. $\mathbf{a}$, $\mathbf{a}'$, $\mathbf{b}$ and $\mathbf{b}'$, and the spin observable

$$\hat{\mathbf{\Pi}} = \frac{\hbar}{2}\hat{\sigma} = \frac{\hbar}{2}(\sigma_x, \sigma_y, \sigma_z)^T \tag{A.58}$$

where the σ_i are the Pauli matrices. Then the observables can be set as

$$\hat{A} = \hat{\sigma}.\mathbf{a} \qquad \hat{A}' = \hat{\sigma}.\mathbf{a}' \qquad \hat{B} = \hat{\sigma}.\mathbf{b} \qquad \hat{B}' = \hat{\sigma}.\mathbf{b}' \tag{A.59}$$

Considering maximally entangled Bell states

$$\begin{aligned} |\Psi^{\pm}\rangle &= \frac{1}{\sqrt{2}}\left(|01\rangle \pm |10\rangle\right) \\ |\Phi^{\pm}\rangle &= \frac{1}{\sqrt{2}}\left(|00\rangle \pm |11\rangle\right) \end{aligned} \tag{A.60}$$

yields straightforwardly

$$\begin{aligned} &\langle\hat{\sigma}_x \otimes \hat{\sigma}_x\rangle_{\Psi^{\pm}} = \langle\hat{\sigma}_y \otimes \hat{\sigma}_y\rangle_{\Psi^{\pm}} = \pm 1 \qquad \langle\hat{\sigma}_z \otimes \hat{\sigma}_z\rangle_{\Psi^{\pm}} = -1 \\ &\langle\hat{\sigma}_x \otimes \hat{\sigma}_x\rangle_{\Phi^{\pm}} = -\langle\hat{\sigma}_y \otimes \hat{\sigma}_y\rangle_{\Phi^{\pm}} = \pm 1 \qquad \langle\hat{\sigma}_z \otimes \hat{\sigma}_z\rangle_{\Phi^{\pm}} = +1 \end{aligned} \tag{A.61}$$

with all the cross-terms $\langle\hat{\sigma}_r \otimes \hat{\sigma}_s\rangle$ where $r \neq s$ vanishing for all Bell states. Therefore from

$$\langle\hat{\sigma}_r \otimes \hat{\sigma}_s\rangle_{\Psi^-} = -\delta_{rs} \tag{A.62}$$

one obtains immediately

$$\langle\hat{A}\hat{B}\rangle_{\Psi^-} = \sum_{r,s} a_r b_s \langle\hat{\sigma}_r \otimes \hat{\sigma}_s\rangle_{\Psi^-} = -\sum_{r,s} a_r b_s \delta_{rs} = -\mathbf{a}.\mathbf{b} = -\cos\theta \tag{A.63}$$

In order to maximise the left-hand side $|\langle\hat{\mathscr{B}}^{(i,j,k)}\rangle|$ of the inequality (A.57), one must extremize

$$\langle\hat{\mathscr{B}}\rangle_{\Psi^-} = -\mathbf{a}.\mathbf{b} - \mathbf{a}'.\mathbf{b} - \mathbf{a}.\mathbf{b}' + \mathbf{a}'.\mathbf{b}' = -(\mathbf{a} + \mathbf{a}').\mathbf{b} - (\mathbf{a} - \mathbf{a}').\mathbf{b}' \tag{A.64}$$

[6] This is not possible for non commuting quantum observables $\hat{A}$ and $\hat{A}'$ (or $\hat{B}$ and $\hat{B}'$) but the example helps understanding the upper and lower bounds of classical observations.Let us remark here that the observations by Alice and those by Bob do commute : hence, in the following, the tensor product structure of the observable describing a "simultaneous" observation by Alice and Bob with one of their respective observables.

One writes

$$k_+\boldsymbol{a}_+ = \boldsymbol{a} + \boldsymbol{a}' \qquad k_-\boldsymbol{a}_- = \boldsymbol{a} - \boldsymbol{a}' \tag{A.65}$$

which implies, for $\boldsymbol{a}.\boldsymbol{a}' = \cos\varphi$,

$$k_+^2 = 4\cos^2\frac{\varphi}{2} \qquad k_-^2 = 4\sin^2\frac{\varphi}{2} \tag{A.66}$$

One is left with

$$\langle\hat{\mathscr{B}}\rangle_{\Psi^-} = -2\cos\frac{\varphi}{2}\mathbf{a}_+.\mathbf{b} - 2\sin\frac{\varphi}{2}\mathbf{a}_-.\mathbf{b}' \tag{A.67}$$

This last expression looks like $f(\phi) = x\cos\phi + y\sin\phi = \rho\cos(\phi-\varphi)$ for $x = \rho\cos\varphi$ and $y = \rho\sin\varphi$. Then one sees that f is maximum for $f_{\max} = \rho$ and since $\rho^2 = x^2 + y^2$ one can maximize $\langle\hat{\mathscr{B}}\rangle$ by obtaining for the right hand side of (A.57)

$$2\sqrt{[\mathbf{a}_+.\mathbf{b}]^2 + [\mathbf{a}_-.\mathbf{b}']^2} \tag{A.68}$$

Then aligning $\boldsymbol{b}$ along $\boldsymbol{a}_+$ and $\boldsymbol{b}'$ along $\boldsymbol{a}_-$[7] one obtains the maximization

$$\max|\langle\hat{\mathscr{B}}\rangle|_{\Psi^-} = 2\sqrt{2} \tag{A.69}$$

which violates inequality (A.57). One can see from this maximization that all the vectors lie in the same plane. By going back to (A.61) it can be seen that for any Bell state a plane can be found where (A.63) holds, thus making it possible to maximize in a similar way the violation of Bell's inequality to $2\sqrt{2}$ with all Bell states[8].
The upper bound of the violation, also called Cirel'son bound [159], can intuitively be found by considering that

$$\langle\hat{\mathscr{B}}\rangle^2 \leq \langle\hat{\mathscr{B}}^2\rangle \tag{A.70}$$

With operators such as the Pauli matrices which verify

$$(\mathbf{n}.\hat{\sigma})^2 = \mathbb{1} \tag{A.71}$$

one obtains

$$\hat{\mathscr{B}}^2 = 4\mathbb{1} - [\hat{A},\hat{A}'][\hat{B},\hat{B}'] \tag{A.72}$$

Recalling the algebra of the Pauli matrices, i.e.

$$[\hat{\sigma}_i,\hat{\sigma}_j] = 2i\epsilon_{ijk}\hat{\sigma}_k \qquad \{\hat{\sigma}_i,\hat{\sigma}_j\} = 2\delta_{ij}\mathbb{1} \tag{A.73}$$

one obtains

$$\langle\hat{\mathscr{B}}^2\rangle \leq 8 \quad \Rightarrow \quad \langle\hat{\mathscr{B}}\rangle \leq \sqrt{8} \tag{A.74}$$

A.4 . Analytic maximization of $\langle\hat{\mathscr{B}}^{(i|j)}\rangle$

In this appendix we present the maximisation of the expectation value of the CHSH operator (4.210). The well-known maximization procedure can also be found, for example, in Refs. [191, 192]. With $r, s \in$

[7] This amounts for example, with $\mathbf{a}.\mathbf{a}' = \mathbf{0}$, to take

$$\mathbf{a}.\mathbf{b} = \mathbf{a}'.\mathbf{b} = \mathbf{a}.\mathbf{b}' = \cos\frac{\pi}{4} = \frac{1}{\sqrt{2}} \qquad \mathbf{a}'.\mathbf{b}' = \cos\frac{3\pi}{4} = -\frac{1}{\sqrt{2}}$$

with all the vectors lying in the same plane.

[8] More precisely one must choose the xy plane for Ψ_+, the xz plane for Φ_+ and the yz for Φ_-. For these three states one would get $\langle\hat{A}\hat{B}\rangle = +\cos\theta$ in (A.63).

$\{x,y,z\}$ and $\hat{\Pi}$ a pseudo-spin operator acting in the space of particle i or j, one has

$$\begin{aligned}
\langle\hat{\mathscr{B}}^{(i,j)}\rangle &= \langle\mathbf{a}.\hat{\mathbf{\Pi}}^{(\mathbf{i})}\otimes\mathbf{b}.\hat{\mathbf{\Pi}}^{(\mathbf{j})}\rangle+\langle\mathbf{a}'.\hat{\mathbf{\Pi}}^{(\mathbf{i})}\otimes\mathbf{b}.\hat{\mathbf{\Pi}}^{(\mathbf{j})}\rangle+\langle\mathbf{a}.\hat{\mathbf{\Pi}}^{(\mathbf{i})}\otimes\mathbf{b}'.\hat{\mathbf{\Pi}}^{(\mathbf{j})}\rangle-\langle\mathbf{a}'.\hat{\mathbf{\Pi}}^{(\mathbf{i})}\otimes\mathbf{b}'.\hat{\mathbf{\Pi}}^{(\mathbf{j})}\rangle\\
&= \sum_{r,s}[\langle a_r\hat{\Pi}_r^{(i)}\otimes b_s\hat{\Pi}_s^{(j)}\rangle+\langle a'_r\hat{\Pi}_r^{(i)}\otimes b_s\hat{\Pi}_s^{(j)}\rangle+\langle a_r\hat{\Pi}_r^{(i)}\otimes b'_s\hat{\Pi}_s^{(j)}\rangle-\langle a'_r\hat{\Pi}_r^{(i)}\otimes b'_s\hat{\Pi}_s^{(j)}\rangle]\\
&= \sum_r[a_r\sum_s\mathcal{T}_{rs}^{(ij)}b_s+a'_r\sum_s\mathcal{T}_{rs}^{(ij)}b_s+a_r\sum_s\mathcal{T}_{rs}^{(ij)}b'_s-a'_r\sum_s\mathcal{T}_{rs}^{(ij)}b'_s]\\
&= \sum_r[a_r\,(\mathcal{T}\mathbf{b})_r+a'_r\,(\mathcal{T}\mathbf{b})_r+a_r\,(\mathcal{T}\mathbf{b}')_r-a'_r\,(\mathcal{T}\mathbf{b}')_r]\\
&= \mathbf{a}.(\mathcal{T}\mathbf{b})+\mathbf{a}'.(\mathcal{T}\mathbf{b})+\mathbf{a}.(\mathcal{T}\mathbf{b}')-\mathbf{a}'.(\mathcal{T}\mathbf{b}')\\
&= (\mathbf{a}+\mathbf{a}').(\mathcal{T}\mathbf{b})+(\mathbf{a}-\mathbf{a}').(\mathcal{T}\mathbf{b}')
\end{aligned}\tag{A.75}$$

As previously in section (A.3), let us define

$$k_+\mathbf{a}_+=\mathbf{a}+\mathbf{a}'\qquad\qquad k_-\mathbf{a}_-=\mathbf{a}-\mathbf{a}'\tag{A.76}$$

This implies $\mathbf{a}_+.\mathbf{a}_-=0$. Then, taking $\mathbf{a}_\pm$, $\mathbf{a}$ and $\mathbf{a}'$ normalized to one and $\mathbf{a}.\mathbf{a}'=\cos\theta$ with $\theta\in[0,\pi]$ one gets

$$k_+=2\cos\frac{\theta}{2}\qquad\qquad k_-=2\sin\frac{\theta}{2}\tag{A.77}$$

that is to say

$$\langle\hat{\mathscr{B}}^{(i,j)}\rangle=\mathbf{a}_+.(\mathcal{T}\mathbf{b})2\cos\frac{\theta}{2}+\mathbf{a}_-.(\mathcal{T}\mathbf{b}')2\sin\frac{\theta}{2}\tag{A.78}$$

Again, this last expression looks like $f(\phi)=x\cos\phi+y\sin\phi=\rho\cos(\phi-\varphi)$ for $x=\rho\cos\varphi$ and $y=\rho\sin\varphi$. Then one sees that f is maximum for $f_{\max}=\rho$ and since $\rho^2=x^2+y^2$ one can maximize $\langle\hat{\mathscr{B}}^{(i,j,k)}\rangle$ by obtaining for the right hand side of (A.75)

$$2\sqrt{[\mathbf{a}_+.(\mathcal{T}\mathbf{b})]^2+[\mathbf{a}_-.(\mathcal{T}\mathbf{b}')]^2}\tag{A.79}$$

Clearly, one can see that this expression is maximal for $\mathbf{a}_+.\mathcal{T}\mathbf{b}=\|\mathbf{a}_+\|\|\mathcal{T}\mathbf{b}\|\cos\phi_+$ and for $\mathbf{a}_-.\mathcal{T}\mathbf{b}=\|\mathbf{a}_-\|\|\mathcal{T}\mathbf{b}'\|\cos\phi_-$ with ϕ_+ and ϕ_- equal to 0 or π. But since the two scalar products and all the components of the matrix and of the vectors are here real, taking the hermitian conjugate of the previous relations, one has $\mathbf{a}_+.\mathcal{T}\mathbf{b}=\mathbf{b}.\hat{\mathcal{T}}^T\mathbf{a}_+$ and $\mathbf{a}_-.\mathcal{T}\mathbf{b}'=\mathbf{b}'.\hat{\mathcal{T}}^T\mathbf{a}_-$. Thus one has also $\mathbf{b}.\mathcal{T}^{\mathbf{T}}\mathbf{a}_+=\|\mathbf{b}\|\|\mathcal{T}^{\mathbf{T}}\mathbf{a}_+\|\cos\varphi_+$ and $\mathbf{b}'.\mathcal{T}^{\mathbf{T}}\mathbf{a}_-=\|\mathbf{b}'\|\|\mathcal{T}^{\mathbf{T}}\mathbf{a}_-\|\cos\varphi_-$ which is of course still maximal for φ_+ and φ_- equal to 0 or π. With the vectors $\mathbf{b}$ and $\mathbf{b}'$ normalized to unity, this implies that the previous expression for the r.h.s of (A.75) is just

$$2\sqrt{||\hat{\mathcal{T}}^T\mathbf{a}_+||^2+||\hat{\mathcal{T}}^T\mathbf{a}_-||^2}\tag{A.80}$$

which has still to be maximized with the conditions $\mathbf{a}_+.\mathbf{a}_-=0$ and $\mathbf{a}_{+/-}$ normalized. As shown in [192], in the previous relation, one has the scalar product for example $[a_+]_r\mathcal{T}_{rt}\mathcal{T}_{ts}^T[a_+]_s$. The matrix $\mathcal{T}\mathcal{T}^T$ being symmetric it can be diagonalized and has real eigenvalues. In order to maximize our relation one must take in this scalar product $\mathbf{a}_+$ as being the eigenvector of the extremal (maximal or minimal) eigenvalue λ_1 of the matrix $\mathcal{T}\mathcal{T}^T$. Then, since $\mathbf{a}_+$ and $\mathbf{a}_-$ are orthogonal one must take $\mathbf{a}_-$ as being the eigenvector of the second extremal (maximal or minimal) eigenvalue λ_2 of the matrix $\mathcal{T}\mathcal{T}^T$. One is finally left with

$$\max_{\mathbf{a}_+,\mathbf{a}_-}||\hat{\mathcal{T}}^T\mathbf{a}_+||^2+||\hat{\mathcal{T}}^T\mathbf{a}_-||^2=\lambda_1^2+\lambda_2^2\tag{A.81}$$

Let us remark that one could have also defined from (A.75) the $\mathbf{a}_\pm$ vectors not as given in (A.76) but as $k_+\mathbf{a}_+=\mathbf{b}+\mathbf{b}'$ and $k_-\mathbf{a}_-=\mathbf{a}-\mathbf{a}'$. In this case one would have ended up with a maximization of (A.75) given by

$$\max_{\mathbf{a}_+,\mathbf{a}_-}||\hat{\mathcal{T}}\mathbf{a}_+||^2+||\hat{\mathcal{T}}\mathbf{a}_-||^2=\lambda_1^2+\lambda_2^2\tag{A.82}$$

which implies that $\mathcal{T}\mathcal{T}^T$ and $\mathcal{T}^T\mathcal{T}$ have same eigenvalues[9]. Thus the CHSH parameter $B^{(i|2)}(\omega)$ defined in (4.211) reads

$$B^{(i|2)}=2\sqrt{\lambda_1+\lambda_2}\,,\tag{A.83}$$

[9]The two matrices have different off-diagonal terms at non zero temperature for $j=2$ but their eigenvalues given in (A.88) are the same even if for $\mathcal{T}\mathcal{T}^T$ one has $C=\mathcal{T}_{xx}^{(ij)}\mathcal{T}_{yx}^{(ij)}+\mathcal{T}_{yy}^{(ij)}\mathcal{T}_{xy}^{(ij)}$ which differs by a minus sign from the C given in (A.87).

where λ_1 and λ_2 are the two largest eigenvalues of matrix $\mathcal{T}^{\mathrm{T}}\mathcal{T}$ where $\mathcal{T}(\omega)$ is the 3×3 matrix with entries

$$\mathcal{T}_{rs}^{(ij)} = \left\langle \hat{\Pi}_r^{(i)} \otimes \hat{\Pi}_s^{(j)} \right\rangle, \tag{A.84}$$

with $(r,s)\in\{x,y,z\}^2$ (see Eq. (4.194)) and $(ij)=(01),(02)$ or (12). The similar procedure for obtaining the upper bound of expression (A.83), also known as the Cirel'son bound, has already been mentioned at the end of Appendix A.3. Therefore the upper bound of $B^{(i|2)}$ corresponds to the value $2\sqrt{2}$ given in (A.74).

At zero temperature or at any finite temperature in a generic basis where the covariance matrix $\sigma_{\mathbf{e}}$ is *not* necessarily in its standard form, the 3×3 hermitian matrix $\mathcal{T}^T\mathcal{T}$ given in (A.82) must be diagonalized in order to obtain the two extremal eigenvalues needed to maximize (A.80) through (A.81) : then $\mathbf{a}_+$ and $\mathbf{a}_-$ will be the two eigenvectors of this matrix corresponding to the two extremal eigenvalues [10]. The results presented in Appendix A.10.2 show that in all the cases we consider the matrix $\mathcal{T}(\omega)$ is block diagonal[11] :

$$\mathcal{T} = \begin{pmatrix} \mathcal{T}_{xx} & \mathcal{T}_{xy} & 0 \\ \mathcal{T}_{yx} & \mathcal{T}_{yy} & 0 \\ 0 & 0 & \mathcal{T}_{zz} \end{pmatrix}, \tag{A.85}$$

and thus

$$\mathcal{T}^{\mathrm{T}}\mathcal{T} = \begin{pmatrix} A & C & 0 \\ C & B & 0 \\ 0 & 0 & \mathcal{T}_{zz}^2 \end{pmatrix}, \tag{A.86}$$

with

$$A = \mathcal{T}_{xx}^2 + \mathcal{T}_{yx}^2 \quad B = \mathcal{T}_{yy}^2 + \mathcal{T}_{xy}^2 \quad C = \mathcal{T}_{xx}\mathcal{T}_{xy} + \mathcal{T}_{yy}\mathcal{T}_{yx} \tag{A.87}$$

one obtains the eigenvalues

$$\begin{aligned} \lambda_1 &= \mathcal{T}_{zz}^2 \\ \lambda_2 &= \frac{A+B+\sqrt{(A-B)^2+4C^2}}{2} \\ \lambda_3 &= \frac{A+B-\sqrt{(A-B)^2+4C^2}}{2} \end{aligned} \tag{A.88}$$

defined in such a way that

$$\lambda_1 \underset{T=0}{\to} \mathcal{T}_{zz}^2\Big|_{T=0} \qquad \lambda_2 \underset{T=0}{\to} \mathcal{T}_{xx}^2\Big|_{T=0} \qquad \lambda_3 \underset{T=0}{\to} \mathcal{T}_{yy}^2\Big|_{T=0} \tag{A.89}$$

with the largest eigenvalues of matrix $\mathcal{T}^{\mathrm{T}}\mathcal{T}$ for zero or finite temperature being always λ_1 and λ_2 as can be seen from the final remarks in Appendix A.10.2. For the two-mode state $i2$ with $i=0,1$ they can be computed from Expressions (4.196), (4.198) and (A.87). The detailed computations for all the (ij) states are given in Appendix A.10.2. With this in mind, Eq. (A.83) determines the value of the CHSH parameter (4.211).

As a final remark we can recall here that instead of choosing to work in the basis of the c-modes, one may perform a Local Linear Unitary BOgoliubov transformation (LLUBO) for attempting to simplify the form of the covariance matrix. As already stated in Appendix 4.3.3, in the bipartite case, the 4×4 covariance matrix (4.175) associated with the reduced two-mode state $(i|2)$ can be brought by an appropriately chosen LLUBO to a standard form where the matrix ε_{i2} are diagonal [117]. Working in this basis does not alter the entanglement properties of the system (they remain unaffected compared to that of the c-modes), but makes the computations easier and may improve the signal of nonlocality. In this basis the result (4.196) is not affected and *at any (zero or finite) temperature* expressions (4.198) modify to

$$\begin{aligned} \mathcal{T}_{xx} &= \frac{2}{\pi}\arctan\frac{2\left|\langle \hat{c}_i \hat{c}_2\rangle\right|}{\sqrt{A_{i2}}} = -A_{i2}\mathcal{T}_{yy}, \\ \mathcal{T}_{xy} &= \mathcal{T}_{yx} = 0, \end{aligned} \tag{A.90}$$

[10] For $j=1$ and therefore $i=0$ the matrix $\mathcal{T}$ is hermitian and therefore the eigenvalues of $\mathcal{T}^T\mathcal{T}$ are just the eigenvalues of $\mathcal{T}$ squared.

[11] For simplicity we write $\mathcal{T}_{rs}^{(ij)}$ simply as $\mathcal{T}_{rs}$ since the i and j can easily be restored.

where A_{i2} is defined in Eq. (4.199). The matrix $\mathcal{T}$ is thus diagonal and λ_2 in expression (A.88) is equal to $\mathcal{T}_{xx}^2$. Equation (A.83) then reads

$$B^{(i|2)} = 2\sqrt{\mathcal{T}_{xx}^2 + \mathcal{T}_{zz}^2} \tag{A.91a}$$

$$= 2\sqrt{\frac{4}{\pi^2}\arctan^2\left(\frac{2|\langle \hat{c}_i \hat{c}_2\rangle|}{\sqrt{A_{i2}}}\right) + \frac{1}{A_{i2}^2}}\,. \tag{A.91b}$$

We note here that the difference between the result (A.83) evaluated in the c-mode basis and expression (A.91b) is always small. The reason is that, in the c-mode basis, the off diagonal entries of the upper left blocks of matrix (A.85) and (A.86) are always small compared to the diagonal ones, because at all temperature $|\mathrm{Im}\,\langle \hat{c}_i \hat{c}_2\rangle| \ll |\mathrm{Re}\,\langle \hat{c}_i \hat{c}_2\rangle|$. However, our numerical checks always demonstrate a small increase of the Bell parameter (A.91b) compared to the one evaluated using (A.83) in the c-mode basis. We thus present our numerical results in Figs. 4.2, 4.3, 4.3, 4.4, 4.7 and 4.7 using formula (A.91b).

To summarize, the result (A.91b) should be considered as an optimized value of the witness of non-locality $B^{(i|2)}$. We note here that we do not have a general proof of the better efficiency of the method which consists in using the basis in which the covariance matrix is in its standard form, but we believe that a general mathematical result of this type would be quite useful.

A.5 . Tripartite Cirel'son bound and analytic maximization of $\langle \hat{\mathscr{S}}^{(0|1|2)}(\omega = 0)\rangle$

In this section we first study the upper bound of the quantity $S^{(0|1|2)}(\omega)$ defined in (4.216) and then study the possibility of maximisation of the average $\langle \hat{\mathscr{S}}^{(0|1|2)}\rangle$ of the operator (4.215) by an appropriate choice of the measurement directions $\boldsymbol{a}$, $\boldsymbol{a}'$, $\boldsymbol{b}$, $\boldsymbol{b}'$, $\boldsymbol{c}$ and $\boldsymbol{c}'$. Denoting as $\hat{A} = \boldsymbol{a}\cdot\hat{\boldsymbol{\Pi}}^{(0)}$, $\hat{A}' = \boldsymbol{a}'\cdot\hat{\boldsymbol{\Pi}}^{(0)}$, $\hat{B} = \boldsymbol{b}\cdot\hat{\boldsymbol{\Pi}}^{(1)}$, etc. makes it possible to write the square of the tripartite Svetlichny operator (4.215) as

$$\begin{aligned} 4\left(\hat{\mathscr{S}}^{(0|1|2)}\right)^2 =& 8 + \{\hat{A},\hat{A}'\}\otimes\{\hat{B},\hat{B}'\}\otimes\{\hat{C},\hat{C}'\} \\ &- 2[\hat{A},\hat{A}']\otimes[\hat{B},\hat{B}']\otimes\mathbb{1}^{(2)} \\ &- 2\mathbb{1}^{(0)}\otimes[\hat{B},\hat{B}']\otimes[\hat{C},\hat{C}'] \\ &- 2[\hat{A},\hat{A}'].\otimes\mathbb{1}^{(1)}\otimes[\hat{C},\hat{C}'], \end{aligned} \tag{A.92}$$

where $[\cdot,\cdot]$ and $\{\cdot,\cdot\}$ denote the commutator and the anticommutator, respectively. From the SU(2) algebra of the pseudo-spins it is easily proven that

$$[\hat{A},\hat{A}'] = 2i(\boldsymbol{a}\times\boldsymbol{a}')\cdot\hat{\boldsymbol{\Pi}}^{(0)}, \tag{A.93a}$$

$$\{\hat{A},\hat{A}'\} = 2(\boldsymbol{a}\cdot\boldsymbol{a}')\mathbb{1}^{(0)}, \tag{A.93b}$$

with similar formulae for the quantities $\hat{B}$, $\hat{B}'$ and $\hat{C}$, $\hat{C}'$. Since the operators $\hat{A}$, $\hat{B}$ and $\hat{C}$ operate in different Hilbert spaces, one can assume without loss of generality that all the vector products of type (A.93a) appearing in (A.92) are colinear with $\boldsymbol{e}_z$. In this case all the unit vectors $\boldsymbol{a}$, $\boldsymbol{a}'$, $\boldsymbol{b}$, $\boldsymbol{b}'$, $\boldsymbol{c}$ and $\boldsymbol{c}'$ lie in the xy plane. Denoting as θ_a the angle between $\boldsymbol{a}'$ and $\boldsymbol{a}$, θ_b the angle between $\boldsymbol{b}'$ and $\boldsymbol{b}$, and θ_c the angle between $\boldsymbol{c}'$ and $\boldsymbol{c}$ (all these angles being in $[0,\pi]$), one gets

$$\begin{aligned} \left(\hat{\mathscr{S}}^{(0|1|2)}\right)^2 =& 2 + 2\cos\theta_a\cos\theta_b\cos\theta_c \\ &+ 2\sin\theta_a\sin\theta_b\,\hat{\Pi}_z^{(0)}\otimes\hat{\Pi}_z^{(1)}\otimes\mathbb{1}^{(2)} \\ &+ 2\sin\theta_b\sin\theta_c\,\mathbb{1}^{(0)}\otimes\hat{\Pi}_z^{(1)}\otimes\hat{\Pi}_z^{(2)} \\ &+ 2\sin\theta_a\sin\theta_c\,\hat{\Pi}_z^{(0)}\otimes\mathbb{1}^{(1)}\otimes\hat{\Pi}_z^{(2)} \end{aligned} \tag{A.94}$$

It is a simple matter to check that when θ_a, θ_b and θ_c run each through $[0,2\pi]$ the eigenvalues of the operator appearing in the right hand side of the above formula are all comprised in $[0,8]$. The extremal values 0 and 8 are reached for $(\theta_a,\theta_b,\theta_c) = (0,0,\pi)$ and $(\pi/2,\pi/2,\pi/2)$, respectively. It then follows that for any choice of the measurement directions $\boldsymbol{a}$, $\boldsymbol{a}'$, $\boldsymbol{b}$, $\boldsymbol{b}'$, $\boldsymbol{c}$ and $\boldsymbol{c}'$

$$\left\langle \hat{\mathscr{S}}^{(0|1|2)}\right\rangle^2 \leq \left\langle (\hat{\mathscr{S}}^{(0|1|2)})^2\right\rangle \leq 8 \tag{A.95}$$

and thus the tripartite entanglement parameter (4.216) verifies

$$S^{(0|1|2)}(\omega) \leq 2\sqrt{2} \tag{A.96}$$

This is the tripartite equivalent of Cirel'son bound.

In the remaining of this Appendix we consider a related but somehow different problem. In order to violate as much as possible the Svetlichny inequality $S^{(0|1|2)} < 2$ we aim at choosing measurement directions $\boldsymbol{a}$, $\boldsymbol{a}'$, $\boldsymbol{b}$, $\boldsymbol{b}'$, $\boldsymbol{c}$ and $\boldsymbol{c}'$ which maximize the expectation value of $\hat{\mathscr{S}}^{(0|1|2)}$. This can be done numerically as explained in Appendix A.6. We show here that this maximization can also be performed analytically in a particular instance. As previously in section (A.3), let us define

$$k_+\mathbf{a}_+ = \mathbf{a} + \mathbf{a}' \qquad k_-\mathbf{a}_- = \mathbf{a} - \mathbf{a}' \tag{A.97}$$

This implies $\mathbf{a}_+.\mathbf{a}_- = 0$. Then, taking $\mathbf{a}_\pm$, $\mathbf{a}$ and $\mathbf{a}'$ normalized to one and $\mathbf{a}.\mathbf{a}' = \cos\theta$ with $\theta \in [0, \pi]$ one obtains

$$k_+ = 2\cos\frac{\theta}{2} \qquad k_- = 2\sin\frac{\theta}{2} \tag{A.98}$$

which yields in (4.216)

$$\begin{aligned}\langle\hat{\mathscr{S}}^{(0,1,2)}\rangle \;=\; &+\cos\frac{\theta}{2}\langle\mathbf{a}_+.\hat{\mathbf{\Pi}}^{(\mathbf{0})}\otimes\mathbf{b}.\hat{\mathbf{\Pi}}^{(\mathbf{1})}\otimes\mathbf{c}'.\hat{\mathbf{\Pi}}^{(\mathbf{2})}\rangle + \sin\frac{\theta}{2}\langle\mathbf{a}_-.\hat{\mathbf{\Pi}}^{(\mathbf{0})}\otimes\mathbf{b}'.\hat{\mathbf{\Pi}}^{(\mathbf{1})}\otimes\mathbf{c}'.\hat{\mathbf{\Pi}}^{(\mathbf{2})}\rangle \\ &+\cos\frac{\theta}{2}\langle\mathbf{a}_+.\hat{\mathbf{\Pi}}^{(\mathbf{0})}\otimes\mathbf{b}'.\hat{\mathbf{\Pi}}^{(\mathbf{1})}\otimes\mathbf{c}.\hat{\mathbf{\Pi}}^{(\mathbf{2})}\rangle - \sin\frac{\theta}{2}\langle\mathbf{a}_-.\hat{\mathbf{\Pi}}^{(\mathbf{0})}\otimes\mathbf{b}.\hat{\mathbf{\Pi}}^{(\mathbf{1})}\otimes\mathbf{c}.\hat{\mathbf{\Pi}}^{(\mathbf{2})}\rangle\end{aligned} \tag{A.99}$$

Defining

$$\begin{aligned}W &= \langle\mathbf{a}_+.\hat{\mathbf{\Pi}}^{(\mathbf{i})}\otimes\mathbf{b}.\hat{\mathbf{\Pi}}^{(\mathbf{j})}\otimes\mathbf{c}'.\hat{\mathbf{\Pi}}^{(\mathbf{k})}\rangle \\ Z &= \langle\mathbf{a}_+.\hat{\mathbf{\Pi}}^{(\mathbf{i})}\otimes\mathbf{b}'.\hat{\mathbf{\Pi}}^{(\mathbf{j})}\otimes\mathbf{c}.\hat{\mathbf{\Pi}}^{(\mathbf{k})}\rangle \\ X &= \langle\mathbf{a}_-.\hat{\mathbf{\Pi}}^{(\mathbf{i})}\otimes\mathbf{b}'.\hat{\mathbf{\Pi}}^{(\mathbf{j})}\otimes\mathbf{c}'.\hat{\mathbf{\Pi}}^{(\mathbf{k})}\rangle \\ Y &= \langle\mathbf{a}_-.\hat{\mathbf{\Pi}}^{(\mathbf{i})}\otimes\mathbf{b}.\hat{\mathbf{\Pi}}^{(\mathbf{j})}\otimes\mathbf{c}.\hat{\mathbf{\Pi}}^{(\mathbf{k})}\rangle\end{aligned} \tag{A.100}$$

the previous expression (A.99) giving the average of the three-mode operator (4.215) becomes, taking $\theta = \phi/2$,

$$\langle\hat{\mathscr{S}}^{(0|1|2)}\rangle = (W+Z)\cos\phi + (X-Y)\sin\phi, \tag{A.101}$$

One can then easily see that, exactly as previously in section (A.3), this last expression looks like $f(\phi) = x\cos\phi + y\sin\phi = \rho\cos(\phi-\varphi)$ for $x = \rho\cos\varphi$ and $y = \rho\sin\varphi$. Then one sees that f is maximum for $f_{\max} = \rho$ with $\rho^2 = x^2 + y^2$. Therefore it is convenient to introduce temporarily the notations

$$W + Z = \rho\cos\varphi, \quad X - Y = \rho\sin\varphi \tag{A.102}$$

which make it possible to cast (A.101) under the simple form

$$\langle\hat{\mathscr{S}}^{(0|1|2)}\rangle = \rho\cos(\phi-\varphi) \tag{A.103}$$

The maximum value of this expression is ρ, i.e.

$$\max_\theta\langle\hat{\mathscr{S}}^{(0|1|2)}\rangle = \sqrt{(W+Z)^2 + (X-Y)^2}. \tag{A.104}$$

The next step of the maximization procedure is easily performed at zero temperature and zero energy ($\omega = 0$). The reason is that, as illustrated in a typical case by (A.114), the explicit expressions of the W, X, Y, Z coefficients in (A.100) and (A.104) involve combinations of terms of the type $\mathcal{T}_{rst}$ (as defined in Eq. (4.195)) that take on particularly simple values at $T = 0$ and $\omega = 0$. Firstly, all the $\mathcal{T}_{rst}$ with at least one component along x vanish. Therefore, the contribution of the components along x of the different

vectors involved in (A.100) cancels. It is thus enough to perform the maximization only considering vectors $\boldsymbol{a}_\pm$, $\boldsymbol{b}$, $\boldsymbol{b}'$, $\boldsymbol{c}$ and $\boldsymbol{c}'$ lying in the y,z plane. A second simplification stems from the fact that, in the y,z plane, all the $\mathcal{T}_{rst}$'s with an odd number of y cancel at $T=0$ and $\omega=0$. In the waterfall and delta peak configurations[12] the only non-zero coefficients are (see the discussion in Appendix 4.3.1)

$$\mathcal{T}_{zzz}=\mathcal{T}_{yyz}=\mathcal{T}_{yzy}=-\mathcal{T}_{zyy}=1. \tag{A.105}$$

In this case, the particular choice

$$\boldsymbol{a}_+=\boldsymbol{b}=\boldsymbol{c}'=\boldsymbol{e}_z,\quad \boldsymbol{a}_-=-\boldsymbol{b}'=-\boldsymbol{c}=\boldsymbol{e}_y, \tag{A.106}$$

plugged in Eqs. (A.100) leads to

$$\begin{aligned} W+Z&=\mathcal{T}_{zzz}+\mathcal{T}_{zyy}=2,\\ X-Y&=-\mathcal{T}_{yyz}+\mathcal{T}_{yzy}=2. \end{aligned} \tag{A.107}$$

and expression (A.104) then shows that the upper bound (A.96) is reached. It is therefore not possible that another arrangement of vectors $\boldsymbol{a}$, $\boldsymbol{a}'$, $\boldsymbol{b}$, $\boldsymbol{b}'$, $\boldsymbol{c}$ and $\boldsymbol{c}'$ reaches a higher value and thus

$$S^{(0|1|2)}(\omega=0)\underset{T=0}{=}2\sqrt{2}. \tag{A.108}$$

The situation is completely different at finite temperature. In this case, as explained in Appendix 4.3.1 all the averages of the type (4.195) cancel when $\omega\to 0$. It then follows that the quantities (A.100) behave in the same way and thus

$$S^{(0|1|2)}(\omega=0)\underset{T\neq 0}{=}0. \tag{A.109}$$

A final remark regarding the maximal value of $S^{(0|1|2)}(\omega)$ at zero temperature when computed in the $\{\mathbf{f}\}$ basis. In this basis, at zero temperature, one has at all energies

$$\mathcal{T}_{rst}\underset{\{\mathbf{f}\}}{=}\langle\hat{\Pi}_r^{(f_0)}\otimes\hat{\Pi}_s^{(f1)}\otimes\hat{\Pi}_t^{(f2)}\rangle=\langle\hat{\Pi}_r^{(f_0)}\rangle\langle\hat{\Pi}_s^{(f1)}\otimes\hat{\Pi}_t^{(f2)}\rangle \tag{A.110}$$

with

$$\langle\hat{\Pi}_z^{(f_0)}\rangle=1\qquad\langle\hat{\Pi}_y^{(f_0)}\rangle=0\qquad\langle\hat{\Pi}_x^{(f_0)}\rangle=0 \tag{A.111}$$

Then, one can take in (A.100) and (A.104) the vector $\boldsymbol{a}_+=\pm\boldsymbol{e}_z$ and one is therefore left with

$$\max_\theta\langle\hat{\mathscr{S}}^{(f_0|f_1|f_2)}(\omega)\rangle\big|_{T=0}=|\langle\mathbf{b}.\hat{\mathbf{\Pi}}^{(f_1)}\otimes\mathbf{c}'.\hat{\mathbf{\Pi}}^{(f_2)}\rangle+\langle\mathbf{b}'.\hat{\mathbf{\Pi}}^{(f_1)}\otimes\mathbf{c}.\hat{\mathbf{\Pi}}^{(f_2)}\rangle| \tag{A.112}$$

Since in this basis $\langle\hat{T}_\rho\rangle_{zz}^{(f_1,f_2)}=1$ at all energies and since the vector $\boldsymbol{b}$, $\boldsymbol{b}'$, $\boldsymbol{c}$ and $\boldsymbol{c}'$ are not constrained with respect to each other one can take them all to be $+\boldsymbol{e}_z$, thus obtaining

$$S^{(f_0|f_1|f_2)}(\omega)\underset{T=0}{=}2 \tag{A.113}$$

Taking $a_-=\pm\boldsymbol{e}_z$ instead of a_+ doesn't change the result of the maximization. Therefore, at any energy, there is never violation of the Svetlichny inequality when the average (4.216) of the Svetlichny operator is computed in the $\{\mathbf{f}\}$ basis since at zero temperature, in this basis, the system is in a genuine bipartite (i.e. not tripartite) state (see section 4.6.5).

[12] The situation is slightly different in the case of a flat profile configuration, where $\mathcal{T}_{yyz}=-1$ and $\mathcal{T}_{zzz}=\mathcal{T}_{zyy}=\mathcal{T}_{yzy}=1$, with all other coefficients also vanishing. Once this modification is accounted for, the maximization procedure yields the same final result.

A.6 . Numerical maximization of $\langle \hat{\mathscr{S}}^{(0|1|2)} \rangle$

As explained in Sec. 4.6, the maximal value of the three-mode Bell operator $\langle \hat{\mathscr{S}}^{(0|1|2)} \rangle$ can be found by optimizing the orientation of the unit vectors $\boldsymbol{a}$, $\boldsymbol{a}'$, $\boldsymbol{b}$, $\boldsymbol{b}'$, $\boldsymbol{c}$ and $\boldsymbol{c}'$. However, solving this optimization problem analytically proves challenging due to the need to maximize a function depending on 12 real parameters. Indeed, the orientation of each of the six previous normalized vectors in the 3-dimensional physical space corresponds to six times two degrees of freedom, leading in total to twelve parameters.

Consequently, we resort to a numerical method to evaluate the maximal violation of Bell inequalities and determine the corresponding optimal orientations for the vectors $\boldsymbol{a}$, $\boldsymbol{a}'$, $\boldsymbol{b}$, $\boldsymbol{b}'$, $\boldsymbol{c}$, and $\boldsymbol{c}'$. More explicitly, we use a genetic algorithm which has proved very efficient for optimizing a function over a large parameter space [193]. This algorithm is based on natural selection : the code starts with a random set of solutions (in our case each of them consists of 12 parameters) which form all together what we call a population. For each set of vectors $(\boldsymbol{a}, \boldsymbol{a}', \boldsymbol{b}, \boldsymbol{b}', \boldsymbol{c}, \boldsymbol{c}')$, the expectation value $\langle \hat{\mathscr{S}}^{(0|1|2)} \rangle$ is then computed by means of the technique exposed in 4.3.1. For instance the contribution of the term $\langle \boldsymbol{a} \cdot \hat{\boldsymbol{\Pi}}^{(0)} \otimes \boldsymbol{b} \cdot \hat{\boldsymbol{\Pi}}^{(1)} \otimes \boldsymbol{c} \cdot \hat{\boldsymbol{\Pi}}^{(2)} \rangle$ to $\langle \hat{\mathscr{B}}^{(0|1|2)} \rangle$ can be evaluated from the knowledge of the terms $\mathcal{T}_{rst}$ defined in Eq. (4.195) :

$$\langle \boldsymbol{a} \cdot \hat{\boldsymbol{\Pi}}^{(0)} \otimes \boldsymbol{b} \cdot \hat{\boldsymbol{\Pi}}^{(1)} \otimes \boldsymbol{c} \cdot \hat{\boldsymbol{\Pi}}^{(2)} \rangle = \sum_{r,s,t} a_r b_s c_t \mathcal{T}_{rst} \tag{A.114}$$

where the sum runs over the indices $(r, s, t) \in \{x, y, z\}^3$. At variance with the bipartite case, at finite temperature it not not possible to find a Local Linear Unitary BOgoliubov transformation (LLUBO) enabling to cast the 6×6 covariance matrix (4.146) under a standard form where all the ε_{ij} matrices are diagonal (see the discussion in 4.3.3). The expectation values are thus computed in the natural basis of the c-modes where the values of the $\mathcal{T}_{rst}$ coefficients are given by Eqs. (4.202), (4.203), (4.204) and (4.205).

At each step of the algorithm the code computes the expectation value $\langle \hat{\mathscr{S}}^{(0|1|2)} \rangle$ for a set of vectors $(\boldsymbol{a}, \boldsymbol{a}', \boldsymbol{b}, \boldsymbol{b}', \boldsymbol{c}, \boldsymbol{c}')$ and ranks the members of the population by computing a *fitness scaling function*, a kind of selection rule : only the members of the population with the lowest fitness value will be retained – they are called the parents – and used to generate new sets of solutions, called the children. Then, at the next step, the selection rules are applied to the children, some of them become parents in turn and engender a new generation. The algorithm stops when all children look like their parents, or, in other words, when

$$|\boldsymbol{v}_{\ell+1} - \boldsymbol{v}_\ell| < \delta, \tag{A.115}$$

where $\boldsymbol{v}_\ell = (\boldsymbol{a}, \boldsymbol{a}', \boldsymbol{b}, \boldsymbol{b}', \boldsymbol{c}, \boldsymbol{c}')$ is the set of solutions at step ℓ of the algorithm, and δ is the chosen convergence precision fixed before the beginning of the selection process.

In our case, the fitness scaling function is simply the opposite of the average $\langle \hat{\mathscr{S}}^{(0|1|2)} \rangle$ of the three-mode Bell operator. Trying to obtain the lowest fitness score is thus equivalent to maximize the Bell operator. For a given set of vectors $\boldsymbol{v}_\ell$ at step ℓ, the next generation is computed as follows : $\boldsymbol{v}_{\ell+1} = \boldsymbol{v}_\ell + \boldsymbol{w}_\ell$, where $\boldsymbol{w}_\ell$ is a random weight which controls the mutations between the parents $\boldsymbol{v}_\ell$ and the children $\boldsymbol{v}_{\ell+1}$, and which tends to decrease when the code starts to converge. For a detailed presentation of the algorithm we refer to Ref. [194]. Note finally that the procedure just presented is also used for determining the optimized Mermin parameter (4.232).

A.7 . Basis dependent expressions of the covariance matrix of the system

A.7.1 . Rotated covariance matrix of the three-mode state at any finite temperature

Recalling that (4.173) is given by

$$[\sigma_i]_e = \begin{pmatrix} A_i & 0 \\ 0 & A_i \end{pmatrix} \quad [\epsilon_{01}]_e = \begin{pmatrix} F_{01} & G_{01} \\ -G_{01} & F_{01} \end{pmatrix} \quad [\epsilon_{i2}]_e = \begin{pmatrix} F_{i2} & -G_{i2} \\ -G_{i2} & -F_{i2} \end{pmatrix} \tag{A.116}$$

one has explicitly

$$\sigma_e = \begin{pmatrix} [\sigma_0]_e & [\epsilon_{01}]_e & [\epsilon_{02}]_e \\ [\epsilon_{01}^T]_e & [\sigma_1]_e & [\epsilon_{12}]_e \\ [\epsilon_{02}^T]_e & [\epsilon_{12}^T]_e & [\sigma_2]_e \end{pmatrix} = \begin{pmatrix} A_0 & 0 & F_{01} & G_{01} & F_{02} & -G_{02} \\ 0 & A_0 & -G_{01} & F_{01} & -G_{02} & -F_{02} \\ F_{01} & -G_{01} & A_1 & 0 & F_{12} & -G_{12} \\ G_{01} & F_{01} & 0 & A_1 & -G_{12} & -F_{12} \\ F_{02} & -G_{02} & F_{12} & -G_{12} & A_2 & 0 \\ -G_{02} & -F_{02} & -G_{12} & -F_{12} & 0 & A_2 \end{pmatrix} \tag{A.117}$$

The determinant of the matrix σ_e is

$$\det \sigma_e = D^2 \tag{A.118}$$

with

$$\begin{aligned} D &= A_0A_1A_2 - A_0(F_{12}^2 + G_{12}^2) - A_1(F_{02}^2 + G_{02}^2) - A_2(F_{01}^2 + G_{01}^2) \\ &\quad -2F_{02}G_{01}G_{12} + 2F_{12}G_{01}G_{02} + 2F_{01}G_{02}G_{12} + 2F_{01}F_{02}F_{12} \end{aligned} \tag{A.119}$$

Then, setting

$$\begin{aligned} A_{ij} &\underset{i<j}{=} A_iA_j - (F_{ij}^2 + G_{ij}^2) \\ B_0 &= -A_0F_{12} + F_{01}F_{02} + G_{01}G_{02} \\ B_1 &= -A_1F_{02} + F_{01}F_{12} - G_{01}G_{12} \\ B_2 &= -A_2F_{01} + F_{02}F_{12} + G_{02}G_{12} \end{aligned} \tag{A.120}$$

and

$$\begin{aligned} C_0 &= -A_0G_{12} - F_{02}G_{01} + G_{02}F_{01} \\ C_1 &= -A_1G_{02} + F_{12}G_{01} + G_{12}F_{01} \\ C_2 &= -A_2G_{01} - F_{02}G_{12} + G_{02}F_{12} \end{aligned} \tag{A.121}$$

the inverse of the matrix σ_e is

$$[\sigma_e]^{-1} = \frac{1}{D} \begin{pmatrix} A_{12} & 0 & B_2 & C_2 & B_1 & -C_1 \\ 0 & A_{12} & -C_2 & B_2 & -C_1 & -B_1 \\ B_2 & -C_2 & A_{02} & 0 & B_0 & -C_0 \\ C_2 & B_2 & 0 & A_{02} & -C_0 & -B_0 \\ B_1 & -C_1 & B_0 & -C_0 & A_{01} & 0 \\ -C_1 & -B_1 & -C_0 & -B_0 & 0 & A_{01} \end{pmatrix} \tag{A.122}$$

One can also check [13] that

$$\begin{aligned} A_{01}A_{02} - (B_0^2 + C_0^2) &= A_0D \\ A_{01}A_{12} - (B_1^2 + C_1^2) &= A_1D \\ A_{02}A_{12} - (B_2^2 + C_2^2) &= A_2D \end{aligned} \tag{A.123}$$

At $T = 0$ in a standard form basis one has also

$$\begin{aligned} B_1B_2 - A_{12}B_0 &\underset{T=0}{=} F_{12}D \\ B_0B_2 - A_{02}B_1 &\underset{T=0}{=} F_{02}D \\ B_0B_1 - A_{01}B_2 &\underset{T=0}{=} F_{01}D \end{aligned} \tag{A.124}$$

[13] These are useful relations for computing the Wigner function integrals.

Relation (A.122) is a generic definition of the inverse covariance matrix of our system and it is valid for any (zero or finite) temperature. The zero temperature inverse covariance matrix is obtained by taking the values at $T = 0$ of its components using the zero temperature expressions of (4.172). Furthermore, at zero temperature, an appropriate rotation can always be found in order to obtain the standard form of the inverse covariance matrix.

A.7.2 . Rotated covariance matrix of the 3-mode state at zero temperature

When, in the idealised case, the system is considered to be at zero temperature, the average $\langle ... \rangle$ is taken over the vacuum of the incoming modes and is given by $\langle ... \rangle_0$: in this section, in order to lighten the notation, we will consider $\langle ... \rangle$ to be $\langle ... \rangle_0$. One can then take $\sigma_e = S_R \sigma_c S_R^T$ of (4.157) with

$$S_R = \text{diag}\{R(\varphi_{02}), R(\varphi_{12}), R(-\varphi_{22})\} \tag{A.125}$$

that is to say

$$\begin{aligned} \Phi_{i2} &\underset{i\neq 2}{=} \varphi_{i2} \\ \Phi_{22} &= -\varphi_{22} \end{aligned} \tag{A.126}$$

with the φ_{ij} given by (4.64). In the *vacuum state*, relations (4.59), (4.64) and (4.65) imply

$$\langle \hat{c}_0 \hat{c}_1^\dagger \rangle = |S_{00}||S_{10}| e^{i(\varphi_{00}-\varphi_{10})} + |S_{01}||S_{11}| e^{i(\varphi_{01}-\varphi_{11})} = |S_{02}||S_{12}| e^{i(\varphi_{02}-\varphi_{12})} \tag{A.127}$$

and therefore

$$\begin{aligned} |\langle \hat{c}_0 \hat{c}_1^\dagger \rangle| &= |S_{02}||S_{12}| \\ Re\langle \hat{c}_0 \hat{c}_1^\dagger \rangle &= |\langle \hat{c}_0 \hat{c}_1^\dagger \rangle| \cos(\varphi_{02} - \varphi_{12}) \\ Im\langle \hat{c}_0 \hat{c}_1^\dagger \rangle &= |\langle \hat{c}_0 \hat{c}_1^\dagger \rangle| \sin(\varphi_{02} - \varphi_{12}) \end{aligned} \tag{A.128}$$

Similarly one has

$$\langle \hat{c}_i \hat{c}_2 \rangle \underset{i\neq 2}{=} |S_{i0}||S_{20}| e^{i(\varphi_{i0}-\varphi_{20})} + |S_{i1}||S_{21}| e^{i(\varphi_{i1}-\varphi_{21})} = |S_{i2}||S_{22}| e^{i(\varphi_{i2}-\varphi_{22})} \tag{A.129}$$

and therefore

$$\begin{aligned} |\langle \hat{c}_i \hat{c}_2 \rangle| &\underset{i\neq 2}{=} |S_{i2}||S_{22}| \\ Re\langle \hat{c}_i \hat{c}_2 \rangle &\underset{i\neq 2}{=} |\langle \hat{c}_i \hat{c}_2 \rangle| \cos(\varphi_{i2} - \varphi_{22}) \\ Im\langle \hat{c}_i \hat{c}_2 \rangle &\underset{i\neq 2}{=} |\langle \hat{c}_i \hat{c}_2 \rangle| \sin(\varphi_{i2} - \varphi_{22}) \end{aligned} \tag{A.130}$$

Furthermore, using (4.59) one gets

$$\begin{aligned} \langle \hat{c}_i^\dagger \hat{c}_i \rangle &\underset{i\neq 2}{=} |S_{i2}|^2 \\ \langle \hat{c}_2^\dagger \hat{c}_2 \rangle &= |S_{20}|^2 + |S_{21}|^2 = |S_{22}|^2 - 1 \end{aligned} \tag{A.131}$$

where to obtain the last equality of the second line we have used (4.62). Then, looking at (A.128) and (A.130), one can write from (A.131)

$$\begin{aligned} |\langle \hat{c}_0 \hat{c}_1^\dagger \rangle| &= |S_{02}||S_{12}| = \sqrt{\langle \hat{c}_0^\dagger \hat{c}_0 \rangle} \sqrt{\langle \hat{c}_1^\dagger \hat{c}_1 \rangle} \\ |\langle \hat{c}_i \hat{c}_2 \rangle| &\underset{i\neq 2}{=} |S_{i2}||S_{22}| = \sqrt{\langle \hat{c}_i^\dagger \hat{c}_i \rangle} \sqrt{1 + \langle \hat{c}_2^\dagger \hat{c}_2 \rangle} \end{aligned} \tag{A.132}$$

Finally, writing

$$a_i = 1 + 2\langle \hat{c}_i^\dagger \hat{c}_i \rangle \tag{A.133}$$

one obtains, considering (4.165),

$$\begin{aligned} [\sigma_i]_e &= a_i \, \mathbb{1}_2 \\ [\epsilon_{01}]_e &= \sqrt{a_0 - 1}\sqrt{a_1 - 1}\, \mathbb{1}_2 = b_{01} \mathbb{1}_2 \\ [\epsilon_{i2}]_e &\underset{i\neq 2}{=} \sqrt{a_i - 1}\sqrt{a_2 + 1}\, \sigma_z = b_{i2} \sigma_z \end{aligned} \tag{A.134}$$

with σ_z the Pauli matrix and

$$b_{01} = \sqrt{a_0 - 1}\sqrt{a_1 - 1} \qquad b_{i2} \underset{i\neq 2}{=} \sqrt{a_i - 1}\sqrt{a_2 + 1} \tag{A.135}$$

In terms of the scattering matrix components one has therefore

$$a_0 = 1 + 2|S_{02}|^2 \qquad a_1 = 1 + 2|S_{12}|^2 \qquad a_2 = -1 + 2|S_{22}|^2 \tag{A.136}$$

and

$$b_{01} = 2|S_{02}||S_{12}| \qquad b_{02} = 2|S_{02}||S_{22}| \qquad b_{12} = 2|S_{12}||S_{22}| \tag{A.137}$$

A.7.3 . Covariance matrix in the $\{\hat{f}\}$ basis

At any zero or finite temperature, one obtains in the $\hat{\mathbf{f}}$ basis, the general expressions

$$[\sigma_i]_f = \begin{pmatrix} A_i & 0 \\ 0 & A_i \end{pmatrix} \tag{A.138}$$

and

$$[\epsilon_{01}]_f = \begin{pmatrix} F_{01} & G_{01} \\ -G_{01} & F_{01} \end{pmatrix} \quad [\epsilon_{02}]_f = \begin{pmatrix} F_{02} & G_{02} \\ G_{02} & F_{02} \end{pmatrix} \quad [\epsilon_{12}]_f = \begin{pmatrix} F_{12} & 0 \\ 0 & -F_{12} \end{pmatrix} \tag{A.139}$$

for the $[\sigma_i]_f$ and $[\epsilon_{ij}]_f$ of the covariance matrix, with

$$\begin{aligned}
A_0 &= 1 + 2\langle \hat{f}_0^\dagger \hat{f}_0 \rangle \quad \underset{T=0}{\rightarrow} \quad a_0 = 1 \\
A_1 &= 1 + 2\langle \hat{f}_1^\dagger \hat{f}_1 \rangle \quad \underset{T=0}{\rightarrow} \quad a_1 = -1 + 2|S_{22}|^2 \\
A_2 &= 1 + 2\langle \hat{f}_2^\dagger \hat{f}_2 \rangle \quad \underset{T=0}{\rightarrow} \quad a_2 = -1 + 2|S_{22}|^2 \\
F_{01} &= 2\, Re\langle \hat{f}_0 \hat{f}_1^\dagger \rangle \quad \underset{T=0}{\rightarrow} \quad 0 \\
G_{01} &= 2\, Im\langle \hat{f}_0 \hat{f}_1^\dagger \rangle \quad \underset{T=0}{\rightarrow} \quad 0 \\
F_{12} &= 2\, Re\langle \hat{f}_1 \hat{f}_2 \rangle = 2\langle \hat{f}_1 \hat{f}_2 \rangle \quad \underset{T=0}{\rightarrow} \quad f_{12} = 2|S_{22}|\sqrt{|S_{22}|^2 - 1} \\
F_{02} &= 2\, Re\langle \hat{f}_0 \hat{f}_2 \rangle \quad \underset{T=0}{\rightarrow} \quad 0 \\
G_{02} &= 2\, Im\langle \hat{f}_0 \hat{f}_2 \rangle \quad \underset{T=0}{\rightarrow} \quad 0
\end{aligned} \tag{A.140}$$

as can be seen from (4.180). At **zero temperature** then one can see that mode 0 decouples from the two other modes and therefore

$$[\sigma]_f \underset{T=0}{=} \sigma^{(f_0)} \oplus \sigma^{(f_1|f_2)} \tag{A.141}$$

Then,

$$[\sigma_i]_f \underset{T=0}{=} \begin{pmatrix} a_i & 0 \\ 0 & a_i \end{pmatrix} \quad [\epsilon_{01}]_f \underset{T=0}{=} [\epsilon_{02}]_f = \mathbf{0}_{2\times 2} \quad [\epsilon_{12}]_f \underset{T=0}{=} \begin{pmatrix} f_{12} & 0 \\ 0 & -f_{12} \end{pmatrix} \tag{A.142}$$

or, explicitly,

$$\sigma_f \underset{T=0}{=} \begin{pmatrix} [\sigma_0]_f & [\epsilon_{01}]_f & [\epsilon_{02}]_f \\ [\epsilon_{01}^T]_f & [\sigma_1]_f & [\epsilon_{12}]_f \\ [\epsilon_{02}^T]_f & [\epsilon_{12}^T]_f & [\sigma_2]_f \end{pmatrix} \underset{T=0}{=} \begin{pmatrix} 1 & 0 & 0 & 0 & 0 & 0 \\ 0 & 1 & 0 & 0 & 0 & 0 \\ 0 & 0 & a_1 & 0 & f_{12} & 0 \\ 0 & 0 & 0 & a_1 & 0 & -f_{12} \\ 0 & 0 & f_{12} & 0 & a_2 & 0 \\ 0 & 0 & 0 & -f_{12} & 0 & a_2 \end{pmatrix} \tag{A.143}$$

The determinant of the matrix σ_f is

$$\det \sigma_f \underset{T=0}{=} [d]^2 \tag{A.144}$$

with

$$d = a_1 a_2 - [f_{12}]^2 = 1 \tag{A.145}$$

Then, setting

$$a_{12} = a_1 a_2 - [f_{12}]^2 = d = 1 \qquad a_{02} = a_2 \qquad a_{01} = a_1 \qquad b_0 = -f_{12} \tag{A.146}$$

the inverse of the matrix σ_f is

$$[\sigma_f]^{-1} \underset{T=0}{=} \begin{pmatrix} 1 & 0 & 0 & 0 & 0 & 0 \\ 0 & 1 & 0 & 0 & 0 & 0 \\ 0 & 0 & a_{02} & 0 & b_0 & 0 \\ 0 & 0 & 0 & a_{02} & 0 & -b_0 \\ 0 & 0 & b_0 & 0 & a_{01} & 0 \\ 0 & 0 & 0 & -b_0 & 0 & a_{01} \end{pmatrix} \tag{A.147}$$

Let us remark here that the maximized violation of Bell's inequalities for the three-mode system at zero temperature in the $\hat{\mathbf{f}}$ basis has been computed in (A.113). Regarding the maximized violation for the two-mode system one has at any temperature and **after tracing out the $\hat{f}_0$ mode** :

$$\sigma_f^{(12)} = \begin{pmatrix} A_1 & 0 & F_{12} & 0 \\ 0 & A_1 & 0 & -F_{12} \\ F_{12} & 0 & A_2 & 0 \\ 0 & -F_{12} & 0 & A_2 \end{pmatrix} \underset{T=0}{=} \begin{pmatrix} a_1 & 0 & f_{12} & 0 \\ 0 & a_1 & 0 & -f_{12} \\ f_{12} & 0 & a_2 & 0 \\ 0 & -f_{12} & 0 & a_2 \end{pmatrix} \tag{A.148}$$

The determinant of the $\sigma_f^{(12)}$ matrix is then

$$\det[\sigma_f^{(12)}] \underset{i\neq 2}{=} [A_1 A_2 - F_{12}^2]^2 = [(1+2\bar{n}_{01})(1+2\bar{n}_2)]^2 \underset{T=0}{=} 1 \tag{A.149}$$

The determinant of $\sigma_f^{(12)}$ is therefore always one at all energies at all temperatures (zero or finite). The inverse of $\sigma_f^{(12)}$ is

$$[\sigma_f^{(12)}]^{-1} = \frac{1}{A_{12}} \begin{pmatrix} A_2 & 0 & -F_{12} & 0 \\ 0 & A_2 & 0 & F_{12} \\ -F_{12} & 0 & A_1 & 0 \\ 0 & F_{12} & 0 & A_1 \end{pmatrix} \underset{T=0}{=} \begin{pmatrix} a_2 & 0 & -f_{12} & 0 \\ 0 & a_2 & 0 & f_{12} \\ -f_{12} & 0 & a_1 & 0 \\ 0 & f_{12} & 0 & a_1 \end{pmatrix} \tag{A.150}$$

with here, since here $G_{12} = 0$,

$$A_{12} = A_1 A_2 - F_{12}^2 \tag{A.151}$$

To obtain the maximization of the violation in the $\hat{\mathbf{f}}$ after tracing out mode $\hat{f}_0$ one must then simply use the same $\mathcal{T}_{rst}$ as for the Hawking-Partner pair, i.e. pair $(1,2)$, but replacing the different terms by the corresponding expression obtained in this section : especially one must take $G_{12} = 0$ and $A_{12} = A_1 A_2 - F_{12}^2$ at all energies and all temperatures (zero or finite).

A.8 . Rotated covariance matrices of the two-mode states

The Hawking-Partner state and the Companion-Partner state

Tracing out of our system state either the Hawking (particle 0) or the Companion (particle 1), i.e. taking

$$\hat{\boldsymbol{\xi}}^{(i2)} \underset{i\neq 2}{=} \sqrt{2}(\hat{q}_i, \hat{p}_i, \hat{q}_2, \hat{p}_2)^T \tag{A.152}$$

one straightforwardly obtains from (4.146) the rotated two mode covariance matrix

$$\sigma_e \underset{i\neq 2}{=} \begin{pmatrix} [\sigma_i]_e^{(i2)} & [\epsilon_{i2}]_e \\ [\epsilon_{i2}^T]_e & [\sigma_2]_e \end{pmatrix} = \begin{pmatrix} A_i & 0 & F_{i2} & -G_{i2} \\ 0 & A_i & -G_{i2} & -F_{i2} \\ F_{i2} & -G_{i2} & A_2 & 0 \\ -G_{i2} & -F_{i2} & 0 & A_2 \end{pmatrix} \underset{T=0}{=} \begin{pmatrix} a_i & 0 & b_{i2} & 0 \\ 0 & a_i & 0 & -b_{i2} \\ b_{i2} & 0 & a_2 & 0 \\ 0 & -b_{i2} & 0 & a_2 \end{pmatrix} \tag{A.153}$$

where the last relation points out that it always possible to find a rotation that put the covariance matrix in the standard form[14]. The determinant of the σ_e matrix is then

$$\det[\sigma_e^{(i2)}] \underset{i\neq 2}{=} A_{i2}^2 \underset{T=0}{\to} a_{i2}^2 \tag{A.154}$$

and the inverse is

$$[\sigma_e^{(i2)}]^{-1} \underset{i\neq 2}{=} \frac{1}{A_{i2}} \begin{pmatrix} A_2 & 0 & -F_{i2} & G_{i2} \\ 0 & A_2 & G_{i2} & F_{i2} \\ -F_{i2} & G_{i2} & A_i & 0 \\ G_{i2} & F_{i2} & 0 & A_i \end{pmatrix} \underset{T=0}{=} \frac{1}{a_{i2}} \begin{pmatrix} a_2 & 0 & -b_{i2} & 0 \\ 0 & a_2 & 0 & b_{i2} \\ -b_{i2} & 0 & a_i & 0 \\ 0 & b_{i2} & 0 & a_i \end{pmatrix} \tag{A.155}$$

The Hawking-Companion state

Tracing out of our system state the Partner (particle 2), i.e. taking

$$\hat{\boldsymbol{\xi}}^{(01)} \underset{i\neq 2}{=} \sqrt{2}(\hat{q}_0, \hat{p}_0, \hat{q}_1, \hat{p}_1)^T \tag{A.156}$$

one straightforwardly obtains from (4.146) the rotated two mode covariance matrix

$$\sigma_e^{(01)} = \begin{pmatrix} [\sigma_0]_e & [\epsilon_{01}]_e \\ [\epsilon_{01}^T]_e & [\sigma_2]_e \end{pmatrix} = \begin{pmatrix} A_0 & 0 & F_{01} & G_{01} \\ 0 & A_0 & -G_{01} & F_{01} \\ F_{01} & -G_{01} & A_1 & 0 \\ G_{01} & F_{01} & 0 & A_1 \end{pmatrix} \underset{T=0}{=} \begin{pmatrix} a_0 & 0 & b_{01} & 0 \\ 0 & a_0 & 0 & b_{01} \\ b_{01} & 0 & a_1 & 0 \\ 0 & b_{01} & 0 & a_1 \end{pmatrix} \tag{A.157}$$

The determinant of the σ_e matrix is

$$\det[\sigma_e^{(01)}] = A_{01}^2 \underset{T=0}{\to} a_{01}^2 \tag{A.158}$$

and the inverse is

$$[\sigma_e^{(01)}]^{-1} = \frac{1}{A_{01}} \begin{pmatrix} A_1 & 0 & -F_{01} & -G_{01} \\ 0 & A_1 & G_{01} & -F_{01} \\ -F_{01} & G_{01} & A_0 & 0 \\ -G_{01} & -F_{01} & 0 & A_0 \end{pmatrix} \underset{T=0}{=} \frac{1}{a_{01}} \begin{pmatrix} a_1 & 0 & -b_{01} & 0 \\ 0 & a_1 & 0 & -b_{01} \\ -b_{01} & 0 & a_0 & 0 \\ 0 & -b_{01} & 0 & a_0 \end{pmatrix} \tag{A.159}$$

A.9 . Gaussian Wigner function

A.9.1 . Gaussian Wigner function for the 3-mode state

[14] Therefore the notation $T = 0$ implies the existence of such a rotation but doesn't mean that all the basis at zero temperature lead to the standard form.

For our 3-mode state, i.e. for $\boldsymbol{q} = \{q_0, q_1, q_2\}$ and $\boldsymbol{p} = \{p_0, p_1, p_2\}$, i.e. for

$$\hat{\boldsymbol{\xi}} \underset{i\neq 2}{=} \sqrt{2}(\hat{q}_0, \hat{p}_0, \hat{q}_1, \hat{p}_1, \hat{q}_2, \hat{p}_2)^T \tag{A.160}$$

the Wigner function is given by

$$W_{\hat{\rho}}(\boldsymbol{q}, \boldsymbol{p}) = \mathcal{N}_3 \, W_+(\boldsymbol{q}) W_-(\boldsymbol{p}) W(\boldsymbol{q}, \boldsymbol{p}) \tag{A.161}$$

where

$$\begin{aligned}
\mathcal{N}_3 &= \frac{1}{\pi^3 D} \\
W_+(\boldsymbol{q}) &= \exp\left\{-\frac{A_{12}q_0^2 + A_{02}q_1^2 + A_{01}q_2^2 + 2B_2 q_0 q_1 + 2B_1 q_0 q_2 + 2B_0 q_1 q_2}{D}\right\} \\
W_-(\boldsymbol{p}) &= \exp\left\{-\frac{A_{12}p_0^2 + A_{02}p_1^2 + A_{01}p_2^2 + 2B_2 p_0 p_1 - 2B_1 p_0 p_2 - 2B_0 p_1 p_2}{D}\right\} \\
W(\boldsymbol{q}, \boldsymbol{p}) &= \exp\left\{-\frac{2C_2(q_0 p_1 - q_1 p_0) - 2C_1(q_0 p_2 + q_2 p_0) - 2C_0(q_1 p_2 + q_2 p_1)}{D}\right\}
\end{aligned} \tag{A.162}$$

Then one can check [15] that (A.162) is normalized as

$$\int_{-\infty}^{+\infty} dq_0 dp_0 dq_1 dp_1 dq_2 dp_2 W_{\hat{\rho}}(q_0, p_0, q_1, p_1, q_2, p_2) = \mathrm{Tr}\{\hat{\rho}\} = 1 \tag{A.163}$$

A.9.2 . Gaussian Wigner function for the 2-mode states

For our entangled two-mode state where $N = 2$ for the dimension of $\boldsymbol{q}$ with $\boldsymbol{q} \underset{j>i}{=} \{q_i, q_j\}$ and $\boldsymbol{p} \underset{j>i}{=} \{p_i, p_j\}$, i.e.

$$\hat{\boldsymbol{\xi}}^{(ij)} \underset{j>i}{=} \sqrt{2}(\hat{q}_i, \hat{p}_i, \hat{q}_j, \hat{p}_j)^T \tag{A.164}$$

the Wigner function is given by

$$W_{\hat{\rho}}(\boldsymbol{q}, \boldsymbol{p}) = \mathcal{N}^{(ij)} \, W_-(\boldsymbol{q}) W_\pm(\boldsymbol{p}) W^\pm(\boldsymbol{q}, \boldsymbol{p}) \tag{A.165}$$

where

$$\begin{aligned}
\mathcal{N}^{(ij)} &\underset{j>i}{=} \frac{1}{\pi^2 A_{ij}} \\
W_-(\boldsymbol{q}) &\underset{j>i}{=} \exp\left\{-\frac{A_j q_i^2 + A_i q_j^2 - 2F_{ij} q_i q_j}{A_{ij}}\right\} \\
W_\pm(\boldsymbol{p}) &\underset{j>i}{=} \exp\left\{-\frac{A_j p_i^2 + A_i p_j^2 \pm 2F_{ij} p_i p_j}{A_{ij}}\right\} \\
W^\pm(\boldsymbol{q}, \boldsymbol{p}) &\underset{i\neq 2}{=} \exp\left\{-\frac{2G_{ij}\left[q_j p_i \pm q_i p_j\right]}{A_{ij}}\right\}
\end{aligned} \tag{A.166}$$

[15] Using the "completing the square" formula (with a real and positive)

$$\int_{-\infty}^{+\infty} dx \, e^{-ax^2 + bx + c} = \sqrt{\frac{\pi}{a}} e^{\frac{b^2}{4a} + c}$$

with $W_{\pm}$ and $W^{\pm}$ respectively being W_{+} and W^{+} for $j=2$ (i.e. $i=0,1$) or W_{-} and W^{-} for $j=1$ (i.e. $i=0$). This means that one has explicitly

$$\begin{aligned} W_{\hat{\rho}}(\boldsymbol{q},\boldsymbol{p}) &= \mathcal{N}^{(i2)}\, W_{-}(\boldsymbol{q})W_{+}(\boldsymbol{p})W^{+}(\boldsymbol{q},\boldsymbol{p}) \\ W_{-}(\boldsymbol{q}) &\underset{i\neq 2}{=} \exp\left\{-\frac{A_i q_2^2 + A_2 q_i^2 - 2F_{i2}q_i q_2}{A_{i2}}\right\} \\ W_{+}(\boldsymbol{p}) &\underset{i\neq 2}{=} \exp\left\{-\frac{A_i p_2^2 + A_2 p_i^2 + 2F_{i2}p_i p_2}{A_{i2}}\right\} \\ W^{+}(\boldsymbol{q},\boldsymbol{p}) &\underset{i\neq 2}{=} \exp\left\{-\frac{2G_{i2}\left[q_i p_2 + q_2 p_i\right]}{A_{i2}}\right\} \end{aligned} \tag{A.167}$$

and

$$\begin{aligned} W_{\hat{\rho}}(\boldsymbol{q},\boldsymbol{p}) &= \mathcal{N}^{(01)}\, W_{-}(\boldsymbol{q})W_{-}(\boldsymbol{p})W^{-}(\boldsymbol{q},\boldsymbol{p}) \\ W_{-}(\boldsymbol{q}) &= \exp\left\{-\frac{A_0 q_1^2 + A_1 q_2^2 - 2F_{01}q_0 q_1}{A_{01}}\right\} \\ W_{-}(\boldsymbol{p}) &= \exp\left\{-\frac{A_0 p_1^2 + A_1 p_0^2 - 2F_{01}p_0 p_1}{A_{01}}\right\} \\ W^{-}(\boldsymbol{q},\boldsymbol{p}) &= \exp\left\{-\frac{2G_{01}\left[q_1 p_0 - q_0 p_1\right]}{A_{01}}\right\} \end{aligned} \tag{A.168}$$

Again one can check that (A.165) is normalized as

$$\int_{-\infty}^{+\infty} dq_i dp_i dq_j dp_j W_{\hat{\rho}}(q_i,p_i,q_j,p_j) = \mathsf{Tr}\{\hat{\rho}\} = 1 \tag{A.169}$$

A.10 . Expectation values for continuous variables through the Wigner function

A.10.1 . Wigner function of the GKMR pseudo-spins

Using the $|q_i\rangle$ basis with $i=\{0,1,2\}$, one obtains

$$\begin{aligned} W_{\hat{\Pi}_z}(q_i,p_i) &= \int_{-\infty}^{+\infty} dz_i\, e^{ip_i z_i} \left\langle q_i - \tfrac{1}{2}z_i\right| \hat{\Pi}_z \left|q_i + \tfrac{1}{2}z_i\right\rangle \\ &= \int_{-\infty}^{+\infty} dz_i\, e^{ip_i z_i} \left\langle q_i - \tfrac{1}{2}z_i\right| \left[\int_{-\infty}^{+\infty} dq_i' \left|q_i'\right\rangle \left\langle -q_i'\right|\right] \left|q_i + \tfrac{1}{2}z_i\right\rangle \\ &= \int_{-\infty}^{+\infty} dz_i\, e^{ip_i z_i} \int_{-\infty}^{+\infty} dq_i' \left\langle q_i - \tfrac{1}{2}z_i | q_i'\right\rangle \left\langle -q_i' | q_i + \tfrac{1}{2}z_i\right\rangle \\ &= \delta(2q_i) \int_{-\infty}^{+\infty} dz_i\, e^{ip_i z_i} \\ &= 2\pi\, \delta(2q_i)\delta(p_i) \\ &= \pi\, \delta(q_i)\delta(p_i) \end{aligned} \tag{A.170}$$

where a change of variable $Z_i = z_i/2$ has been performed before integration over Z in order to take into account the scaling properties of the δ function. Similarly, one obtains

$$\begin{aligned} W_{\hat{\Pi}_y}(q_i,p_i) &= \int_{-\infty}^{+\infty} dz_i\, e^{ip_iz_i}\, \langle q_i - \tfrac{1}{2}z_i|\, \hat{\Pi}_y\, |q_i + \tfrac{1}{2}z_i\rangle \\ &= \int_{-\infty}^{+\infty} dz_i\, e^{ip_iz_i}\, \langle q_i - \tfrac{1}{2}z_i| \left[i\int_0^{+\infty} dq_i' \,|q_i'\rangle\,\langle -q_i'| - i\int_0^{+\infty} dq_i' \,|-q_i'\rangle\,\langle q_i'| \right] |q_i + \tfrac{1}{2}z_i\rangle \\ &= 2i\,\delta(2q_i) e^{-2ip_iq_i} \int_0^{+\infty} dq_i' \left[e^{-2ip_iq_i'} - e^{2ip_iq_i'} \right] \\ &= i\,\delta(q_i) \int_0^{+\infty} dq_i' \left[e^{-2ip_iq_i'} - e^{2ip_iq_i'} \right] \\ &= i\,\delta(q_i) \left[\int_0^{+\infty} dq_i'\, \mathrm{sgn}(q_i') e^{-2ip_iq_i'} + \int_{-\infty}^{0} dq_i'\, \mathrm{sgn}(q_i') e^{-2ip_iq_i'} \right] \\ &= i\,\delta(q_i) \int_{-\infty}^{+\infty} dq_i'\, \mathrm{sgn}(q_i') e^{-2ip_iq_i'} \end{aligned} \tag{A.171}$$

The last line can also be written $-\delta(q_i)\mathrm{p.v.}(1/p_i)$ using $\lim_{\varepsilon\to 0^+} \int_0^{+\infty} dq_i' e^{\pm 2ip_iq_i'} e^{-\varepsilon q'}$ to compute the integrals of the third last line. Finally one gets also

$$\begin{aligned} W_{\hat{\Pi}_x}(q_i,p_i) &= \int_{-\infty}^{+\infty} dz_i\, e^{ip_iz_i}\, \langle q_i - \tfrac{1}{2}z_i|\, \hat{\Pi}_x\, |q_i + \tfrac{1}{2}z_i\rangle \\ &= \int_{-\infty}^{+\infty} dz_i\, e^{ip_iz_i}\, \langle q_i - \tfrac{1}{2}z_i| \left[\int_0^{+\infty} dq_i' \,|q_i'\rangle\,\langle q_i'| - \int_0^{+\infty} dq_i' \,|-q_i'\rangle\,\langle -q_i'| \right] |q_i + \tfrac{1}{2}z_i\rangle \\ &= 2e^{-2ip_iq_i} \int_0^{+\infty} dq_i' \left[e^{2ip_iq_i'}\delta(2q_i - 2q_i') - e^{-2ip_iq_i'}\delta(2q_i + 2q_i') \right] \\ &= 2\int_0^{+\infty} dq_i' \left[\delta(2q_i - 2q_i') - \delta(2q_i + 2q_i') \right] \\ &= \int_0^{+\infty} dq_i' \left[\delta(q_i - q_i') - \delta(q_i + q_i') \right] \\ &= \Theta(q_i) - \Theta(-q_i) \\ &= \mathrm{sgn}(q_i) \end{aligned} \tag{A.172}$$

where we used the definition of the Heaviside function $\Theta(x-a) = \int_{-\infty}^{x} dx\,\delta(x-a)$ to compute the second last line after taking $q_i' \to -q_i'$ whereas the sign function in the last line is defined as $\mathrm{sgn}(q_i) = +1$ for q_i positive, $\mathrm{sgn}(q_i) = -1$ for q_i negative and $\mathrm{sgn}(q_i) = 0$.

A.10.2 . Expectation values of the GKMR pseudo-spins for the 2-mode states

From (4.194), (A.165) (A.170), (A.171) and (A.172) one has

$$\begin{aligned} \langle \hat{\Pi}_z^{(i)} \otimes \hat{\Pi}_z^{(j)} \rangle &\underset{j>i}{=} \int_{-\infty}^{+\infty} dq_i \int_{-\infty}^{+\infty} dp_i \int_{-\infty}^{+\infty} dq_j \int_{-\infty}^{+\infty} dp_j\, W_{\hat{\rho}}(q_i,p_i,q_j,p_j)\, W_{\hat{\Pi}_z}(q_i,p_i) W_{\hat{\Pi}_z}(q_j,p_j) \\ &\underset{j>i}{=} \int_{-\infty}^{+\infty} dq_i \int_{-\infty}^{+\infty} dp_i \int_{-\infty}^{+\infty} dq_j \int_{-\infty}^{+\infty} dp_j\, W_{\hat{\rho}}(q_i,p_i,q_j,p_j)\, \pi^2 \delta(q_i)\,\delta(p_i)\,\delta(q_j)\,\delta(p_j) \\ &\underset{j>i}{=} \pi^2 \mathcal{N} \\ &\underset{j>i}{=} \frac{1}{A_{ij}} \end{aligned} \tag{A.173}$$

The previous result is obtained in the general case of a thermal distribution. Setting the occupation numbers to zero one gets the result for the vacuum state. Summarizing one has

$$\begin{aligned} \langle \hat{\Pi}_z^{(i)} \otimes \hat{\Pi}_z^{(j)} \rangle_{th} &\underset{j>i}{=} \frac{1}{A_{ij}} \\ \langle \hat{\Pi}_z^{(i)} \otimes \hat{\Pi}_z^{(j)} \rangle_{0} &\underset{j>i}{=} \frac{1}{a_{ij}} \end{aligned} \tag{A.174}$$

The computation for $\langle \hat{\Pi}_x^{(i)} \otimes \hat{\Pi}_x^{(j)} \rangle$ is more involved : it requires (and so does $\langle \hat{\Pi}_y^{(i)} \otimes \hat{\Pi}_y^{(j)} \rangle$) some integration steps by completing the square. One has

$$\begin{aligned} \langle \hat{\Pi}_x^{(i)} \otimes \hat{\Pi}_x^{(j)} \rangle &\underset{j>i}{=} \int_{-\infty}^{+\infty} dq_i \int_{-\infty}^{+\infty} dp_i \int_{-\infty}^{+\infty} dq_j \int_{-\infty}^{+\infty} dp_j \, W_{\hat{\rho}}(q_i, p_i, q_j, p_j) \, W_{\hat{\Pi}_x}(q_i, p_i) W_{\hat{\Pi}_x}(q_j, p_j) \\ &= \mathcal{N} \int_{-\infty}^{+\infty} dq_i dq_j W_-(q_i, q_j) \, \mathrm{sgn}(q_i) \, \mathrm{sgn}(q_j) \int_{-\infty}^{+\infty} dp_i dp_j W_{\pm}(p_i, p_j) \end{aligned} \tag{A.175}$$

Writing $B_{ij} = 1/A_{ij}$ and $C_{ij} = 1/[A_i A_j - F_{ij}^2]$, the integration over p gives by completing the square

$$\begin{aligned} \int_{-\infty}^{+\infty} dp_i dp_j W_{\pm}(p_i, p_j) &\underset{j>i}{=} \int_{-\infty}^{+\infty} dp_i \, e^{-B_{ij}[A_j p_i^2 + 2G_{ij} q_j p_i]} \\ &\quad \times \int_{-\infty}^{+\infty} dp_j \, e^{-B_{ij}[A_i p_j^2 \pm 2(G_{ij} q_i + F_{ij} p_i) p_j]} \\ &\underset{j>i}{=} \frac{\pi \sqrt{C_{ij}}}{B_{ij}} e^{G_{ij}^2 B_{ij} C_{ij} \left[A_j q_i^2 + A_i q_j^2 - 2F_{ij} q_i q_j \right]} \end{aligned} \tag{A.176}$$

and therefore

$$\begin{aligned} \langle \hat{\Pi}_x^{(i)} \otimes \hat{\Pi}_x^{(j)} \rangle &\underset{j>i}{=} \frac{\mathcal{N} \pi \sqrt{C_{ij}}}{B_{ij}} \int_{-\infty}^{+\infty} dq_i dq_j \, \mathrm{sgn}(q_i) \, \mathrm{sgn}(q_j) e^{-C_{ij} \left[A_j q_i^2 + A_i q_j^2 - 2F_{ij} q_i q_j \right]} \\ &\underset{j>i}{=} \frac{\mathcal{N} \pi \sqrt{C_{ij}}}{B_{ij}} \left[\int_0^{+\infty} dq_i \, e^{-C_{ij} A_j q_i^2} \int_0^{+\infty} dq_j e^{[-C_{ij} A_i q_j^2 + 2C_{ij} F_{ij} q_i q_j]} \right. \\ &\quad - \int_{-\infty}^{0} dq_i \, e^{-C_{ij} A_j q_i^2} \int_0^{+\infty} dq_j \, e^{[-C_{ij} A_i q_j^2 + 2C_{ij} F_{ij} q_i q_j]} \\ &\quad - \int_0^{+\infty} dq_i \, e^{-C_{ij} A_j q_i^2} \int_{-\infty}^{0} dq_j e^{[-C_{ij} A_i q_j^2 + 2C_{ij} F_{ij} q_i q_j]} \\ &\quad \left. + \int_{-\infty}^{0} dq_i \, e^{-C_{ij} A_j q_i^2} \int_{-\infty}^{0} dq_j \, e^{[-C_{ij} A_i q_j^2 + 2C_{ij} F_{ij} q_i q_j]} \right] \end{aligned} \tag{A.177}$$

Using the formula for a real

$$\int_p^q dx \, e^{-ax^2 + bx + c} = e^{\frac{b^2}{4a} + c} \int_P^Q dX \, e^{-aX^2} = e^{\frac{b^2}{4a} + c} \left[\frac{1}{2} \sqrt{\frac{\pi}{a}} \left[\mathrm{erf}(Q\sqrt{a}) - \mathrm{erf}(P\sqrt{a}) \right] \right] \tag{A.178}$$

where $\mathrm{erf}(x)$ is the error function, with $\mathrm{erf}(\pm\infty) = \pm 1$, $\mathrm{erf}(0) = 0$ and $\mathrm{erf}(-x) = -\mathrm{erf}(x)$, and where we have performed the change of variable

$$\begin{aligned} X &= x - \frac{b}{2a} \\ P &= p - \frac{b}{2a} \\ Q &= q - \frac{b}{2a} \end{aligned} \tag{A.179}$$

one is left with only

$$\langle \hat{\Pi}_x^{(i)} \otimes \hat{\Pi}_x^{(j)} \rangle \underset{j>i}{=} \frac{\mathcal{N} \pi \sqrt{C_{ij}}}{B_{ij}} \left[2 \sqrt{\frac{\pi}{a}} \int_0^{+\infty} dq_i \, e^{-C_{ij} A_j q_i^2} e^{\frac{b^2}{4a} + c} \, \mathrm{erf} \left(\frac{b}{2\sqrt{a}} \right) \right] \tag{A.180}$$

with $a = C_{ij} A_i$, $b = 2C_{ij} F_{ij} q_i$ and $c = 0$, that is to say

$$\langle \hat{\Pi}_x^{(i)} \otimes \hat{\Pi}_x^{(j)} \rangle \underset{j>i}{=} 2 \frac{\mathcal{N} \pi}{B_{ij}} \sqrt{\frac{\pi}{A_i}} \int_0^{+\infty} dq_i \, e^{-\frac{1}{A_i} q_i^2} \, \mathrm{erf} \left(\frac{\sqrt{C_{ij}} F_{ij} q_i}{\sqrt{A_i}} \right) \tag{A.181}$$

Using the Taylor expansion of the error function [16], the integral in the previous expression is, after the change of variable $Q_i = (1/A_i) q_i^2$, just

$$\sqrt{\frac{A_i}{\pi}} \sum_{n=0}^{+\infty} \frac{(-1)^n}{n!(2n+1)} \left(F_{ij} \sqrt{C_{ij}} \right)^{2n+1} \int_0^{+\infty} dQ_i e^{-Q_i} Q_i^n \tag{A.182}$$

[16] i.e. $\mathrm{erf}(x) = \frac{2}{\sqrt{\pi}} \sum_{n=0}^{+\infty} \frac{(-1)^n x^{2n+1}}{n!(2n+1)}$

Since the remaining integral is just the definition of the gamma function $\Gamma(n+1) = \int_0^{+\infty} dt\, e^{-t}\, t^n = n!$ and that, for $x \in [-1,1]$, one has

$$\arctan(x) = \sum_{n=0}^{+\infty} \frac{(-1)^n x^{2n+1}}{(2n+1)} \tag{A.183}$$

one is finally left with

$$\langle \hat{\Pi}_x^{(i)} \otimes \hat{\Pi}_x^{(j)} \rangle \underset{j>i}{=} 2\frac{\mathcal{N}\pi}{B_{ij}} \arctan\left(F_{ij}\sqrt{C_{ij}}\right) \tag{A.184}$$

that is to say, after restoring the initial variables,

$$\langle \hat{\Pi}_x^{(i)} \otimes \hat{\Pi}_x^{(j)} \rangle \underset{j>i}{=} \frac{2}{\pi} \arctan\left(\frac{F_{ij}}{\sqrt{A_i A_j - F_{ij}^2}}\right) \tag{A.185}$$

The previous result is obtained in the general case of a thermal distribution. Setting the occupation numbers to zero one gets the result for the vacuum state. Summarizing one has

$$\begin{aligned} \langle \hat{\Pi}_x^{(i)} \otimes \hat{\Pi}_x^{(j)} \rangle_{th} &\underset{j>i}{=} \frac{2}{\pi} \arctan\left(\frac{F_{ij}}{\sqrt{A_i A_j - F_{ij}^2}}\right) \\ \langle \hat{\Pi}_x^{(i)} \otimes \hat{\Pi}_x^{(j)} \rangle_0 &\underset{j>i}{=} \frac{2}{\pi} \arctan\left(\frac{b_{ij}}{\sqrt{a_{ij}}}\right) \end{aligned} \tag{A.186}$$

Regarding $\langle \hat{\Pi}_y^{(i)} \otimes \hat{\Pi}_y^{(j)} \rangle$ one has

$$\begin{aligned} \langle \hat{\Pi}_y^{(i)} \otimes \hat{\Pi}_y^{(j)} \rangle &\underset{j>i}{=} \int_{-\infty}^{+\infty} dq_i \int_{-\infty}^{+\infty} dp_i \int_{-\infty}^{+\infty} dq_j \int_{-\infty}^{+\infty} dp_j\, W_{\hat{\rho}}(q_i,p_i,q_j,p_j)\, W_{\hat{\Pi}_y}(q_i,p_i) W_{\hat{\Pi}_y}(q_j,p_j) \\ &= -\mathcal{N} \int_{-\infty}^{+\infty} dq_i' dq_j'\, \mathrm{sgn}(q_i')\, \mathrm{sgn}(q_j') \int_{-\infty}^{+\infty} dp_i dp_j W_{\pm}(p_i,p_j) e^{-2ip_i q_i'} e^{-2ip_j q_j'} \end{aligned} \tag{A.187}$$

The integration over p gives by completing the square

$$\begin{aligned} \int_{-\infty}^{+\infty} dp_i dp_j W_{\pm}(p_i,p_j) e^{-2ip_i q_i'} e^{-2ip_j q_j'} &\underset{j>i}{=} \int_{-\infty}^{+\infty} dp_i\, e^{-B_{ij}A_j p_i^2 - 2ip_i q_i'} \\ &\quad \times \int_{-\infty}^{+\infty} dp_j\, e^{-B_{ij}A_i p_j^2 - 2\left(iq_i' \pm B_{ij}F_{ij}p_i\right)p_j} \\ &\underset{j>i}{=} \frac{\pi\sqrt{C_{ij}}}{B_{ij}} e^{-\frac{C_{ij}}{B_{ij}}\left[A_i q_i'^2 + A_j q_j^2 \mp 2F_{ij}q_i'q_j'\right]} \end{aligned} \tag{A.188}$$

where we used at the very end $1 + C_{ij}F_{ij}^2 = A_i A_j C_{ij}$. Thus one obtains

$$\begin{aligned} \langle \hat{\Pi}_y^{(i)} \otimes \hat{\Pi}_y^{(j)} \rangle &\underset{j>i}{=} -\frac{\mathcal{N}\pi\sqrt{C_{ij}}}{B_{ij}} \Bigg[\int_0^{+\infty} dq_i'\, e^{-\frac{C_{ij}}{B_{ij}}A_i q_i'^2} \int_0^{+\infty} dq_j' e^{-\frac{C_{ij}}{B_{ij}}A_j q_j^2 \pm 2\frac{C_{ij}}{B_{ij}}F_{ij}q_i'q_j'} \\ &\quad - \int_{-\infty}^{0} dq_i'\, e^{-\frac{C_{ij}}{B_{ij}}A_i q_i'^2} \int_0^{+\infty} dq_j'\, e^{-\frac{C_{ij}}{B_{ij}}A_j q_j^2 \pm 2\frac{C_{ij}}{B_{ij}}F_{ij}q_i'q_j'} \\ &\quad - \int_0^{+\infty} dq_i'\, e^{-\frac{C_{ij}}{B_{ij}}A_i q_i'^2} \int_{-\infty}^{0} dq_j' e^{-\frac{C_{ij}}{B_{ij}}A_j q_j^2 \pm 2\frac{C_{ij}}{B_{ij}}F_{ij}q_i'q_j'} \\ &\quad + \int_{-\infty}^{0} dq_i'\, e^{-\frac{C_{ij}}{B_{ij}}A_i q_i'^2} \int_{-\infty}^{0} dq_j'\, e^{-\frac{C_{ij}}{B_{ij}}A_j q_j^2 \pm 2\frac{C_{ij}}{B_{ij}}F_{ij}q_i'q_j'} \Bigg] \end{aligned} \tag{A.189}$$

which is analogous to (A.177). We can therefore apply once again (A.178) and obtain straightforwardly

$$\langle \hat{\Pi}_y^{(i)} \otimes \hat{\Pi}_y^{(j)} \rangle \underset{j>i}{=} -\frac{\mathcal{N}\pi\sqrt{C_{ij}}}{B_{ij}} \left[2\sqrt{\frac{\pi}{a}} \int_0^{+\infty} dq_i'\, e^{-\frac{C_{ij}}{B_{ij}}A_i q_i'^2} e^{\frac{b^2}{4a}+c}\, \mathrm{erf}\left(\frac{b}{2\sqrt{a}}\right) \right] \tag{A.190}$$

with $a = \frac{C_{ij}}{B_{ij}}A_j$, $b = \pm 2\frac{C_{ij}}{B_{ij}}F_{ij}q_i'$ and $c = 0$, that is to say

$$\langle \hat{\Pi}_y^{(i)} \otimes \hat{\Pi}_y^{(j)} \rangle \underset{j>i}{=} \mp 2\mathcal{N}\pi\sqrt{\frac{\pi}{B_{ij}A_j}} \int_0^{+\infty} dq_i'\, e^{-\frac{1}{B_{ij}A_j}q_i'^2}\, \mathrm{erf}\left(\sqrt{\frac{C_{ij}}{B_{ij}A_j}} F_{ij} q_i'\right) \tag{A.191}$$

Using the Taylor expansion of the error function once again, the integral of the previous expression is, after the change of variable $Q_i = \frac{1}{B_{ij}A_j}[q_i']^2$, just

$$\sqrt{\frac{B_{ij}A_j}{\pi}} \sum_{n=0}^{+\infty} \frac{(-1)^n}{n!(2n+1)} \left(\sqrt{C_{ij}}F_{ij}\right)^{2n+1} \int_0^{+\infty} dQ_i e^{-Q_i} Q_i^n \tag{A.192}$$

where once again we recognize in the integral over Q_i the gamma function $\Gamma(n+1) = n!$. Considering again the Taylor expansion of the arctan function one is left with

$$\langle \hat{\Pi}_y^{(i)} \otimes \hat{\Pi}_y^{(j)} \rangle \underset{j>i}{=} \mp 2\pi\mathcal{N} \arctan\left(F_{ij}\sqrt{C_{ij}}\right) \tag{A.193}$$

that is to say, after restoring the initial variables,

$$\langle \hat{\Pi}_y^{(i)} \otimes \hat{\Pi}_y^{(j)} \rangle \underset{j>i}{=} \mp \frac{2}{\pi A_{ij}} \arctan\left(\frac{F_{ij}}{\sqrt{A_iA_j - F_{ij}^2}}\right) \tag{A.194}$$

with the upper sign (here "$-$") for $j = 2$ and the lower sign (here "$+$") for $j = 1$. The previous result is obtained in the general case of a thermal distribution. Setting the occupation numbers to zero one gets the result for the vacuum state. Summarizing one has

$$\begin{aligned} \langle \hat{\Pi}_y^{(i)} \otimes \hat{\Pi}_y^{(j)} \rangle_{th} &\underset{j>i}{=} \mp \frac{2}{\pi A_{ij}} \arctan\left(\frac{F_{ij}}{\sqrt{A_iA_j - F_{ij}^2}}\right) \\ \langle \hat{\Pi}_y^{(i)} \otimes \hat{\Pi}_y^{(j)} \rangle_0 &\underset{j>i}{=} \mp \frac{2}{\pi a_{ij}} \arctan\left(\frac{b_{ij}}{\sqrt{a_{ij}}}\right) \end{aligned} \tag{A.195}$$

We are left with the cross-terms. One has

$$\begin{aligned} \langle \hat{\Pi}_x^{(i)} \otimes \hat{\Pi}_z^{(j)} \rangle &\underset{j>i}{=} \int_{-\infty}^{+\infty} dq_i \int_{-\infty}^{+\infty} dp_i \int_{-\infty}^{+\infty} dq_j \int_{-\infty}^{+\infty} dp_j \, W_{\hat{\rho}}(q_i, p_i, q_j, p_j) \, W_{\hat{\Pi}_x}(q_i, p_i) W_{\hat{\Pi}_z}(q_j, p_j) \\ &\underset{j>i}{=} \mathcal{N}\pi \int_{-\infty}^{+\infty} dq_i \int_{-\infty}^{+\infty} dp_i \int_{-\infty}^{+\infty} dq_j \int_{-\infty}^{+\infty} dp_j \, W_-(q) W_\pm(p) W_\pm(q,p) \, \mathrm{sgn}(q_i)\delta(q_j)\delta(p_j) \\ &\underset{j>i}{=} \mathcal{N}\pi \left[\int_{-\infty}^{+\infty} dq_i \, \mathrm{sgn}(q_i) e^{-B_{ij}A_j q_i^2}\right] \left[\int_{-\infty}^{+\infty} dp_i e^{-B_{ij}A_j p_i^2}\right] \\ &\underset{j>i}{=} 0 \end{aligned} \tag{A.196}$$

and a similar computation leads to same results for $\langle \hat{\Pi}_z^{(i)} \otimes \hat{\Pi}_x^{(j)} \rangle$. Furthermore one has

$$\begin{aligned} \langle \hat{\Pi}_y^{(i)} \otimes \hat{\Pi}_z^{(j)} \rangle &\underset{j>i}{=} \int_{-\infty}^{+\infty} dq_i \int_{-\infty}^{+\infty} dp_i \int_{-\infty}^{+\infty} dq_j \int_{-\infty}^{+\infty} dp_j \, W_{\hat{\rho}}(q_i, p_i, q_j, p_j) \, W_{\hat{\Pi}_y}(q_i, p_i) W_{\hat{\Pi}_z}(q_j, p_j) \\ &\underset{j>i}{=} i\mathcal{N}\pi \int_{-\infty}^{+\infty} dq_i \int_{-\infty}^{+\infty} dp_i \int_{-\infty}^{+\infty} dq_j \int_{-\infty}^{+\infty} dp_j \, W_-(q) W_\pm(p) W_\pm(q,p) \\ &\qquad \times \delta(q_i)\delta(q_j)\delta(p_j) \int_{-\infty}^{+\infty} dq_i' \mathrm{sgn}(q_i') e^{-2ip_iq_i'} \\ &\underset{j>i}{=} i\mathcal{N}\pi \int_{-\infty}^{+\infty} dq_i' \, \mathrm{sgn}(q_i') \int_{-\infty}^{+\infty} dp_i e^{-B_{ij}A_j p_i^2 - 2iq_i'p_i} \\ &\underset{j>i}{=} i\mathcal{N}\pi \sqrt{\frac{\pi}{B_{ij}A_j}} \int_{-\infty}^{+\infty} dq_i' \, \mathrm{sgn}(q_i') e^{-\frac{B_{ij}}{A_j} q_i'^2} \\ &\underset{j>i}{=} 0 \end{aligned} \tag{A.197}$$

and a similar computation leads to the same results for for $\langle \hat{\Pi}_z^{(i)} \otimes \hat{\Pi}_y^{(j)} \rangle$. Finally one has

$$\begin{aligned}
\langle \hat{\Pi}_x^{(i)} \otimes \hat{\Pi}_y^{(j)} \rangle &\underset{j>i}{=} \int_{-\infty}^{+\infty} dq_i \int_{-\infty}^{+\infty} dp_i \int_{-\infty}^{+\infty} dq_j \int_{-\infty}^{+\infty} dp_j \, W_{\hat{\rho}}(q_i, p_i, q_j, p_j) \, W_{\hat{\Pi}_x}(q_i, p_i) W_{\hat{\Pi}_y}(q_j, p_j) \\
&\underset{j>i}{=} i\mathcal{N} \int_{-\infty}^{+\infty} dq_i \int_{-\infty}^{+\infty} dp_i \int_{-\infty}^{+\infty} dq_j \int_{-\infty}^{+\infty} dp_j \, W_-(q) W_\pm(p) W_\pm(q,p) \\
&\quad \times \mathrm{sgn}(q_i) \delta(q_j) \int_{-\infty}^{+\infty} dq_j' \mathrm{sgn}(q_j') e^{-2ip_j q_j'} \\
&\underset{j>i}{=} i\mathcal{N} \frac{\pi}{B_{ij}} \sqrt{C_{ij}} \int_{-\infty}^{+\infty} dq_i \, \mathrm{sgn}(q_i) e^{-C_{ij} A_j q_i^2} \\
&\quad \times \int_{-\infty}^{+\infty} dq_j' \mathrm{sgn}(q_j') e^{-\frac{C_{ij}A_j}{B_{ij}} q_j'^2 \pm 2i A_j C_{ij} G_{ij} q_i q_j'} \\
&\underset{j>i}{=} \mp 4\mathcal{N} \frac{\pi}{B_{ij}} \sqrt{C_{ij}} \int_0^{+\infty} dq_i \, e^{-C_{ij} A_j q_i^2} \int_0^{+\infty} dq_j' e^{-\frac{C_{ij}A_j}{B_{ij}} q_j'^2} \sin\left(2 A_j C_{ij} G_{ij} q_i q_j'\right)
\end{aligned} \tag{A.198}$$

and a similar computation leads to

$$\langle \hat{\Pi}_y^{(i)} \otimes \hat{\Pi}_x^{(j)} \rangle \underset{j>i}{=} -4\mathcal{N} \frac{\pi}{B_{ij}} \sqrt{C_{ij}} \int_0^{+\infty} dq_j \, e^{-C_{ij} A_i q_j^2} \int_0^{+\infty} dq_i' e^{-\frac{C_{ij}A_i}{B_{ij}} q_i'^2} \sin\left(2 A_i C_{ij} G_{ij} q_j q_i'\right) \tag{A.199}$$

Performing a change of variables in the two previous expressions, one is left with

$$\begin{aligned}
\langle \hat{\Pi}_x^{(i)} \otimes \hat{\Pi}_y^{(j)} \rangle &\underset{j>i}{=} \mp \frac{4}{\pi A_j \sqrt{C_{ij} A_{ij}}} \int_0^{+\infty} dQ_i \int_0^{+\infty} dQ_j' \, e^{-Q_i^2 - Q_j'^2} \sin\left(2 \frac{G_{ij}}{\sqrt{A_{ij}}} Q_i Q_j'\right) \\
\langle \hat{\Pi}_y^{(i)} \otimes \hat{\Pi}_x^{(j)} \rangle &\underset{j>i}{=} - \frac{4}{\pi A_i \sqrt{C_{ij} A_{ij}}} \int_0^{+\infty} dQ_j \int_0^{+\infty} dQ_i' \, e^{-Q_j^2 - Q_i'^2} \sin\left(2 \frac{G_{ij}}{\sqrt{A_{ij}}} Q_j Q_i'\right)
\end{aligned} \tag{A.200}$$

Both expressions are proportional to an expression of the form

$$\int_0^{+\infty} dx \int_0^{+\infty} dy \, e^{-x^2 - y^2} \sin(axy) \tag{A.201}$$

which contains terms like

$$\int_0^{+\infty} dy \, e^{-y^2 + \gamma i a x y} = e^{-\frac{a^2}{4} x^2} \int_{-\gamma i \frac{ax}{2}}^{+\infty} dY e^{-Y^2} \tag{A.202}$$

with $\gamma = \pm 1$ and where in the second step we have performed the change of variable $Y = y - \gamma i \frac{ax}{2}$. An evaluation of such a term using (A.178) yields, after simplification and using $\mathrm{erf}(z^*) = -\mathrm{erf}(z)$, to

$$\frac{\sqrt{\pi}}{2i} \int_0^{+\infty} dx \, e^{-\left(1 + \frac{a^2}{4}\right) x^2} \mathrm{erf}\left(i \frac{ax}{2}\right) \tag{A.203}$$

Then one performs the change of variable $X = \left(1 + \frac{a^2}{4}\right) x^2$ and $dX = 2\sqrt{\left(1 + \frac{a^2}{4}\right) X} dx$ and then the Taylor expansion of the error function which allows to introduce in the expression the gamma function $\int_0^{+\infty} dX \, e^{-X} X^n = \Gamma(n+1) = n!$. One is finally left with

$$\frac{1}{2\sqrt{1 + \frac{a^2}{4}}} \sum_{n=0}^{\infty} \frac{1}{2n+1} \left(\frac{a}{2\sqrt{1 + \frac{a^2}{4}}} \right)^{2n+1} = \frac{1}{2\sqrt{1 + \frac{a^2}{4}}} \mathrm{arctanh}\left(\frac{a}{2\sqrt{1 + \frac{a^2}{4}}} \right) \tag{A.204}$$

Then using

$$\begin{aligned}
\mathrm{arsinh}(u) &= \ln\left(u + \sqrt{1 + u^2}\right) \\
\mathrm{arctanh}(u) &= \ln\left(\sqrt{\frac{u+1}{u-1}}\right)
\end{aligned} \tag{A.205}$$

it can easily be shown that

$$\mathrm{arsinh}(u) = \mathrm{arctanh}\left(\frac{u}{\sqrt{1 + u^2}}\right) \tag{A.206}$$

hence the final relation

$$\int_0^{+\infty} dx \int_0^{+\infty} dy\, e^{-x^2-y^2} \sin(axy) = \frac{1}{\sqrt{4+a^2}} \operatorname{arsinh}\left(\frac{a}{2}\right) \tag{A.207}$$

Therefore, after restoring the initial values, one ends up with

$$\begin{aligned} \langle \hat{\Pi}_x^{(i)} \otimes \hat{\Pi}_y^{(j)} \rangle &\underset{j>i}{=} \mp \frac{2}{\pi A_j} \operatorname{arsinh}\left(\frac{G_{ij}}{\sqrt{A_{ij}}}\right) \\ \langle \hat{\Pi}_y^{(i)} \otimes \hat{\Pi}_x^{(j)} \rangle &\underset{j>i}{=} -\frac{2}{\pi A_i} \operatorname{arsinh}\left(\frac{G_{ij}}{\sqrt{A_{ij}}}\right) \end{aligned} \tag{A.208}$$

where the upper line in $\mp$ is for $j = 2$ and the lower line for $j = 1$ and $i = 0$.
One can see that at zero temperature, since then the G_{ij} vanish, one has

$$\langle \hat{\Pi}_x^{(i)} \otimes \hat{\Pi}_y^{(j)} \rangle \underset{T=0}{=} \langle \hat{\Pi}_y^{(i)} \otimes \hat{\Pi}_x^{(j)} \rangle \underset{T=0}{=} 0 \tag{A.209}$$

Therefore at zero temperature, when a standard form basis is considered, the 3×3 matrix $\mathcal{T}_{rs}^{(ij)}$ given in (4.194) is already diagonal (and so is consequently the matrix $\mathcal{T}^T\mathcal{T}$ given in (A.82)) since in this case all the G_{ij} vanish. From the previous results, since at zero temperature and at any finite temperature $\det \sigma_e \geq 1$ and $|\arctan(x)| \leq \frac{\pi}{2}$, one can also see that

$$\begin{aligned} |\langle \hat{\Pi}_z^{(i)} \otimes \hat{\Pi}_z^{(j)} \rangle| &\underset{j>i}{=} \frac{1}{\sqrt{\det \sigma_e}} \leq 1 \\ |\langle \hat{\Pi}_x^{(i)} \otimes \hat{\Pi}_x^{(j)} \rangle| &\underset{j>i}{\leq} 1 \end{aligned} \tag{A.210}$$

Furthermore one can easily see that

$$|\langle \hat{\Pi}_y^{(i)} \otimes \hat{\Pi}_y^{(j)} \rangle| \underset{j>i}{=} |\langle \hat{\Pi}_z^{(i)} \otimes \hat{\Pi}_z^{(j)} \rangle| |\langle \hat{\Pi}_x^{(i)} \otimes \hat{\Pi}_x^{(j)} \rangle| \tag{A.211}$$

Because of the two previous relations (A.210) and (A.211) one has therefore

$$\begin{aligned} |\langle \hat{\Pi}_y^{(i)} \otimes \hat{\Pi}_y^{(j)} \rangle| &\underset{j>i}{\leq} |\langle \hat{\Pi}_z^{(i)} \otimes \hat{\Pi}_z^{(j)} \rangle| \\ |\langle \hat{\Pi}_y^{(i)} \otimes \hat{\Pi}_y^{(j)} \rangle| &\underset{j>i}{\leq} |\langle \hat{\Pi}_x^{(i)} \otimes \hat{\Pi}_x^{(j)} \rangle| \end{aligned} \tag{A.212}$$

All the previous relations are true at zero temperature and at any finite temperature.

A.10.3 . Expectation values of the GKMR pseudo-spins for three-mode state

Following the same line of reasoning as in (A.10.2) one obtains, after some algebra, the expectation values of the GKMR pseudo-spins for three-mode systems $\mathcal{T}_{rst}$ as defined in (4.195). For three z one has

$$\mathcal{T}_{zzz} = \frac{1}{D} \underset{T=0}{=} \frac{1}{d} \tag{A.213}$$

For two z and one x, because of the delta functions in (A.170), one has $W(\boldsymbol{q}, \boldsymbol{p}) = 1$ and for the integral over q_i one is left only with

$$\int_{-\infty}^{+\infty} dq_i \operatorname{sgn}(q_i) e^{-\frac{A_{jk}}{D} q_i^2} \tag{A.214}$$

which is zero. Hence at any temperature

$$\mathcal{T}_{xzz} = \mathcal{T}_{zxz} = \mathcal{T}_{zzx} = 0 \tag{A.215}$$

Similarly for two z and one y, one has $W_+(\boldsymbol{q}) = 1$ and $W(\boldsymbol{q}, \boldsymbol{p}) = 1$, and after integration over the remaining momentum q_i one is left with

$$\int_{-\infty}^{+\infty} dq_i' \operatorname{sgn}(q_i') e^{-\frac{D}{A_{jk}} q_i'^2} \tag{A.216}$$

Hence at any temperature

$$\mathcal{T}_{yzz} = \mathcal{T}_{zyz} = \mathcal{T}_{zzy} = 0 \tag{A.217}$$

For two x and one z one obtains :

$$\begin{aligned} \mathcal{T}_{zxx} &= -\frac{2}{\pi A_0} \arctan\left(\frac{B_0}{\sqrt{A_{01}A_{02} - B_0^2}}\right) \\ &\underset{T=0}{=} \frac{2}{\pi a_0} \arctan\left(\frac{b_{01}b_{02} - a_0 b_{12}}{\sqrt{a_0 d}}\right) \end{aligned} \tag{A.218}$$

$$\begin{aligned} \mathcal{T}_{xzx} &= -\frac{2}{\pi A_1} \arctan\left(\frac{B_1}{\sqrt{A_{01}A_{12} - B_1^2}}\right) \\ &\underset{T=0}{=} \frac{2}{\pi a_1} \arctan\left(\frac{b_{01}b_{12} - a_1 b_{02}}{\sqrt{a_1 d}}\right) \end{aligned} \tag{A.219}$$

$$\begin{aligned} \mathcal{T}_{xxz} &= -\frac{2}{\pi A_2} \arctan\left(\frac{B_2}{\sqrt{A_{02}A_{12} - B_2^2}}\right) \\ &\underset{T=0}{=} \frac{2}{\pi a_2} \arctan\left(\frac{b_{02}b_{12} - a_2 b_{01}}{\sqrt{a_2 d}}\right) \end{aligned} \tag{A.220}$$

For two y and one z one gets :

$$\begin{aligned} \mathcal{T}_{zyy} &= +\frac{2}{\pi D} \arctan\left(\frac{B_0}{\sqrt{A_{01}A_{02} - B_0^2}}\right) \\ &\underset{T=0}{=} -\frac{2}{\pi d} \arctan\left(\frac{b_{01}b_{02} - a_0 b_{12}}{\sqrt{a_0 d}}\right) \end{aligned} \tag{A.221}$$

$$\begin{aligned} \mathcal{T}_{yzy} &= +\frac{2}{\pi D} \arctan\left(\frac{B_1}{\sqrt{A_{01}A_{12} - B_1^2}}\right) \\ &\underset{T=0}{=} -\frac{2}{\pi d} \arctan\left(\frac{b_{01}b_{12} - a_1 b_{02}}{\sqrt{a_1 d}}\right) \end{aligned} \tag{A.222}$$

$$\begin{aligned} \mathcal{T}_{yyz} &= -\frac{2}{\pi D} \arctan\left(\frac{B_2}{\sqrt{A_{02}A_{12} - B_2^2}}\right) \\ &\underset{T=0}{=} +\frac{2}{\pi d} \arctan\left(\frac{b_{02}b_{12} - a_2 b_{01}}{\sqrt{a_2 d}}\right) \end{aligned} \tag{A.223}$$

For terms with one x, one y and one z, because of the definition (A.170) of the Wigner function of $\hat{\Pi}_z$, one retrieve expressions similar to the ones already computed in the 2-mode case. More specifically, one obtains (using (A.123)) after integration over the momentum space $\boldsymbol{p}$

$$\frac{i}{\pi\sqrt{A_{jk}A_{ij} - J_j^2}} \int_{-\infty}^{+\infty} dq_i dQ_i \mathrm{sgn}(q_i)\mathrm{sgn}(Q_k) e^{\frac{A_{jk}}{A_{jk}A_{ij} - J_j^2}\left(-A_j q_i^2 - DQ_k^2 - 2iE_{jk}Q_k q_i\right)} \tag{A.224}$$

where one has taken $W^{(j)}_{\hat{S}_z}$, $W^{(k)}_{\hat{S}_y}$ and $W^{(i)}_{\hat{S}_x}$ with A_{jk} being A_{jk} for $k > j$ or A_{kj} for $j > k$ (and similarly for A_{ij}), $E_{jk} = +C_j$ for $j \neq 2$ and $k \neq 1$, $E_{21} = -C_2$ and finally $J_j = B_j$ for $j \neq 2$ and $J_2 = -B_2$. At zero

temperature $E_{jk} \underset{T=0}{=} 0$ and therefore both the integral vanish. Just by writing explicitly the sign functions and by a change of variables the previous expression can be rewritten as

$$\frac{4}{\pi A_{jk}}\sqrt{\frac{A_{jk}A_{ij}-J_j^2}{A_j D}}\int_{-\infty}^{+\infty} dq_i dQ_i\, e^{-q_i^2-Q_k^2}\sin\left(aq_iQ_k\right) \tag{A.225}$$

with $a = 2E_{jk}/\sqrt{A_j D}$. Then applying (A.207) one obtains straightforwardly

$$\frac{2}{\pi A_{jk}}\operatorname{arsinh}\left(\frac{E_{jk}}{\sqrt{A_j D}}\right) \tag{A.226}$$

Therefore one ends up with

$$\mathcal{T}_{xyz} = -\frac{2}{\pi A_{12}}\operatorname{arsinh}\left(\frac{C_2}{\sqrt{A_2 D}}\right) \underset{T=0}{=} 0 \tag{A.227}$$

$$\mathcal{T}_{yxz} = +\frac{2}{\pi A_{02}}\operatorname{arsinh}\left(\frac{C_2}{\sqrt{A_2 D}}\right) \underset{T=0}{=} 0 \tag{A.228}$$

$$\mathcal{T}_{yzx} = +\frac{2}{\pi A_{01}}\operatorname{arsinh}\left(\frac{C_1}{\sqrt{A_1 D}}\right) \underset{T=0}{=} 0 \tag{A.229}$$

$$\mathcal{T}_{xzy} = +\frac{2}{\pi A_{12}}\operatorname{arsinh}\left(\frac{C_1}{\sqrt{A_1 D}}\right) \underset{T=0}{=} 0 \tag{A.230}$$

$$\mathcal{T}_{zxy} = +\frac{2}{\pi A_{02}}\operatorname{arsinh}\left(\frac{C_0}{\sqrt{A_0 D}}\right) \underset{T=0}{=} 0 \tag{A.231}$$

$$\mathcal{T}_{zyx} = +\frac{2}{\pi A_{01}}\operatorname{arsinh}\left(\frac{C_0}{\sqrt{A_0 D}}\right) \underset{T=0}{=} 0 \tag{A.232}$$

In the case of $\mathcal{T}_{yyy}$ considered at any temperature, because of the three $\delta(q_i)$ in $W^{(i)}_{\hat{S}_y}$, one has $W_+(\boldsymbol{q}) = 1$ and $W(\boldsymbol{q},\boldsymbol{p}) = 1$. After integration over the momentum space $\boldsymbol{p}$, one finds an expression that is proportional to

$$\int_{-\infty}^{+\infty} dQ_0 dQ_1 dQ_2\, \mathrm{sgn}(Q_0)\,\mathrm{sgn}(Q_1)\,\mathrm{sgn}(Q_1) e^{AQ_0^2+BQ_1^2+CQ_2^2+DQ_0Q_1+EQ_0Q_2+FQ_1Q_2} \tag{A.233}$$

with A, B, C, D, E, F all *real* coefficients and with the Q_i corresponding to the q_i' of (A.171). This expression is proven straightforwardly to be zero without evaluating the integrals. In the case of $\mathcal{T}_{xxx}$, even if $W_+(\boldsymbol{q})$ and $W(\boldsymbol{q},\boldsymbol{p})$ are no longer equal to one, after integration over the momentum space $\boldsymbol{p}$, one finds an expression analogous to (A.233) with with the Q_i corresponding to the q_i of (A.172). Then $\mathcal{T}_{xxx}$ is also zero at any temperature. For any permutation in the x and y for expressions such as $\mathcal{T}_{yxx}$ or $\mathcal{T}_{yyx}$, after integration over the momentum space $\boldsymbol{p}$, one finds, in addition to square terms such as q_i^2 or $q_j'^2$, terms such as q_iq_j' and $q_i'q_j'$ for expressions with two y or q_iq_j' and q_iq_j' for expressions with two x in the remaining exponential (to be evaluated respectively over $dq_idq_j'dq_k'$ or $dq_idq_j'dq_k$ with $i \neq j \neq k$). Again the expression are analogous to (A.233) but with coefficients D, E and F being *complex* when associated to products such as q_iq_j' and *real* for any product such as q_iq_j or $q_i'q_j'$: there are therefore straightforwardly proven to be zero. All together one has at any tempertature :

$$\mathcal{T}_{xxx} = \mathcal{T}_{xxy} = \mathcal{T}_{xyx} = \mathcal{T}_{yxx} = \mathcal{T}_{yyx} = \mathcal{T}_{yxy} = \mathcal{T}_{xyy} = \mathcal{T}_{yyy} = 0 \tag{A.234}$$

The previous results show that the only non vanishing coefficients are those which have a correspondent expression in the 2-mode mean value of $\hat{\mathcal{T}}_\rho$, i.e. once one of the modes is traced out (which is equivalent

to have in the 3-mode expression at least an index being z since $W^{(i)}_{\hat{\Pi}_z} \propto \delta(q_i)\delta(p_i)$ basically "traces out" the mode i)[17].

[17] One can retrieve the two-mode expressions from the three mode ones just by applying the following informal procedure. Take a three mode with at least one z, then if z in position i :

$$\begin{array}{lcl} A_i & \rightarrow & 1 \\ A_{ij} & \rightarrow & A_i A_j \rightarrow A_j \\ B_i & \rightarrow & -A_i F_{hk} \rightarrow -F_{hk} \text{ with } h \text{ and } k \text{ different from } i \\ D & \rightarrow & A_{hk} \text{with } h \text{ and } k \text{ different from } i \end{array}$$

.

B - BACK-REACTION IN AN ANALOG BLACK HOLE

B.1 . Back-reaction equations from 2nd order expansion of the field operator in the Gross-Pitaevskii equation

The back reaction equations are obtained by averaging equations (5.19) and (5.20) over the system state, as this is done in (5.28). For (5.22) and (5.23) holding at zeroth order, the second order quantum fluctuations terms appearing in (5.19) and (5.20) to be considered are respectively :

$$-\frac{\hbar}{2\sqrt{\rho_0}}\hat{L}_t^{(0)}\{\delta\hat{\rho}_0,\delta\hat{\theta}_0\}+\hat{L}_{GP}^{(0)}\sqrt{\rho_0}\delta\hat{\theta}_0^2+i\left(\hat{L}_{GP}^{(0)}-2g\rho_0\right)\frac{[\delta\hat{\rho}_0,\delta\hat{\theta}_0]}{2\sqrt{\rho_0}}+\left(\hat{L}_{GP}^{(0)}-4g\rho_0\right)\frac{\delta\hat{\rho}_0^2}{4\rho_0^{3/2}} \tag{B.1}$$

$$\begin{aligned}&\hbar\sqrt{\rho_0}\left(\hat{L}_t^{(0)}-(\nabla.\mathbf{v}_0)\right)\delta\hat{\theta}_0^2+\frac{\hbar}{4\rho_0^{3/2}}\left(\hat{L}_t^{(0)}+(\nabla.\mathbf{v}_0)\right)\delta\hat{\rho}_0^2\\&+i\frac{\hbar}{2\sqrt{\rho_0}}\hat{L}_t^{(0)}[\delta\hat{\rho}_0,\delta\hat{\theta}_0]+\left(\hat{L}_{GP}^{(0)}+2g\rho_0\right)\frac{\{\delta\hat{\rho}_0,\delta\hat{\theta}_0\}}{2\sqrt{\rho_0}}\end{aligned} \tag{B.2}$$

By the same reasoning, substituting $\rho(\mathbf{x},t)\rightarrow\rho_0(\mathbf{x},t)+\rho_{BR}(\mathbf{x},t)$ and $\rho(\mathbf{x},t)\rightarrow\theta_0(\mathbf{x},t)+\theta_{BR}(\mathbf{x},t)$ in the zeroth order quantum fluctuations terms of (5.19) and (5.20), with (5.22) and (5.23) still holding, one should be left with terms linear in ρ_{BR} and θ_{BR} since these are already second order terms. Using expansion (5.27) for (5.18) it follows that

$$-2\hat{L}_{GP}\sqrt{\rho}=-2\sqrt{\rho_0}\left(\frac{-\hbar^2}{4m\rho_0}\nabla.\left(\rho_0\nabla\frac{\rho_{BR}}{\rho_0}\right)+m\mathbf{v}_0.\mathbf{v}_{BR}+g\rho_{BR}+\hbar\partial_t\theta_{BR}\right) \tag{B.3}$$

$$\frac{-\hbar}{\sqrt{\rho}}\hat{L}_t\rho=\frac{-\hbar}{\sqrt{\rho_0}}\left(\partial_t\rho_{BR}+\nabla(\rho_{BR}\mathbf{v}_0+\rho_0\mathbf{v}_{BR})\right) \tag{B.4}$$

The right-hand-side terms of relations (B.3) and (B.4) will appear in our back-reaction equations added to the average over the system state of the terms respectively in (B.1) and (B.2). In order to write these equations in a more efficient form we systematicaly apply the same procedure. Recalling the definition of $\hat{L}_{GP}$ and $\hat{L}_t$ given in (5.18), and noticing that, for any two operators $\hat{A}$ and $\hat{B}$, one has

$$\hat{L}_{GP}^{(0)}\hat{A}\hat{B}=(\hat{L}_{GP}^{(0)}\hat{A})\hat{B}-\hat{A}\frac{\hbar^2}{2m}(\nabla^2\hat{B})-\frac{\hbar^2}{m}(\nabla\hat{A}).(\nabla\hat{B}) \tag{B.5}$$

$$\hat{L}_t^{(0)}\hat{A}\hat{B}=\hat{A}(\hat{L}_t^{(0)}\hat{B})+(\hat{L}_t^{(0)}\hat{A})\hat{B}-(\nabla.\mathbf{v}_0)\hat{A}\hat{B} \tag{B.6}$$

one can apply zeroth order equations (5.22) and (5.23), by setting $\hat{A}$ to either $\sqrt{\rho_0}$ or ρ_0, or first order relations (5.24) and (5.25) with $\hat{A}$ and $\hat{B}$ being either $\delta\rho_0$ or $\delta\theta_0$. This is already what we have done with the zeroth order equations to obtain relations (B.3) and (B.4). Therefore let us now consider the terms in (B.1) and (B.2) to obtain more efficient formulations [1]. Let us start with the terms of (B.1). Introducing as $\hat{A}$ a $\sqrt{\rho_0}$ in relation (B.5) and applying this relation, i.e. systematically simplifying the expression with (5.22), one obtains with little algebra :

$$\begin{aligned}\hat{L}_{GP}^{(0)}\sqrt{\rho_0}\delta\hat{\theta}_0^2&=-2\sqrt{\rho_0}\left(\frac{\hbar^2}{4m\rho_0}\nabla\left(\rho_0\nabla\delta\hat{\theta}_0^2\right)\right)\\i\left(\hat{L}_{GP}^{(0)}-2g\rho_0\right)\frac{[\delta\hat{\rho}_0,\delta\hat{\theta}_0]}{2\sqrt{\rho_0}}&=-2\sqrt{\rho_0}\left(\frac{\hbar^2}{4m\rho_0}\nabla\left(\rho_0\nabla\frac{i[\delta\hat{\rho}_0,\delta\hat{\theta}_0]}{2\rho_0}\right)+g\rho_0\frac{i[\delta\hat{\rho}_0,\delta\hat{\theta}_0]}{2\rho_0}\right)\\\left(\hat{L}_{GP}^{(0)}-4g\rho_0\right)\frac{\delta\hat{\rho}_0^2}{4\rho_0^{3/2}}&=-2\sqrt{\rho}\left(\frac{\hbar^2}{4m\rho_0}\nabla\left(\rho_0\nabla\frac{\delta\hat{\rho}_0^2}{4\rho_0^2}\right)+g\rho_0\frac{\delta\hat{\rho}_0^2}{2\rho_0^2}\right)\end{aligned} \tag{B.7}$$

[1] One can notice that in relation (B.5), without reversing the order of $\hat{A}$ and $\hat{B}$, the operator $\hat{L}_{GP}^{(0)}$ can also be applied to $\hat{B}$ instead of $\hat{A}$: in this case ∇^2 should be applied to $\hat{A}$, the last term of the right-hand-side remaining the same.

Finally noticing that the first term in (B.1) is just

$$-\frac{\hbar}{2\sqrt{\rho_0}}\hat{L}_t^{(0)}\{\delta\hat{\rho}_0,\delta\hat{\theta}_0\}=-2\sqrt{\rho_0}\left(\frac{\hbar}{4\rho_0}(\partial_t+(\nabla.\mathbf{v}_0)+\mathbf{v}_0.\nabla)\{\delta\hat{\rho}_0,\delta\hat{\theta}_0\}\right) \tag{B.8}$$

all the terms for the first back reaction equation have now been rewritten. Regarding the terms for the second back reaction equation in (B.2) the computations to obtain more efficient expressions are a bit more involved. First of all, since for index μ being t or $\mathbf{x}$, one has $\partial_\mu\delta\hat{\theta}_0^2=\{\partial_\mu\delta\hat{\theta}_0,\delta\hat{\theta}_0\}$, the same being true for $\delta\hat{\rho}_0$, one obtains :

$$\begin{aligned}\hbar\sqrt{\rho_0}\left(\hat{L}_t^{(0)}-(\nabla.\mathbf{v}_0)\right)\delta\hat{\theta}_0^2 &= \sqrt{\rho_0}\left\{\hbar\left(\hat{L}_t^{(0)}-(\nabla.\mathbf{v}_0)\right)\delta\hat{\theta}_0,\delta\hat{\theta}_0\right\}\\ &= -\frac{1}{2}\left\{\hat{L}_{GP}^{(0)}\frac{\delta\hat{\rho}_0}{\sqrt{\rho_0}},\delta\hat{\theta}_0\right\}-g\sqrt{\rho_0}\left\{\delta\hat{\rho}_0,\delta\hat{\theta}_0\right\}\\ &= \frac{\hbar^2\sqrt{\rho_0}}{4m}\left\{\nabla^2\frac{\delta\hat{\rho}_0}{\rho_0},\delta\hat{\theta}_0\right\}+\frac{\hbar^2(\nabla\rho_0)}{4m\sqrt{\rho_0}}\left\{\nabla\frac{\delta\hat{\rho}_0}{\rho_0},\delta\hat{\theta}_0\right\}\\ &\quad -g\sqrt{\rho_0}\left\{\delta\hat{\rho}_0,\delta\hat{\theta}_0\right\}\end{aligned} \tag{B.9}$$

where to go from the first to the second line the first order equation (5.24) has been applied and to go from the second to the third line we have set $\delta\hat{\rho}_0/\sqrt{\rho_0}=\sqrt{\rho_0}\delta\hat{\rho}_0/\rho_0$ and then again set $\hat{A}$ to $\sqrt{\rho_0}$ in relation (B.5) to simplify the expression by applying the zeroth order equation (5.22). Furthermore one obtains

$$\begin{aligned}\frac{\hbar}{4\rho_0^{3/2}}\left(\hat{L}_t^{(0)}+(\nabla.\mathbf{v}_0)\right)\delta\hat{\rho}_0^2 &= \frac{1}{4\rho_0^{3/2}}\left\{\hbar\hat{L}_t^{(0)}\delta\hat{\rho}_0,\delta\hat{\rho}_0\right\}\\ &= \frac{1}{2\rho_0}\left\{\hat{L}_{GP}^{(0)}\sqrt{\rho_0}\delta\hat{\theta}_0,\delta\hat{\rho}_0\right\}\\ &= \frac{-\hbar^2}{4m\sqrt{\rho_0}}\left\{\nabla^2\delta\hat{\theta}_0,\delta\hat{\rho}_0\right\}-\frac{\hbar^2(\nabla\rho_0)}{4m\rho_0^{3/2}}\left\{\nabla\delta\hat{\theta}_0,\delta\hat{\rho}_0\right\}\end{aligned} \tag{B.10}$$

where in the first line we have used $\delta\hat{\rho}_0^2=\{\delta\hat{\rho}_0,\delta\hat{\rho}_0\}/2$ whereas to go from the first to the second line the first order equation (5.25) has been applied and to go from the second to the third line we have again set $\hat{A}$ to $\sqrt{\rho_0}$ in relation (B.5) to simplify the expression by applying the zeroth order equation (5.22). Similarly one has

$$\begin{aligned}\left(\hat{L}_{GP}^{(0)}+2g\rho_0\right)\frac{\{\delta\hat{\rho}_0,\delta\hat{\theta}_0\}}{2\sqrt{\rho_0}} &= \frac{-\hbar^2\sqrt{\rho_0}}{2m}\nabla^2\frac{\{\delta\hat{\rho}_0,\delta\hat{\theta}_0\}}{2\rho_0}-\frac{\hbar^2\nabla\rho_0}{2m\sqrt{\rho_0}}\nabla\frac{\{\delta\hat{\rho}_0,\delta\hat{\theta}_0\}}{2\rho_0}\\ &\quad +g\sqrt{\rho_0}\{\delta\hat{\rho}_0,\delta\hat{\theta}_0\}\\ &= \frac{-\hbar^2\sqrt{\rho_0}}{4m}\{\nabla^2\frac{\delta\hat{\rho}_0}{\rho_0},\delta\hat{\theta}_0\}-\frac{\hbar^2}{4m\sqrt{\rho_0}}\{\delta\hat{\rho}_0,\nabla^2\delta\hat{\theta}_0\}\\ &\quad +\frac{\hbar^2(\nabla\rho_0)}{4m\rho_0^{3/2}}\{\delta\hat{\rho}_0,\nabla\delta\hat{\theta}_0\}-\frac{\hbar^2}{2m\sqrt{\rho_0}}\{\nabla\delta\hat{\rho}_0,\nabla\delta\hat{\theta}_0\}\\ &\quad -\frac{\hbar^2(\nabla\rho_0)}{4m\sqrt{\rho_0}}\{\nabla\frac{\delta\hat{\rho}_0}{\rho_0},\delta\hat{\theta}_0\}+g\sqrt{\rho_0}\{\delta\hat{\rho}_0,\delta\hat{\theta}_0\}\end{aligned} \tag{B.11}$$

where to obtain the right-hand-side of the first line we have set $\{\delta\hat{\rho}_0,\delta\hat{\theta}_0\}/\sqrt{\rho_0}=\sqrt{\rho_0}\{\delta\hat{\rho}_0,\delta\hat{\theta}_0\}/\rho_0$ and again set $\hat{A}$ to $\sqrt{\rho_0}$ in relation (B.5) to simplify the expression by applying the zeroth order equation (5.22). Then, going from the obtained expression to the last expression requires only little algebra. Adding all the terms of the previous expressions (B.9), (B.10) and (B.11), leaves only

$$-\frac{\hbar^2}{2m\sqrt{\rho_0}}\{\delta\hat{\rho}_0,\nabla^2\delta\hat{\theta}_0\}-\frac{\hbar^2}{2m\sqrt{\rho_0}}\{\nabla\delta\hat{\rho}_0,\nabla\delta\hat{\theta}_0\}=-\frac{\hbar}{\sqrt{\rho_0}}\left(\frac{\hbar}{2m}\nabla\{\delta\hat{\rho}_0,\nabla\delta\hat{\theta}_0\}\right) \tag{B.12}$$

We are now left with a last term in (B.2). Just by applying (B.6), one sees that :

$$\begin{aligned} +i\frac{\hbar}{2\sqrt{\rho_0}}\hat{L}_t^{(0)}[\delta\hat{\rho}_0,\delta\hat{\theta}_0] &= i\frac{1}{2\sqrt{\rho_0}}\left([\hbar\hat{L}_t^{(0)}\delta\hat{\rho}_0,\delta\hat{\theta}_0]+[\delta\hat{\rho}_0,\hbar\hat{L}_t^{(0)}\delta\hat{\theta}_0]-\hbar(\nabla.\mathbf{v}_0)[\delta\hat{\rho}_0,\delta\hat{\theta}_0,]\right) \\ &= i\frac{1}{2\sqrt{\rho_0}}\left(\frac{-2\sqrt{\rho_0}\hbar^2}{2m}[\nabla^2\sqrt{\rho_0}\delta\hat{\theta}_0,\delta\hat{\theta}_0]+\frac{\hbar^2}{4m\sqrt{\rho_0}}[\delta\hat{\rho}_0,\nabla^2\frac{\delta\hat{\rho}_0}{\sqrt{\rho_0}}]\right) \\ &= 0 \end{aligned} \tag{B.13}$$

where from the first to the second line we have applied the first order equations (5.24) and (5.25) knowing that $\delta\hat{\rho}_0$ and $\delta\hat{\theta}_0$ commute respectively with themselves, whereas from the second to the third line we have also applied relation (5.11) that states that $\delta\hat{\rho}_0$ and $\delta\hat{\theta}_0$ commute respectively with their own *spatial* derivatives.
We are now ready to summarize our computations in our back-reaction equations. Indeed, on the one hand, taking the average of equation (5.19) over the system state, that is to say applying the first line of (5.28), remembering that all the first order quantum fluctuations terms vanish, and resuming all the remaining terms of (B.1) as we have written them in relations (B.3), (B.7) and (B.8), one finally obtains, after dividing by $-2\sqrt{\rho_0}$, the *first back-reaction equation* :

$$\begin{aligned} &\hbar\partial_t\theta_{BR}+m\mathbf{v}_0.\mathbf{v}_{BR}+\frac{\hbar}{2\rho_0}(\partial_t+(\nabla.\mathbf{v}_0)+\mathbf{v}_0.\nabla)Re\langle\delta\hat{\rho}_0\delta\hat{\theta}_0\rangle \\ &+g\rho_0\left(\frac{\rho_{BR}}{\rho_0}+\frac{\langle\delta\hat{\rho}_0^2\rangle}{2\rho_0^2}-\frac{\delta(\mathbf{0})}{2\rho_0}\right)-\frac{\hbar^2}{4m\rho_0}\nabla\left(\rho_0\nabla\left(\frac{\rho_{BR}}{\rho_0}-\left(\frac{\langle\delta\hat{\rho}_0^2\rangle}{4\rho_0^2}+\langle\delta\hat{\theta}_0^2\rangle-\frac{\delta(\mathbf{0})}{2\rho_0}\right)\right)\right)=0 \end{aligned} \tag{B.14}$$

where we have written $\langle\{\delta\hat{\rho}_0,\delta\hat{\theta}_0\}\rangle = 2Re\langle\delta\hat{\rho}_0\delta\hat{\theta}_0\rangle$ and $\langle[\delta\hat{\rho}_0,\delta\hat{\theta}_0]\rangle = \langle i\delta(\mathbf{0})\rangle = i\delta(\mathbf{0})$. Dividing this equation by m, one can introduce the coefficients $c(t,\mathbf{x})\xi(t,\mathbf{x}) = \hbar/m$ and $c^2(t,\mathbf{x}) = g(t,\mathbf{x})\rho_0(t,\mathbf{x})/m$ with c the velocity of sound in the fluid and ξ the healing length.

On the other hand, taking the average of equation (5.20) over the system state, that is to say applying the second line of (5.28), remembering that all the first order quantum fluctuations terms vanish, and resuming all the remaining terms of (B.2) as we have written them in relations (B.4) and (B.12), one finally obtains, after dividing by $-\hbar/\sqrt{\rho_0}$, the *second back-reaction equation* :

$$\partial_t\rho_{BR}+\nabla\left(\rho_{BR}\mathbf{v}_0+\rho_0\mathbf{v}_{BR}+\frac{\hbar}{m}Re\langle\delta\hat{\rho}_0\nabla\delta\hat{\theta}_0\rangle\right)=0 \tag{B.15}$$

where we have written $\langle\{\delta\hat{\rho}_0,\nabla\delta\hat{\theta}_0\}\rangle = 2Re\langle\delta\hat{\rho}_0\nabla\delta\hat{\theta}_0\rangle$.

B.2 . Source terms in the 1-D Back-Reaction equations

Let us now consider a stationary one-dimensional transonic flow. In relation (5.6) we defined the operator $\hat{\Psi}(t,\mathbf{x})$ in the density-phase representation. Expanding at *first* order, for a one-dimensional configuration, this definition yields

$$\hat{\Psi}(t,x)\approx\varphi_0(x)+\varphi_0(x)\left(\frac{\delta\hat{\rho}_0(t,x)}{2\rho_0(x)}+i\delta\hat{\theta}_0(t,x)\right) \tag{B.16}$$

where

$$\varphi_0(x)=e^{i\,\theta_0(x)}\sqrt{\rho_0(x)} \tag{B.17}$$

is defined for $\rho_0(x)$ and $\theta_0(x)$ being *stationary* solutions of the zeroth order equations (5.22) and (5.23) whereas $\delta\hat{\rho}_0(t,x)$ $\delta\hat{\theta}_0(t,x)$ are solutions of the first order equations (5.24) and (5.25) parametrized by $\rho_0(x)$ and $\theta_0(x)$. Comparing the expansion (B.16) to the Bogoliubov approximation

$$\hat{\Psi}(t,x)=\phi(x)+\delta\hat{\Psi}(t,x) \tag{B.18}$$

where $\langle\hat{\Psi}(t,x)\rangle = \phi(x)$ and $\langle\delta\hat{\Psi}(t,x)\rangle = 0$ with $\delta\hat{\Psi}(t,x)$ a first order quantum fluctuation. When $\hat{\Psi}(t,x)$ is taken up to first order, $\phi(x)$ is just the zeroth order term $\varphi_0(x)$. Then, comparing the expansion (B.16) to the Bogoliubov approximation (B.18) at first order yields immediately

$$\begin{aligned}\delta\hat{\rho}_0(t,x) &= \varphi_0(x)\delta\hat{\Psi}^\dagger(t,x) + \varphi_0^*(x)\delta\hat{\Psi}(t,x)\\ \delta\hat{\theta}_0(t,x) &= \frac{i}{2\rho_0(x)}\left(\varphi_0(x)\delta\hat{\Psi}^\dagger(t,x) - \varphi_0^*(x)\delta\hat{\Psi}(t,x)\right)\end{aligned} \tag{B.19}$$

which also shows that $\delta\hat{\rho}_0$ and $\delta\hat{\theta}_0$ are hermitian operators. Taking the definition of $\varphi_0(x)$ from relation (4) in reference [38] one has :

$$\varphi_0(X_\alpha) = \sqrt{n_\alpha}e^{i\,m_\alpha X_\alpha}\phi_\alpha(X_\alpha) \tag{B.20}$$

where we have defined $x = X_\alpha\xi_\alpha$ with ξ_α the healing length and m_α the Mach number for α meaning u (upstream) or d (downstream). With this definition one sees that

$$\rho_0(X_\alpha) = |\varphi_0(X_\alpha)|^2 = n_\alpha|\phi_\alpha(X_\alpha)|^2 \tag{B.21}$$

From relation (45) still in reference [38] one has

$$\begin{aligned}\delta\hat{\Psi}(t,X_\alpha) = e^{im_\alpha X_\alpha}\int_0^\infty\frac{d\omega}{\sqrt{2\pi}}\sum_{L\in[U,D1]}\left[\bar{u}_L(X_\alpha,\omega)e^{-i\omega t}b_L(\omega) + \bar{v}_L^*(X_\alpha,\omega)e^{i\omega t}b_L^\dagger(\omega)\right]\\ + e^{im_\alpha X_\alpha}\int_0^\Omega\frac{d\omega}{\sqrt{2\pi}}\left[\bar{u}_{D2}(X_\alpha,\omega)e^{-i\omega t}b_{D2}^\dagger(\omega) + \bar{v}_{D2}^*(X_\alpha,\omega)e^{i\omega t}b_{D2}(\omega)\right]\end{aligned} \tag{B.22}$$

Applying these definitions at equal time, we want to compute the source terms in the back-reaction equations (5.29) and (5.30) with the state of the system being the vacuum of quasi-particles. Let us start with the term

$$\frac{\langle\delta\hat{\rho}_0^2\rangle}{4\rho_0^2} + \langle\delta\hat{\theta}_0^2\rangle - \frac{\delta(0)}{2\rho_0} \tag{B.23}$$

in (5.29). To this end, for L being U, $D1$ or $D2$ one defines

$$\begin{aligned}\tilde{u}_L(X_\alpha,\omega) &= \bar{u}_L(X_\alpha,\omega)\phi_\alpha^*(X_\alpha)\\ \tilde{v}_L(X_\alpha,\omega) &= \bar{v}_L(X_\alpha,\omega)\phi_\alpha(X_\alpha)\end{aligned} \tag{B.24}$$

Then, dropping for convenience the ω and X_α dependence of $\tilde{u}_L$ and $\tilde{v}_L$ and the X_α dependence of ϕ_α, one can write

$$\begin{aligned}\delta\hat{\rho}_0 = \sqrt{n_\alpha}\int_0^\infty\frac{d\omega}{\sqrt{2\pi}}\sum_{L\in[U,D1]}\left[[\tilde{u}_L+\tilde{v}_L]e^{-i\omega t}b_L(\omega) + [\tilde{u}_L^*+\tilde{v}_L^*]e^{i\omega t}b_L^\dagger(\omega)\right]\\ + \sqrt{n_\alpha}\int_0^\Omega\frac{d\omega}{\sqrt{2\pi}}\left[[\tilde{u}_{D2}+\tilde{v}_{D2}]e^{-i\omega t}b_{D2}^\dagger(\omega) + [\tilde{u}_{D2}^*+\tilde{v}_{D2}^*]e^{i\omega t}b_{D2}(\omega)\right]\end{aligned} \tag{B.25}$$

and

$$\begin{aligned}\delta\hat{\theta}_0 = \frac{i}{2\sqrt{n_\alpha}|\phi_\alpha|^2}\int_0^\infty\frac{d\omega}{\sqrt{2\pi}}\sum_{L\in[U,D1]}\left[[\tilde{v}_L-\tilde{u}_L]e^{-i\omega t}b_L(\omega) + [\tilde{u}_L^*-\tilde{v}_L^*]e^{i\omega t}b_L^\dagger(\omega)\right]\\ + \frac{i}{2\sqrt{n_\alpha}|\phi_\alpha|^2}\int_0^\Omega\frac{d\omega}{\sqrt{2\pi}}\left[[\tilde{v}_{D2}-\tilde{u}_{D2}]e^{-i\omega t}b_{D2}^\dagger(\omega) + [\tilde{u}_{D2}^*-\tilde{v}_{D2}^*]e^{i\omega t}b_{D2}(\omega)\right]\end{aligned} \tag{B.26}$$

With these definitions in mind, recalling that one has always $\langle\hat{b}_L(\omega)\hat{b}_{L'}(\omega')\rangle$ and $\langle\hat{b}_L(\omega)\hat{b}_{L'}(\omega')\rangle$ equal to zero and, when averaging on the vacuum state, $\langle\hat{b}_L^\dagger(\omega)\hat{b}_{L'}(\omega')\rangle = 0$ and $\langle\hat{b}_L(\omega)\hat{b}_{L'}^\dagger(\omega')\rangle = \delta_{L,L'}\delta(\omega-\omega')$, one obtains

$$\langle\delta\hat{\rho}_0^2\rangle = n_\alpha\int_0^\infty\frac{d\omega}{2\pi}\sum_{L\in[U,D1]}|\tilde{u}_L+\tilde{v}_L|^2 + n_\alpha\int_0^\Omega\frac{d\omega}{2\pi}|\tilde{u}_{D2}+\tilde{v}_{D2}|^2 \tag{B.27}$$

$$\langle \delta\hat{\theta}_0^2 \rangle = \frac{1}{4n_\alpha|\phi_\alpha|^4}\int_0^\infty \frac{d\omega}{2\pi}\sum_{L\in[U,D1]}|\tilde{u}_L-\tilde{v}_L|^2 + \frac{1}{4n_\alpha|\phi_\alpha|^4}\int_0^\Omega \frac{d\omega}{2\pi}|\tilde{u}_{D2}-\tilde{v}_{D2}|^2 \tag{B.28}$$

$$\begin{aligned}\langle \delta\hat{\rho}_0\delta\hat{\theta}_0\rangle = &\frac{i}{2|\phi_\alpha|^2}\int_0^\infty \frac{d\omega}{2\pi}\sum_{L\in[U,D1]}\left[|\tilde{u}_L|^2+2iIm(\tilde{u}_L^*\tilde{v}_L)-|\tilde{v}_L|^2\right]\\ &+\frac{i}{2|\phi_\alpha|^2}\int_0^\Omega \frac{d\omega}{2\pi}\left[|\tilde{v}_{D2}|^2+2iIm(\tilde{u}_{D2}^*\tilde{v}_{D2})-|\tilde{u}_{D2}|^2\right]\end{aligned} \tag{B.29}$$

$$\begin{aligned}\langle \delta\hat{\theta}_0\delta\hat{\rho}_0\rangle = &\frac{i}{2|\phi_\alpha|^2}\int_0^\infty \frac{d\omega}{2\pi}\sum_{L\in[U,D1]}\left[|\tilde{v}_L|^2+2iIm(\tilde{u}_L^*\tilde{v}_L)-|\tilde{u}_L|^2\right]\\ &+\frac{i}{2|\phi_\alpha|^2}\int_0^\Omega \frac{d\omega}{2\pi}\left[|\tilde{u}_{D2}|^2+2iIm(\tilde{u}_{D2}^*\tilde{v}_{D2})-|\tilde{v}_{D2}|^2\right]\end{aligned} \tag{B.30}$$

One can see that all these quadratic terms are time independent. It is also straightforward to obtain

$$\langle[\delta\hat{\rho}_0,\delta\hat{\theta}_0]\rangle = \frac{i}{|\phi_\alpha|^2}\int_0^\infty \frac{d\omega}{2\pi}\sum_{L\in[U,D1]}\left[|\tilde{u}_L|^2-|\tilde{v}_L|^2\right] + \frac{i}{|\phi_\alpha|^2}\int_0^\Omega \frac{d\omega}{2\pi}\left[|\tilde{v}_{D2}|^2-|\tilde{u}_{D2}|^2\right] \tag{B.31}$$

Then, adding these last relations together and recalling that $-\delta(0) = i\langle[\delta\hat{\rho}_0,\delta\hat{\theta}_0]\rangle$ one finally ends up with

$$\boxed{\frac{\langle\delta\hat{\rho}_0^2\rangle}{4\rho_0^2}+\langle\delta\hat{\theta}_0^2\rangle-\frac{\delta(0)}{2\rho_0} = \frac{1}{n_\alpha|\phi_\alpha|^2}\int_0^\infty \frac{d\omega}{2\pi}\sum_{L\in[U,D1]}|\bar{v}_L|^2+\frac{1}{n_\alpha|\phi_\alpha|^2}\int_0^\Omega\frac{d\omega}{2\pi}|\bar{u}_{D2}|^2} \tag{B.32}$$

In the same way one obtains in (5.29) the terms

$$\boxed{Re\langle\delta\hat{\rho}_0\delta\hat{\theta}_0\rangle = \int_0^\infty\frac{d\omega}{2\pi}\sum_{L\in[U,D1]}Im\left(\frac{\phi_\alpha^*}{\phi_\alpha}\bar{u}_L\bar{v}_L^*\right)+\int_0^\Omega\frac{d\omega}{2\pi}Im\left(\frac{\phi_\alpha^*}{\phi_\alpha}\bar{u}_{D2}\bar{v}_{D2}^*\right)} \tag{B.33}$$

and

$$\boxed{\begin{aligned}\frac{\langle\delta\hat{\rho}_0^2\rangle}{2\rho_0^2}-\frac{\delta(0)}{2\rho_0} =&\frac{1}{n_\alpha|\phi_\alpha|^4}\int_0^\infty\frac{d\omega}{2\pi}\sum_{L\in[U,D1]}\left[|\tilde{v}_L|^2+Re(\tilde{u}_L\tilde{v}_L^*)\right]\\ &+\frac{1}{n_\alpha|\phi_\alpha|^4}\int_0^\Omega\frac{d\omega}{2\pi}\left[|\tilde{u}_{D2}|^2+Re(\tilde{u}_{D2}\tilde{v}_{D2}^*)\right]\end{aligned}} \tag{B.34}$$

Now let us compute also the terms with the derivatives. From (B.33) one has immediately

$$\partial_{X_\alpha}Re\langle\delta\hat{\rho}_0\delta\hat{\theta}_0\rangle = \int_0^\infty\frac{d\omega}{2\pi}\sum_{L\in[U,D1]}\partial_{X_\alpha}Im\left(\frac{\phi_\alpha^*}{\phi_\alpha}\bar{u}_L\bar{v}_L^*\right)+\int_0^\Omega\frac{d\omega}{2\pi}\partial_{X_\alpha}Im\left(\frac{\phi_\alpha^*}{\phi_\alpha}\bar{u}_{D2}\bar{v}_{D2}^*\right) \tag{B.35}$$

Furthermore one has

$$\begin{aligned}\langle\delta\hat{\rho}_0\partial_{X_\alpha}\delta\hat{\theta}_0\rangle =&\frac{i}{2}\int_0^\infty\frac{d\omega}{2\pi}\sum_{L\in[U,D1]}\left[(\tilde{u}_L+\tilde{v}_L)\partial_{X_\alpha}\left(\frac{\bar{u}_L^*}{\phi_\alpha^*}-\frac{\bar{v}_L^*}{\phi_\alpha}\right)\right]\\ &+\frac{i}{2}\int_0^\Omega\frac{d\omega}{2\pi}\left[(\tilde{u}_{D2}^*+\tilde{v}_{D2}^*)\partial_{X_\alpha}\left(\frac{\bar{v}_{D2}}{\phi_\alpha^*}-\frac{\bar{u}_{D2}}{\phi_\alpha}\right)\right]\end{aligned} \tag{B.36}$$

and

$$\begin{aligned}\langle(\partial_{X_\alpha}\delta\hat{\theta}_0)\delta\hat{\rho}_0\rangle =&\frac{i}{2}\int_0^\infty\frac{d\omega}{2\pi}\sum_{L\in[U,D1]}\left[(\tilde{u}_L^*+\tilde{v}_L^*)\partial_{X_\alpha}\left(\frac{\bar{v}_L}{\phi_\alpha^*}-\frac{\bar{u}_L}{\phi_\alpha}\right)\right]\\ &+\frac{i}{2}\int_0^\Omega\frac{d\omega}{2\pi}\left[(\tilde{u}_{D2}+\tilde{v}_{D2})\partial_{X_\alpha}\left(\frac{\bar{u}_{D2}^*}{\phi_\alpha^*}-\frac{\bar{v}_{D2}^*}{\phi_\alpha}\right)\right]\end{aligned} \tag{B.37}$$

Hence

$$\begin{aligned} Re\langle \delta\hat{\rho}_0 \partial_{X_\alpha} \delta\hat{\theta}_0 \rangle =& \frac{1}{2}\int_0^\infty \frac{d\omega}{2\pi} \sum_{L\in[U,D1]} Im\left[(\tilde{u}_L^* + \tilde{v}_L^*) \partial_{X_\alpha} \left(\frac{\bar{u}_L}{\phi_\alpha} - \frac{\bar{v}_L}{\phi_\alpha^*} \right) \right] \\ &+ \frac{1}{2}\int_0^\Omega \frac{d\omega}{2\pi} Im\left[(\tilde{u}_{D2} + \tilde{v}_{D2}) \partial_{X_\alpha} \left(\frac{\bar{v}_{D2}^*}{\phi_\alpha} - \frac{\bar{u}_{D2}^*}{\phi_\alpha^*} \right) \right] \end{aligned} \tag{B.38}$$

From the last term (B.41) one can also easily deduce that

$$\begin{aligned} Re\langle \delta\hat{\rho}_0 \partial^2_{X_\alpha} \delta\hat{\theta}_0 \rangle =& \frac{1}{2}\int_0^\infty \frac{d\omega}{2\pi} \sum_{L\in[U,D1]} Im\left[(\tilde{u}_L^* + \tilde{v}_L^*) \partial^2_{X_\alpha} \left(\frac{\bar{u}_L}{\phi_\alpha} - \frac{\bar{v}_L}{\phi_\alpha^*} \right) \right] \\ &+ \frac{1}{2}\int_0^\Omega \frac{d\omega}{2\pi} Im\left[(\tilde{u}_{D2} + \tilde{v}_{D2}) \partial^2_{X_\alpha} \left(\frac{\bar{v}_{D2}^*}{\phi_\alpha} - \frac{\bar{u}_{D2}^*}{\phi_\alpha^*} \right) \right] \end{aligned} \tag{B.39}$$

$$\begin{aligned} Re\langle (\partial_{X_\alpha} \delta\hat{\rho}_0) \delta\hat{\theta}_0 \rangle =& \frac{1}{2}\int_0^\infty \frac{d\omega}{2\pi} \sum_{L\in[U,D1]} Im\left[[\partial_{X_\alpha}(\tilde{u}_L^* + \tilde{v}_L^*)] \left(\frac{\bar{u}_L}{\phi_\alpha} - \frac{\bar{v}_L}{\phi_\alpha^*} \right) \right] \\ &+ \frac{1}{2}\int_0^\Omega \frac{d\omega}{2\pi} Im\left[[\partial_{X_\alpha}(\tilde{u}_{D2} + \tilde{v}_{D2})] \left(\frac{\bar{v}_{D2}^*}{\phi_\alpha} - \frac{\bar{u}_{D2}^*}{\phi_\alpha^*} \right) \right] \end{aligned} \tag{B.40}$$

$$\begin{aligned} Re\langle (\partial_{X_\alpha} \delta\hat{\rho}_0) \partial_{X_\alpha} \delta\hat{\theta}_0 \rangle =& \frac{1}{2}\int_0^\infty \frac{d\omega}{2\pi} \sum_{L\in[U,D1]} Im\left[[\partial_{X_\alpha}(\tilde{u}_L^* + \tilde{v}_L^*)] \, \partial_{X_\alpha} \left(\frac{\bar{u}_L}{\phi_\alpha} - \frac{\bar{v}_L}{\phi_\alpha^*} \right) \right] \\ &+ \frac{1}{2}\int_0^\Omega \frac{d\omega}{2\pi} Im\left[[\partial_{X_\alpha}(\tilde{u}_{D2} + \tilde{v}_{D2})] \, \partial_{X_\alpha} \left(\frac{\bar{v}_{D2}^*}{\phi_\alpha} - \frac{\bar{u}_{D2}^*}{\phi_\alpha^*} \right) \right] \end{aligned} \tag{B.41}$$

The first and second derivatives of (B.32) that appear in the first back reaction equation (**??**) are straightforward from (B.32). Still in the first back reaction equation the term (B.35) can alternatively be computed from

$$\partial_{X_\alpha} Re\langle \delta\hat{\rho}_0 \delta\hat{\theta}_0 \rangle = Re\langle (\partial_{X_\alpha} \delta\hat{\rho}_0) \delta\hat{\theta}_0 \rangle + Re\langle \delta\hat{\rho}_0 \partial_{X_\alpha} \delta\hat{\theta}_0 \rangle \tag{B.42}$$

Finally the term of the second back reaction equation (5.30)

$$\partial_{X_\alpha} Re\langle \delta\hat{\rho}_0 \partial_{X_\alpha} \delta\hat{\theta}_0 \rangle = Re\langle (\partial_{X_\alpha} \delta\hat{\rho}_0) \partial_{X_\alpha} \delta\hat{\theta}_0 \rangle + Re\langle \delta\hat{\rho}_0 \partial^2_{X_\alpha} \delta\hat{\theta}_0 \rangle \tag{B.43}$$

is straightforward from the previous terms.

Rewriting the depletion term

The depletion term can be rewritten as

$$\frac{\langle \delta\hat{\rho}_0^2 \rangle}{4\rho_0^2} + \langle \delta\hat{\theta}_0^2 \rangle - \frac{\delta(0)}{2\rho_0} = \frac{1}{2}\left[\frac{\langle \delta\hat{\rho}_0^2 \rangle}{2\rho_0^2} - \frac{\delta(0)}{2\rho_0} \right] + \left[\langle \delta\hat{\theta}_0^2 \rangle - \frac{\delta(0)}{4\rho_0} \right] \tag{B.44}$$

with

$$\begin{aligned} \langle \delta\hat{\theta}_0^2 \rangle - \frac{\delta(0)}{4\rho_0} =& \frac{1}{2n_\alpha |\phi_\alpha|^4} \int_0^\infty \frac{d\omega}{2\pi} \sum_{L\in[U,D1]} \left[|\tilde{v}_L|^2 - Re(\tilde{u}_L \tilde{v}_L^*) \right] \\ &+ \frac{1}{2n_\alpha |\phi_\alpha|^4} \int_0^\Omega \frac{d\omega}{2\pi} \left[|\tilde{u}_{D2}|^2 - Re(\tilde{u}_{D2} \tilde{v}_{D2}^*) \right] \end{aligned} \tag{B.45}$$

Then one can check numerically that

$$\begin{aligned} \partial_x \left[\langle \delta\hat{\theta}_0^2 \rangle - \frac{\delta(0)}{4\rho_0} \right] =& \frac{1}{2n_\alpha \xi_\alpha} \int_0^\infty \frac{d\omega}{2\pi} \sum_{L\in[U,D1]} \left[\partial_{X_\alpha} \frac{|\bar{v}_L|^2}{|\phi_\alpha|^2} - \partial_{X_\alpha} \frac{1}{|\phi_\alpha|^2} Re\left(\frac{\phi_\alpha^*}{\phi_\alpha} \bar{u}_L \bar{v}_L^* \right) \right] \\ &+ \frac{1}{2n_\alpha \xi_\alpha} \int_0^\Omega \frac{d\omega}{2\pi} \left[\partial_{X_\alpha} \frac{|\bar{u}_{D2}|^2}{|\phi_\alpha|^2} - \partial_{X_\alpha} \frac{1}{|\phi_\alpha|^2} Re\left(\frac{\phi_\alpha^*}{\phi_\alpha} \bar{u}_{D2} \bar{v}_{D2}^* \right) \right] \end{aligned} \tag{B.46}$$

is zero.

Source terms for a homogeneous 1D flow

For a homogeneous flow one has $|\phi_\alpha|^2 = 1$ and the vectors to be used are the ones defined in relations (27-31) of reference [38]. One has

$$\begin{aligned} \frac{1}{\xi_\alpha}\langle \delta\hat{\rho}_0 \partial_{X_\alpha} \delta\hat{\theta}_0 \rangle &= \frac{c_\alpha}{4\pi\xi_\alpha^2} \sum_{l\in u \text{ or } d1,d2 \text{ in/out}} \int_0^{e_l} d\varepsilon_\alpha \, \frac{Q_l}{|V_g(Q_l)|} \, \text{sgn}(E_l) \\ &= \frac{1}{4\pi\xi_\alpha^2} \sum_{l\in u \text{ or } d1,d2 \text{ in/out}} \int_{c_0^l}^{c_\infty^l} dQ_l \, Q_l \, \text{sgn}(E_l V_g(Q_l)) \end{aligned} \tag{B.47}$$

where we used for the first line $e_l \underset{l\neq d2}{=} \infty$ and $e_{d2} = \Omega$, and for the second line $V_g(Q_l)dQ_l = c_\alpha d\varepsilon_\alpha$ and defined $Q_l \underset{\varepsilon\to i}{\to} c_i^l$. One obtains for $Q_\alpha = q\xi_\alpha$

$$\frac{1}{\xi_\alpha}\langle \delta\hat{\rho}_0 \partial_{X_\alpha} \delta\hat{\theta}_0 \rangle = \frac{1}{4\pi\xi_\alpha^2} \int_{-\infty}^{+\infty} dQ_\alpha Q_\alpha \tag{B.48}$$

This term therefore diverges but it is x-independent. The source term proportional to the $G_2 = g_2(0)^2 - \rho_0^2$ is given in relation (183) of Ref. [89]. It reads

$$\frac{\langle \delta\hat{\rho}_0^2 \rangle}{2\rho_0^2} - \frac{\delta(0)}{2\rho_0} = \frac{G_2}{2\rho_0^2} = -\frac{1}{\pi n_\alpha \xi_\alpha} \tag{B.49}$$

The term $Re\langle \delta\hat{\rho}_0 \delta\theta_0 \rangle$ is zero for a homogenous flow.

Bibliography

[1] L. D. Landau and E. M. Lifschitz. *The Classical Theory of Fields*, volume II of *Course of Theoretical Physics*. Butterworth Heinemann, 1975 [1973].

[2] Y. Choquet-Bruhat. *Introduction to General Relativity, Black Holes and Cosmology*. Oxford University Press, 2015.

[3] K. Schwarschild. Über das Gravitationsfeld eines Massenpunktes nach der Einsteinschen Theorie. *Sitzungsberichte der Königlich Preussischen Akademie der Wissenschaften*, pages 189–196, Feb 1916.

[4] A. Einstein, B. Podolsky, and N. Rosen. Can Quantum-Mechanical Description of Physical Reality Be Considered Complete ? *Physical Review*, 47:777–780, 1935.

[5] E. Schrödinger. Discussion of Probability Relations between Separated systems. In *Mathematical Proceedings of the Cambridge Philosophical Society*, volume 31, pages 555–563. 1935.

[6] N. Bohr. Can Quantum-Mechanical Description of Physical Reality Be Considered Complete ? *Physical Review*, 48:696–702, 1935.

[7] J. S. Bell. On the Einstein Podolsky Rosen paradox. *Physics Physique Fizika*, 1:195–200, Nov 1964.

[8] Samuel L. Braunstein and Peter van Loock. Quantum information with continuous variables. *Rev. Mod. Phys.*, 77:513, April 2005.

[9] S. L. Braunstein, M. Faizal, L.M. Krauss, and F. Marino and. N. A. Shah. Analogue simulations of quantum gravity with fluids. *Nature Reviews Physics*, 5(1):612–622, October 2023.

[10] S. W. Hawking. Black Hole Explosions? *Nature (London)*, 248:30, 1974.

[11] S. W. Hawking. Particle Creation by Black Holes. *Commun. Math. Phys.*, 43:199, 1975.

[12] W.G. Unruh. Notes on black-hole evaporation? *Physical Review D*, 14(14):870–892, August 1976.

[13] R. Penrose and R. M. Floyd. Extraction of Rotational Energy from a Black Hole. *Nature Physical Science*, 229:177, 1971.

[14] Ya. B. Zel'dovich. Generation of Waves by a Rotating Body. *JETP Lett.*, 14:180, 1971.

[15] Ya. B. Zel'dovich. Amplification of Cylindrical Electromagnetic Waves Reflected from a Rotating Body. *Sov. Phys. JETP*, 36:1085, 1972.

[16] W. G. Unruh. Experimental Black-hole Evaporation? *Phys. Rev. Lett.*, 46:1351–1353, May 1981.

[17] M. Visser. Acoustic black holes : horizons, ergospheres, and Hawking radiation. *Classical and Quantum Gravity*, 15(17):1767, 1998.

[18] G. Rousseaux et al. Horizon effects with surface waves on moving water. *New Journal of Physics*, 12, 2010.

[19] S. Weinfurtner, E. W. Tedford, M. C. J. Penrice, W. G. Unruh, and G. A. Lawrence. Measurement of Stimulated Hawking Emission in an Analogue System. *Phys. Rev. Lett.*, 106:021302, Jan 2011.

[20] L.-P. Euvé, F. Michel, R. Parentani, T. G. Philbin, and G. Rousseaux. Observation of Noise Correlated by the Hawking Effect in a Water Tank. *Phys. Rev. Lett.*, 117:121301, Sep 2016.

[21] T. Torres, S. Patrick, A. Coutant, M. Richartz, E. W. Tedford, and S. Weinfurtner. Rotational Superradiant Scattering in a Vortex Flow. *Nat. Phys.*, 13:833, 2017.

[22] L.-P. Euvé, S. Robertson, N. James, A. Fabbri, and G. Rousseaux. Scattering of Co-Current Surface Waves on an Analogue Black Hole. *Phys. Rev. Lett.*, 124:141101, Apr 2020.

[23] T. Torres, S. Patrick, M. Richartz, and S. Weinfurtner. Quasinormal Mode Oscillations in an Analogue Black Hole Experiment. *Phys. Rev. Lett.*, 125:011301, Jul 2020.

[24] M. Cromb, G. M. Gibson, E. Toninelli, M. J. Padgett, E. M. Wright, and D. Faccio. Amplification of waves from a rotating body. *Nat. Phys.*, 16:1069, 2020.

[25] T. G. Philbin, C. Kuklewicz, S. Robertson, S. Hill, F. König, and U. Leonhardt. Fiber-Optical Analog of the Event Horizon. *Science*, 319(5868):1367–1370, 2008.

[26] M. Elazar, V. Fleurov, and S. Bar-Ad. All-optical event horizon in an optical analog of a Laval nozzle. *Phys. Rev. A*, 86:063821, Dec 2012.

[27] J. Drori, Y. Rosenberg, D. Bermudez, Y. Silberberg, and U. Leonhardt. Observation of Stimulated Hawking Radiation in an Optical Analogue. *Phys. Rev. Lett.*, 122:010404, 2019.

[28] M. C. Braidotti, R. Prizia, C. Maitland, F. Marino, A. Prain, I. Starshynov, N. Westerberg, E. M. Wright, and D. Faccio. Measurement of Penrose Superradiance in a Photon Superfluid. *Phys. Rev. Lett.*, 128:013901, Jan 2022.

[29] H. S. Nguyen, D. Gerace, I. Carusotto, D. Sanvitto, E. Galopin, A. Lemaître, I. Sagnes, J. Bloch, and A. Amo. Acoustic Black Hole in a Stationary Hydrodynamic Flow of Microcavity Polaritons. *Phys. Rev. Lett.*, 114:036402, Jan 2015.

[30] M. J. Jacquet, T. Boulier, F. Claude, A. Maître, E. Cancellieri, C. Adrados, A. Amo, S. Pigeon, Q. Glorieux, A. Bramati, and E. Giacobino. Polariton fluids for analogue gravity physics. *Phil. Trans. R. Soc. A*, 378(2177):20190225, 2020.

[31] K. Falque, Q. Glorieux, E. Giacobino, A. Bramati, and M. J Jacquet. Spectroscopic measurement of the excitation spectrum on effectively curved spacetimes in a polaritonic fluid of light, 2023.

[32] O. Lahav, A. Itah, A. Blumkin, C. Gordon, S. Rinott, A. Zayats, and J. Steinhauer. Realization of a Sonic Black Hole Analog in a Bose-Einstein Condensate. *Phys. Rev. Lett.*, 105:240401, Dec 2010.

[33] J. Steinhauer. Observation of quantum Hawking radiation and its entanglement in an analogue black hole. *Nat. Phys.*, 12(10):959–965, October 2016.

[34] J. R. M. de Nova, K. Golubkov, V. I. Kolobov, and J. Steinhauer. Observation of thermal Hawking radiation and its temperature in an analogue black hole. *Nature*, 569(7758):688–691, May 2019.

[35] V. I. Kolobov, K. Golubkov, J. R. Muñoz de Nova, and J. Steinhauer. Observation of stationary spontaneous Hawking radiation and the time evolution of an analogue black hole. *Nat. Phys.*, 17(3):362–367, March 2021.

[36] R. Balbinot, A. Fabbri, S. Fagnocchi, A. Recati, and I. Carusotto. Nonlocal density correlations as a signature of Hawking radiation from acoustic black holes. *Phys. Rev. A*, 78, 2008.

[37] P.-E. Larré. *Fluctuations quantiques et effets non-linéaires dans les condensats de Bose-Einstein*. PhD thesis, Université Paris 11 - Orsay, 2013.

[38] P.-É. Larré, A. Recati, I. Carusotto, and N. Pavloff. Quantum fluctuations around black hole horizons in Bose-Einstein condensates. *Phys. Rev. A*, 85:013621, Jan 2012.

[39] M. Isoard and N. Pavloff. Departing from Thermality of Analogue Hawking Radiation in a Bose-Einstein Condensate. *Phys. Rev. Lett.*, 124:060401, Feb 2020.

[40] L. Pitaevskii and S. Stringari. Uncertainty principle, quantum fluctuations, and broken symmetries. *J. Low Temp. Phys.*, 85:377–388, 1991.

[41] S. N. Bose. Plancks Gesetz und Lichtquantenhypothese. *Zeitschrift für Physik*, 26:178–181, 1924.

[42] A. Einstein. Quantentheorie des einatomigen idealen Gases. *Sitzungsberichte der Preussischen Akademie der Wissenschaften*, pages 261–267, 1924.

[43] N.N. Bogoliubov. On the theory of superfluidity. *J. Phys. (USSR)*, 11:23–32, 1947.

[44] J. F. Allen and A. D. Misener. Flow of liquid helium ii. *Nature*, 141:75, 1938.

[45] J. F. Allen and A. D. Misener. Viscosity of liquid helium below the λ-point. *Nature*, 141:71, 1938.

[46] F. W. London. The λ-phenomenon of liquid helium and the Bose–Einstein degeneracy. *Nature*, 141:643–644, 1938.

[47] L. Onsager. Statistical Hydrodynamics. *Il Nuovo Cimento*, 6:279–287, 1949.

[48] O. Penrose. On the quantum mechanics of helium ii. *Philosophical Magazine*, 42:1373–1377, 1951.

[49] R. P. Feynman. Application of Quantum Mechanics to Liquid Helium. In C. J. Gorter, editor, *Progress in Low Temperature Physics*, volume 1, chapter II, pages 17–53. Elsevier, New-York, 1955.

[50] E. P. Gross. Structure of a quantized vortex in boson systems. *Nuovo Cimento*, 20:454–477, 1961.

[51] L. P. Pitaevskii. Vortex lines in an imperfect Bose gas. *Soviet Physics Journal of Experimental and Theoretical Physics*, 13:451–454, 1961.

[52] M. H. Anderson, J. R. Ensher, M. R. Matthews, C. E. Wieman, and E. A. Cornell. Observation of Bose–Einstein condensation in a dilute atomic vapor. *Science*, 269:198–201, 1995.

[53] K. B. Davis, M. O. Mewes, M. R. Andrews, N. J. van Druten, D. S. Durfee, D. M. Kurn, and W. Ketterle. Bose–Einstein condensation in a gas of sodium atoms. *Physical Review Letters*, 75:3969–3973, 1995.

[54] J. Steinhauer. Measuring the entanglement of analogue Hawking radiation by the density-density correlation function. *Phys. Rev. D*, 92:024043, Jul 2015.

[55] P. C. Hohenberg. Existence of long-range order in one and two dimensions. *Phys. Rev.*, 158:383–386, 1967.

[56] N. D. Mermin and H. Wagner. Absence of ferromagnetism or antiferromagnetism in one- or two-dimensional isotropic heisenberg models. *Phys. Rev. Lett.*, 17:1133–1136, 1966.

[57] C. Menotti and S. Stringari. Collective oscillations of a one-dimensional trapped Bose-Einstein gas. *Phys. Rev. A*, 66:043610, Oct 2002.

[58] S. Stringari L. Pitaevskii. *Bose-Einstein Condensation*. Clarendon Press Oxford, 2003.

[59] M. J. Lighthill. Introduction. Boundary Layer theory. In L. Rosenhead, editor, *Laminar Boundary Layer*, chapter II, page 46. Dover Publications, New York, 1966.

[60] A.E. Perry and B.D. Fairlie. Critical Points in Flow Patterns. In F.N. Frenkiel and R.E. Munn, editors, *Turbulent Diffusion in Environmental Pollution*, volume 18B of *Advances in Geophysics*, pages 299–315. Elsevier, 1975.

[61] H. K. Moffatt. The topology of scalar fields in 2D and 3D turbulence. In Tsutomu Kambe, Tohru Nakano, and Toshio Miyauchi, editors, *IUTAM Symposium on Geometry and Statistics of Turbulence*, pages 13–22, Dordrecht, 2001. Springer Netherlands.

[62] L. Rossi, J. C. Vassilicos, and Y. Hardalupas. Multiscale Laminar Flows with Turbulentlike Properties. *Phys. Rev. Lett.*, 97:144501, Oct 2006.

[63] N. T. Ouellette and J. P. Gollub. Dynamic topology in spatiotemporal chaos. *Phys. Fluids*, 20(6):064104, 2008.

[64] J. M. García de la Cruz, J. C. Vassilicos, and L. Rossi. Topologies of velocity-field stagnation points generated by a single pair of magnets in free-surface electromagnetic experiments. *Phys. Rev. E*, 90:043001, Oct 2014.

[65] S. S. Smith, J. Arenson, E. Roberts, S. Sindi, and K. A. Mitchell. Topological chaos in a three-dimensional spherical fluid vortex. *EPL*, 117:60005, 2017.

[66] James C. McWilliams. The emergence of isolated coherent vortices in turbulent flow. *J. Fluid Mech.*, 146:21–43, 1984.

[67] A. Babiano, C. Basdevant, B. Legras, and R. Sadourny. Vorticity and passive-scalar dynamics in two-dimensional turbulence. *J. Fluid Mech.*, 183:379–397, 1987.

[68] R. Benzi, S. Patarnello, and P. Santangelo. On the statistical properties of two-dimensional decaying turbulence. *Europhys. Lett.*, 3(7):811, apr 1987.

[69] M. E. Brachet, M. Meneguzzi, H. Politano, and P. L. Sulem. The dynamics of freely decaying two-dimensional turbulence. *J. Fluid Mech.*, 194:333–349, 1988.

[70] G. Boffetta and R. E. Ecke. Two-Dimensional Turbulence. *Annu. Rev. Fluid Mech.*, 44(Volume 44, 2012):427–451, 2012.

[71] S. Nazarenko and M. Onorato. Wave turbulence and vortices in Bose–Einstein condensation. *Physica D*, 219(1):1–12, 2006.

[72] Angela C. White, Brian P. Anderson, and Vanderlei S. Bagnato. Vortices and turbulence in trapped atomic condensates. *Proc. Natl. Acad. Sci.*, 111(supplement_1):4719–4726, 2014.

[73] T. W. Neely, A. S. Bradley, E. C. Samson, S. J. Rooney, E. M. Wright, K. J. H. Law, R. Carretero-González, P. G. Kevrekidis, M. J. Davis, and B. P. Anderson. Characteristics of Two-Dimensional Quantum Turbulence in a Compressible Superfluid. *Phys. Rev. Lett.*, 111:235301, Dec 2013.

[74] Y. P. Sachkou, C. G. Baker, G. I. Harris, O. R. Stockdale, S. Forstner, M. T. Reeves, Xin He, D. L. McAuslan, A. S. Bradley, M. J. Davis, and W. P. Bowen. Coherent vortex dynamics in a strongly interacting superfluid on a silicon chip. *Science*, 366(6472):1480–1485, 2019.

[75] G. Gauthier, M. T. Reeves, X. Yu, A. S. Bradley, M. A. Baker, T. A. Bell, H. Rubinsztein-Dunlop, M. J. Davis, and T. W. Neely. Giant vortex clusters in a two-dimensional quantum fluid. *Science*, 364(6447):1264–1267, 2019.

[76] S. P. Johnstone, A. J. Groszek, P. T. S., C. J. Billington, T. P. Simula, and K. Helmerson. Evolution of large-scale flow from turbulence in a two-dimensional superfluid. *Science*, 364(6447):1267–1271, 2019.

[77] A. Eloy, O. Boughdad, M. Albert, P.-É. Larré, F. Mortessagne, M. Bellec, and C. Michel. Experimental observation of turbulent coherent structures in a superfluid of light. *Europhys. Lett.*, 134(2):26001, apr 2021.

[78] M. Baker-Rasooli, W. Liu, T. Aladjidi, A. Bramati, and Q. Glorieux. Turbulent dynamics in a two-dimensional paraxial fluid of light. *Phys. Rev. A*, 108:063512, Dec 2023.

[79] R. Panico, P. Comaron, M. Matuszewski, A. S. Lanotte, D. Trypogeorgos, G. Gigli, M. De Giorgi, V. Ardizzone, D. Sanvitto, and D. Ballarini. Onset of vortex clustering and inverse energy cascade in dissipative quantum fluids. *Nat. Photonics*, 17:451, 2023.

[80] T. Jacobson. Black Holes and Hawking Radiation in Spacetime and Its Analogues. In D. Faccio, F. Belgiorno, S. Cacciatori, V. Gorini, S. Liberati, and U. Moschella, editors, *Analogue Gravity Phenomenology*, chapter 1, pages 1–30. Springer, 2013.

[81] R. Balbinot, I. Carusotto, A. Fabbri, C. Mayoral, and A. Recati. Understanding Hawking Radiation from Simple Models of Atomic Bose-Einstein Condensates. In D. Faccio, F. Belgiorno, S. Cacciatori, V. Gorini, S. Liberati, and U. Moschella, editors, *Analogue Gravity Phenomenology*, chapter 9, pages 181–217. Springer, 2013.

[82] A. Fabbri and J. Navarro-Salas. *Modeling Black Hole Evaporation*. Imperial College Press, 2005.

[83] F. Michel. *Nonlinear and quantum effects in analogue gravity*. PhD thesis, Université Paris-Saclay Paris-Sud, 2017.

[84] A. Fabbri and N. Pavloff. Momentum Correlations as Signature of Sonic Hawking Radiation in Bose-Einstein Condensates. *SciPost Phys.*, 4:019, 2018.

[85] I. Carusotto, S. Fagnocchi, A. Recati, R. Balbinot, and A. Fabbri. Numerical Observation of Hawking Radiation from Acoustic Black Holes in Atomic Bose-Einstein condensates. *New J. Phys.*, 10:103001, 2008.

[86] M. Isoard, N. Milazzo, N. Pavloff, and O. Giraud. Bipartite and tripartite entanglement in a Bose-Einstein acoustic black hole. *Phys. Rev. A*, 104:063302, Dec 2021.

[87] J.-P. Blaizot and G. Ripka. *Quantum Theory of Finite Systems*. MIT Press, 1986.

[88] F. Dalfovo, A. Fracchetti, A. Lastri, L. Pitaevskii, and S. Stringari. Quantum Evaporation from the Free Surface of Superfluid ^{4}He. *Journal of Low Temperature Physics*, 104:367–397, 1996.

[89] C. Mora and Y. Castin. Extension of Bogoliubov theory to quasicondensates. *Physical Review A*, 67(053615):1–24, 2003.

[90] M. Isoard. *Theoretical study of quantum correlations and nonlinear fluctuations in quantum gases*. PhD thesis, Université Paris-Saclay, 2020.

[91] S. Emig. Violation of Bell inequality in Analogue Gravity, 2021.

[92] S. J. Robertson. The theory of Hawking radiation in laboratory analogues. *J. Phys. B: At. Mol. Opt. Phys.*, 45(16):163001, aug 2012.

[93] J. Macher and R. Parentani. Black-hole radiation in Bose-Einstein condensates. *Phys. Rev. A*, 80:043601, Oct 2009.

[94] A. Recati, N. Pavloff, and I. Carusotto. Bogoliubov theory of acoustic Hawking radiation in Bose-Einstein condensates. *Phys. Rev. A*, 80:043603, Oct 2009.

[95] N. Brunner, D. Cavalcanti, S. Pironio, V. Scarani, and S. Wehner. Bell nonlocality. *Rev. Mod. Phys.*, 86:419–478, Apr 2014.

[96] R. Schmied, J.-D. Bancal, B. Allard, M. Fadel, V. Scarani, P. Treutlein, and N. Sangouard. Bell correlations in a Bose-Einstein condensate. *Science*, 352(6284):441–444, 2016.

[97] M. Fadel, T. Zibold, B. Décamps, and P. Treutlein. Spatial entanglement patterns and Einstein-Podolsky-Rosen steering in Bose-Einstein condensates. *Science*, 360(6387):409–413, 2018.

[98] P. Kunkel, M. Prüfer, H. Strobel, D. Linnemann, A. Frölian, T. Gasenzer, M. Gärttner, and M. K. Oberthaler. Spatially distributed multipartite entanglement enables EPR steering of atomic clouds. *Science*, 360(6387):413–416, 2018.

[99] P. Colciaghi, Y. Li, P. Treutlein, and T. Zibold. Einstein-Podolsky-Rosen Experiment with Two Bose-Einstein Condensates. *Phys. Rev. X*, 13:021031, May 2023.

[100] S. Piano and G. Adesso. Genuine Tripartite Entanglement and Nonlocality in Bose-Einstein Condensates by Collective Atomic Recoil. *Entropy*, 15:1875–1886, 2013.

[101] R. J. Lewis-Swan and K. V. Kheruntsyan. Proposal for a motional-state Bell inequality test with ultracold atoms. *Phys. Rev. A*, 91:052114, May 2015.

[102] K. F. Thomas, B. M. Henson, Y. Wang, R. J. Lewis-Swan, K. V. Kheruntsyan, S. S. Hodgman, and A. G. Truscott. A matter-wave Rarity–Tapster interferometer to demonstrate non-locality. *Eur. Phys. J. D*, 76:244, 2022.

[103] D. Bohm and Y. Aharonov. Discussion of Experimental Proof for the Paradox of Einstein, Rosen and Podolski. *Physical Review*, 108(4):1070–1076, Nov. 15, 1957.

[104] G. Grynberg, A. Aspect, and C. Fabre. Polarization-entangled photons and violation of Bell's inequalities. In *Introduction to Quantum Optics*, chapter 5C, pages 413–433. Cambridge University Press, New York, 2010.

[105] J. F. Clauser, M. A. Horne, A. Shimony, and R. A. Holt. Proposed Experiment to Test Local Hidden-Variable Theories. *Phys. Rev. Lett.*, 23:880–884, Oct 1969.

[106] G. Gour, F.C. Khanna, A. Mann, and M. Revzen. Optimization of Bell's inequality violation for continuous variable systems. *Phys. Lett. A*, 324(5):415–419, 2004.

[107] The Nobel Committee for Physics. *For Experiments with Entangled Photons, Establishing the Violation of Bell Inequalities and Pioneering Quantum Information Science*. THE ROYAL SWEDISH ACADEMY OF SCIENCES, Oct 2022.

[108] S. J. Freedman and J. F. Clauser. Experimental Test of Local Hidden-Variable Theories. *Physical Review Letters*, 28(14):938–941, Apr. 3, 1972.

[109] A. Aspect, J. Dalibard, and G. Roger. Experimental Test of Bell's Inequalities Using Time-Varying Analyzers. *Physical Review Letters*, 49(25):1804–1807, Dec. 20, 1982.

[110] J.-W. Pan, D. Bouwmeester, M. Daniell, H. Weinfurter, and A. Zeilinger. Experimental test of quantum nonlocality in three-photon Greenberger-Horne-Zeilinger entanglement. *Nature*, 403:515–519, Feb. 3, 2000.

[111] N. D. Mermin. Extreme quantum entanglement in a superposition of macroscopically distinct states. *Phys. Rev. Lett.*, 65:1838–1840, Oct 1990.

[112] N. D. Mermin. Quantum mysteries revisited. *Am. J. Phys.*, 58(8):731–734, 08 1990.

[113] Christian Weedbrook, Stefano Pirandola, Raúl García-Patrón, Nicolas J. Cerf, Timothy C. Ralph, Jeffrey H. Shapiro, and Seth Lloyd. Gaussian quantum information. *Rev. Mod. Phys.*, 84:621–669, May 2012.

[114] J. S. Bell. EPR Correlations and EPW Distributions. *Ann. N.Y. Acad. Sci.*, 480(1):263–266, 1986.

[115] C. H. Bennett, D. P. DiVincenzo, J. A. Smolin, and W. K. Wootters. Mixed-state entanglement and quantum error correction. *Phys. Rev. A*, 54:3824–3851, Nov 1996.

[116] G. Adesso and F. Illuminati. Continuous Variable Tangle, Monogamy Inequality, and Entanglement Sharing in Gaussian States of Continuous Variable Systems. *New J. Phys.*, 8:15, 2006.

[117] L.-M. Duan, G. Giedke, J. I. Cirac, and P. Zoller. Inseparability Criterion for Continuous Variable Systems. *Phys. Rev. Lett.*, 84:2722–2725, 2000.

[118] I. Agullo, A. J. Brady, and D. Kranas. Quantum Aspects of Stimulated Hawking Radiation in an Optical Analog White-Black Hole pair. *Phys. Rev. Lett.*, 128:091301, Feb 2022.

[119] A. J. Brady, I. Agullo, and D. Kranas. Symplectic circuits, entanglement, and stimulated Hawking radiation in analogue gravity. *Phys. Rev. D*, 106:105021, Nov 2022.

[120] W. B. Case. Wigner functions and Weyl transforms for pedestrians. *Am. J. Phys.*, 76(10):937–946, 2008.

[121] W. P. Schleich. *Quantum Optics in Phase Space*. John Wiley & Sons, Ltd, 2001.

[122] Lars M Johansen. EPR correlations and EPW distributions revisited. *Phys. Lett. A*, 236(3):173–176, 1997.

[123] K. Banaszek and K. Wódkiewicz. Nonlocality of the Einstein-Podolsky-Rosen state in the Wigner representation. *Phys. Rev. A*, 58:4345–4347, Dec 1998.

[124] M. Revzen, P. A. Mello, A. Mann, and L. M. Johansen. Bell's inequality violation with non-negative Wigner functions. *Phys. Rev. A*, 71:022103, Feb 2005.

[125] A. Serafini. *Quantum Continuous Variables: A Primer of Theoretical Methods*. CRC Press, Boca Raton London New York, 2017.

[126] G. Adesso, A. Serafini, and F. Illuminati. Multipartite entanglement in three-mode Gaussian states of continuous-variable systems: Quantification, sharing structure, and decoherence. *Phys. Rev. A*, 73:032345, Mar 2006.

[127] J. R. M. de Nova, F. Sols, and I. Zapata. Violation of Cauchy-Schwarz inequalities by spontaneous Hawking radiation in resonant boson structures. *Phys. Rev. A*, 89:043808, Apr 2014.

[128] X. Busch and R. Parentani. Quantum Entanglement in Analogue Hawking Radiation: When Is the Final State Nonseparable? *Phys. Rev. D*, 89:105024, 2014.

[129] D. Boiron, A. Fabbri, P.-É. Larré, N. Pavloff, C. I. Westbrook, and P. Ziń. Quantum Signature of Analog Hawking Radiation in Momentum Space. *Phys. Rev. Lett.*, 115:025301, Jul 2015.

[130] J R M de Nova, F Sols, and I Zapata. Entanglement and Violation of Classical Inequalities in the Hawking Radiation of Flowing Atom Condensates. *New J. Phys.*, 17:105003, 2015.

[131] A. Coutant and S. Weinfurtner. Low-frequency analogue Hawking radiation: The Bogoliubov-de Gennes model. *Phys. Rev. D*, 97:025006, Jan 2018.

[132] S. Finazzi and I. Carusotto. Entangled phonons in atomic Bose-Einstein condensates. *Phys. Rev. A*, 90:033607, Sep 2014.

[133] S. Robertson, F. Michel, and R. Parentani. Assessing degrees of entanglement of phonon states in atomic Bose gases through the measurement of commuting observables. *Phys. Rev. D*, 96:045012, Aug 2017.

[134] B. Horstmann, R. Schützhold, B. Reznik, S. Fagnocchi, and J. I. Cirac. Hawking radiation on an ion ring in the quantum regime. *New J. Phys.*, 13(4):045008, apr 2011.

[135] M. J. Jacquet and F. Koenig. The influence of spacetime curvature on quantum emission in optical analogues to gravity. *SciPost Phys. Core*, 3:5, 2020.

[136] I. Agullo, A. J. Brady, and D. Kranas. Robustness of entanglement in Hawking radiation for optical systems immersed in thermal baths. *Phys. Rev. D*, 107:085009, Apr 2023.

[137] A. Delhom, K. Guerrero, P. Calizaya, K. Falque, A. J. Brady, I. Agullo, and M. J. Jacquet. Entanglement from superradiance and rotating quantum fluids of light, 2023.

[138] S. Giovanazzi. Entanglement Entropy and Mutual Information Production Rates in Acoustic Black Holes. *Phys. Rev. Lett.*, 106:011302, Jan 2011.

[139] D. E. Bruschi, N. Friis, I. Fuentes, and S. Weinfurtner. On the robustness of entanglement in analogue gravity systems. *New J. Phys.*, 15(11):113016, November 2013.

[140] R. Simon. Peres-Horodecki Separability Criterion for Continuous Variable Systems. *Phys. Rev. Lett.*, 84:2726–2729, Mar 2000.

[141] J. J. Williamson. On the algebraic problem concerning the normal forms of linear dynamical systems. *Amer. J. Math.*, 58(1):141–163, 1936.

[142] A. Peres. Separability Criterion for Density Matrices. *Phys. Rev. Lett.*, 77:1413–1415, Aug 1996.

[143] Michał Horodecki, Paweł Horodecki, and Ryszard Horodecki. Separability of mixed states: necessary and sufficient conditions. *Phys. Lett. A*, 223(1):1–8, 1996.

[144] G. Adesso and I. Fuentes-Schuller. Correlation loss and multipartite entanglement across a black hole horizon. *Quantum Info. Comput.*, 9(7):657–665, jul 2009.

[145] E. G. Cavalcanti, C. J. Foster, M. D. Reid, and P. D. Drummond. Bell Inequalities for Continuous-Variable Correlations. *Phys. Rev. Lett.*, 99:210405, Nov 2007.

[146] R. S. Barbosa, T. Douce, P.-E. Emeriau, E. Kashefi, and S. Mansfield. Continuous-Variable Nonlocality and Contextuality. *Commun. Math. Phys.*, 391(3):1047–1089, 2022.

[147] Arthur Fine. Hidden Variables, Joint Probability, and the Bell inequalities. *Phys. Rev. Lett.*, 48:291–295, Feb 1982.

[148] S. Abramsky and A. Brandenburger. The sheaf-theoretic structure of non-locality and contextuality. *New J. Phys.*, 13(11):113036, nov 2011.

[149] U. Leonhardt and J. A. Vaccaro. Bell correlations in phase space: application to quantum optics. *J. Mod. Opt.*, 42(5):939–943, 1995.

[150] A. Gilchrist, P. Deuar, and M. D. Reid. Contradiction of Quantum Mechanics with Local Hidden Variables for Quadrature Phase Amplitude Measurements. *Phys. Rev. Lett.*, 80:3169–3172, Apr 1998.

[151] G. Auberson, G. Mahoux, S.M. Roy, and Virendra Singh. Bell Inequalities in Phase Space and their Violation in Quantum Mechanics. *Phys. Lett. A*, 300(4):327–333, 2002.

[152] J. Wenger, M. Hafezi, F. Grosshans, R. Tualle-Brouri, and P. Grangier. Maximal violation of Bell inequalities using continuous-variable measurements. *Phys. Rev. A*, 67:012105, Jan 2003.

[153] R. García-Patrón, J. Fiurášek, N. J. Cerf, J. Wenger, R. Tualle-Brouri, and Ph. Grangier. Proposal for a Loophole-Free Bell Test Using Homodyne Detection. *Phys. Rev. Lett.*, 93:130409, Sep 2004.

[154] J. Martin and V. Vennin. Obstructions to Bell CMB experiments. *Phys. Rev. D*, 96:063501, Sep 2017.

[155] Y. Xiang, B. Xu, L. Mišta, T. Tufarelli, Q. He, and G. Adesso. Investigating Einstein-Podolsky-Rosen steering of continuous-variable bipartite states by non-Gaussian pseudospin measurements. *Phys. Rev. A*, 96:042326, Oct 2017.

[156] R. Chatterjee and A. S. Majumdar. Bell-inequality violation by dynamical Casimir photons in a superconducting microwave circuit. *Phys. Rev. A*, 106:042224, Oct 2022.

[157] K. Banaszek and K. Wódkiewicz. Testing Quantum Nonlocality in Phase Space. *Phys. Rev. Lett.*, 82:2009–2013, Mar 1999.

[158] Z.-B. Chen, J.-W. Pan, G. Hou, and Y.-D. Zhang. Maximal Violation of Bell's Inequalities for Continuous Variable Systems. *Phys. Rev. Lett.*, 88:040406, Jan 2002.

[159] B.S. Cirel'son. Quantum generalizations of Bell's inequality. *Lett. Math. Phys.*, 4:93–100, 1980.

[160] K. Banaszek and K. Wódkiewicz. Nonlocality of the Einstein-Podolsky-Rosen state in the phase space. *Acta Phys. Slov.*, 49:491, 1999.

[161] G. Svetlichny. Distinguishing three-body from two-body nonseparability by a Bell-type inequality. *Phys. Rev. D*, 35:3066–3069, May 1987.

[162] J.-D. Bancal, N. Brunner, N. Gisin, and Y.-C. Liang. Detecting Genuine Multipartite Quantum Nonlocality: A Simple Approach and Generalization to Arbitrary Dimensions. *Phys. Rev. Lett.*, 106:020405, Jan 2011.

[163] D. Collins, N. Gisin, S. Popescu, D. Roberts, and V. Scarani. Bell-Type Inequalities to Detect True n-Body Nonseparability. *Phys. Rev. Lett.*, 88:170405, Apr 2002.

[164] D.N. Klyshko. The Bell and GHZ theorems: a possible three-photon interference experiment and the question of nonlocality. *Phys. Lett. A*, 172(6):399–403, 1993.

[165] A. Serafini, G. Adesso, and F. Illuminati. Unitarily localizable entanglement of Gaussian states. *Phys. Rev. A*, 71:032349, Mar 2005.

[166] T. Jacobson. Black-hole evaporation and ultrashort distances. *Phys. Rev. D*, 44:1731–1739, Sep 1991.

[167] W. G. Unruh. Sonic analogue of black holes and the effects of high frequencies on black hole evaporation. *Phys. Rev. D*, 51:2827–2838, Mar 1995.

[168] S. Corley and T. Jacobson. Hawking spectrum and high frequency dispersion. *Phys. Rev. D*, 54:1568–1586, Jul 1996.

[169] S. Corley. Computing the spectrum of black hole radiation in the presence of high frequency dispersion: An analytical approach. *Phys. Rev. D*, 57:6280–6291, May 1998.

[170] S. Robertson, F. Michel, and R. Parentani. Nonlinearities induced by parametric resonance in effectively 1D atomic Bose condensates. *Phys. Rev. D*, 98:056003, Sep 2018.

[171] A. Chatrchyan, K. T. Geier, M. K. Oberthaler, J. Berges, and P. Hauke. Analog cosmological reheating in an ultracold Bose gas. *Phys. Rev. A*, 104:023302, Aug 2021.

[172] S. Butera and I. Carusotto. Numerical Studies of Back Reaction Effects in an Analog Model of Cosmological preheating. *Phys. Rev. Lett.*, 130:241501, Jun 2023.

[173] J. R. M. de Nova and F. Sols. Black-hole laser to Bogoliubov-Cherenkov-Landau crossover: From nonlinear to linear quantum amplification. *Phys. Rev. Res.*, 5:043282, Dec 2023.

[174] S. W. Hawking. Breakdown of predictability in gravitational collapse. *Phys. Rev. D*, 14:2460–2473, Nov 1976.

[175] P. R. Anderson, A. Fabbri, and R. Balbinot. Low frequency gray-body factors and infrared divergences: Rigorous results. *Physical Review D*, 91(064061):1–18, 2015.

[176] R. H. Kraichnan. Inertial Ranges in Two-Dimensional Turbulence. *The Physics of Fluids*, 10(7):1417–1423, 1967.

[177] T. Simula, M. J. Davis, and K. Helmerson. Emergence of Order from Turbulence in an Isolated Planar Superfluid. *Phys. Rev. Lett.*, 113:165302, Oct 2014.

[178] J. F. Nye, J. V. Hajnal, and J. H. Hannay. Phase saddles and dislocations in two-dimensional waves such as the tides. *Proc. R. Soc. A*, 417(1852):7–20, 1988.

[179] Natalya Shvartsman and Isaac Freund. Speckle spots ride phase saddles sidesaddle. *Opt. Commun.*, 117(3):228, 1995.

[180] T. Congy, P. Azam, R. Kaiser, and N. Pavloff. Topological Constraints on the Dynamics of Vortex Formation in a Two-Dimensional Quantum Fluid. *Phys. Rev. Lett.*, 132:033804, Jan 2024.

[181] D. Caputo, N. Bobrovska, D. Ballarini, M. Matuszewski, M. De Giorgi, L. Dominici, K. West, L. N. Pfeiffer, G. Gigli, and D. Sanvitto. Josephson vortices induced by phase twisting a polariton superfluid. *Nat. Photonics*, 13:488–493, 2019.

[182] S. Nazarenko and M. Onorato. Freely decaying Turbulence and Bose–Einstein Condensation in Gross–Pitaevski Model. *J. Low Temp. Phys.*, 146:31–46, 2007.

[183] A. J. Groszek, T. P. Simula, D. M. Paganin, and K. Helmerson. Onsager vortex formation in Bose-Einstein condensates in two-dimensional power-law traps. *Phys. Rev. A*, 93:043614, 2016.

[184] M. Karl and T. Gasenzer. Strongly anomalous non-thermal fixed point in a quenched two-dimensional Bose gas. *New J. Phys.*, 19(9):093014, sep 2017.

[185] A. W. Baggaley and C. F. Barenghi. Decay of homogeneous two-dimensional quantum turbulence. *Phys. Rev. A*, 97:033601, 2018.

[186] Toshiaki Kanai and Chuanwei Zhang. Dynamical Transition of Quantum Vortex-Pair Annihilation in a Bose-Einstein Condensate, 2024.

[187] A. M. Polyakov. The theory of turbulence in two dimensions. *Nucl. Phys. B*, 396:367–385, 1993.

[188] D. Bernard, G. Boffetta, A. Celani, and G. Falkovich. Conformal invariance in two-dimensional turbulence. *Nat. Phys.*, pages 124–128, 2006.

[189] L. Puggioni, A. G. Kritsuk, S. Musacchio, and G. Boffetta. Conformal invariance of weakly compressible two-dimensional turbulence. *Phys. Rev. E*, 102:023107, Aug 2020.

[190] R. Panico, A. S. Lanotte, D. Trypogeorgos, G. Gigli, M. De Giorgi, D. Sanvitto, and D. Ballarini. Conformal invariance of 2D quantum turbulence in an exciton–polariton fluid of light. *Appl. Phys. Rev.*, 10:041418, 2023.

[191] Sandu Popescu and Daniel Rohrlich. Generic quantum nonlocality. *Phys. Lett. A*, 166(5):293–297, 1992.

[192] R. Horodecki, P. Horodecki, and M. Horodecki. Violating Bell inequality by mixed spin-$\frac{1}{2}$ states: necessary and sufficient condition. *Phys. Lett. A*, 200(5):340–344, 1995.

[193] K. De Jong, D. Fogel, and H.-P. Schwefel. *Handbook of Evolutionary Computation*. CRC Press, 01 1997.

[194] H.-G. Beyer and H.-P. Schwefel. Evolution strategies - A comprehensive introduction. *Natural Computing*, 1(1):3–52, 2002.